

Characterization of Natural Products from Actinobacteria of the Tübingen Strain Collection – Screening, Isolation & Structure Elucidation

Dissertation

der Mathematisch-Naturwissenschaftlichen Fakultät

der Eberhard Karls Universität Tübingen

zur Erlangung des Grades eines

Doktors der Naturwissenschaften

(Dr. rer. nat.)

vorgelegt von

Nico Ortlieb

aus Berlin

Tübingen

2019

Gedruckt mit Genehmigung der Mathematisch-Naturwissenschaftlichen Fakultät der Eberhard Karls Universität Tübingen.

Tag der mündlichen Qualifikation:	01.07.2019
Dekan:	Prof. Dr. Wolfgang Rosenstiel
1. Berichterstatter:	Prof. Dr. Timo H. J. Niedermeyer
2. Berichterstatter:	Prof. Dr. Harald Groß

**Nicht weil es schwer ist, wagen wir es nicht,
sondern weil wir es nicht wagen, ist es schwer.**

Lucius Annaeus Seneca

List of papers

This thesis includes the following papers, which will be referred to in the text by their alphabetic character (**A**; **B**):

A. Xanthocidin Derivatives from the Endophytic *Streptomyces* sp. AcE210 Provide Insight into Xanthocidin Biosynthesis

Ortlieb, Nico; Bretzel, Karin; Kulik, Andreas; Haas, Julian; Lüdeke, Steffen; Keilhofer, Nadine; Schrey, Silvia Diane; Gross, Harald; Niedermeyer, Timo Horst Johannes

ChemBioChem 19, 2472–2480 (2018); doi: 10.1002/cbic.201800467

Author	Author position	Scientific ideas [%]	Data generation [%]	Analysis & interpretation [%]	Paper writing [%]
Nico Ortlieb	1	60	35	50	50
Karin Bretzel	2	10	15	10	0
Andreas Kulig	3	0	5	0	0
Julian Haas	4	0	2.5	2.5	2.5
Steffen Lüdeke	5	0	2.5	2.5	2.5
Nadine Keilhofer	6	2.5	7.5	5	2.5
Sylvia Diane Schrey	7	2.5	7.5	5	2.5
Harald Gross	8	10	15	10	15
Timo Horst Johannes Niedermeyer	9	15	10	15	25
Titel of paper:		Xanthocidin Derivatives from the Endophytic <i>Streptomyces</i> sp. AcE210 Provide Insight into Xanthocidin Biosynthesis			
Status in publication process:		Published; 09.10.2018			

B. Draft Genome Sequence of the Xanthocidin-Producing Strain *Streptomyces* sp.

AcE210, Isolated from a Root Nodule of *Alnus glutinosa* (L.)

Ortlieb, Nico; Keilhofer, Nadine; Schrey, Silvia Diane; Gross, Harald; Niedermeyer, Timo Horst Johannes;

Microbiol Resour Announc 14, 277 (2018); doi: 10.1128/MRA.01190-18

Author	Author position	Scientific ideas [%]	Data generation [%]	Analysis & interpretation [%]	Paper writing [%]
Nico Ortlieb	1	40	35	40	20
Karin Bretzel	2	0	5	0	0
Nadine Keilhofer	3	0	5	0	0
Sylvia Diane Schrey	4	0	5	0	0
Harald Gross	5	40	40	40	70
Timo Horst Johannes Niedermeyer	6	20	10	20	10
Titel of paper:		Draft Genome Sequence of the Xanthocidin-Producing Strain <i>Streptomyces</i> sp. AcE210, Isolated from a Root Nodule of <i>Alnus glutinosa</i> (L.)			
Status in publication process:		Published; 11.10.2018			

Table of contents

A Zusammenfassung.....	12
B Summary	14
1. Introduction.....	16
1.1 Natural products as lead structures for drug development	16
1.2 The importance of Actinobacteria in the identification of new bioactive NPs.....	18
1.3 Anti-infectives.....	20
1.3.1 Strategies to overcome resistances – Antivirulence concept	22
1.3.2 The QS networks of <i>S. aureus</i>	24
1.4 Phenotypic screening approach	28
1.5 Aim of the Thesis	30
2. Material & Methods.....	31
2.1 Chemicals & Instruments	31
2.2 Strain cultivation	32
2.2.1 Media.....	32
2.2.2 <i>E. coli</i> K12, <i>B. subtilis</i> 168 & <i>S. aureus</i> PC322	34
2.2.3 Cultivation of <i>Streptomyces</i> sp. Tü2700 and <i>Streptomyces</i> sp. Tü2401	34
2.2.3.1 Preparation of Pre-cultures	34
2.2.3.2 Preparation of cryopreserved spores	35
2.2.4 Fermentation in the bioreactor.....	35
2.3 Bioassays.....	35
2.3.1 Agar diffusion assays.....	35
2.3.2 Bioactivity assay against <i>S. aureus</i> PC322	36
2.3.3 <i>yorB</i> Reporter gene assay.....	36
2.3.4 Bioautography.....	36
2.4 Sample preparation and extraction	37
2.4.1 Preparation of cell free supernatant (CFS) samples.....	37
2.4.2 Preparation of CFS extract samples	37
2.4.3 Preparation of biomass extracts.....	37
2.4.4 Processing of fermentation broth	37
2.4.4.1 Extraction of the fermentation broth of <i>S. sp.</i> Tü2700	37
2.4.4.2 Extraction of the fermentation broth of <i>S. sp.</i> Tü2401	38
2.4.5 Agar extraction of <i>S. sp.</i> Tü2401.....	38
2.4.6 Determination of extraction conditions for <i>S. sp.</i> Tü2401 submers cultures	38
2.4.7 Determination of extraction conditions for <i>S. sp.</i> Tü2401 reverse extract.....	38
2.5 Lyophilisation	39
2.6 Bioactivity- guided isolation	39

2.6.1	Thin-layer chromatography	39
2.6.1.1	Staining agents	40
2.6.1.1.1	Orcinol.....	40
2.6.1.1.2	Bromocresol green	40
2.6.1.1.3	Ninhydrin.....	40
2.6.2	Size-exclusion chromatography.....	40
2.6.3	MPLC	41
2.6.4	Analytical HPLC and MS	42
2.6.5	HPLC-HR-MS analysis	45
2.6.6	Preparative HPLC.....	46
2.7	Stability analysis of oxazolomycin A	46
2.8	NMR analysis.....	47
2.9	DNA Isolation	47
3.	Results & Discussion.....	48
3.1	Screening of the Tübingen strain collection of Actinobacteria.....	48
3.1.1	Development of a cultivation system.....	48
3.1.2	Development of the screening system	50
3.1.3	Bioactivity screening against <i>S. aureus</i> PC322.....	52
3.3	<i>Streptomyces</i> sp. Tü2700.....	56
3.3.1	Taxonomy.....	56
3.3.2	Primary screening	58
3.3.2.1	Cultivation in different media	58
3.3.2.2	Biological screening	59
3.3.2.3	Microfractionation and dereplication of the bioactive Extract	60
3.3.3	Fermentation & extraction of <i>Streptomyces</i> sp. Tü2700	61
3.3.4	Chromatographic isolation	62
3.3.4.1	Sephadex™ LH-20.....	62
3.3.4.2	pHPLC.....	64
3.3.5	Identification of oxazolomycin A.....	65
3.3.6	Genome analysis.....	70
3.3.8	Stability testing	72
3.4	<i>Streptomyces</i> sp. Tü2401.....	75
3.4.1	Taxonomy.....	75
3.4.2	Primary screening	77
3.4.2.1	Biological activity	77
3.4.2.2	Comparison of production media.....	79
3.4.3	Genome analysis.....	80
3.4.3.1	Identification of putative biosynthetic gene cluster	80

3.4.4	Agar extraction.....	86
3.4.4.1	Dereplication of the bioactive compound produced on solid medium.....	87
3.4.5	Purification of hydrophilic metabolites from <i>S. sp.</i> Tü2401 submerge cultures ...	90
3.4.5.1	Gel filtration chromatography	94
3.4.5.2	HPLC	101
3.4.5.3	Dereplication of the hydrophilic metabolites from <i>S. sp.</i> Tü2401 liquid cultures	107
3.5	<i>Streptomyces sp.</i> AcE210.....	112
4.	Conclusion.....	126
4.1	Development of a screening system	126
4.2	Exploitation of the developed system to search for bioactive compounds.....	126
4.3	Investigations of the xanthocidin biosynthesis.....	129
5.	References.....	130
6.	Appendix	143
6.1	List of abbreviations.....	143
6.2	Supporting Information <i>Streptomyces sp.</i> AcE210.....	145
6.3	Acknowledgments.....	169
6.4	Rights of use for third party property.....	170

A Zusammenfassung

Die Ordnung der Actinomycetales ist bekannt für die Produktion einer Vielzahl von Naturstoffen mit unterschiedlichen Indikationen. Im Rahmen dieser Arbeit wurden daher neue Naturstoffe innerhalb der Tübinger Stammsammlung, welche mehr als 1000 Stämme von Actinomycetales umfasst, gesucht. Dafür wurde ein bisher einzigartiges Wachstumssystem entwickelt, dass die zeitgleiche Kultivierung von bis zu 96 Stämmen von Actinomycetales auf Agar in einer Mikrotiterplatte erlaubt. Darüber hinaus ermöglichen die eigens dafür konstruierten Stempelplatten die Übertragung der Stämme als Agar Blöcke, in Petrischalen um mit ihnen Agardiffusionstests gegen unterschiedlichste Zielorganismen durchzuführen. Im Zuge dessen wurde die Tübinger Stammsammlung gegen den Monitorstamm *Staphylococcus aureus* PC322 gescreent. Dieser Stamm zeigt sowohl Verbindungen an, die mit dem *agr* System von *S. aureus* PC322 interagieren, welches u.a. an der Regulation des Quorum sensing beteiligt ist, als auch solche, die das Wachstum von *S. aureus* PC322 hemmen. Innerhalb dieses Screenings wurden 82 Stämme identifiziert, die mit dem *agr* System interagierten, sowie 284 Stämme, die das Wachstum von *S. aureus* PC322 inhibierten. Die jeweils vielversprechendsten Stämme wurden daraufhin hinsichtlich der für die Bioaktivität verantwortlichen Verbindungen untersucht.

Der Stamm *Streptomyces* sp. Tü2700 zeigte in den Agardiffusionstests eine starke Interaktion mit dem *agr* System von *S. aureus* PC322. Mit Hilfe mehrerer chromatographischer und spektroskopischer Verfahren konnte die Aktivität auf das bekannte Oxazol-polyene- γ -lactam/ β -lacton Antibiotikum Oxazolomycin A zurückgeführt werden. Die beobachtete Aktivität resultiert dabei weniger aus einer Interaktion mit dem *agr* System, als vielmehr aus einer sublethalen Inhibition von *S. aureus*, was einen Phänotyp des Monitorstamms ergibt, der dem einer echter Inhibition des *agr* Systems sehr ähnelt.

Der Stamm *Streptomyces* sp. Tü2401 zeigte eine intensive Hemmung des Wachstums von *S. aureus* PC322. Abhängig von den Kultivierungsbedingungen von *Streptomyces* sp. Tü2401 wurden unterschiedliche Substanzen isoliert und identifiziert, die für dessen Bioaktivität verantwortlich sind. Kultivierung auf Agar führte zur Biosynthese des stark zytotoxischen Endiins C-1027. Diese Verbindung befindet sich derzeit in klinischen Studien zur Behandlung von Leberzellkarzinomen.

Die Entwicklung spezieller Aufreinigungsmethoden führte zur Identifizierung der, in submerser Kultivierung von *Streptomyces* sp. Tü2401 produzierten, stark hydrophilen Sideromycine Albomycin δ_1 und δ_2 . Untersuchungen konnten deren außerordentliche Bioaktivität auch gegen multiresistente Gram-negative Bakterien belegen, bei gleichzeitigem günstigem toxikologischem Profil in *in-vivo* Studien, was sie zu vielversprechenden Wirkstoffkandidaten macht. Aufgrund seines vielseitigen Biosynthesepotentials ist der Stamm *S. sp.* Tü2401 ein attraktiver Organismus für zukünftige biotechnologische Optimierungen hinsichtlich der Ausbeute, sowie der Erzeugung von Derivaten mit veränderter Wirksamkeit und Toxizität.

Im Rahmen dieser Arbeit ist es zudem gelungen aus *Streptomyces* sp. AcE210 Xanthocidin und sechs weitere, bisher unbekannte Derivate mit Hilfe von Flash Chromatographie, SPE und semipräparativer HPLC zu isolieren. Deren Strukturen wurden mittels HRMS, NMR, Polarimetrie und VCD-Spektroskopie aufgeklärt. Bei den Verbindungen handelt es sich um Dihydroxanthocidin, Homoxanthocidin, Xanthocidin B, Homoxanthocidin B, Xanthocidin C und Homoxanthocidin C. Aufgrund der strukturellen Analogie der Xanthocidine zu Methylenomycin A, B, und C konnte erstmals eine Hypothese für die Xanthocidin Biosynthese entwickelt werden. Laut dieser verläuft die Biosynthese ähnlich der von Methylenomycin. Der entscheidende Unterschied ist die Substratspezifität der, dem MmyC entsprechenden, KASIII in *Streptomyces* sp. AcE210 für verzweigte Startereinheiten wie Isobutyryl-CoA oder 2-Methylbutyryl-CoA. Fütterungsexperimente mit Isotopen markiertem [$^{13}\text{C}_5$]-L-Valin zeigten den Einbau von Isobutyryl-CoA, welches ein Abbauprodukt von L-Valin ist, in das Xanthocidin Gerüst. Zudem konnte innerhalb der Genomsequenz von *Streptomyces* sp. AcE210 ein Cluster mit Homologien zu den an der Methylenomycin Biosynthese beteiligten *mmy* Genen identifiziert werden.

B Summary

The phylum of Actinobacteria is well known for its ability to produce a variety of bioactive compounds with various areas of application. Thus, within this thesis, the Tübingen strain collection, which currently comprises more than 1000 selected Actinobacteria strains, has been chosen as a biological source for the discovery of new natural products. In order to facilitate a time and space efficient cultivation of the strains, a unique tool was developed, allowing for the contemporaneous cultivation of 96 strains on agar in stainless steel microtiter plates. Moreover, the custom-built plungers enabled the transfer of the strains as agar blocks into petri dishes, for subsequent agar diffusion assays comprising different target organisms and various bioactivity read-outs. As a proof of concept, the Tübingen strain collection was screened against the monitor strain *Staphylococcus aureus* PC322 which has been developed to identify compounds that interfere with *agr*, a key player of quorum sensing (QS) signal transduction.

Within the screening, 82 strains showed QS inhibition activity, while 284 strains exhibited antibacterial activity. Two of the most promising strains from the screening have been analysed in regard to their bioactive compounds with *Streptomyces* sp. Tü2700 exhibiting QS inhibition activity, and *Streptomyces* sp. Tü2401 showing antibacterial activity.

By various chromatographic and spectroscopic techniques, the oxazole polyene γ -lactam/ β -lactone antibiotic oxazolomycin A was identified as the bioactive compound produced by *Streptomyces* sp. Tü2700. However, instead of a specific interaction with the *agr* system, the bioactivity is rather based on a sublethal inhibition of *S. aureus* PC322, both resulting in similar phenotypes of the monitor strain.

Characterization of *Streptomyces* sp. Tü2401 revealed that this strain was able to produce two different compounds depending on the cultivation conditions. On agar, the highly antibacterial and cytotoxic compound C-1027 was produced. which is currently being tested as new drug candidate against hepatoma in phase II clinical trials.

The development of a specific purification procedure led to the identification of the hydrophilic sideromycins albomycin δ_1 and δ_2 , which were produced in submerge cultures of *Streptomyces* sp. Tü2401. Detailed characterization revealed their great potential especially against multi resistant Gram-negative, bacteria, while being at the same time well tolerated in *in-vivo* studies. In current times where multi resistant strains are on the rise, and antibiotics active against Gram-negative bacteria are scarce, albomycins are promising drug candidates.

Within the course of this thesis, xanthocidin and six new derivatives were identified from the endophytic *Streptomyces* sp. AcE210 using flash chromatography, SPE and semi preparative HPLC. The structure of dihydroxanthocidin, homoxanthocidin, xanthocidin B, homoxanthocidin B, xanthocidin C and homoxanthocidin C were elucidated by HRMS, NMR, polarimetry and VCD spectroscopy. The structural resemblance of the xanthocidins to methylenomycin A, B, and C, led to a hypothesis for the xanthocidin biosynthesis, which is similar to the biosynthesis of methylenomycin. The decisive difference is the substrate specificity for branched chain starter units such as isobutyryl-CoA or 2-methylbutyryl-CoA of the MmyC-corresponding KASIII in *Streptomyces* sp. AcE210. Isobutyryl-CoA is a degradation product of L-valine. Feeding studies with isotopically labelled [$^{13}\text{C}_5$]-L-valine confirmed that *Streptomyces* sp. AcE210 incorporates an isobutyryl-CoA starter unit, resulting in a branched side chain in xanthocidin. Moreover, analysis of the genome sequence of *Streptomyces* sp. AcE210 revealed a cluster of homologues to the *mmy* genes involved in methylenomycin biosynthesis.

1. Introduction

1.1 Natural products as lead structures for drug development

The human evolution has always been closely connected to the use of natural goods to cover basic needs such as shelter, clothes, and food, but also for more advanced applications like spices, dyes, and also remedies. Sumerian clay tablets inscribed in cuneiform from ~ 2600 BC represent the first records of the medical application of plants, describing approximately 1000 plant-derived drugs.¹ Among these are oils of *Glycyrrhiza glabra*, *Papaver somniferum*, and *Aloe barbadensis* as remedies for respiratory tract infections, pain, diarrhea or constipations.² Up to now, the monographs of these plants are an important part of European pharmaceutical codices. Other examples of ancient descriptions of phytopharmaceutical products include the Egyptian “Ebers Papyrus” from around 1500 BC, the Chinese “Wushi'er Bingfang” from around 1100 BC; the Indian “Charaka Samhita” from about 100 BC, and the ancient Greek “History of Plants” from about 300 BC.²⁻⁶ All these prequels of the modern pharmacopeia share the common fact that either the plant itself or a sort of plant extract is administered.

In 1802, the German pharmacist Friedrich Wilhelm Adam Sertürner was the first to isolate a pure compound from opium, which is the dried latex obtained from *Papaver somniferum*. He termed this soporific, crystalline product “morphium”, after the Greek god of dreams, Morpheus.^{7,8} Soon after, in 1827, the Prussian Government triggered the industrial production of drugs, which could be otherwise only obtained by time consuming processes, by allowing physicians and pharmacists in Germany to acquire drugs from factories.⁹ The pharmacist Heinrich Emanuel Merck can be considered as the first one producing and selling a pure natural product (NP), morphium, in an industrial scale.^{10,11} With the improvement in general manufacturing processes, semi-synthetic drugs have been introduced into the market, as well. The first commercially available derivative of a natural product was acetylsalicylic acid, being sold by Bayer under the name “Aspirin®” since 1899.^{2,12} These findings in the late 18th /early 19th century started the intensive research on natural products.

One key factor to the fascination of NPs comes from their chemical diversity and complexity. Their molecular weights range from small molecules with only a few Dalton (e.g. coumarin with 146 Da) to large biopolymers featuring several thousand Dalton (e.g. chitosan, approx. 322 kDa). In contrast to synthetic compounds, many NPs possess a considerable number

of asymmetric carbons.¹³ Studies of the relationship between the stereochemistry and the bioactivity of various compounds revealed that only certain stereoisomers were able to trigger a biological response.¹⁴ Therefore, their stereochemistry, optimized throughout evolution, might be one reason why the number of NPs with bioactivity is significantly higher (0,6 %) compared to the number of synthetic bioactive compounds (0,005 %).¹⁵ However, it should be noted that the 1000-fold difference might also arise from the fact that NPs are mostly discovered in bioactivity screenings aiming for the identification of bioactive compounds whereas the whole of synthetic compounds is not only derived from various, non-medicinal fields, including the automobile or packaging industries, but also the creation of big compound libraries.

Up to now, around 250 000 NPs with bioactive or other useful characteristics have been identified covering multiple classes from antimicrobials, antivirals, cytotoxic and immunosuppressive compounds to antidiabetics, enzyme inhibitors, nutraceuticals, polymers, surfactants, herbicides and even vaccines.^{16,17} Furthermore, among the 1211 small molecule drugs approved by the U.S. Food and Drug Administration (FDA) from 1981 to 2014, 65 % were native NPs, NP mimics or compounds with a NP-derived pharmacophore.¹⁸ However, the numbers vary depending on the fields of application. For instance, the main medical use of NPs consists in the treatment of infectious diseases and cancer with up to 78 % of the drugs being NPs.¹⁶ The significance of NPs in drug development is also reflected in the ratio of NPs among the 25 best-selling drugs in 1997 - 42 % of these were NPs or NP derived drugs. It is an incontrovertible fact that the market has changed within the last 20 years and monoclonal antibodies have become more important therapeutics.^{18,19} This might explain why, within the 10 best-selling drugs in 2017 no NPs were present but instead five of these were monoclonal antibodies.²⁰ These drugs are advantageous in certain indications like autoimmune diseases or cancer, since they are specific for one antigenic target and less prone for side effects.²¹ However, NPs still play an important role in drug development, since approx. 25 % of all by the U.S. FDA newly approved drugs in 2015 were NPs or NP derived.¹⁸

Whereas in the past, the higher plants had served as main sources for bioactive NPs, the discovery of penicillin by Fleming in 1928 revealed a new, important class of potential producers: microorganisms.²² Still, about 60 % of all bioactive NPs identified today are derived from

plants. The remaining 40 % is mostly produced by microorganisms, with only a few compounds coming from animal sources (e.g. Casein, Chitosan, Collagen, steroid hormones).^{16,23,24}

According to the dictionary of natural products (version 27.2), around 44 000 NPs from microorganisms are known to date. Of these, 50 % are produced by fungi and about ~23 % by filamentous bacteria – more specifically the phylum Actinobacteria.²⁵

1.2 The importance of Actinobacteria in the identification of new bioactive NPs

The Actinobacteria constitute one of the most species-rich, diverse phylum within the domain of bacteria.²⁶ They are Gram-positive, filamentous bacteria, which are widely distributed in terrestrial and aquatic as well as marine eco systems.²⁷ Actinomycetes possess several distinctive features, including a high Guanin and Cytosin content in their genomic DNA, a mycelial life cycle, and the ability to undergo a complex morphological differentiation. Their typical type of growth, characterized by a unique combination of branching of the hyphae and tip extension, gave them their name, which is the combination of the Greek words for ray (aktis or aktin) and fungi (mukes).²⁸ In addition to their characteristic life cycle, Actinobacteria exhibit an extensive secondary metabolism, leading to the production of many different compounds by one single strain, depending on growth conditions and sampling time.^{29,30}

The phylum of Actinobacteria comprises various families ranging from Corynebacteriaceae, Mycobacteriaceae, Nocardiaceae to Micromonosporaceae and Streptomycetaceae. While the first three include pathogenic species, Micromonosporaceae, and Streptomycetaceae are more famous for their ability to produce a wide range of secondary metabolites, including but not limited to antibiotics, anticancer or immunosuppressive drugs, which all have a great influence on our daily life.^{28,31,32} Especially the family of Streptomycetaceae comprises the arguably largest antibiotic-producing genus, namely *Streptomyces*, which is responsible for the production of 80 % of the clinically used antibiotics.^{33,34} American Nobel laureate (1952) Selman Abraham Waksman became the first scientist to discover an antibiotic from the genus *Streptomyces*. He managed to isolate actinomycin from *Streptomyces antibioticus* at Rutgers University, USA, in 1940.^{35,36} However, it took four additional years and the discovery of streptomycin from *Streptomyces griseus* before a more systematic screening for bioactive compounds in this genus was initiated.^{37–40}

In general, more than half of the antibiotics in clinical use are produced by the phylum of Actinobacteria including β -lactams, tetracyclins, rifamycins, aminoglycosides, macrolides and glycopeptides.^{16,41,42}

Furthermore, the significance of Actinobacteria can also be attributed to their ability to produce a variety of other bioactive compounds, such as herbicides, insecticides, antifungals, antivirals, antitumor and immunosuppressive drugs, antiparasitic, as well as anthelmintic agents.^{28,43} Nevertheless, it has become progressively difficult to obtain novel compounds. Limitations in culturing methods combined with high rates of rediscovery of already known compounds have significantly hampered our current drug screening efforts. This is also reflected in a 30 % decrease in NP-based drugs entering clinical studies from 2001 to 2008.^{44,45} However, whole genome sequencing and genome mining have revealed that most strains harbour more biosynthetic gene clusters than already identified compounds.⁴⁶ Smanski *et al.* have estimated that the genus *Streptomyces* might be able to produce more than 150 000 secondary metabolites, of which approximately 5% are known so far.⁴⁷ In order to access so-called “silent” or “cryptic” gene clusters, two strategies are currently applied. First, empirical optimisation of the growth conditions, addition of chemical elicitors (e.g. trace metal ions) to the production medium, ribosome engineering and optimisation of regulatory genes are all useful methods applied in the past to target the cryptic gene cluster.^{45,48–51} Secondly, it has been shown that the identification and exploitation of new non-streptomycetes and novel *Streptomyces* strains also can lead to the discovery of new NPs.^{52,53} As a result, until 2005 approximately 2250 new bioactive natural products have been discovered from so called “rare” actinomycetes like e.g. *Micromonospora*, *Nocardia*, *Actinomadura*, *Actinoplanes*, *Streptoverticillium* and *Saccharopolyspora* e.g. abyssomycin and proximicin from *Verrucosisspora maris*.^{45,54–57}

Despite recent progresses in cultivation techniques, the majority of bacterial strains is still considered to be unculturable. According to 16S rRNA analysis, it has been estimated that to date only 1 % of the bacteria can be cultured under laboratory conditions.^{45,58} Therefore, methods and concepts have been and are currently being developed to exploit this “dark matter”.⁵⁸ One approach that has already been employed for the discovery of new NPs focuses on the screening of large metagenomic libraries.^{45,59} For this purpose, environmental DNA (eDNA), obtained

from environmental samples is transferred into a heterologous host. Using this culture-independent approach resulted in the identification of malacidins, a novel class of antibacterials targeting lipid II, a cell wall precursor, that, in a complex with calcium, leads to the destruction of the cell wall.⁶⁰

Taken together, these examples show that, despite current limitations, the discovery of new NP from Actinobacteria is still a promising, not yet exhausted field of research.^{41,45}

1.3 Anti-infectives

Any drug capable of inhibiting infectious disease is termed anti-infective, encompassing anti-fungals, anthelmintics, antimalarials, antiprotozoals, antituberculosis agents, antivirals, and antibiotics. The term *antibiotic* was coined in 1947 by Selman Waksman as follows: “An antibiotic is a chemical substance, produced by micro-organisms, which has the capacity to inhibit the growth of and even to destroy bacteria and other micro-organisms.”⁶¹ This definition has later been broadened in order to include also those antibacterial compounds of solely synthetic origin as well, e.g. quinolone antibiotics.⁶²

The so-called antibacterial era was initiated by the two German scientists Alfred Bertheim and Paul Ehrlich, who discovered what can be considered being the first synthetic antibacterial compound in 1907. Arsphenamin, also known as salvarsan, a cyclopolyarsenin, was used as remedy for syphilis.^{63,64}

However, it was Sir Alexander Fleming, who, by his serendipitous discovery of penicillin in 1928, kicked off the extensive research on antibacterial drugs for the following decades.²² During this so-called golden era of antibacterial drug discovery, most of the antibiotic classes known today, came into clinical use such as e.g. the aminoglycosides (1944), tetracyclines (1950), and macrolides (1952).^{62,65}

During this time, several research groups and companies initiated their efforts to establish strain collections to improve discovery of novel, NP-based drug leads. Some of these groups carrying out systematic screenings of bacterial strain collections include that of Selman Waksman in the United States, in Europe by Hans Zähler at the University of Tübingen and in Japan by Hamao Umezawa at the Institute for Antibiotics in Tokyo and Satoshi Omura at the Kitasato University in Tokyo. Their combined efforts led to the discovery of more than 1000 new NP,

including several antibiotics, like kanamycin, josamycin, several erythromycin derivatives and other macrolide antibiotics.¹³ However, the efficacy of those screening pipelines dropped in the early 1960s.⁶⁶ As a result, no new class of antibiotics, except for the carbapenems, was discovered between the early 1960s and 2000. During this time, instead of isolating new compounds, the development shifted towards the modification of existing scaffolds in order to improve pharmacological properties or to overcome resistances.^{29,67} Hence, almost all antibiotics approved by the FDA during this time were derivatives of known compounds.⁶⁸ Due to the successful and global application of antibiotics, mortality rates of previously life-threatening bacterial diseases dropped substantially. While infectious diseases used to be the main cause of death worldwide in the 1900s, it has been the second-leading in the world 100 years later, respectively the third-leading in developed countries.^{69,70} Several examples exist to highlight the impact of anti-infectives on global health. One of these is the reduction of the mortality rate of acute meningococcal meningitis from 70–90 % in the pre-antibiotic era to ~ 10 % after subcutaneous sulfanilamide injections began to be employed as treatment.⁷¹

Unfortunately, blinded by their successes, people began to forget the original warnings of Sir Alexander Flemings, who, in his Nobel prize lecture in 1945, mentioned that “it is not difficult to make microbes resistant”.⁷² Hence, during the following decades, antibiotic therapy was further expanded not only in human therapies, but also in animal medicine and farming. This misuse combined with the increased mobility of people in a more globalized world and increased industrialisation have led to the evolution and spread of resistant bacteria.⁷³ Some pathogenic bacteria have even acquired resistances against multiple antibiotics and, as a result, are referred to as multiresistant pathogens or even “superbugs”. As a consequence of the rise of resistance, the failure of antibiotic therapies has already increased morbidity and mortality and additionally puts an economic burden on the public health systems.⁷⁴

During the same period of time the number of antibacterial drugs, which were newly approved by the FDA, decreased from 2.9 per year in 1960 to 1.6 per year in 2000.⁷¹ The reasons for this decline are many, one of the more important being the decreased efforts of the major pharmaceutical companies in research on anti-infectives. Here, especially the expenses associated with the development of new drugs, which have been estimated to be around 1 billion US\$, have limited the company’s interest in this field.⁷⁵ Instead, many companies shifted their focus

towards chronic diseases, which promise better margins.⁷⁶ As a result, only four major pharmaceutical companies pursued research on antibiotics in 2010, namely AstraZeneca (London, UK), Novartis (Basel, Switzerland), GSK (London, UK) and Sanofi (Paris, France) whereas, 20 years earlier, the number was 18.⁷⁷

Ultimately, these opposing trends have provoked a growing fear of the occurrence of non-treatable “superbugs” and the return to the pre-antibiotic era.⁷⁸ In order to combat this, it is essential to develop new anti-infectives with properties that can aid in overcoming existing resistances and at the same time being less prone to develop new ones.⁷⁹

However, the concerted efforts of researchers, companies and governments led to the discovery of 25 new antibacterial drugs, which have been approved by the FDA in the time between 2000 to 2015.^{80,81} Most of these are derivatives of known ones, but five represent members of new antibiotic classes: Linezolid (oxazolidinone), daptomycin (lipopeptide), retapamulin (pleuromutilin), fidaxomicin (tiacumicin) and bedaquiline (diarylquinoline).^{77,80} Unfortunately, one major limitation of all of these new classes are the lack of activity against gram-negative bacteria. Gram-negative bacteria represent the majority of antibiotic-resistant bacteria. The Infectious Diseases Society of America (IDSA) has highlighted six pathogens as so-called “ESKAPE” organisms (*Enterococcus faecium*, *Staphylococcus aureus*, *Klebsiella pneumoniae*, *Acinetobacter baumannii*, *Pseudomonas aeruginosa* and *Enterobacteriaceae*), of which five are gram negative. They are the clinically most relevant pathogens as they have developed resistances allowing them to “escape” most of the common antibacterial therapies including the drug of last resort vancomycin.⁸² Following the IDSA, the WHO has named *Acinetobacter baumannii*, *Pseudomonas aeruginosa*, *Enterobacteriaceae* and *Staphylococcus aureus* among others as the most problematic pathogens for which new antibiotics are urgently needed.⁸³

Although the research dealing with discovery of new anti-infectives is on the right track, there is still an urgent need for the development of new strategies to overcome resistances.

1.3.1 Strategies to overcome resistances – Antivirulence concept

Concepts to overcome antibiotic resistances are as diverse as the resistance mechanisms developed by pathogens. One example is the combination of a drug which is susceptible to efflux

or enzymatic degradation with an efflux pump or enzyme inhibitor.^{84–86} Additionally, the enhancement of binding affinity of the drug towards the target or the reduction of side effects by structural optimization of the anti-infective compound are examples of two very distinguished approaches for a higher efficacy.⁸⁷ Furthermore, as mentioned above, the development/discovery of novel antibiotic classes remains an important research topic as well as the identification of novel drug targets.⁸⁸ However, what all these approaches have in common is that they are targeting bacterial compartments or functions that are crucial for survival or proliferation of the pathogen. Therefore, these approaches still bear the risk of provoking new resistances due to selection pressure in the pathogens.⁷⁸

A promising approach to overcome the obstacle of selection pressure in pathogen presents itself with the anti-virulence concept in which neither cell viability nor bacterial fitness are targeted, but rather virulence-associated mechanisms.^{86,89–91} Hence, this approach aims at disarming pathogens and thereby enabling the host's immune system to effectively clear the pathogen by itself having little to no impact on the native human microbiota.^{86,91} Since these so-called patho- or virulence blockers ideally should not interfere with bacterial growth (bacteriostatic) or viability (bactericidal), the selective pressure is alleviated.⁹¹ Thereby, it has been assumed, that those drugs possess a reduced likelihood for the emergence of resistance relative to current antibiotics.^{86,92–97} However, this remains to be verified empirically.⁹¹

Factors or mechanisms crucial for the initiation of infections or for causing diseases are promising, potential targets for the development of antivirulence therapies. More specifically, these include pathogenicity factors promoting cell adhesion, cell invasion, mechanisms to evade or overcome host immune defence, intracellular replication and damage of host tissues, stress adaptation and metabolic functions important to adapt to the different host environments, biofilm formation as well as maintenance, and control systems regulating the expression of virulence-relevant genes.⁸⁶ Especially these approaches seem promising for the development of new anti-infective drugs, that target classical virulence factors, such as adhesins/invasins, which inhibit pathogen-induced host signalling disruption by toxins, effectors, and immune modulators, manipulating microbial signal transduction and regulation, or interfere with functions required for bacterial survival and/or persistence during the infection.⁸⁶

Interfering with bacterial cell-to-cell communication, also referred to as quorum sensing (QS), has been found to be a promising way to disrupt bacterial virulence.^{90,98–104} The term “quorum sensing” is used to describe intercellular communication systems which allow bacteria to sense their direct environment in order to examine their particular cell density.^{105–107} The communication system relies on small molecules, which are constantly synthesized and secreted. The small molecules are recognized by the surrounding bacteria via cognate receptors present either on the surface of the bacterial cells (Gram-positive bacteria) or in the intracellular matrix (Gram-negative bacteria).^{105–109} When a certain threshold concentration is reached, gene expression in the respective bacteria changes, and they start to behave as multicellular organisms, producing for example biofilms or virulence factors. Since inhibition of these systems can lower the virulence of pathogenic microorganisms without affecting their growth, they are seen as promising leads for new anti-infectives, since emergence of resistance is less prone to happen.^{110–113} Unfortunately, as shown for *Pseudomonas aeruginosa*, the potency of quorum sensing inhibitors (QSI) is influenced by the presence of active efflux mechanisms.¹¹⁴ There are several possibilities to inhibit QS, including (I) lowering the activity of the autoinducer synthase and thereby reducing the production of signal molecules, or (II) through degradation of the autoinducer, or (III) by allosterically or competitively blocking the respective signal receptors.^{90,110,115}

Although extensive research on quorum sensing inhibition (QSI) has been carried out in recent years and several QS-inhibiting compounds have been identified, such as hamamelitannin, furanone C-30, or fimbrolide (F1), none of them has yet entered the market, due to critical side effects or reduced activity in animal studies.^{115–117}

1.3.2 The QS networks of *S. aureus*

Staphylococcus aureus is a Gram-positive, facultative anaerobic, coccus-shaped bacterium.¹¹⁸ It is at the same time a commensal bacterium, colonizing approximately 30 % of the human population, and at the same time a human pathogen.¹¹⁹ Since it has the potential to cause a variety of infections, including bacteremia, skin and soft tissue infections, infective endocarditis, pleuropulmonary, device-related infections and osteomyelitis, *S. aureus* is considered to be the leading cause of nosocomial infections worldwide.^{118,120–122}

For decades, β -lactam antibiotics such as penicillin have been used as the classical course of treatment for *S. aureus* infections. However, already in 1950, approximately 40 % of all *S. aureus* hospital isolates were penicillin-resistant. Only ten years later, in 1960, this number rose up to 80 %.¹²³ This stunning increase in spread of resistances is most likely due to natural selection or horizontal gene transfer. With the emergence of strains having acquired resistances to multiple β -lactam antibiotics, including the penicillin-derivative methicillin, the treatment of *Staphylococcus* infections has become increasingly challenging.¹²⁴ Glycopeptides such as teicoplanin and vancomycin are currently the first-line treatments for serious, invasive methicillin-resistant *S. aureus* (MRSA) infections.¹²⁴ However, the first cases of vancomycin-resistant *S. aureus* (VRSA) were already reported in 2002.¹²⁵

S. aureus employs a biphasic strategy for invasion and infection. At low cell densities, the bacteria express protein factors for attachment and colonization such as Protein A encoded by the gene *spa*. However, at high cell densities these pathways are suppressed in order to initiate secretion of toxins such as α -hemolysin encoded by *hla*, and proteases, which are most likely necessary for dissemination.^{106,126–128} For the regulation of virulence, *S. aureus* uses at least two different QS systems: The *agr* system and the RAP/TRAP system.^{120,129} These two circuits employ on one hand cyclic peptides, the so-called autoinducing peptides (AIP) and on the other hand the RNAlII-activating protein (RAP).^{120,130}

Although three AIP families are known, *Staphylococcus* spp. only uses AIP of the thiolactone class. Within this class, four different groups can be distinguished based on the amino acid sequence in *S. aureus*.¹²⁰ After posttranslational modification, the functional AIP can only induce its own *agr* expression. Furthermore, AIP of one group can even act as inhibitors for other groups.¹³¹ In addition to this, structure-activity relationship studies have revealed that the tail of the AIP is necessary for the activation of the *agr* system whereas the macrocycle is responsible for antagonistic activity, which has led to the synthesis of truncated AIPs.^{127,129,132,133}

The cognate receptors of the AIPs are transmembrane histidine protein kinase receptors called AgrC. They consist of a N-terminal transmembrane sensor domain, which is highly variable, and a conserved C-terminal histidine protein kinase domain.¹³⁴ After activation by the respective AIP, it has been speculated that AgrC, like other histidine protein kinases, forms a dimer and undergoes autophosphorylation followed by the transfer of one phosphoryl group to the

response regulator AgrA.^{120,135} In turn, the phosphorylated AgrA activates the transcription of the two promoters P2 and P3, completing a positive feedback loop.^{129,136} The P2 transcripts are responsible for the activation of the *agrBDCA* operon, whose gene products are responsible for the production, export, and import of AIP.¹²⁹ The transmembrane endopeptidase AgrB processes the propeptide AgrD by cleaving segments from the C-terminal end followed by a condensation between the cysteine residue and a C-terminal carboxyl group resulting in the typical thiolactone ring.¹³⁷ P3 is the promoter region of a RNAlII encoding gene.¹²⁰ Besides encoding the 26 amino acid peptide δ -hemolysin, which is presumably involved in biofilm integrity, the regulatory RNA RNA-III downregulates the transcription of genes involved in adhesion (e.g. *spa*) and activates the transcription of virulence genes encoding for example hemolysins (*hla*), Panton-Valentin leucocidin, and enterotoxins (see **Figure 1**).^{120,131,135}

The second signalling molecule employed by *S. aureus* in QS is RAP.¹³⁸ Not much is known about this QS circuit, neither about its synthesis nor its secretion. It has been speculated that RAP binds to the cognate receptor TRAP after a certain extracellular threshold has been reached resulting in the phosphorylation of the latter. Subsequently, the *agr* system and thereby RNA-III transcription is activated. Nonetheless, the role of RAP in QS is still part of a lively discussion.¹²⁰ This is also why it is still uncertain whether RAP really operates as a second QS signal in *S. aureus*.^{120,139,140}

The presence of a third QS circuit in *S. aureus*, which employs autoinducer-2 (AI-2), is currently under discussion. Genes encoding the metalloenzyme LuxS, which is the key enzyme in the production of AI-2, a mixture of signalling molecules originating from 4-,5-dihydroxy-2,3-pentanedione (DPD), are widely conserved in both gram-negative and gram-positive bacteria including in *S. aureus*.^{120,141,142} However, genomic analysis has also revealed that the cognate receptor LuxR is not present in *Staphylococcus* ssp.¹⁴³ Additionally, the exact structure of active DPD in *Staphylococcus* spp. is still unknown. Although it has been demonstrated that LuxS/AI-2 can regulate cellular functions in *S. aureus* through the KdpDE two-component system, the exact mechanisms of interaction are still unknown.^{144,145} Thus, it remains uncertain whether *S. aureus* can employ AI-2 as signalling molecule.^{120,144,146}

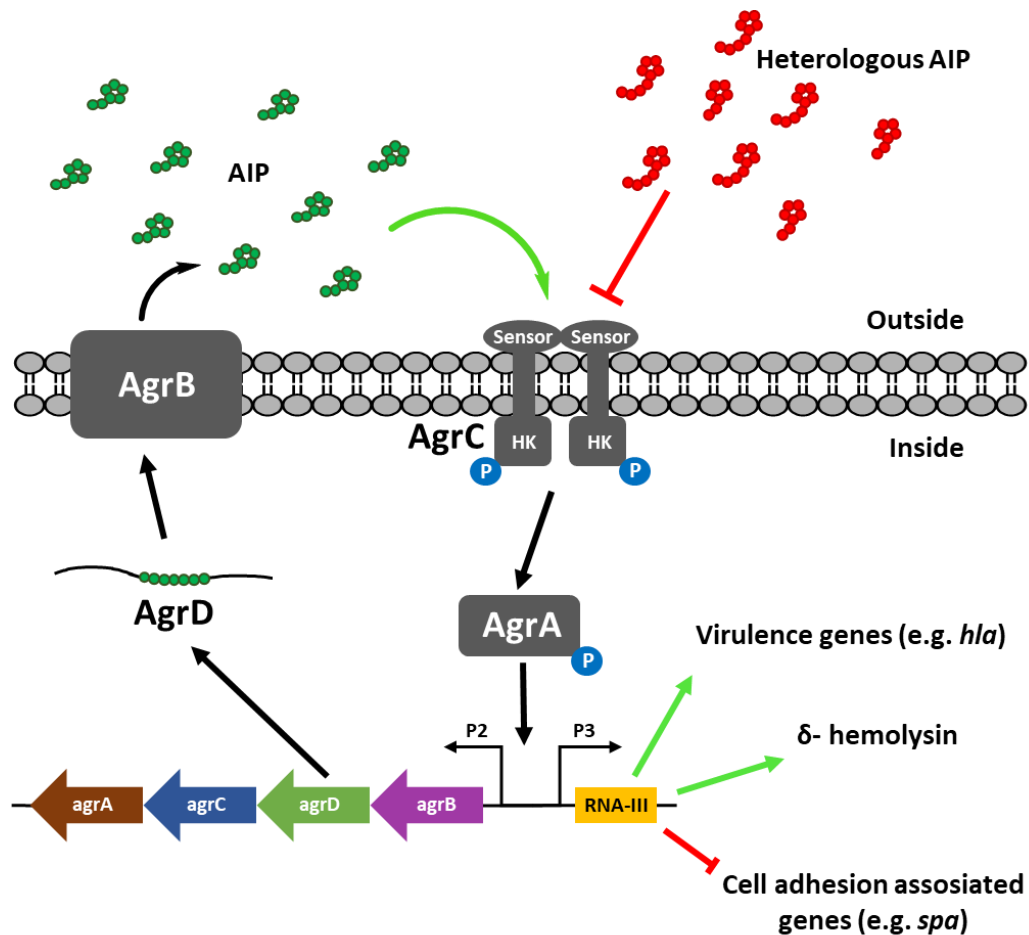


Figure 1. Schematic figure of the agr quorum sensing system in *S. aureus*. Autoinducing peptides (AIP, green) acts on the N-terminal transmembrane sensor domain of AgrC, inducing autophosphorylation followed by the transfer of one phosphoryl group to the response regulator AgrA. Phosphorylated AgrA activates the transcription of the two promoters P2 and P3. P2 is completing a positive feedback loop by activating the *agrBDCA* operon, whose gene products lead to the production, export, and import of AIP. The P3 promoter controls the transcription of the regulatory RNA RNA-III, directing the upregulation of virulence genes, as well as the downregulation of genes involved in adhesion (e.g. *spa*). Heterologous, non-cognate AIP can act as inhibitors of the system, when competing with cognate AIP for AgrC receptor binding. (adapted from Novick *et al.*)¹³⁵

Finally, in order to identify new QS inhibitors, Nielsen *et al.* developed a screening assay based on *S. aureus* *LacZ* reporter fusion strains.¹⁴⁷ This assay utilizes the *agr* regulated gene *hla*, which is fused with *LacZ*. Upon activation, AgrC leads the expression of *hla* as well as of *lacZ*, which encodes for a β -galactosidase. That in turn can be detected by the occurrence of a blue colour, resulting from the cleavage of 5-bromo-4-chloro-3-indolyl- β -D-galactopyranoside (X-Gal) mediated by the β -galactosidase.¹⁴⁷ Hence, compounds interfering with *S. aureus* QS

will result in an unstained, hazy zone of inhibition. Accordingly, this assay has led to the identification of several NPs interfering with the *agr* system, e.g. norlichexanthron or solonamides A and B.^{147–149} The first one is a small non-reduced tricyclic polyketide, which is produced by lichen or fungi. It has been shown that norlichexanthron binds to AgrA and thus blocks its ability to bind at the promoter regions P2 and P3, leading to a reduced expression of RNA III and *hla*.¹⁴⁸ The solonamides A and B are cyclodepsipeptides that have been isolated from the marine bacterium *Photobacterium halotolerans*. Due to their structural resemblance with the natural *S. aureus* AIP's they act as competitive inhibitors and interfere with the binding of the AIP to the sensor histidine kinase, AgrC (see **Figure 1**; red AIP), which leads to significant reduction of the expression of RNA III and *hla*.^{149,150}

1.4 Phenotypic screening approach

Within the last century, scientists and companies have used mainly two different approaches to test fermentation broths, extracts or pure compounds for identifying new bioactive compounds: Phenotypic or target based screenings.¹⁵¹ The latter have been the main focus of drug discovery in the past 20 years. The advancements in recombinant DNA technologies and the better understanding of biochemical processes have led to the development of many whole-cell or biochemical assays. They do not only allow for the identification of the mode of action (MoA) of a drug of interest but also feature an enormous throughput and the whole screening process became more rational.^{13,152–154} Thus, by modulating the targets activity, the whole screening process became more rational. However, the modulation of a certain targets activity may either not be of relevance for the disease pathogenicity or the responsible compounds may have an insufficient therapeutic index.¹⁵⁵ Although some companies, such as Roche's Genentech Inc., continue to employ the target-based approach for their drug discovery studies, other companies, including GlaxoSmithKline plc and Novartis AG, are investing more efforts in the classical phenotypic screening approach in order to overcome the limitations in the single-target screenings.¹⁵¹

The phenotypic screening is a target-independent approach, in which extracts or single compounds are analysed, resulting in an appropriate phenotype supposedly associated with a therapeutic effect.¹⁵⁶ In contrast, the phenotypic screening enable the discovery of bioactive compounds without having prior knowledge of their respective targets or MoA.¹³ Additionally, it has been shown that activities from phenotypic screenings can be translated into therapeutic

impact more effectively than those from the target based approaches.¹³ However, identification of the target is even though often challenging and not always crowned with success, beneficial for an approval of the new compound by the FDA. Mark Fishman, president of the Novartis Institutes for BioMedical Research, stated in 2012 that the pass rate for the target identification is “somewhere in the 40 % range”.¹⁵¹ Furthermore, in the process of preclinical and clinical development, it has been shown that substances with unknown targets are more challenging since the mechanism-related toxicities are more difficult to predict.¹⁵¹ In addition, also the optimisation of the molecular properties of the candidate drugs is often an ambitious problem as no prior knowledge of the structural features mandatory for activity exists. Another disadvantage of the phenotypic screening approach is the low time efficiency, in which some of the assays suffer from noticeably lower throughputs than the target-based assays.^{151,155} In the period between 1999 and 2008, 75 first-in-class drugs with new MoA were approved by the FDA. Of these, 50 compounds belonged to the class of small molecules and 25 were biologicals. Interestingly, even though target-based approaches were more prominent during this time, 56 % of these drugs were discovered in phenotypic screenings and only 34 % by target-based approaches.¹⁵⁵ Worth noting is that these numbers vary depending on the therapeutic area. As an example, 63 % of the small molecule anti-cancer therapeutics were derived from target-based screening, whereas 70 % of the small molecule anti-infectives were derived from phenotypic screenings, e.g. daptomycin or retapamulin.^{155,157,158} In this regard, NPs are of significant interest, since their structure, the target, and the MoA have already been optimized through evolution. As a consequence, the combination of the phenotypic screening for anti-infective substances with NPs is a promising approach for the identification of new candidate drugs.¹⁵⁵

1.5 Aim of the Thesis

The aim of this thesis was the identification of new natural products from the phylum Actinobacteria. For this purpose, the Tübingen strain collection, which currently comprises more than 1000 selected Actinobacteria strains, has been chosen as a biological source for the discovery.

Initially, a screening platform, allowing a fast and efficient growth and bioactivity testing of the whole strain collection needed to be developed. Subsequently, in order to identify new anti-infective, or antivirulent natural products, the Tübingen strain collection was screened against the *S. aureus* PC322 assay that has been developed by Nielsen *et al.*¹⁴⁷ This assay has been developed to identify compounds that interfere with the *agr* system of *S. aureus*, which has a key function in the regulation of QS in *S. aureus*.

The biological active compounds of the most promising strains were isolated. Therefore, optimal production conditions for the respective strains were identified. Additionally, extraction and isolation protocols for the individual compounds were developed using e.g. several chromatographic techniques.

Finally, the biological active compounds were dereplicated and their structure elucidated with the help of techniques like MS and NMR.

Additionally, the present work also aimed at the identification and characterisation of new natural products with rare structural features, independent from their bioactivity. Within this scope, *Streptomyces* sp AcE210 was analysed due to its potential to synthesise a rare cyclopentanone antibiotic – xanthocidin.

2. Material & Methods

2.1 Chemicals & Instruments

Table 1. Chemicals & solvents

Chemical	Vendor
Aceton	Sigma-Aldrich, St. Louis (USA)
Acetonitrile (ACN)	J. T. Baker® Avantor Performance Materials, Deventer (NLD)
Acetonitrile- <i>d</i> ₃	Carl Roth GmbH & Co. KG, Karlsruhe (DE)
Agar	Carl Roth GmbH & Co. KG, Karlsruhe (DE)
Ammonium formate	Sigma -Aldrich, St. Louis (USA)
Butanol	Merck KGaA, Darmstadt (DE)
Dichlormethane (DCM)	Fisher Scientific, Loughborough (UK)
Dimethylsulfoxid (DMSO)	Merck KGaA, Darmstadt (DE)
Dimethylsulfoxid- <i>d</i> ₆	Carl Roth GmbH & Co. KG, Karlsruhe (DE)
Ethanol	Sigma-Aldrich, St. Louis (USA)
Ethyl formate	Merck KGaA, Darmstadt (DE)
Ethylacetat (EA)	Sigma-Aldrich, St. Louis (USA)
Formic acid (FA)	Merck KGaA, Darmstadt (DE)
Hamamelitannin	Carl Roth GmbH & Co. KG, Karlsruhe (DE)
Hydrogen chloride (HCl)	VWR International GmbH, Darmstadt (DE)
Methanol (MeOH)	Sigma -Aldrich, St. Louis (USA)
Methanol- <i>d</i> ₄	Sigma-Aldrich, St. Louis (USA)
Methyl acetate	Merck KGaA, Darmstadt (DE)
Sodium hydroxide (NaOH)	VWR International GmbH, Darmstadt (DE)
X-β-Gal	Carl Roth GmbH & Co. KG, Karlsruhe (DE)

Table 2. Components of HPLC systems

System	Specification	Component
Agilent 1200 Series	G1379B	Degasser
	G1312A	Binary Pump
	G1367B	Autosampler
	G1330B	Thermostat
	G1316A	Column Compartment
	G1315B	Diode Array Detector
Agilent 1260 Infinity	G4225A	Degasser
	G1312C	Binary Pump
	G1329B	Autosampler
	G1330B	Thermostat
	G1316A	Column Compartment
	G1315D	Diode Array Detector
	G1346C	Fraction collector
Agilent 6330 IonTrap		
Sedex LT-ELSD	Model 85LT	ELSD

2.2 Strain cultivation

2.2.1 Media

All media were prepared by dissolving the relevant ingredients (see **Table 3**) in MilliQ water and subsequent pH adjustment using NaOH or HCl, respectively. If not stated otherwise, 2 % (w/v) agar (Sigma-Aldrich, St. Louis, USA) were added for solid media. All media were autoclaved at 121°C.

Table 3. Compositions of media

Name	Substance	Vendor	Concentration	pH
KM4 Broth	Yeast extract	Ohly GmbH, Hamburg, D	4 g/l	7.3
	Malt extract	Thermo Fischer Scientific, Waltham, USA	10 g/l	
	Dextrose	Carl Roth, Karlsruhe, D	4 g/l	
TS-Broth	TSB	Thermo Fischer Scientific, Waltham, USA	30 g/l	7.3
TS-Agar	TSA	Becton, Dickinson and Company, Sparks, USA	40 g/l	7.3
LB	LB-Broth	Sigma-Aldrich, St. Louis, USA	20 g/l	7.3
ISP2	Yeast extract	Ohly GmbH, Hamburg, D	4 g/l	7.3
	Malt extract	Thermo Fischer Scientific, Waltham, USA	10 g/l	
	Dextrose	Carl Roth, Karlsruhe, D	4 g/l	
ISP3/OM	Oatmeal Holo Hafergold	Reform Kontor GmbH & Co.KG, Zarrentin, D	20 g/l	7.3

Name	Substance	Vendor	Concentration	pH
	Trace metal mix		5.0 ml	
Trace metal mix	CaCl ₂ · 2H ₂ O		3 g/l	
		N/A		
	Iron(III)-citrate	N/A	1 g/l	
	MnSO ₄ · 1H ₂ O	N/A	200 mg/l	
	ZnCl ₂	N/A	100 mg/l	
	CuSO ₄ · 5H ₂ O	N/A	25 mg/l	
	Na ₂ B ₄ O ₇ · 10H ₂ O	N/A	20 mg/l	
	CoCl ₂ · 6H ₂ O	N/A	4 mg/l	
	Na ₂ MoO ₄ · 2H ₂ O	N/A	10 mg/l	
NL 19	Mannit	Merck KGaA, Darmstadt (DE)	20 g/l	7.5
	Soy meal	Henselwerk, Magstadt (DE)	20 g/l	
NL 200	Mannit	Merck KGaA, Darmstadt (DE)	20 g/l	7.5
	Cornsteep powder	Marcor Development Corporation, Carlstadt (USA)	20 g/l	
NL 300	Mannit	Merck KGaA, Darmstadt (DE)	20 g/l	7.5
	Cotton seed powder	PharmaMedia Dr. Müller GmbH, Leimen (DE)	20 g/l	
NL 333	Dextrose	Carl Roth GmbH & Co. KG, Karlsruhe (DE)	5 g/l	7.0
	Starch, soluble	Carl Roth GmbH & Co. KG, Karlsruhe (DE)	10 g/l	
	Malt extract	Thermo Fischer Scientific, Waltham (USA)	10 g/l	
	Yeast extract	Carl Roth GmbH & Co. KG, Karlsruhe (DE)	3 g/l	
	Bacto™ Peptone	Becton, Dickinson and Company, Sparks (USA)	3 g/l	
	Ammoniumnitrate	Merck KGaA, Darmstadt (DE)	3 g/l	
	CaCO ₃	Merck KGaA, Darmstadt (DE)	2 g/l	
NL 400	Dextrose	Carl Roth GmbH & Co. KG, Karlsruhe (DE)	10 g/l	7.0
	Starch	Carl Roth GmbH & Co. KG, Karlsruhe (DE)	2 g/l	
	Bacto™ Peptone	Becton, Dickinson and Company, Sparks (USA)	3 g/l	
	Yeast extract	Carl Roth GmbH & Co. KG, Karlsruhe (DE)	5 g/l	
	Meat extract	N/A	3 g/l	
	CaCO ₃	Merck KGaA, Darmstadt (DE)	3 g/l	
NL 410	Dextrose	Carl Roth GmbH & Co. KG, Karlsruhe (DE)	10 g/l	7.0
	Glycerol	Sigma-Aldrich, St. Louis (USA)	10 g/l	
	Oat meal	ReformKontor GmbH & Co. KG, Zarrentin (DE)	5 g/l	
	Soy meal	Henselwerk, Magstadt (DE)	10 g/l	
	Yeast extract	Carl Roth GmbH & Co. KG, Karlsruhe (DE)	5 g/l	
	Bacto™ Casaminoacid	Becton, Dickinson and Company, Sparks (USA)	5 g/l	
	CaCO ₃	Merck KGaA, Damrstadt (DE)	1 g/l	

Name	Substance	Vendor	Concentration	pH
NL 500	Starch, soluble	Carl Roth GmbH & Co. KG, Karlsruhe (DE)	10 g/l	8.0
	Dextrose	Sigma-Aldrich, St. Louis (USA)	10 g/l	
	Glycerol	Sigma-Aldrich, St. Louis (USA)	10 g/l	
	Fish meal	Becton, Dickinson and Company, Sparks (USA)	15 g/l	
	Sea salt	Sigma-Aldrich, St. Louis (USA)	10 g/l	
KM5	Yeast extract	Carl Roth GmbH & Co. KG, Karlsruhe (DE)	4 g/l	5.5
	Malt extract	Thermo Fischer Scientific, Waltham (USA)	10 g/l	
	Dextrose	Carl Roth GmbH & Co. KG, Karlsruhe (DE)	4 g/l	

2.2.2 *E. coli* K12, *B. subtilis* 168 & *S. aureus* PC322

E. coli K12, *B. subtilis* 168 were cultivated in LB medium (K12 & 168) at 30 °C (168) or 37 °C (K12). *S. aureus* PC322 was cultivated in TSB, supplemented with 5 µg/ml erythromycin at 37 °C. Strains were either grown in liquid cultures in flasks with baffles and spirals, and shaken at 180 rpm, or on solid media incubating statically. Pre-cultures were either inoculated with single colonies, grown on solid media or with 20 µl of a solution of cryopreserved spores. Pre-cultures were used to inoculate main cultures (1 % (v/v)). Main cultures were incubated for 16 h.

2.2.3 Cultivation of *Streptomyces* sp. Tü2700 and *Streptomyces* sp. Tü2401

Streptomyces sp. Tü2700 and *Streptomyces* sp. Tü2401 were incubated at 29 °C in miscellaneous complex media. Cultures grown on solid medium (ISP2 agar) were inoculated with 50 µl of a pre-culture and incubated until sporulation occurred (Tü2700: 7 d; Tü2401: 4 d). Submerge cultures were inoculated with 1 % (V/V) of pre-culture and incubated in Erlenmeyer flasks (max. 10 % media filling) equipped with baffle and spiral at 180 rpm.

2.2.3.1 Preparation of Pre-cultures

Pre-cultures of *Streptomyces* sp. Tü2700 and *Streptomyces* sp. Tü2401 were inoculated either with spores from the respective agar plates, or with 50 µL of the respective solution of cryopreserved spores. They were incubated in a 100 ml Erlenmeyer flask, filled with 20 ml of NL410 medium for three days at 180 rpm.

2.2.3.2 Preparation of cryopreserved spores

In order to maintain a long-term stock of each bacterial strain, spore suspensions with a final concentration of 37.5 % glycerol were prepared. The respective strains were grown on agar plates until sporulation occurred. The spores were collected by suspending in 5 ml sterile 37.5 % glycerol in water (v/v). The cultures were stored in cryotubes at - 80 °C.

2.2.4 Fermentation in the bioreactor

Streptomyces sp. Tü2700 and *Streptomyces* sp. Tü2401 were cultivated at 27 °C each in a 10 l bioreactor at a rotor speed of 200 rpm, and an airflow of 5 l/min. 500 ml of pre-culture were used to inoculate 9.5 l of the respective medium (see **Table 4**) for fermentation. Therefore, five 500 ml Erlenmeyer flask, equipped with baffle, spiral and a silicon air vent cap (Silicosen®) were each filled with 100 ml NL410 medium (see **Table 3**) and inoculated with 50 µL of the respective solution of cryopreserved spores. In case of foam development during the fermentation, the antifoam agent Ucolub N115® was added (see **Table 4**).

Table 4. Parameters for batch fermentation of *S. sp.* Tü2700 & *S. sp.* Tü2401

Strain	Medium	pH	Incubation period [d]	Amount of Ucolub N115® [ml]
<i>S. sp.</i> Tü2700	NL19	7.5	7	4
<i>S. sp.</i> Tü2401	OM	7.3	5	2

2.3 Bioassays

2.3.1 Agar diffusion assays

Agar diffusion assays against *E. coli* K12 and *B. subtilis* 168 were performed in round ($\varnothing = 92\text{mm}$) or square (120 x 120 mm) petri dishes. Petri dishes were filled with 20 ml (40 ml for square) LB-agar (see **Table 3**) at $T \sim 36\text{ °C}$ containing 50 µl (100 µl for square) of a main culture of *E. coli* K12, or *B. subtilis* 168 (see **2.2.2**). Round wells ($\varnothing = 7\text{ mm}$) were made and filled with 50 µl of sample. Subsequently, plates were first incubated for 1 h, at ambient temperature, before incubating for 16 h at either 30 °C (*B. subtilis* 168) or 37 °C (*E. coli* K12). Unless otherwise stated, 1 µl Gentamicin sulfate [c = 50 mg/ml in water] was spotted on the surface of the agar as positive control.

2.3.2 Bioactivity assay against *S. aureus* PC322

Bioactivity assays against *S. aureus* PC322 were performed in round ($\varnothing = 92\text{mm}$) or square (120 x 120 mm) petri dishes. 320 μl 5-bromo-4-chloro-3-indoxyl- β -D-galactopyranoside (X-Gal) [20 mg/ml in DMSO], and 4 μl erythromycin solution [50 mg/ml in ethanol] were mixed with 40 ml TSA and supplemented with 2 ml of the main culture of PC322 (OD of 0.1).¹⁴⁷ Subsequently, the mixture was filled into petri dishes. After solidification, round wells ($\varnothing = 7\text{ mm}$) were made and filled with 50 μl of sample. Unless otherwise stated, 50 μl hamamelitannin solution [c = 2 mg/ml in DMSO] were used as positive control.¹⁴⁰

2.3.3 *yorB* Reporter gene assay

The yorB reporter gene assays were kindly performed by Katharina Wex (Working group of Prof. Dr. Heike Brötz-Oesterhelt) at the IMIT.

The *yorB* reporter gene assays were performed with *Bacillus subtilis* 1S34 pHJS105-*yorB*-lacZ2 as agar diffusion assays.¹⁵⁹ The assay was performed in square petri dishes (120 x 120 mm). 20 ml LB medium supplemented with 1 mg spectinomycin were inoculated with 500 μl of an overnight culture and grown until reaching the stationary phase. This solution was used to inoculate 50 ml LB soft agar (0.7% agarose) containing 7.5 mg X-Gal up to the defined concentration of 3×10^7 CFU/ml. Subsequently, the mixture was filled into petri dishes. After solidification, round wells ($\varnothing = 7\text{ mm}$) were made and filled with 50 μl of sample. 5 μg ciprofloxacin were used as positive control.

2.3.4 Bioautography

Bioautography was performed subsequently to the TLC analysis of the bioactive fractions of the reverse extract of *S. sp.* Tü2401 submerge cultures derived from GFC (see **2.6.1**). For this purpose, after drying, the TLC plates were transferred (face up) into square petri dishes (120 x 120 mm). Petri dishes were filled with 40 ml LB- agar (see **Table 3**) at $T \sim 36\text{ }^\circ\text{C}$ containing 100 μl of a main culture of *E. coli* K12 (see **2.2.2**). Subsequently, plates were first incubated for 1 h at ambient temperature, before incubating for 16 h at $37\text{ }^\circ\text{C}$ (*E. coli* K12). Unless otherwise stated, 1 μl Gentamicin sulfate [c = 50 mg/ml in water] was spotted on the surface of the agar as positive control.

2.4 Sample preparation and extraction

Extracts and reverse extracts from *Streptomyces* submerge cultures were generally obtained after 4 to 7 days of incubation.

2.4.1 Preparation of cell free supernatant (CFS) samples

1.0 ml of *Streptomyces* submerge culture was transferred into a 2.0 ml tube and subsequently centrifuged for 5 min at 13,000 rpm. Finally, the supernatant was filtered through a 0.2 µm sterile filter. 0.5 ml of this CFS were transferred into an HPLC vial.

2.4.2 Preparation of CFS extract samples

CFS extract samples were prepared by adjusting the pH of CFS (see **2.4.1**) to 5.0. The CFS was extracted with an equal amount of EA in an overhead shaker for 30 min. Subsequently, the organic phase was dried under reduced pressure. The pellet was dissolved in 0.5 ml methanol and centrifuged for 5 min and 13000 rpm. The supernatant was transferred into an HPLC vial.

2.4.3 Preparation of biomass extracts

The biomass was obtained by centrifuging 5 ml *Streptomyces* submerge culture for 5 min at 13,000 rpm. The Pellet was extracted with 10 ml of a mixture of methanol and acetone (1:1; (v/v)) in an overhead shaker for 30 min. Afterwards, the organic phase was dried using a rotary evaporator. The pellet was dissolved in 1 ml methanol and centrifuged for 5 min at 13000 rpm. The supernatant was transferred into an HPLC vial.

2.4.4 Processing of fermentation broth

After termination of the fermentation (see **2.2.4**), 2% Celite® Hyflo Super-cel was added and the entire culture was separated by multiple sheet filtration (Pall T 1500 filter plates; relative retention range 10 - 30 µm) into culture filtrate (CFS) and mycelium.

2.4.4.1 Extraction of the fermentation broth of *S. sp. Tü2700*

The pH of the CFS was adjusted to pH 5 with 1 M HCl and extracted five times for 30 min with each 2.0 l of EA. The organic phases were combined and concentrated under reduced pressure.

2.4.4.2 Extraction of the fermentation broth of *S. sp.* Tü2401

CFS was extracted five times for 30 min with each 2.0 l of EA. The organic phases were combined and concentrated under reduced pressure. The aqueous phase was lyophilized (see 2.5). The residue of the extracted aqueous phase will be called “reverse extract” in the description of further processing steps below.

2.4.5 Agar extraction of *S. sp.* Tü2401

For the extraction from agar, *S. sp.* Tü2401 was cultivated on ISP2 agar plates. 2 plates (approx. 40 ml) were sliced, transferred into a 50 ml tube, and subsequently centrifuged at 20 000 g for 30 min, resulting in 10 ml supernatant. After filtration through a folded filter, the pH was adjusted to pH 4.0 using 0.1 M HCl. After centrifugation, $(\text{NH}_4)_2\text{SO}_4$ was added to the supernatant up to the saturation point and incubated for 4 h at 4 °C. Afterwards, the precipitate was separated and dissolved in 10 ml 0.1 M K_2HPO_4 at a pH of 8.0. Finally, this solution was extracted with 10 ml EA.¹⁶⁰ After drying under reduced pressure, the pellet was dissolved in 2.0 ml MeOH.

2.4.6 Determination of extraction conditions for *S. sp.* Tü2401 submers cultures

*These experiments have been performed by Philipp Schneider during his master thesis under my supervision.*¹⁶¹

In order to determine the extraction conditions for *S. sp.* Tü2401 submerge cultures, twenty 15 ml tubes were filled with 5 ml CFS from *S. sp.* Tü2401 submerge cultures. The pH was adjusted four times to either 2, 5, 7, 9, or 11 with 0.1 M NaOH or 0.1 M HCl. Subsequently, the samples were extracted with EA, methyl acetate, ethyl formate, or butanol. Finally, each phase was tested against *E. coli* K12 (see 2.3.1).

2.4.7 Determination of extraction conditions for *S. sp.* Tü2401 reverse extract

In order to determine the extraction conditions for the reverse extract of *S. sp.* Tü2401, eight 1.5 ml tubes were filled with each app. 10 mg reverse extract from *S. sp.* Tü2401 submerge cultures (2.4.4.2). Subsequently, the extract was dissolved in each 1 ml of a mixtures of MeOH and H_2O (0 %; 30 %; 50 %; 80 % MeOH) each at pH of 2 and 7. After shaking for 30 min in the ultrasonic bath, the tube was centrifuged at 13,000 rpm. The supernatants were removed and

subsequently analysed using *E. coli* K12 agar diffusion assays (see **2.3.1**). The pellets were once more dissolved in 1 ml of the respective mixture and extracted by shaking for 30 min in the ultrasonic bath. After centrifugation at 13,000 rpm, the supernatants were analysed using *E. coli* K12 agar diffusion assays. Meanwhile, the pellets were dried for 10 min at 60 °C and subsequently weighted.

2.5 Lyophilisation

Aqueous solutions, e.g. CFS of *S. sp.* Tü2401, were frozen at – 80 °C and were subsequently dried using the Lyovac GT2 (Heraeus Holding, Hanau; Germany) according to the manufacturers protocol.

2.6 Bioactivity- guided isolation

2.6.1 Thin-layer chromatography

Bioactive fractions derived from GFC of the reverse extract of *S. sp.* Tü2401 submerge cultures were analysed using Thin-layer chromatography (TLC). Two different polar stationary phases were used (Silica gel 60 F₂₅₄, and Silica gel 60 Diol F₂₅₄ (Merck KGaA, Darmstadt, Germany)) with various mobile phase mixtures (see **Table 28**). Samples were applied stepwise, by spotting 2 µl at a time approximately 1.5 cm from the bottom edge of the plate. After evaporation of the solvent, this procedure was repeated until 25 µl of each sample were applied. In the meantime, the TLC chambers were filled with a sufficient amount of the mobile phase to a depth of less than 1 cm. Additionally, filter paper soaked with the same mobile phase was attached to the walls of the chambers. The separation chambers were closed and stored for 30 min at ambient temperature to saturate the air in the chambers with the mobile phase. Subsequently, the plates were placed in the chambers without allowing the sample spots to drown in the mobile phase. When the solvent front reached approx. 90 % of the plates maximum size, the TLC plates were removed from the chambers. After drying, the plates were initially analysed using UV light at $\lambda = 366$ nm (for fluorescent analytes) and at $\lambda = 254$ nm (for fluorescence quenching compounds). Finally, in order to visualize the compounds on the TLC plates, different reagents were sprayed onto the plates (orcinol, bromocresol green, or ninhydrin (see **2.6.1.1**)), or the plates were submitted to bioautography analyses (see **2.3.4**).

2.6.1.1 Staining agents

2.6.1.1.1 Orcinol

The orcinol staining solution was always prepared freshly by mixing the storage solutions A and B (ratio 10:1 (V/V)). Solution A is 10 % sulfuric acid containing 1 % (w/V) Fe(III)Cl₃. Solution B is an ethanolic solution of 6 % (w/V) orcinol. After staining, the TLC plates were stored for 1 min at 60 °C.

2.6.1.1.2 Bromocresol green

The bromocresol green staining solution was prepared by adding 0.04 g of bromocresol green to 100 ml ethanol. Subsequently, 0.1 M NaOH was added until the colour of the solution turned blue.

2.6.1.1.3 Ninhydrin

The ninhydrin staining solution was always prepared freshly by dissolving 0.1 g ninhydrin in a mixture of 100 ml acetone and 0.5 ml acetic acid. After staining, the TLC plates were developed for 5 min at 60 °C.

2.6.2 Size-exclusion chromatography

Gravity flow size-exclusion chromatography columns were prepared by soaking a sufficient amount of stationary phase material in the appropriate mobile phase for 4 h (see **Table 5**) to form slurry. Subsequently, this slurry was thoroughly transferred into the gravity flow glass column. The columns were flushed with the mobile phase for 4 - 5 h at a flow rate of 40 ml/h (Ø 2.5 ml) or 90 ml/h (Ø 5 ml).

Samples were dissolved in 1 ml of the mobile phase (2 ml when loading mass exceeded 200 mg) for 30 min under shaking in an ultrasonic bath. After centrifugation, the supernatant was loaded onto the columns.

500 µl of each fraction were analysed via agar diffusion assays against *S. aureus* PC322 (*S. sp.* Tü2700) or *E. coli* K12 (*S. sp.* Tü2401) (see **2.3**). The active fractions were combined and analysed via HPLC.

Table 5. Characteristics of the SEC columns

Material	Exclusion Limits [Da]	Column dimensions [cm]	Mobile phase	Flow rate [ml/h]	Loading mass [mg]	Fractionation interval [1/h]
Sephadex™ LH20	≤ 5000	2.5 x 90	H ₂ O	34	104	3
Sephadex™ LH20	≤ 5000	2.5 x 78	MeOH	24	200	2
Sephadex™ LH20	≤ 5000	5.0 x 95	MeOH	102	1000	4
Sephadex™ G15	≤ 1500	2.5 x 90	H ₂ O	36	105	3
Bio-Gel® P2	100 - 1800	2.5 x 90	H ₂ O	45	103	3
Toyopearl® HW40	100 - 10000	2.5 x 90	H ₂ O	36	105	3

2.6.3 MPLC

MPLC was performed on a preparative HPLC consisting of an injection valve (Valco C6UW with 5 ml Sample loop; Macherey & Nagel, Düren), Chromatograph LaPrep with two P119 pumps (VWR, Darmstadt), dynamic mixing chamber (Knauer, Berlin), P314 2-channel-UV-Vis detector (VWR) with 2-channel- recorder (Modell N-2, Abimed, Langenfeld). A 12 g Sepacore Silica HP column (Büchi Labortechnik AG, Flawil, Switzerland) with a CV of 17 ml was used for the separations.

Samples were applied via dry loading. Therefore, 40 mg of the bioactive fractions were dissolved in 80 % MeOH/H₂O (V/V) in a round flask. Approximately 1 g silica gel was added and thoroughly mixed with the dissolved fractions. Subsequently, the solvent was removed under reduced pressure. As a result, the bioactive fractions from the GFC adhered to the silica gel. This silica gel was transferred into an empty column and compacted by tamping. Emerging void volume was filled with sea sand until the column was tightly packed.

Prior to the separation the 12 g Sepacore Silica HP column was activated and conditioned for 5 min at a flow rate of 18 ml/min with 100 % MeOH. The flow was stopped and the column containing the sample was connected to the system. For detection, the wavelength 210 nm and 280 nm have been used. The separation was started by executing a gradient from 100 % MeOH to 50 % MeOH/H₂O [pH2] in 15 min at a flow rate of 18 ml/min. Samples were taken every minute and 50 µl were analysed using *E. coli* K12 agar diffusion assays (see 2.3.1). The bioactive fractions were combined and analysed via HPLC.

2.6.4 Analytical HPLC and MS

The components for HPLC and HPLC-MS analysis using either an Agilent Technologies 1260 Infinity (HPLC), or an Agilent Technologies 1000 (HPLC-MS) (Agilent, Waldbronn) are specified in **Table 2**. For analytical measurements, a standard 10 mm flow cell was used, whereas for semi-preparative analysis a 3 mm flow cell was installed. The following tables contain parameters used for different separations. Prior to the analysis, samples were centrifuged at 13000 rpm and supernatants were transferred into HPLC vials. The HPLC data were analysed using the Agilent Chemstation (Version B.04.03). The HPLC-MS data were analysed with Bruker DataAnalysis for 6300 Series IonTrap LC-MS (Version 3.4).

Table 6. Parameter of the HPLC screening method using the Luna® C18 column.

Parameter	Value
Machine	Agilent Technologies 1260 Infinity
Column	Luna® C-18; 5 µm; 100 Å; 4.6 mm x 250 mm
Column oven	30 °C
Solvents	A: H ₂ O + 0.1 % FA; B: ACN + 0.1 % FA
Method	Gradient 5 - 100 % B for 20 min; Plateau 100 % B for 5 min
Flow	2.5 ml/min
Detektor	UV/ DAD: 210-500 nm; ELSD
Injection volume	5 µl (analytical); 50 µl (semi-preparative)
[Fraction collector: time based with timeslices 2/min]	

Table 7. Parameter of the HPLC screening method using the Nucleosil 100 C18 column.

Parameter	Value
Machine	Agilent Technologies 1260 Infinity
Column	Nucleosil 100 C-18; 5 µm; 100 Å; 4.6 mm x 125 mm
Column oven	30 °C
Solvents	A: H ₂ O + 0.1 % FA; B: ACN + 0.1 % FA
Method	Gradient 0 - 100 % B for 15 min; Plateau 100 % B for 3 min
Flow	2.0 ml/min
Detektor	UV/ DAD: 210-500 nm; ELSD
Injection volume	5 µl (analytical); 50 µl (semi-preparative)
[Fraction collector: time based with timeslices 2/min]	

Table 8. Parameter of the HPLC-MS screening method using the Nucleosil 100 C18 column.

Parameter	Value
Machine	Agilent Technologies 1200
Column	Nucleosil 100 C-18; 5 µm; 100 Å; 3.0 mm x 150 mm
Column oven	30 °C
Solvents	A: H ₂ O + 0.1 % FA; B: ACN + 0.06 % FA
Method	Gradient 0 - 100 % B for 15 min; Plateau 100 % B for 2 min
Flow	0.4 ml/min
Detektor	UV/ DAD: 210-500 nm
Injection volume	2.5 µl
Machine	Mass spectrometer 6330 Iontrap LC/MS
Ionisation	Electrospray ionisation (pos. & neg. mode alternating)
Capillary Voltage	3.5 kV
Injector Temperature	350 °C
Target mass	400 m/z; 800 m/z; 1000 m/z

Table 9. Parameter of the HPLC method using the Nucleosil 100 C8 column.

Parameter	Value
Machine	Agilent Technologies 1260 Infinity
Column	Nucleosil 100 C-8; 5 µm; 100 Å; 4.6 mm x 125 mm
Column oven	30 °C
Solvents	A: H ₂ O + 0.1 % FA; B: ACN + 0.1 % FA
Method	Gradient 0 - 100 % B for 15 min; Plateau 100 % B for 3 min
Flow	2.0 ml/min
Detektor	UV/ DAD: 210-500 nm; ELSD
Injection volume	50 µl
Fraction collector	time based with timeslices 2/min

Table 10. Parameter of the HPLC method using the Kinetex® Polar C18 column.

Parameter	Value
Machine	Agilent Technologies 1260 Infinity
Column	Kinetex® Polar C-18; 2.6 µm; 100 Å; 4.6 mm x 150 mm
Column oven	50 °C
Solvents	A: H ₂ O + 0.1 % FA; B: ACN + 0.1 % FA
Method	Gradient 5 - 100 % B for 20 min; Plateau 100 % B for 5 min
Flow	1.2 ml/min
Detektor	UV/ DAD: 210-500 nm; ELSD
Injection volume	25 µl
Fraction collector	time based with timeslices 2/min

Table 11. Parameter of the HPLC method using the Luna® NH₂ column.

Parameter	Value
Machine	Agilent Technologies 1260 Infinity
Column	Luna® NH ₂ ; 5 µm; 100 Å; 4.6 mm x 250 mm
Column oven	30 °C
Solvents	A: H ₂ O + 0.1 % FA; B: ACN + 0.1 % FA
Method	80 % B for 20 min
Flow	2.0 ml/min
Detektor	UV/ DAD: 210-500 nm; ELSD
Injection volume	50 µl
Fraction collector	time based with timeslices 2/min

Table 12. Parameter of the HPLC method using the SeQuant® ZIC®-HILIC column.

Parameter	Value
Machine	Agilent Technologies 1260 Infinity
Column	SeQuant® ZIC®-HILIC; 3.5 µm; 100 Å; 4.6 mm x 150 mm
Column oven	30 °C
Solvents	A: 10 mM NH ₄ CH ₃ COO; B: ACN + 0.1 % FA
Method	80 % B for 20 min
Flow	2.0 ml/min
Detektor	UV/ DAD: 210-500 nm; ELSD
Injection volume	50 µl
Fraction collector	time based with timeslices 2/min

Table 13. Parameter of the HPLC method for the isolation of albomycins using the XBridge BEH Amide column.

Parameter	Value
Machine	Agilent Technologies 1260 Infinity
Column	XBridge BEH Amide; 5 µm; 130 Å; 4.6 mm x 250 mm
Column oven	30 °C
Solvents	A: ACN/H ₂ O/100mM NH ₄ COO pH3 (5:4:1); B: ACN/100mM NH ₄ COO pH3 (9:1)
Method	Plateau 80 % B for 5 min; Gradient 80 - 60 % B for 35 min; Plateau 60 % B for 5 min
Flow	1.0 ml/min
Detektor	UV/ DAD: 210-500 nm; ELSD
Injection volume	50 µl
Fraction collector	time based with timeslices 2/min

Table 14. Parameter of the HPLC method determining the most suitable pH for the separation of albomyces using the XBridge BEH Amide column.

Parameter	Value
Machine	Agilent Technologies 1260 Infinity
Column	XBridge BEH Amide; 5 μ m; 130 \AA ; 4.6 mm x 250 mm
Column oven	30 $^{\circ}$ C
Solvents	A: 10 mM $\text{NH}_4\text{CH}_3\text{COO}$ (pH 3; 6; 8.5); B: ACN
Method	Plateau 95 % B for 5 min; Gradient 95 - 60 % B for 20 min; Plateau 60 % B for 5 min
Flow	1.0 ml/min
Detektor	UV/ DAD: 210-500 nm; ELSD
Injection volume	50 μ l
Fraction collector	time based with timeslices 2/min

Table 15. Parameter of the HPLC method determining the best gradient for the separation of albomyces using the XBridge BEH Amide column.

Parameter	Value
Machine	Agilent Technologies 1260 Infinity
Column	XBridge BEH Amide; 5 μ m; 130 \AA ; 4.6 mm x 250 mm
Column oven	30 $^{\circ}$ C
Solvents	A: ACN/ H_2O /100mM NH_4COO pH3 (5:4:1); B: ACN/100mM NH_4COO pH3 (9:1)
Method	Plateau 95 (70) % B for 5 min; Gradient 95 (70) - 60 % B for 20 min; Plateau 60 % B for 5 min
Flow	1.0 ml/min
Detektor	UV/ DAD: 210-500 nm; ELSD
Injection volume	50 μ l
Fraction collector	time based with timeslices 2/min

2.6.5 HPLC-HR-MS analysis

For HPLC-HR-MS analysis, ESI (positive and negative ionization) was performed in Ultra Scan mode with a capillary voltage of 3.5 kV and drying gas temperature of 350 $^{\circ}$ C. To obtain HR-MS data, samples were applied to a Dionex Ultimate 3000 HPLC system (Thermo Fisher Scientific), coupled to a maXis 4G ESI-QTOF mass spectrometer (Bruker Daltonics). The following solvent composition was used to separate the analytes 0.1 % formic acid in water as solvent A and 0.06 % formic acid in MeOH as solvent B, with a gradient from 10 % to 100 % B over 20 min, followed by 100 % B for 5 min at a flow rate of 0.3 ml/min. The separation was carried out on a Nucleoshell C18 column, 2.7 μ m, 150 \times 2 mm (Macherey-Nagel). The ESI source was operated at a nebulizer pressure of 2.0 bar, and drying gas was set to 8.0 l/min at 350 $^{\circ}$ C. MS/MS spectra were recorded in auto MS/MS mode with collision energy stepping enabled.

The scan rates for full scan and MS/MS spectra were set to 1 Hz and 7 Hz, respectively. Sodium formate was used as internal calibrant in each analysis. Molecular formulae were calculated from monoisotopic masses using the SmartFormula function of DataAnalysis (Bruker Daltonics).

2.6.6 Preparative HPLC

Preparative HPLC was performed on a preparative HPLC consisting of an injection valve (Valco C6UW with 5 ml Sample loop; Macherey-Nagel, Düren), Chromatograph LaPrep with two P119 pumps (VWR, Darmstadt), dynamic mixing chamber (Knauer, Berlin), P314 2-channel-UV-Vis detector (VWR) with 2-channel-recorder (Modell N-2, Abimed, Langenfeld). The separation parameters for the isolation of oxazolomycin are described in **Table 16**. Prior to the analysis, samples were centrifuged at 13000 rpm and supernatants were injected into the HPLC. Fractions were collected peak based by hand, and analysed subsequently via HPLC (see **Table 6**).

Table 16. Parameter of the HPLC method for the isolation of oxazolomycin A using a Luna® C-18 column

Parameter	Value
Machine	Chromatograph LaPrep
Column	Luna® C-18; 5 µm; 100 Å; 10 mm x 250 mm
Column oven	30 °C
Solvents	A: H ₂ O; B: ACN
Method	Isocratic 40 % B for 10 min; Gradient to 100 % B in 1 min; Plateau 100 % B for 5 min
Flow	9.45 ml/min
Detektor	UV: 230 nm; 280 nm
Injection volume	300 µl
Fractionation: peak based by hand	

2.7 Stability analysis of oxazolomycin A

In order to examine the stability of oxazolomycin A, stress tests have been performed. 5 mg of the pure compound were dissolved in 5 ml MeOH [c = 1 mg/ml]. After centrifugation, the supernatant was dispensed equally in 25 HPLC vials. 3 vials were stored under each of the conditions listed in **Table 17**. In order to create an inert atmosphere above the sample solution, the void volume of the HPLC vials was flushed with argon gas for 30 s. Light protection was created by wrapping the HPLC vials in aluminium foil and storing them in a light protective box. Samples were either stored in the fridge at 4 °C, in the hot cabinet at 60 °C, or at ambient

temperature (about 23 °C). The samples were analysed at the start of the experiment, after 17 h and after 77 h via HPLC (see **Table 7**). The maximum peak heights at 280 nm were compared. The degradation [%] was calculated according to formula **(1)**.

$$(1) \quad \text{Degradation [\%]} = \frac{h_{T_0}^{280 \text{ nm}} - h_{T_x}^{280 \text{ nm}}}{h_{T_0}^{280 \text{ nm}}} * 100$$

Table 17. Storage conditions of stability tests of oxazolomycin A

Atmosphere	Light protection	Temperature [°C]
Air	-	23
Air	+	23
Argon	+	23
Argon	+	4
Argon	+	60
Argon	+	23
Argon	-	23

2.8 NMR analysis

The NMR experiments were performed on a Bruker Avance III HD 400 spectrometer at 400 MHz (¹H). The compounds were dissolved in methanol-*d*₄. This solution was filtered through cotton wool and transferred into an NMR tube (filling height: 4 cm). The chemical shifts were referenced to the residual protonated solvent signals of methanol-*d*₄ ($\delta_H = 3.31$ ppm & $\delta_H = 4.78$ ppm; $\delta_C = 49.15$ ppm).

2.9 DNA Isolation

To obtain genomic DNA for sequencing, main cultures of the *Streptomyces* strains were used after 4 d of incubation. To isolate the genomic DNA, the Qiagen Genomic-tip 100/G kit (Qiagen, Hilden, Germany) was used, following the manufacturer's protocol. 50 μ l deionised H₂O were used for elution.

3. Results & Discussion

3.1 Screening of the Tübingen strain collection of Actinobacteria

3.1.1 Development of a cultivation system

Small-scale cultivation systems using microtiter plates (MTP) are widely used in microbiology labs throughout the world.^{162–166} There are even reports of applications of low volume cultivation systems for filamentous organisms like streptomycetes.^{166–171} In recent years, cultivation in an even smaller scale than MTP, in picodroplets, has made great progress.^{172–176} The advantages of these high-throughput (HTP) cultivation systems are apparently the increased time- and space- efficiency while handling and screening large amounts of different bacteria strains.¹⁷⁶ Moreover, the development of picoinjection systems, enabling the injection of reporter cells into the droplets, allowed screening for antimicrobial compounds in picodroplets.¹⁷⁴ However, no new antimicrobial compound has been identified through this new approach yet.¹⁷⁴

As mentioned in the introduction (see **1.2**), Actinobacteria are soil bacteria which undergo a complex life cycle from spore germination over vegetative growth, formation of aerial hyphae, spore formation, and finally spore dispersal.²⁸ However, all cultivation systems reported to date are submerge cultivation systems. Needless to say that these systems led to the identification of a plethora of natural products from Actinobacteria. Nevertheless, cultivation in submerge cultures is still an artificial way of growing, and relatively little is known yet about the morphogenesis of Actinobacteria in submerge cultures.^{177,178} Antibiotic production is influenced by the morphology in submerged cultures, which can range from fragmented growth to dense clumps.²⁸ For example, production of erythromycin in *Saccharopolyspora erythraea* is promoted by clumps of at least 90 μm in diameter. All morphologies differing from these clumps leads to diminished yields.¹⁷⁹

Keeping in mind the tremendous influence of the cultivation conditions on the production of secondary metabolites, this work aimed at the development of an agar based MTP (96 well) cultivation system for Actinobacteria.^{28,30} Additionally, this cultivation system needed to be connectable to a suitable screening system.

In parallel to the development of the cultivation system, the Tübingen strain collection, which currently comprises more than 1000 Actinobacteria strains, was formatted in a 96 well MTP format. Therefore, spores of each strain were harvested according to **2.2.3.2**. But instead of filling the spore solutions into cryotubes, they were transferred into MTPs (96-deepwell, flat bottom, square). These MTPs were stored at -80 °C.

Antibiotic production is growth phase dependent, mostly appearing during vegetative growth.²⁸ Hence, in order to harvest all strains after incubation during their vegetative growth phase, it was necessary to sort strains, whose sporulation occurred around the same time, into the same MTP.

After incubation, the agar blocks, containing the Actinobacteria strains needed to be transferred into petri dishes to subsequently perform bioassays. While using standard MTP, it was impossible to non-destructively remove the agar blocks from the MTP. Removal of the bottoms of the wells was the solution to this problem. Thereby, the agar blocks could be pushed out of the MTP. However, neither could the bottoms been removed sterile nor was it possible to develop a supplementary sterilization method, nor could bottomless MTP been purchased. Standard MTP consists of polystyrene which is not heat stable. Hence treatments like (moist) heat sterilization were not applicable. But also chemical sterilization according to the Centers of Disease Control and Prevention (CDC) Guidelines, employing 7.5 % H₂O₂ for 15 min and 70 % ethanol for 5 min failed in their effectiveness.¹⁸⁰

Due to these sterility problems, the Actinobacteria strains were finally cultivated in bottomless, stainless-steel MTPs (96-well, round). These plates are reusable and could be heat sterilized at 160 °C for 2 h.

Before being used for the cultivation of Actinobacteria, the plates were closed on one site with a silicone mat. Each well was filled with 160 µl of either ISP-2 or ISP-3 agar (see **Figure 2A**). For further processing, it was necessary to increase the amount of agar in the media from 2.0 % to 2.5 %.

A cryo-replicator, developed by Duetz *et al.*, was used for inoculation of these MTPs from the frozen spore stocks.¹⁶⁸ This replicator was designed to remove small aliquots from the frozen stocks, without allowing the whole stock to thaw, since this would lead to a rapid loss of spore

viability (see **Figure 2B**).¹⁶⁸ The replicator consists of 96 spring-borne stainless steel pins. For inoculation, the cryo-replicator is pressed (app. 0.2 N) for 3 s onto the frozen surface of the spore stock.¹⁶⁸ This leads to the melting of app. 0.3 μl of the spore stock, which will form an app. 50 μm film on the tip of the pin.¹⁶⁸ Subsequently, this spore film was used for inoculation of the agar-filled MTPs (see **Figure 2C**). Finally, the MTPs were closed with another silicone matt and incubated at 27 °C for 5 to 10 d, depending on the sporulation times (see **Figure 2D**). In order to prevent the agar from drying during incubation, the MTP were stored in a water saturated atmosphere in desiccators.

Between inoculations, the cryo-replicator was heat sterilized and allowed to cool down to ambient temperature.¹⁶⁸

In order to analyse the possibility of cross contamination, MTPs were prepared, containing an Actinobacteria spore stock only in every third well. This plate was used for iterative inoculations of agar filled MTPs. Throughout this analysis contamination of adjoining wells has never been observed.

3.1.2 Development of the screening system

Agar diffusion assays are basic tools in microbiology. The susceptibility of bacteria towards certain compounds is analysed by spotting the compounds on an agar plate, where bacteria have already been placed. The occurrence of an inhibition zone around the compounds, also called halo, indicates if growth of the bacteria was affected.¹⁸¹ The size of the halo does not only depend on the susceptibility of a bacterium towards the compound, but also on the compounds diffusion coefficient.¹⁸² The discovery of penicillin has been one of the very first reported agar diffusion assays.²² Meanwhile, agar diffusion assays can be used for various applications either to detect the susceptibility of an organism towards a certain compound, to quantify compounds, or to identify mode of actions.^{183–185} Even combinations of agar diffusion test with analytical techniques like TLC or MS have been reported.^{186,187}

However, there are no assays described in the literature that combine agar diffusion assays with MTP cultivation systems. In order to screen the Tübingen strain collection for the production of QS inhibitory metabolites, it was necessary to develop a screening system suitable for the combination of the above mentioned MTP cultivation system with an agar diffusion assay.

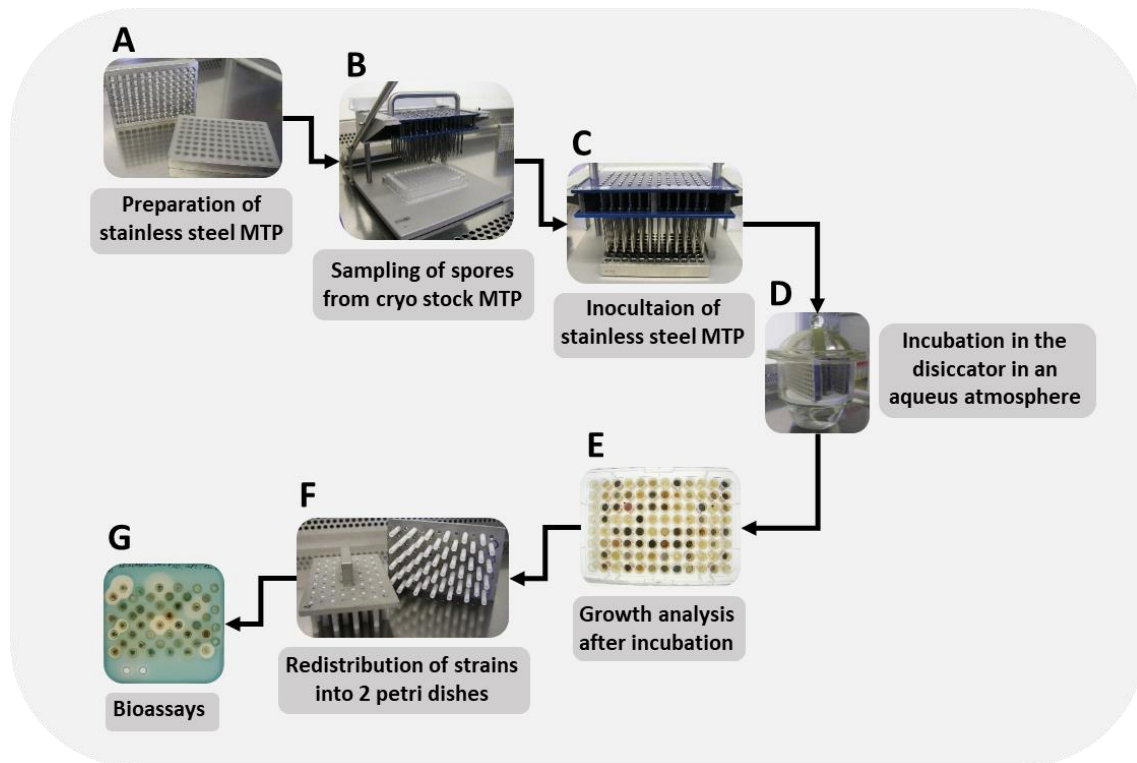


Figure 2. "From spore to bioactivity" - the workflow of the combined MTP cultivation system and an agar diffusion assay. (A) Bottomless, stainless steel MTP were closed with silicone mats and wells were filled with agar. (B) For spore sampling, the cryo-replicator is pressed onto the frozen surface of the spore stock, leading to a 50 μm film on the tip of the pin. (C) The agar filled MTP were inoculated, sealed with another silicone mat and stored in a water filled desiccator (D). (E) After an appropriate time of incubation, the MTP were unsealed and the growth of the bacteria was analysed. (F) With the help of two plungers, agar plugs containing the bacteria were redistributed in two petri dishes. (G) Those plugs were subsequently submitted to bioassays.

To withdraw the agar plugs from the MTPs after the appropriate incubation time, plungers have been developed to push the agar plugs out of the bottomless MTPs (see **Figure 2E&F**). These plungers have been designed to be heat sterilisable, thus consisting of aluminium handles with Teflon pins. Instead of a flat shape the tips of the pins are concaved. This has been found to be necessary to reduce the contact area of the pins and the agar plugs, thus preventing adhesion of the plugs to the pins

In order to create sufficient distance between the agar plugs in the petri dish, it was necessary to distribute the 96 agar plugs of one MTP into two petri dishes (square; 100 x 100 mm). Hence, two plungers each consisting of 48 pins alternating pin and gap, were build.

After transferring the agar plugs into the petri dishes, 40 ml agar, supplemented with the test organism, were carefully poured around the agar plugs (see **Figure 2G**). The agar plates were kept at ambient temperature for 1 h and subsequently incubated over night at either 27 °C or 36 °C, depending on the test organism.

3.1.3 Bioactivity screening against *S. aureus* PC322

1232 strains from the Tübingen strain collection of Actinobacteria have been tested against *S. aureus* PC322, using the combined cultivation / screening system described above (see **3.1.1** & **3.1.2**).¹⁴⁷ As already mentioned, the cultivation conditions have a tremendous impact on the secondary metabolite profile of Actinobacteria, therefore the strains were cultivated on two different media: ISP2 and ISP3 (see **Table 3**).³⁰ These two media have been developed in the course of the International *Streptomyces* Project, representing two recommended media for the cultivation of Actinobacteria.^{188,189}

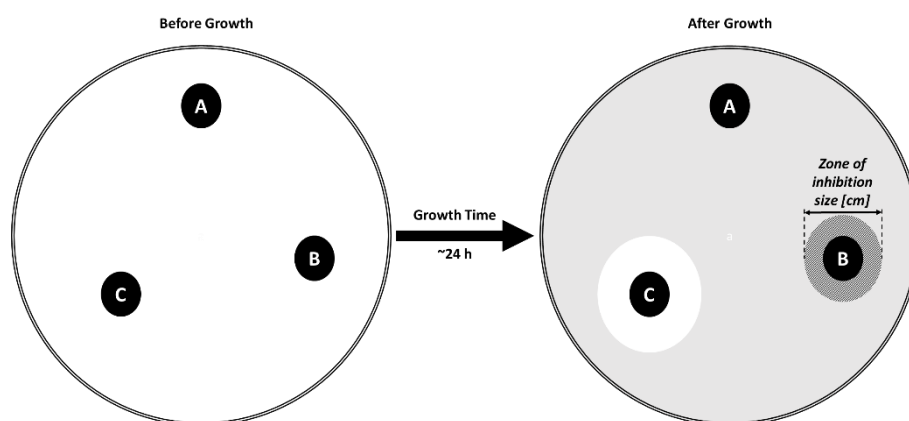


Figure 3. Probable outcomes of the *S. aureus* PC 322 agar diffusion assay (see **2.3.2**). A, B, C represent different Actinobacteria that were grown on agar and have been subsequently placed in a petri dish. Agar supplemented with *S.aureus* PC322, X-Gal and Erythromycin was poured around the plugs. After incubation, 3 different outcomes could be observed. (A) No inhibition, neither of growth nor of QS; (B) quorum sensing inhibition, indicated by hazy, uncolored inhibition zones; (C) growth inhibition, indicated by clear inhibition zones

The combined cultivation/screening experiments were performed in triplicates, in order to reduce the effect of random errors, e.g. growth deficiencies, on the screening results. Only those effects occurring at least two times were taken into account as reliable results.

Three different outcomes could be observed during the screening: A) no bioactivity, B) quorum sensing inhibition activity, and C) antibacterial activity (see **Figure 3**).

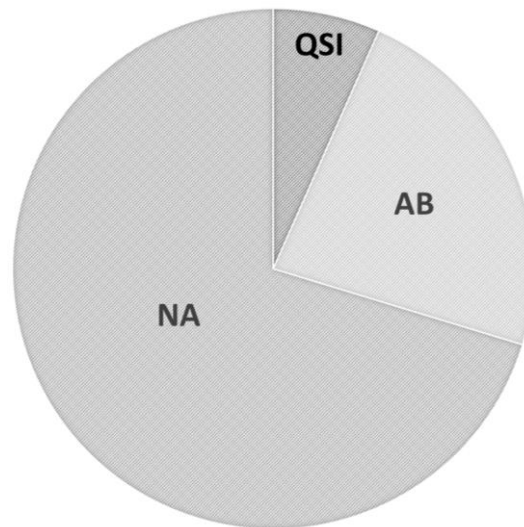


Figure 4. Results from the screening of 1232 Actinobacteria strains from the Tübingen strain collection against *S. aureus* PC322. 82 strains showed quorum sensing inhibition activity (QSI), while 284 strains exhibited antibacterial activity (AB). 866 strains did not reveal any activity (NA).

Independently from the cultivation medium, 82 strains showed quorum sensing inhibition activity, representing approx. 7 % of the tested strains (see **Figure 4**). While the majority of those strains (80 %) only exhibited modest inhibition zones smaller than 0.5 cm, 17 strains showed inhibition zones bigger than 1.0 cm (see **Table 18**). 5 strains (Tü99; Tü1792; Tü2698; Tü2700, and Tü3337) even showed halos of at least 2 cm. However, some data sets showed bad quality, e.g. impurities, short PCR fragments, and thus led to ambiguous resemblance.

The impact of the cultivation conditions is also visible in this screening. Among the strains exhibiting inhibition zones ≥ 1 cm, 4 strains exclusively inhibited QS when cultivated on ISP3 agar, while 9 strains revealed inhibition only when grown on ISP2 agar. 4 strains exhibited QS inhibition independently from the cultivation medium.

Table 18. Strains of the Tübingen strain collection of Actinobacteria exhibiting QS inhibition against the monitor strain *S. aureus* PC322 with inhibition zones ≥ 1 cm. The genus has been determined via 16S rRNABLAST analysis. Ambiguous results are indicated with N/A

ISP-2		ISP-3	
Strain number	Genus	Strain number	Genus
Tü1471	N/A	Tü35	<i>Streptomyces</i>
Tü1792	<i>Streptomyces</i>	Tü99	<i>Streptomyces</i>
Tü2395	<i>Streptomyces</i>	Tü1792	<i>Streptomyces</i>
Tü2431	N/A	Tü2644	<i>Streptomyces</i>
Tü2469	<i>Streptomyces</i>	Tü2698	<i>Streptomyces</i>
Tü2698	<i>Streptomyces</i>	Tü2700	<i>Streptomyces</i>
Tü2700	<i>Streptomyces</i>	Tü3004	N/A
Tü3004	N/A	Tü3676	<i>Streptomyces</i>
Tü3054	<i>Streptomyces</i>		
Tü3084	<i>Streptomyces</i>		
Tü3337	<i>Streptomyces</i>		
Tü3374	N/A		
Tü6438	<i>Streptomyces</i>		

Overall, 284 strains showed antibacterial activity against *S. aureus* PC322, representing 23% of the screened strains (see **Figure 4**). 4 % of the strains even exhibited inhibition zones larger than 2.0 cm (see **Table 19**). Due to 16S-rRNA sequence identity, all of these strains belong to the genus *Streptomyces*. That was revealed by a BLAST search for resemblance of the 16S-rRNA sequence of the strains in the NCBI database, identifying a collection of *Streptomyces* with > 99 % sequences identity.¹⁹⁰ 4 strains exhibited their activity exclusively on ISP2 medium, and 2 strains only on ISP3 medium, which is another confirmation of the OSMAC strategy (see **1.2**). The large amount of 23 % strains exhibiting antibacterial activities is not surprising, since especially the genus *Streptomyces* is well known for its potential to produce antibiotics (see **1.2**), and the Tübingen strain collection contains preselected Actinobacteria strains.

However, 866 strains did not show any activity against the monitor strain *S. aureus* PC322

While among the strains exhibiting QS inhibitory activity, *Streptomyces* sp. Tü2700 was the one with the biggest zone of inhibition (2.5 cm), *Streptomyces* sp. Tü2401 was the most promising strain exhibiting anti-bacterial activity (2.2 cm). Thus these strains were chosen for further analysis, which will be presented in the following chapters.

Table 19. Strains of the Tübingen strain collection of Actinobacteria exhibiting antibacterial activity against the monitor strain *S. aureus* PC322 with inhibition zones ≥ 2 cm. The genus has been determined via 16S rRNA BLAST analysis. When strains have already been characterized for the specialized metabolites they produce, their antibacterial metabolites are also shown.

ISP-2			ISP-3		
Strain number	Genus	Metabolites	Strain number	Genus	Metabolites
Tü735	<i>Streptomyces</i>	Tetracyclin	Tü39	<i>Streptomyces</i>	Actinomycin, Chloractinomycin
Tü2293	<i>Streptomyces</i>	N/A	Tü735	<i>Streptomyces</i>	Tetracyclin
Tü2401	<i>Streptomyces</i>	N/A	Tü2293	<i>Streptomyces</i>	N/A
Tü2687	<i>Streptomyces</i>	N/A	Tü2401	<i>Streptomyces</i>	N/A
Tü3775	<i>Streptomyces</i>	N/A	Tü2687	<i>Streptomyces</i>	N/A
Tü3938	<i>Streptomyces</i>	N/A	Tü3158	<i>Streptomyces</i>	N/A
Tü4116	<i>Streptomyces</i>	N/A	Tü3775	<i>Streptomyces</i>	N/A
F86	<i>Streptomyces</i>	N/A			N/A

3.3 *Streptomyces* sp. Tü2700

3.3.1 Taxonomy

Strain Tü2700 is a member of the genus *Streptomyces*, as shown by its 16S rRNA sequence (> 99 % sequence identity with several Streptomycetaceae).¹⁹⁰ However, this method is unable to reveal the distinct species of *Streptomyces* sp. Tü2700. Therefore, the genomic DNA was isolated, using the Qiagen Genomic-tip 100/G kit (Qiagen, Hilden, Germany) following the manufacturer's protocol. Subsequently, the whole genome was sequenced. Finally, the sequence was submitted to the autoMLST program in order to automatically generate a species phylogeny with reference organisms, identifying the phylogenetic neighbours.^{191–193} As a result, the two type strains *Streptomyces alboflavus* NRRL B-2373 and *Streptomyces aureocirculatus* NRRL ISP5386 appeared as the closest relatives with an estimated average nucleotide identity (ANI) of 86.0 % (Mash distance: 0.1404) for *Streptomyces alboflavus* NRRL B-2373, respectively 85.3 % (Mash distance: 0.1475) for *Streptomyces aureocirculatus* NRRL ISP5386. These results indicate that *Streptomyces* sp. Tü2700 apparently belongs to a yet undescribed species (**Figure 5**). However, in order to confirm this hypothesis further experiments determining its chemotaxonomy, eg. lipid profile, its morphology, and its utilization of different carbon sources are needed.

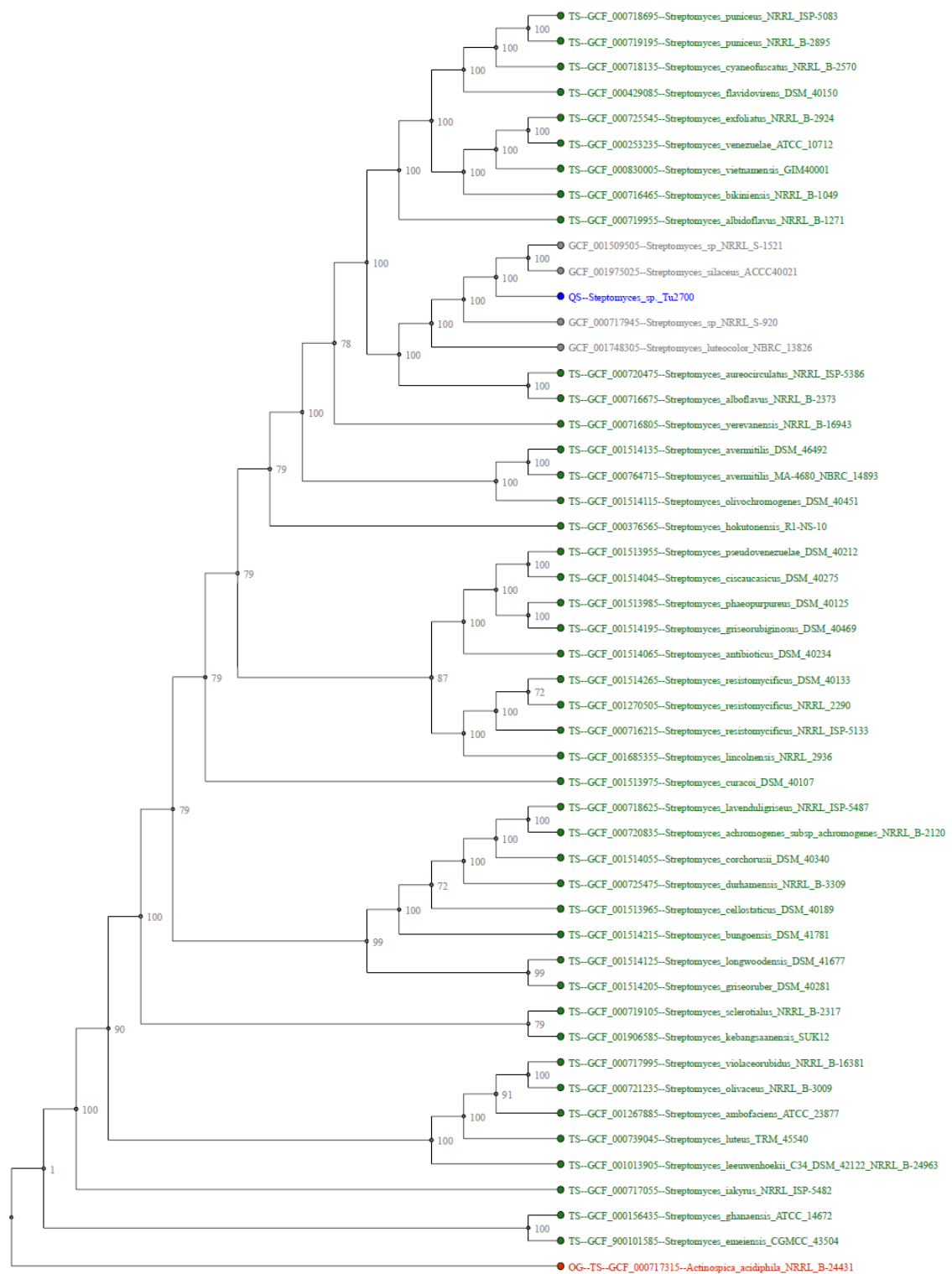


Figure 5. Phylogenetic tree of *S. sp. Tü2700* (blue font) inferred from its gDNA sequence using the software autoMLST. The phylogeny is rooted with *Actinospica acidiphila* NRRL B24431 (red), strains depicted in green font represent *Streptomyces* type strains.

3.3.2 Primary screening

The aim of this primary screening was the analysis of the biosynthetic potential of *Streptomyces* sp. Tü2700, as well as the dereplication of the bioactive compound(s) with the help of an in-house spectral-database.

3.3.2.1 Cultivation in different media

Several sequencing projects have confirmed that Actinobacteria have a huge biosynthetic potential.^{45–47} However, many of the biosynthetic gene clusters remain “silent”. In order to increase the number of secondary metabolites available from one microbial source, Bode *et al.* have investigated the influence of the media composition.³⁰ By altering the cultivation parameter, the so called OSMAC (One strain many compounds) approach resulted in more than 100 compounds, belonging to various structural classes from 6 different organisms.³⁰

Therefore, following this OSMAC approach, *Streptomyces* sp. Tü2700 was cultivated in different media. Subsequently, the potential to produce bioactive secondary metabolites was evaluated using bioactivity tests. Additionally, this primary screening aimed at the dereplication of bioactive compounds utilizing an in-house database.

Streptomyces sp. Tü2700 was cultivated according to **2.2.3**. After 72 h and 120 h, the pH and the amount of biomass were analysed (see **Table 20**). The pH value as well as the biomass show a constant increase over time in most media. Exceptions are NL200, NL400, NL410 and NL500, showing a constant or even decreasing biomass, and NL300, exhibiting a slight decrease of the pH value.¹⁹⁴ A decline in biomass as well as of pH could be a sign of a bacterial colony being already in the death or decline phase of growth.¹⁹⁵ A variety of reasons can be responsible. Either growth of *Streptomyces* sp. Tü2700 is accelerated in these media, which leads to populations being faster in the stationary growth phase. However, this seems unlikely, since media like e.g. NL19 show a similar increase in biomass (60 %) and no decline in pH. Thereby, the most possible explanation is that these media have to some extent a nutrient limitation, leading to smaller populations that reach the stationary growth phase faster.

Table 20. Results of the cultivation experiments of *Streptomyces* sp. Tü2700 in different media after 72 h & 168 h incubation.

	Time [h]	Biomass [%]	pH CFS	Colour Medium	Colour CFS	Colour biomass
NL 19	72	6	7,6	beige	light-grey	beige
	168	10	8.2		light-brown	light-brown
NL 200	72	2	6,7	light-grey	yellow	dark-grey
	168	1	8.9		yellow	light-grey
NL 300	72	7	7,5	dark-brown	light-brown	light-brown
	168	12	7.3		red	light-brown
NL 333	72	3	7,9	light-brown	yellow	light-grey
	168	5	8.4		light-brown	beige
NL 400	72	1	4,5	yellow	yellow	beige
	168	1	4.8		yellow	beige
NL 410	72	5	4,2	light-brown	yellow	light-grey
	168	5	4.5		dark-brown	light-grey
NL 500	72	1	3,9	light-grey	light-grey	dark-grey
	168	1	4.2		beige	dark-grey
OM	72	3	4,7	beige	beige	beige
	168	4	4.8		red	beige

3.3.2.2 Biological screening

In order to analyse the impact of the cultivation conditions on the bioactivity, extracts of the biomass as well as the CFS were prepared according to **2.4** and subsequently tested against *S. aureus* PC322, according to **2.3.2**. The size and the appearance of halos were evaluated after 12 h (see **Table 21**). In general, the extracts of the CFS or the biomass showed higher activity than the CFS itself, which is most probably a concentration effect. Additionally, extracts and CFS of cultures grown in media like NL200, NL400, NL410, NL500 and OM showed only slight activities.

Depending on the media composition and the incubation time, extracts and CFS showed unstained halos varying in size and appearance, either clear or hazy, whereas hazy halos could be an indication for QSI in *S. aureus* PC322.

Two media, NL19 and NL333, showed remarkable inhibition zones, with halo sizes above 1.5 cm. However, this study aimed at the identification of novel QS inhibitors against *S. aureus*. Therefore, since extracts and CFS of cultures grown in NL19 have shown solely hazy halos, further cultivation studies were performed in NL19.¹⁹⁴ Since the bioactivity of the CFS extracts

has increased after 72 h, it can be assumed that the optimal incubation time is longer than 3 days.

Table 21. Results of the bioactivity tests of CFS and extracts of Tü2700 against *S. aureus* PC322 after incubation times of 72 h and 168 h (- ... no bioactivity; + ... halo size \leq 0.5 cm; ++ ... halo size \leq 1.5 cm; +++ ... halo size $>$ 1.5 cm; (c)... clear halo; (h)... hazy halo).

	Time [h]	CFS	CFS extract	Biomass extract
NL 19	72	-	++ (h)	+ (h)
	168	-	+++ (h)	+ (h)
NL 200	72	-	-	+ (h)
	168	-	-	+ (c)
NL 300	72	-	++ (h)	-
	168	+ (c)	++ (c)	+ (c)
NL 333	72	+ (h)	+++ (c)	++ (c)
	168	+ (c)	+++ (c)	++ (c)
NL 400	72	-	-	+ (c)
	168	-	+ (h)	+ (h)
NL 410	72	-	-	-
	168	-	-	-
NL 500	72	-	-	-
	168	+ (h)	+ (h)	+ (h)
OM	72	-	-	-
	168	-	-	+ (c)

3.3.2.3 Microfractionation and dereplication of the bioactive Extract

In a first attempt to dereplicate the potential QS inhibiting compound produced by *Streptomyces* sp. Tü2700, the CFS extract of the culture grown in NL19 was microfractionated (see **Table 6**). The fractions were dried, redissolved in MeOH, and subsequently tested against *S. aureus* PC322 according to **2.3.2**. As a result, only fraction 11 showed a hazy halo. This fraction featured, along some smaller peaks, one very prominent peak. However, comparison of the UV spectra of the peaks with the in-house database did not reveal any accordance. Therefore, it was assumed that the compound responsible for the hazy halo is unknown.

Needless to say, that this dereplication method has limitations, since the in-house database only covers 976 natural products (as at 01/2018). Additionally, signal overlapping of coeluting compounds is a known restraint of dereplication methods using crude extracts. Furthermore, compounds featuring no chromophore in the molecular structure cannot be dereplicated by the use of this method. However, all compounds known so far that interfere with *S. aureus* QS

feature chromophores.^{115,120} Nevertheless, it would have been useful to expand the dereplication efforts and include also external NP databases like the dictionary of natural products. Moreover, since the combination of UHPLC and HR-MS-MS has been shown to be a promising tool for the dereplication of natural products even in complex matrices, the use of those techniques would have been advantageous.^{196–198}

3.3.3 Fermentation & extraction of *Streptomyces* sp. Tü2700

Initially, *Streptomyces* sp. Tü2700 has been cultivated on small scale in 10 ml culture volume in 100 ml shake flasks with spiral and baffler, leading to 10 mg CFS extract. In order to obtain larger amounts of extract, necessary for further purification and structure elucidation, *Streptomyces* sp. Tü2700 was cultivated at a larger scale in a labour-efficient manner, using a continuous stirred tank B20 bioreactor (B. Braun, Melsungen, Germany).

Streptomyces sp. Tü2700 was cultivated according to **2.2.4**. Samples were taken every 24 h, and CFS extracts were prepared as described in **2.4.2**. Subsequently, these extracts were analysed using the *S. aureus* PC322 assay (see **2.3.2**). During the course of the fermentation, the pH decreased slightly from initially 7.5 to 6.6 after 4 days.

The halo size increased during the first three days up to 2.7 cm. After 4 days, the halo size remained constant at 2.7 cm. Hence, the fermentation was stopped after 4 days. Even though 5 ml of polyethylene glycol had been added to the batch during the fermentation, excessive amounts of foam have formed which got partly lost, decreasing the yield to only 18 l culture broth. After filtration, 14 l CFS were obtained. Finally, extraction with ethyl acetate resulted in 3.8 g crude extract (see **2.4.4**).

This fermentation has shown that it is possible to cultivate *Streptomyces* sp. Tü2700 in a 20 l scale in a bioreactor, maintaining its capability to produce the QS inhibiting compound. Moreover, 3.8 g of crude extract, containing substantial amounts of the active compound, could be obtained, which are necessary for further purification and structure elucidation. However, knowledge of the chemistry of the active compound could be used for further optimization of the fermentation, in order to increase the amount of active compound. Moreover, in future fermentations in a bioreactor, the addition of sufficient amounts of PEG or other suitable anti-foam agents is advisable to prevent loss of CFS through excessive foam formation.

3.3.4 Chromatographic isolation

3.3.4.1 Sephadex™ LH-20

A well-established method for the isolation and separation of peptides, but also for other small molecules like terpenoids and lipids, is size-exclusion chromatography.^{199–201} For separations of low molecular weight peptides (~35 aa residues), Sephadex™ LH-20 is often used as stationary phase in combination with water or mixtures of water and miscible solvents like MeOH.²⁰² Sephadex™ LH-20 is a beaded cross-linked hydroxy-propylene dextrane that exhibits at the same time hydrophilic as well as hydrophobic properties.²⁰² It swells in water and also in numerous organic solvents. The separation principle is mainly based on size exclusion, while the exclusion limit depends on the solvent(s) used for swelling. However, due to the amphiphilic character of the material also adsorption effects play a role during the separation.²⁰²

Initially, a pilot column of 2.5 cm x 78 cm filled with Sephadex™ LH-20 as stationary phase and MeOH as mobile phase has been used to determine the purification parameters for the bioactive compound (see **2.6.2**). Using this column, 0.2 g of the crude extract have been fractionated, and fractions have subsequently been subjected to a bioassay, since this was the only established method of detection for the bioactive compound. As a result, two bioactive fractions could be detected. One, eluting after 11.5 h showing hazy, not stained halos, and the second one, eluting after 31 h, exhibiting clear halos. Additionally, all bioactive fractions have been analysed via HPLC. A comparison of the UV- spectrum of the antibiotic compound with the in-house database revealed accordance with the known isoflavone genistein. It has been shown that this compound can act as a topoisomerase II inhibitor and also exhibited antibacterial activity against *S. aureus*.^{203,204} Due to its low molecular weight of 270.2 g/mol, it was able to interact with the pores of the stationary phase, resulting in a t_R of 31 h. Genistein is a natural product that can be found in plants including lupin and coffee plants as well as in soy beans.^{205,206} Even though Actinobacteria are able to produce isoflavonoids, it is most likely that genistein originates from the cultivation medium, since *Streptomyces* sp. Tü2700 has been cultivated in NL19 media, which contains 2 % soy flour (see **Table 3**).²⁰⁷ For the samples containing the putative QS inhibitory compound, none of the UV-spectra of the respective peaks matched to the spectra in the in-house database. However, fraction 24 putatively contained only one compound, since it showed a single significant peak at a t_R of 9.2 min (see **2.6.4; Table 7**),

exhibiting UV maxima at 230 nm and 280 nm with shoulders at 265 and 285 nm. This sample was subsequently submitted to HPLC-ESIMS analyses (see **2.6.4; Table 8**) in order to determine the molecular mass of the compound. This analyses revealed a m/z $[M+H]^+$ of 656. MS analyses also revealed impurities in the sample. Therefore, it was necessary to perform further purification steps using different chromatographic methods, e.g. pHPLC. Moreover, these initial separations using the pilot column have confirmed the benefit of using SEC with Sephadex™ LH-20 as stationary phase as an initial chromatographic step for the separation of the crude extract of *Streptomyces* sp. Tü2700.

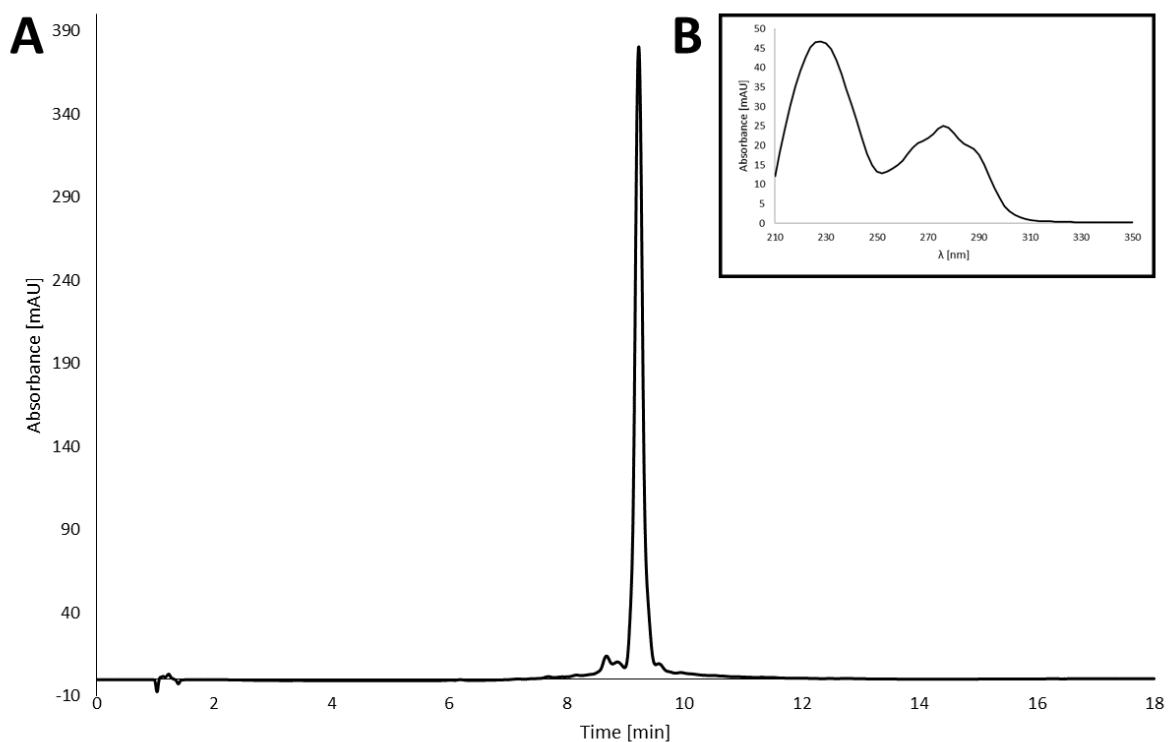


Figure 6. (A): HPLC-DAD chromatogram of extract A after purification using Sephadex™ LH-20 chromatography at 280 nm, exhibiting a significant peak at $t_R = 9.2$ min; **(B) UV-Spectrum** at $t_R = 9.2$ min, exhibiting maxima at 230 nm and 280 nm with shoulders at 265 and 285 nm

In order to increase the operational capacity, a wider column (5 cm x 95 cm) was used to fractionate the remaining 3.6 g of crude extract (see **2.6.2**). As in-process control, all bioactive fractions have been analysed via analytical HPLC (see **2.6.4; Table 6**). Fractions containing only a single peak were combined separately. All remaining bioactive fractions have also been combined. Finally, the two extracts were dried under reduced pressure, resulting in 20 mg of an

extract, exhibiting a single peak (A) and 200 mg of an extract whose chromatogram shows multiple peaks (B).

The three most pronounced peaks in extract B (**1** ($t_R = 7.5$ min), **2** ($t_R = 8.5$ min) and **3** ($t_R = 9.2$ min)) as well as the single peak in extract A (t_R of 9.2 min) exhibit the same UV-spectra with maxima at 230 nm and 280 nm (see **Figure 6**). HPLC-ESIMS analysis revealed m/z values of $[M+H]^+$ 674 for **1** and $[M+H]^+$ 656 for **3**. The data for compound **2** are ambiguous. Due to their comparable behaviour during the separation, and the fact that all three compounds feature a similar UV- spectrum, it is tempting to speculate that these compounds share the same chemical scaffold. The mass difference of 18 could be due to the loss or addition of one water molecule (e.g. as the result of a hydrolysis reaction of an intramolecular ester or ether bond).

3.3.4.2 pHPLC

In order to isolate the bioactive compound from extract A, preparative HPLC was applied, since the compounds could be separated already during analytical HPLC with a good resolution. Therefore, based on the initial analytical method (**Table 6**) a suitable preparative method has been developed.

It was necessary to scale up the analytical method from the Phenomenex Luna C18 250 x 4.6 mm column to the respective semi-preparative column with 10 mm inner diameter (see **Table 16**). Therefore, the flow was increased from 2 ml/min to 9.45 ml/min. After optimization of the gradient in terms of time efficiency and peak resolution, the best method for the isolation of the single compound proved to be an isocratic mixture of 60 % water and 40 % ACN without any modifiers for 10 min. The t_R of the bioactive compound was 7.2 min. This method yielded in 8 mg of a pure compound from extract A.

The whole isolation scheme of this bioactivity guided isolation, starting from the culture filtrate and ending with the pure compound, is depicted in **Figure 7**.

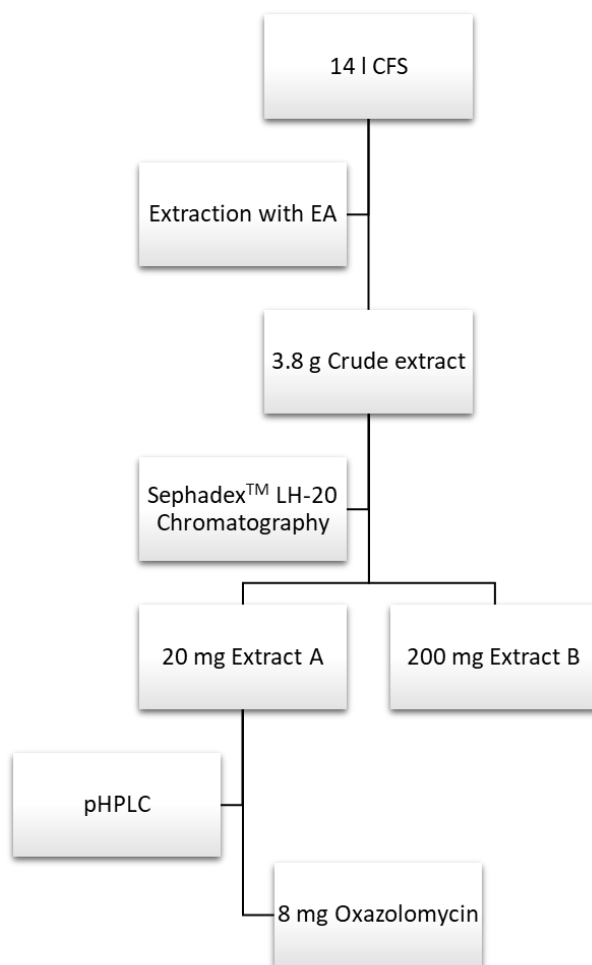


Figure 7. Isolation scheme for oxazolomycin.

3.3.5 Identification of oxazolomycin A

Dereplication is a crucial step for the identification of NPs.¹⁹⁷ The aim of dereplication is to identify already known compounds as quickly as possible in order to avoid time consuming isolation and structure elucidation processes. Thus, dereplication should be performed as early in the process and with as many data in hand as possible. During this study, the bioactive compound could not be dereplicated before isolation, using the in-house HPLC-MS and UV databases.

After isolation of the bioactive compound (**3**) (see section 3.3.4.2) from extract A, it was analysed using HR-MS (2.6.5). This method confirmed on one hand the purity of the isolate, and on the other hand it indicated an accurate mass of m/z $[M+H]^+$ of 656,35435. These data were used to calculate molecular formulae, using the Universal mass calculator tool. This calculation led to 4 different formulae with mass accuracies less than 1 ppm, $C_{35}H_{50}N_3O_9^+$, $C_{34}H_{44}N_{10}O_4^+$,

$C_{20}H_{46}N_{15}O_{10}^+$, $C_{21}H_{52}N_8O_{15}^+$. A repetition of the search in the dictionary of NPs using the neutral molecular formulae, showed no entries except for the formula $C_{35}H_{49}N_3O_9$, revealing oxazolomycin A as compound having this molecular formula.

In order to confirm that the compound isolated from extract A is truly oxazolomycin A or a member of this family, UV spectra of oxazolomycin A and the isolated compound were compared. The UV spectrum of oxazolomycin A shows maxima at 265 (e, 28000), 275 (e, 34000), and 285 nm (e, 27000) due to the triene system, and one maximum at 230 nm due to the conjugated diene chromophore.²⁰⁸ As described above (see section 3.3.4.1) the spectrum of the isolated compound exhibits UV maxima at 230 nm and 280 nm with shoulders at 265 and 285 nm. Therefore, additionally to potentially sharing the same molecular formula, both compounds feature the same UV absorption pattern.

To finally prove that both compounds are identical, **3** was dissolved in $MeOH-d_4$ and a proton NMR spectrum was recorded (see section 0) (see **Figure 8**). Comparison of the 1H NMR spectrum with literature data revealed that all observed signals were consistent with those previously described.²⁰⁹ Therefore, **3** was confirmed to be indeed oxazolomycin A. Compound **1** showing a m/z $[M+H]^+$ difference of 18, while exhibiting the same UV- spectrum of **3** is most likely a derivative of oxazolomycin A, which potentially contains an additional hydroxyl group.

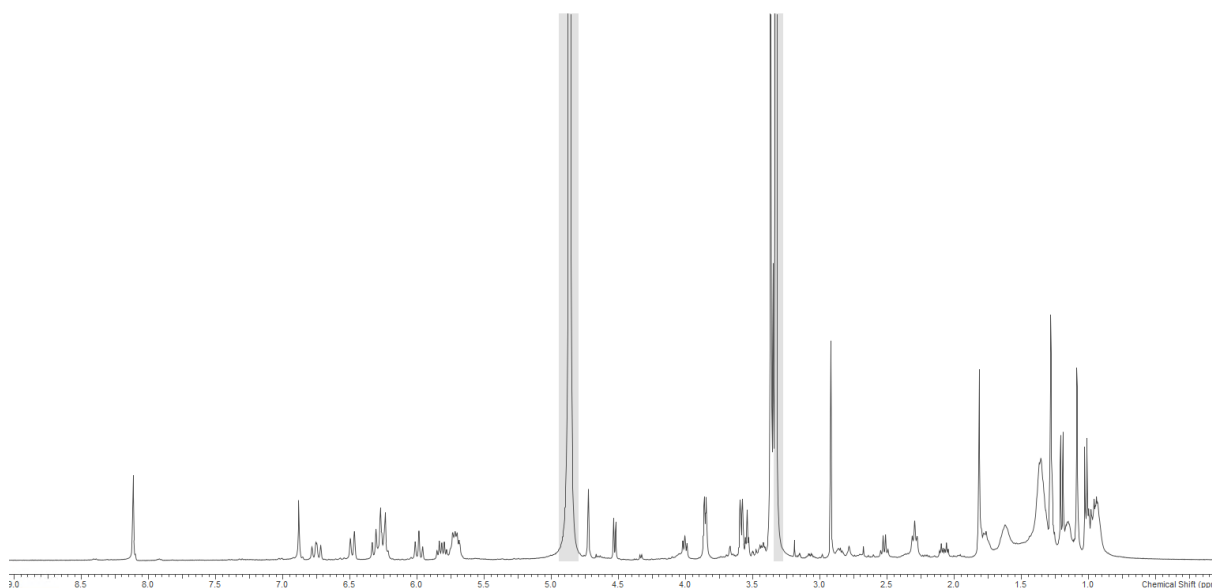
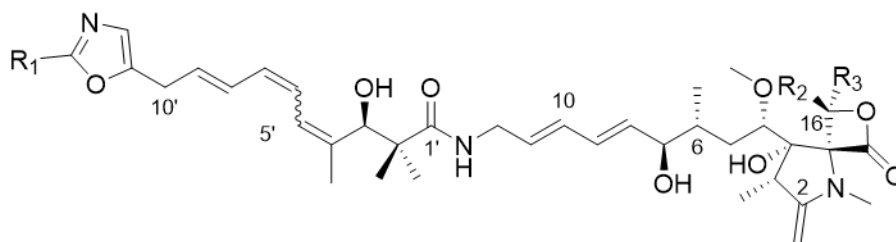


Figure 8 1H NMR spectrum of oxazolomycin A (400 MHz; methanol- d_4), grey- shaded areas are residual solvent signals of methanol- d_4



Oxazolomycin A: R1 = H, R2 = H, R3 = H; 4'Z,6'Z,8'E

Oxazolomycin B: R1 = H, R2 = H, R3 = H; 4'E,6'E,8'E

Oxazolomycin C: R1 = H, R2 = H, R3 = H; 4'Z,6'E,8'E

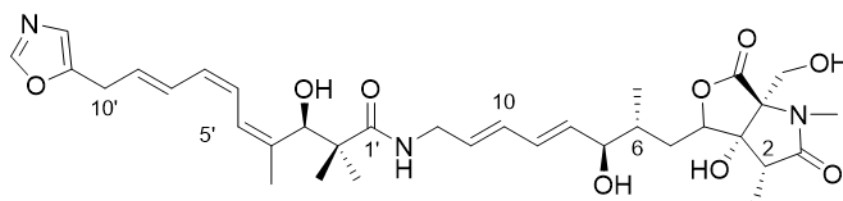
16-Methyloxazolomycin: R1 = H, R2 = H, R3 = CH₃; 4'Z,6'Z,8'E (2R, 3S, 15S and 16R)

Curromycin A: R1 = CH₃, R2 = CH₃OCH₂, R3 = H; 4'Z,6'Z,8'E

Curromycin B: R1 = CH₃, R2 = H, R3 = CH₃; 4'Z,6'Z,8'E

KSM-2690 B: R1 = H, R2 = H, R3 = CH₃; 4'Z,6'Z,8'E (2R, 3R, 15S and 16S)

KSM-2690 C: R1 = H, R2 = H, R3 = CH₃; 4'Z,6'E,8'E



Neooxazolomycin; 4'Z,6'Z,8'E

Figure 9 Structures of oxazolomycins. Adapted from Moloney et al. (2004)

Oxazolomycin A was first described in 1985. It was found during a screening campaign for new NPs from *Streptomyces* sp. with inhibitory activity against Ehrlich ascites tumour.²¹⁰ However, Mori *et al.* noted, that the compound that they described as oxazolomycin might be identical to a compound described in 1971 as resistaphylin.^{210,211} Since the structure of resistaphylin has not been determined at this time, Mori *et al.* findings are considered being the first report of oxazolomycin.²¹¹ It has become the parent and eponymous member of a growing group of NPs (see **Figure 9**) that have all been isolated from several *Streptomyces* species. Characteristic for this group of NPs is the unusual spiro fused β -lactone/ γ -lactam linked via a triene and (*E,E'*)-diene spacer to an oxazole terminal residue. Variations occur either in the geometry of the triene double bond (oxazolomycins A-C) or the substituents of the β -lactone ring (curromycin A, B and 16-methyloxazolomycin).²⁰⁸

The oxazolomycins exhibit wide ranging antibiotic activity against Gram positive bacteria like *Bacillus subtilis* (e.g. 16- methyloxazolomycin, MIC = 5 $\mu\text{g/ml}$), and also antiviral activity against vaccinia, herpes simplex type I, and influenza A.^{208,212,213} Additionally, the oxazolomycins have shown activity as in-vivo antitumor agents (LD_{50} = 10.6 mg/kg for intraperitoneal injection in mice).²⁰⁸ Moreover, these compounds have been described as novel plant transformation inhibitors upon infection with *Agrobacterium tumefaciens*.^{214,215} Only limited biological studies on the MoA of the oxazolomycin A have been performed.^{216,217} In an artificial lipid membrane model, it has been shown that oxazolomycin A is a protonophore at pH 4.7 - 7.0, and thus increases membrane conductivity. Above pH 7.5 it is able to convey protons as well as monovalent cations like potassium.²¹⁷ It can be assumed that the bioactivities of oxazolomycin A are correlated with these ionophoric properties.²⁰⁸ In case of the antiviral activity, these drugs inhibit the membrane fusion mediated by haemagglutinin by raising the pH of the normally acidic endosomes, like amantadine, which is an approved drug for the treatment of influenza. The membrane fusion with the host cells is a crucial step within the viral life-cycle, since it leads to the dispersal of the viral RNA into the host cell cytoplasm.²⁰⁸ In regard to their cytotoxic and antibacterial behaviour, it is most likely that the activity is related to the membranophilic behaviour of the oxazolomycins. However, this needs to be further investigated.²⁰⁸

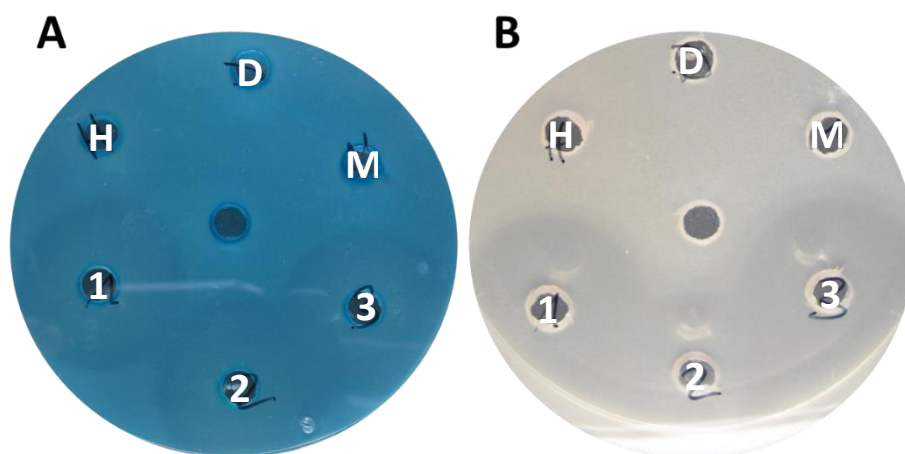


Figure 10. Results of the bioactivity assays of oxazolomycin A against *S. aureus* PC322; 1-3: oxazolomycin A [c = 50 $\mu\text{g/ml}$]; H: hamamelitannin [c = 2 mg/ml]; D: DMSO; M: MeOH A: Assay was performed as usual (see 2.3.2), using X-Gal, resulting in hazy, less stained halos with a diameter of 22.0 mm. B: A: Assay was performed as usual (see 2.3.2), but without using X-Gal, resulting in hazy, halos with a diameter of 22.0 mm, indicating antibacterial behaviour of oxazolomycin A.

So far oxazolomycin A is solely known for its antiviral, cytotoxic and antibacterial behaviour, as well as its potential to inhibit plant transformation. In order to analyse its antivirulence activity, the *S. aureus lacZ* reporter assay monitoring transcriptional activity of the *hla* promoter has been performed with a 50 µg/ml solution of the isolated oxazolomycin A as described in **2.3.2**. As a result, hazy, less stained halos with a diameter of 22.0 mm occurred (see **Figure 10**). In parallel, the same assay was performed with a 50 µg/ml solution of the isolated oxazolomycin A, but without X-Gal. Exclusive reduction of the *hla* expression in *S. aureus* would cause no inhibition zones, since bacterial growth should not be affected. However, the wells containing the oxazolomycin A solution were surrounded by hazy halos with a diameter of 22.0 mm (see **Figure 10**). This experiment confirms that oxazolomycin A is not a QS inhibitor, but instead exhibits partial antibacterial activity against *S. aureus* PC322. This behaviour has never been described for oxazolomycin A, but is in accordance with reports about the bioactivity of its methylated derivative KSM-2690 B (see **Figure 9**). According to the authors, this compound also showed hazy inhibition zones of 25.0 mm diameter at concentrations of 50 µg/ml against *S. aureus* Smith.²¹⁸

As already mentioned (see section 1.3.2), the assay utilized in this study has led to the identification of several compounds, interfering with the *agr* system, e.g. norlichexanthon, solonamide A & B, ngercheumicin F, G, H & I and savirin.^{148–150,219,220} Yet, so far no compounds except for glucose have been reported that decrease the expression of *hla* independently of *agr*.^{221,222} Oxazolomycin A and presumably also KSM-2690 B appear in the assay as QS inhibitors by exhibiting hazy less stained halos. Through only partly inhibited bacterial growth, halos still appear hazy, and due to the reduced cell number also less stained. Hence, it can be assumed that all compounds, which not entirely kill *S. aureus* cells will interfere with this assay and can be considered as false positive hits. Therefore, in order to eliminate those compounds early in the screening process, it would be advisable to analyse every positive hit in a second assay. This second assay should be performed exactly as the usual *S. aureus* PC322 assay (see **2.3.2**), but without supplementing X-Gal in the agar. Compounds interfering with bacterial growth will still result in halos. Compounds that are exclusively interfering with the expression of *hla* will cause no inhibition zones.

3.3.6 Genome analysis

To analyse the capability of *Streptomyces* sp. Tü2700 to produce oxazolomycin, its genomic DNA was isolated (see 2.9) and subsequently fully sequenced. It was obtained as one single contig, comprising 8,019,152 bp with a GC content of 72.0 %. For the identification of biosynthetic gene clusters, the sequence was submitted to the antibiotics and Secondary Metabolite Analysis Shell (antiSMASH).²²³ In total, 28 clusters have been identified. Of these, 6 clusters showed ≥ 90 % similarity to already characterized clusters. Among these are biosynthetic gene clusters (BGC) for compounds widespread amongst bacteria like the osmolyte ectoin, the carotenoid isorenieratene, the sesquiterpene albaflavenon, the membrane constituent hopene and the peptide siderophore coelichelin, but also a BGC having 90 % similarity to the known cluster of oxazolomycin. For a more profound insight into the resemblance of the respective genes, the genome analysis was complemented with manual BLAST analyses (see **Table 22**).¹⁹⁰ It revealed the presence of homologues to all genes that have previously been annotated as *ozm* genes in the oxazolomycin (*ozm*) BGC, being also arranged in the same way as in the *ozm* gene cluster.^{224,224}

Table 22. Results of the BLAST analysis – comparison of the *ozm* gene cluster of *S. albus* JA3453 and the putative oxazolomycin gene cluster of *S. sp.* Tü2700 ²²⁴

Gene	AA Identity [%]	AA Similarity [%]	AA Gaps [%]	Annotation/ Proposed function
512084 to 513457	94	97	0	<i>ozmA</i> (Antibiotic efflux protein)
510941 to 512041	91	93	0	<i>ozmB</i> (Glyceryltransferase/ phosphatase)
509988 to 510941	96	97	0	<i>ozmC</i> (Acyltransferase)
508849 to 509943	92	94	0	<i>ozmD</i> (Acyl-dehydrogenase)
508578 to 508853	96	95	1	<i>ozmE</i> (ACP)
507898 to 508560	92	96	0	<i>ozmF</i> (O-Methyltransferase)
507035 to 507895	90	93	0	<i>ozmG</i> (3-Hydroxyacyl-CoA- dehydrogenase)
487455 to 505880	83	86	2	<i>ozmH</i> (Hybrid NRPS/PKS)
473236 to 479409	85	87	2	<i>ozmJ</i> (PKS)
469644 to 473216	86	88	1	<i>ozmK</i> (PKS)
463567 to 469563	90	93	0	<i>ozmL</i> (NRPS)
460391 to 463507	87	90	1	<i>ozmM</i> (Acyltransferase/ oxidoreductase)
451545 to 460241	82	85	2	<i>ozmN</i> (PKS)
441772 to 443862	85	89	0	<i>ozmO</i> (NRPS)
440473 to 441618	97	98	0	<i>ozmP</i> (Unknown)
438034 to 440460	86	90	0	<i>ozmQ</i> (PKS)
435537 to 436403	90	95	0	<i>ozmR</i> (Transcriptional regulator)
434858 to 435490	95	95	0	<i>ozmS</i> (Transporter)
433544 to 434836	87	93	0	<i>ozmT</i> (Thr-tRNA synthetase)
429651 to 432455	91	92	0	<i>ozmU</i> (Transcriptional activator)

3.3.8 Stability testing

Stability of the bioactive compounds and the drug product is a crucial parameter in drug development, since it has an influence on the storage conditions and the shelf life.

In order to examine the stability of **3**, stress tests evaluating parameters which are known to enhance degradation reactions using the pure compound dissolved in MeOH at a concentration of 1 mg/ml have been performed (see **2.7**). Those parameters are light, since it is known to trigger radical reactions like substitution, addition, or polymerisation; oxygen, due to its potential to act as initiator of radical reactions; and temperature, since it is a crucial parameter and general accelerator of degradation reactions.

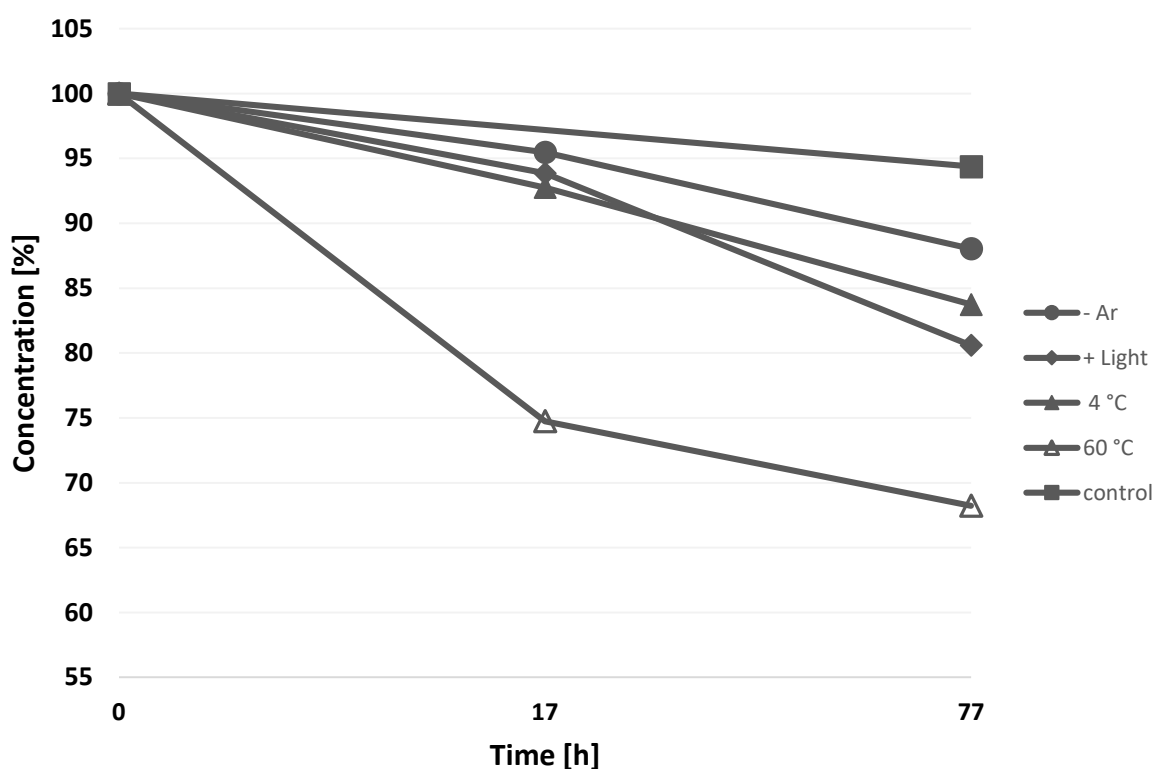


Figure 11. Results of the stability testings of oxazolomycin A. This graphic depicts the concentration [%] of oxazolomycin A [1mg/ml in MeOH] under different storage conditions. The control samples were stored at atmospheric conditions, at ambient temperature, and not protected from light. Unless otherwise stated, all other samples were stored under exclusion of light in an argon atmosphere at ambient temperature (23 °C). One of these parameters was changed at a time, “- Ar” indicating, an air atmosphere, “+ Light” indicating samples with light exposure, 4 °C/60 °C indicating variations in the storage temperature. Samples were analysed after 17 h, and 77 h of storage.

At the beginning of the study, all samples have been evaluated via HPLC-UV. All samples were prepared as triplicates. The samples were stored under the respective conditions and analysed again after 17 h (~ 1 d) and 77 h (~ 3 d). Finally, the maximum peak heights at 280 nm were compared. The Degradation [%] was calculated according to formula (1).

The results were ambiguous since e.g. the control samples that were neither protected from light, nor oxygen and stored at ambient temperature were less prone for degradation after 77 h than the samples that were protected from light and oxygen and stored at 4 °C. However, a trend is noticeable, since, after 77 h, all samples showed a degradation of 10 - 20 % (see **Figure 11**). Light exposure and an increased temperature might lead to an increased degradation process. The concentration of the samples stored at 60 °C decreased after 17 h already to 74.7 %, reaching 68.2 % after 77 h (see **Figure 11**).

In the chromatograms, except for those of the samples that were stored at 60 °C, no degradation products became visible (no appearance of additional peaks). An additional peak only appeared in the samples stored at 60 °C. HPLC-MS analysis (see **2.6.4; Table 8**) of these samples revealed that this additional peak has a m/z $[M+H]^+$ of 688, which is an increase in weight by 32. Since **3** was dissolved in MeOH, a transesterification of the β -lactone substructure of oxazolomycin A with MeOH via nucleophilic substitution could be the reason for the degradation, leading to the opening of the β -lactone ring and the addition of a MeOH molecule (see **Figure 11**).

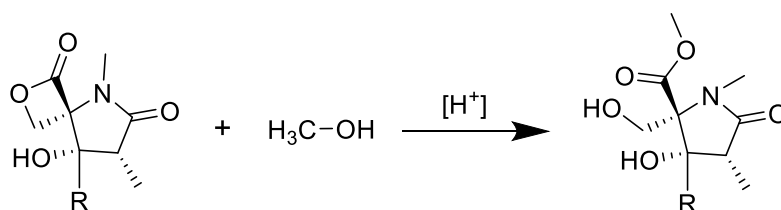


Figure 12. Putative ring opening and transesterification of the β -lactone substructure of oxazolomycin A via nucleophilic substitution with MeOH during the stability tests at 60 °C

The ring opening of the β -lactone is likely to occur via nucleophilic substitution, in which the nucleophile MeOH attacks the sp^2 carbonyl to form a tetrahedral intermediate which subsequently leads to the ring opening.²²⁵ These reactions are usually either acid or base catalysed. In view of the known pK_a values for oxazole (0.8) and isoxazole (3.0), these two substructures

exhibit weak basic properties. Thus, mild basic conditions within the pure oxazolomycin A samples can be expected.²²⁶ Since transesterifications are known to be temperature and pressure dependent, an increased storage temperature of 60 °C could indeed accelerate the degradation of oxazolomycin A.²²⁷ However, in order to finally prove this hypothesis, further analysis of the by-product is necessary to confirm its structure.

Even though instabilities of oxazolomycin derivatives have been reported, this is the first time stability tests have been performed with oxazolomycin A.²¹⁸ Due to their earlier mentioned ambiguous outcome in regard of the control samples, it would be beneficial to repeat these experiments with a larger batch size and with more sampling time points. Additionally, since humidity is another crucial parameter for stability, its influence on the stability of oxazolomycin A would also be worth to examine. Unfortunately, these experiments could not be performed in the scope of this thesis, since the compound was completely degraded after a few weeks even though it was stored under light protection in an argon atmosphere at 8 °C.

3.4 *Streptomyces* sp. Tü2401

3.4.1 Taxonomy

Comparison of the 16S-rRNA sequence of strain Tü2401 with the NCBI database using the Basic local-alignment search tool (BLAST) revealed a number of sequences with > 99 % sequence identity, all belonging to the genus *Streptomyces*.¹⁹⁰ Therefore, it can be assumed that strain Tü2401 is also a member of the genus *Streptomyces*. However, this method is insufficient to assign *Streptomyces* sp. Tü2401 to a specific species.

Therefore the genomic DNA was isolated (2.9) and subsequently, the whole genome was sequenced using single-molecule real-time (SMRT) sequencing, also known as PacBio sequencing, honouring its developer Pacific BioSciences (PacBio). Finally, for the de-novo assembly of the sequence, the software FALCON was used to identify and connect overlapping contig ends. In order to automatically generate a species phylogeny with reference organisms, the sequence was submitted to the autoMLST program.^{191–193} As a result, the strain *Streptomyces globisporus* C-1027 was identified as the closest relative with an estimated average nucleotide identity (ANI) of 92.0 % (Mash distance: 0.0803). These results confirm the strain *Streptomyces* sp. Tü2401 as a member of the genus *Streptomyces*, being a close relative to *Streptomyces globisporus* C-1027 (**Figure 13**)

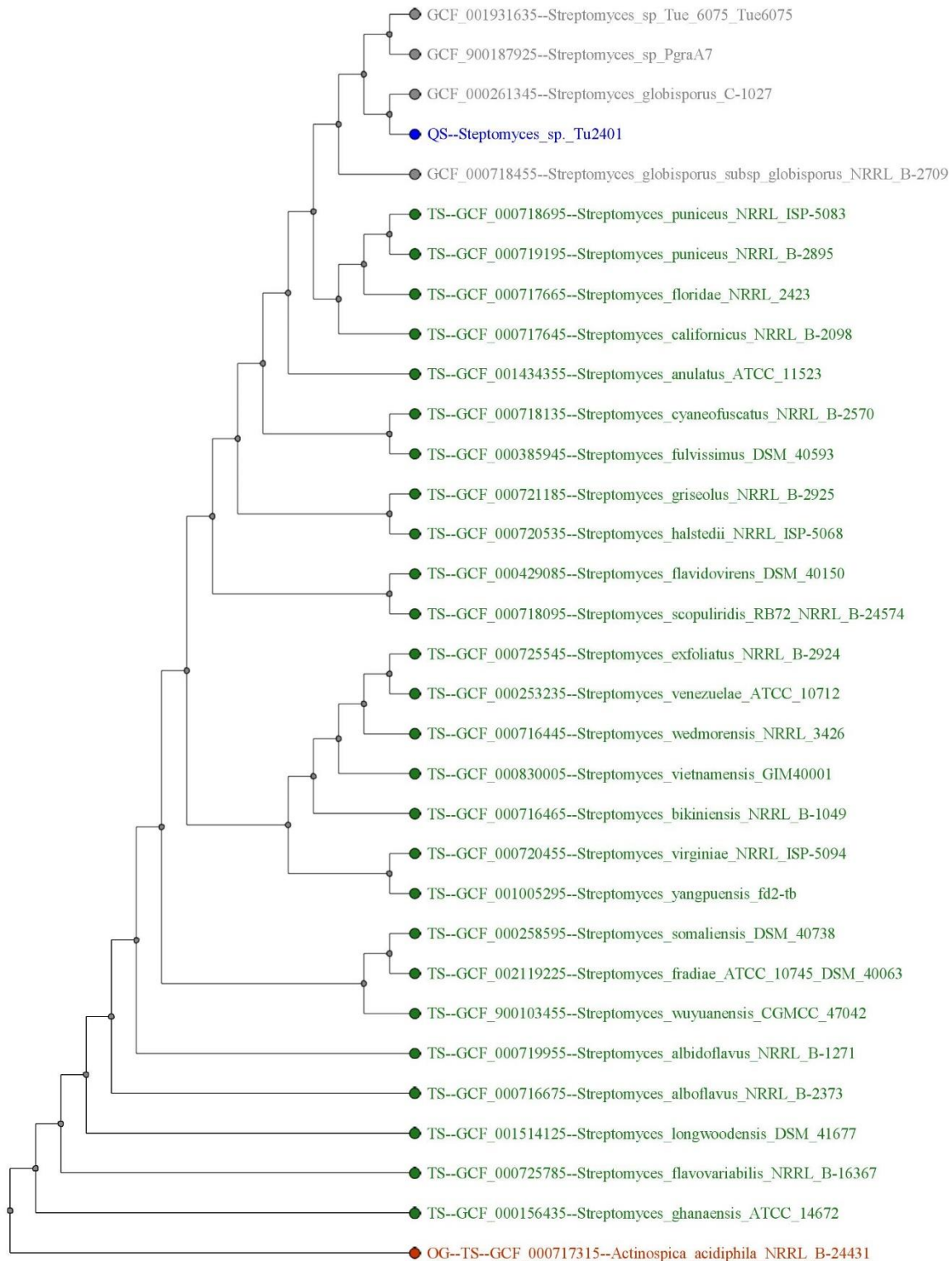


Figure 13. Phylogenetic tree of *S. sp. Tü2401* (blue font) inferred from gDNA sequence using the software autoMLST. The phylogeny is rooted with *Actinospica acidiphila* NRRL B24431 (red font), strains depicted in green font represent type strains.

3.4.2 Primary screening

The primary screening aimed at the analysis of the biosynthetic potential of *Streptomyces* sp. Tü2401 in silico (see 3.4.3.1), as well as in vivo (see 3.4.4.1 & 3.4.5.3). Another crucial part of the primary screening is dereplication of the bioactive compound(s), in order to identify already known compounds prior to time-consuming isolation efforts.

3.4.2.1 Biological activity

In the initial agar-plug based screening (see section 3.1) against the Gram-positive *S. aureus* PC322 (see 2.3.2), *Streptomyces* sp. Tü2401 was highly bioactive with clear inhibition zones (> 2 cm), indicating no QS inhibition, but antibiosis. Subsequent bioactivity assays of *Streptomyces* sp. Tü2401 grown on ISP2 agar as well as in submerge cultures against the also Gram-positive *B. subtilis* 168 and the Gram-negative *E. coli* K12 (see 2.3.1) revealed additional antibiotic effects (> 2 cm) against those microorganisms.

The antibiotic class of aminoglycosides is known to be produced by Actinobacteria and active against Gram-positive and Gram-negative bacteria likewise.²²⁸ These compounds are particularly hard to identify in classical screenings, since they are highly hydrophilic and most often do not contain a chromophore.²²⁸ Therefore, in order to rule out that the bioactive compound(s) belong to the aminoglycosides, *S. sp.* Tü2401 culture broth has been tested against a series of *E. coli* strains. Those strains harbour one or more resistance genes that decrease their susceptibility towards various antibiotics, including aminoglycosides like streptomycin, spectinomycin, neomycin and gentamicin (see **Table 23**). Constant activity against all tested strains indicated that the resistance genes present in the tested *E. coli* strains did not confer resistance against the compound(s) produced by *S. sp.* Tü2401. Most of these resistances (see **Table 23**) enhance export or degradation of the particular antibiotic. However, some of them, namely *rpsL150*, *gyrA91* and *rpoB318* modify cellular targets.^{161,229} Decreased streptomycin binding is conveyed by *rpsL150*, through an altered 30S ribosomal subunit. Binding of nalidixic acid to the DNA gyrase is decreased by mutation of *gyrA91*. Additionally, rifampicin binding to the DNA dependent RNA-polymerase is decreased by mutations of *rpoB318*.¹⁶¹ Since the viability of none of those strains is improved, *S. sp.* Tü2401 presumably produces a compound with an alternative MoA.

Table 23. List of strains tested against *S. sp.* Tü2401, indicating their mutations and resistances

Name	Mutation	Resistance
<i>E. coli</i> K12	/	/
<i>E. coli</i> H5434	<i>yebA::cam yibP::spc</i>	streptomycin, chloramphenicol, spectinomycin
<i>E. coli</i> H5309	<i>araD139 D(argF lac)U169 rspL150 relA1 flbB5301 deoC1 ptsF25 rbsR aroB fiu::MudX feoB::Tn5 corA::Tn10</i>	streptomycin, am- picillin, neomycin, tetracyclin
<i>E. coli</i> H5313	<i>araD139 D(argF lac)U169 rspL150 relA1 flbB5301 deoC1 ptsF25 rbsR aroB entC::MudX ftnspc</i>	streptomycin, spectinomycin, ampicillin
<i>E. coli</i> JF486	<i>ara-55 delta(lac)3 thi-1 asnB::50 nagB2 gyrA91 relA1 spoT1 asnA31 rpoB318</i>	nalidixic acid, ri- fampicin
<i>E. coli</i> BL21	<i>B F⁻ ompT gal dcm lon hsdS_B(r_B⁻m_B⁻) [malB⁺]_{K-12}(λ^S)</i>	gentamicin
<i>E. coli</i> BL21pWBT	<i>B F⁻ ompT gal dcm lon hsdS_B(r_B⁻m_B⁻) [malB⁺]_{K-12}(λ^S)</i>	gentamicin
<i>S. aureus</i> PC322	<i>hla::lacZ</i>	/
<i>B. subtilis</i> 1S34	<i>pHJS105-yorB-lacZ2</i>	/

In order to get deeper insights into the MoAs of the compound(s) produced by *S. sp.* Tü2401, bioactivity assays using *B. subtilis* 1S34 pHJS105-yorB-lacZ2 (see **2.3.3**) revealed that cultures grown on solid medium, but not submerge cultures are able to induce the *yorB* reporter system. However, antibacterial activity in the reporter system was shown to be present regardless of the growth conditions of *S. sp.* Tü2401. In previous studies, *yorB* was found to be up-regulated during flourquinolone treatment.^{161,230} Additional studies strengthened the hypothesis that the upregulation of *yorB* is a stress response triggered by inhibition of the topoisomerase II α subunit, causing DNA damage.^{161,230–232} Nonetheless, the identification of other inducers of the *yorB* reporter system with diverse MoA indicate (see **Table 24**) that this reporter system is appropriate for the identification of compounds interfering with bacterial DNA or DNA replication in general. Therefore, it is most likely that *S. sp.* Tü2401 is, when grown on agar, producing a compound with either of these or even both as its target(s).

Cultures from *S. sp.* Tü2401 both grown on agar as well as submerge culture have been analysed in the *yorB* reporter assay, but only the cultures grown on agar were able to induce the *yorB* reporter system, while the others only showed antibiosis. Therefore, it is likely that *S. sp.* Tü2401 is producing at least two different compounds with different MoA, but similar activity spectra. The significance of the growth conditions of Actinobacteria on their secondary metabolite production is well known and has been aforementioned (see 1.2).³⁰

Table 24. Inducers of the *yorB* reporter system. Substances with determined MoA that induce the *yorB* reporter system in *B. subtilis*.^{161,230,232} (Adapted from Schneider *et al.* 2018)

MoA	Compound	Origin
RNA polymerase inhibition	8-Hydroxyquinoline	Synthetic
	Juglone	<i>Carya illinonensis</i>
DNA gyrase inhibition	Novobiocin	<i>S. niveus</i>
DNA strand breaking	Alternariol monomethyl ether	<i>Alternaria sp.</i>
	Bleomycin	<i>S. verticillus</i>
	Myxin	<i>Sorangium sp.</i>
	Phleomycin	<i>S. verticillus</i>
DNA intercalation	Streptonigrin	<i>S. flocculus</i>
	Chromomycin	<i>S. griseus</i>
	Daunorubicin	<i>S. peucetius</i>
	Doxorubicin	<i>S. peucetius</i>
DNA binding	Anthramycin	<i>S. refuineus</i>
	Desmethylethersibiromycin	<i>Streptomyces spp.</i>
DNA crosslinking	Porfiromycin	<i>S. arduus</i>

S. sp. Tü2401 is a noticeable example of the genus of Actinobacteria and their huge potential of producing diverse bioactive secondary metabolites (see also 1.2).

3.4.2.2 Comparison of production media

In order to determine the best production medium for the hydrophilic metabolites from submerge cultures, *S. sp.* Tü2401 was cultivated in NL200, NL300, NL500 and OM complex media (composition see **Table 3**) for seven days. The CFS was analysed after 4 and 7 days in standard *E. coli* K12 agar diffusion bioassays (see 2.3.1). Most samples revealed halos of more than 1 cm. CFS of NL500 after 7 d and CFS of OM after 4 & 7 d showed the biggest zones of inhibition (> 1.5 cm).¹⁶¹ Due to these findings, OM was considered to be the best production medium,

since it already exhibited the largest inhibition zones already after 4 days. Therefore, all further experiments were performed with CFS of cultures grown in OM for four days.

3.4.3 Genome analysis

To investigate the biosynthetic potential of *Streptomyces* sp. Tü2401, its genome was sequenced and analysed. Therefore, the genomic DNA of *S.* sp. Tü2401 was isolated, sequenced and aligned as described in 3.4.1. The final sequence consists of 8,139,204 base pairs with a GC content of 71.4 % allocated to 5 contigs.

3.4.3.1 Identification of putative biosynthetic gene cluster

In order to identify known biosynthetic gene clusters (BGC), the whole sequence was analysed using the antibiotic and Secondary Metabolite Analysis SHell (antiSMASH 4.0.2).²³³ In total 26 clusters have been identified throughout the genome, including 7 that show a similarity of ≥ 95 % to already characterised BGC (see **Table 25**).

Table 25. Output of antiSMASH analysis of *S.* sp. Tü2401, showing BGC with ≥ 95 % similarity to known biosynthetic gene clusters

Cluster	Type	Most similar known cluster	Similarity [%]
4	Bacteriocin-T1 PKS-NRPS	Frontalamide, Heat-Stable Antifungal Factor	100
10	Lanthipeptide	AmfS	100
14	Terpene	Isorenieratene	100
17	NRPS	Griseobactin	100
21	Ectoine	Ectoin	100
24	Siderophore	Desferrioxamine B	100
26	T1 PKS-NRPS	C-1027	100

As cluster 4 the software detected a Type1-PKS-NRPS hybrid cluster containing genes with high similarity to genes known from the frontalamide BGC (BGC0000996) and the heat-stable antifungal factor (HSAF) BGC (BGC0000999).^{234,235} The frontalamides and the HSAF both share the same structural feature of polycyclic tetramate macrolactams (PTMs) (see **Figure 14**). Frontalamide A & B and also the HSAF are on the one hand known for their antifungal bioactivity, a common MoA among bacterial PTM, and on the other hand for their activity against plant pathogens like *Bipolaris sorokiniana*, *Fusarium graminearum*, *F. verticilloides* and *Ophiostoma*

minus.^{234–238} PTM gene clusters could be identified in more than 50 % of the sequenced *Streptomyces* species and are highly conserved.²³⁴ However, the PTM clusters have been also identified in a broad variety of other bacterial families, for example in the Gram-negative *Xanthomonadaceae*.^{161,234,239}

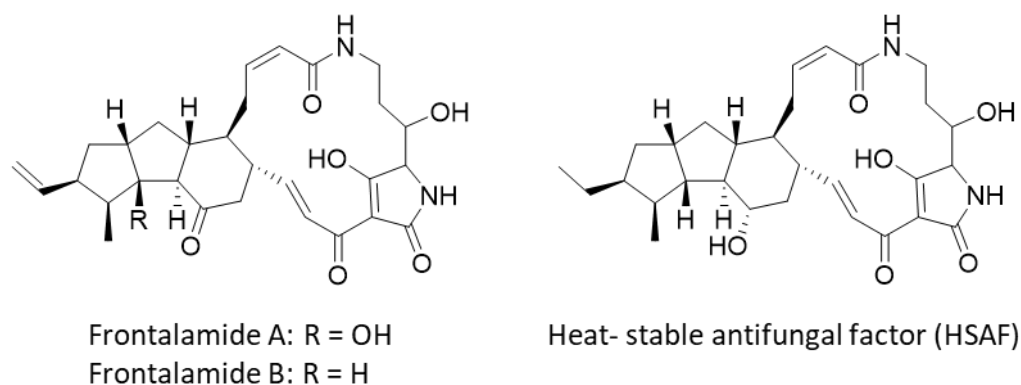


Figure 14. Structures of polycyclic tetramate macrolactams (PTM). Adapted from Mo *et al.* (2014).²³⁸

The existence of a PTM cluster in the genome of *S. sp.* Tü2401 implies its potential to produce antifungals. However, neither has this bioactivity been tested yet, nor could frontalamide A, B or HSAF been identified in the supernatant via HPLC-DAD or HPLC-MS.

Cluster 10 was identified by antiSMASH as lanthipeptide BGC, at which the genes show high similarity to the AnfS BGC (BGC0000496). The peptide AmfS is considered being an extracellular morphogen without any anti-infective bioactivity. The *amf* gene cluster has been identified as a regulator of the initiation of aerial-mycelium formation in *Streptomyces griseus*.^{161,240}

A terpenoid cluster has been predicted by antiSMASH as cluster 14. The genes showed high homology with an isorenieratene BGC, originally identified from *Streptomyces griseus* (MIBiG BGC-ID: BGC0000664).¹⁶¹ Isorenieratene (see **Figure 15**) is an extensively conjugated compound, belonging to the carotenoids. Even though the biological function of isorenieratene in Actinobacteria is still unknown, it has been speculated that it is a response to blue or UV light, due to its large conjugated system.^{161,241,242} However, neither the bacteria themselves, nor the culture broth took on the orange colour, which is typical for carotenoids. Therefore, either this cluster was not expressed under the cultivation conditions, or the cluster was

expressed, but the amount of biosynthesised isorenieratene had no impact on the appearance of *S. sp.* Tü2401.

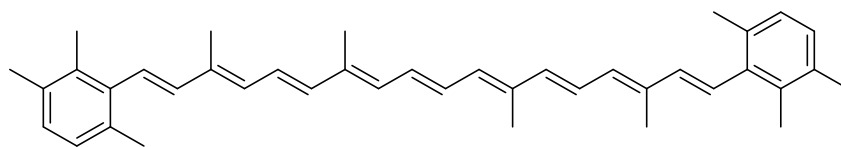


Figure 15. Structure of isorenieratene

Cluster 17 was predicted by antiSMASH to be a NRPS cluster. The genes were almost identical to a griseobactin BGC (BGC0000368) from *Streptomyces sp.* ATCC 700974. Griseobactin is a siderophore produced under iron limitation (see **Figure 16**). Typical siderophores synthesised by *Streptomyces sp.* are desferrioxamines.²⁴³ However, other structurally different siderophores, coproduced with desferrioxamines have been reported, namely coelichelin in *Streptomyces coelicolor*, enterobactin in *Streptomyces tendae*, and the catechol-peptide griseobactin from *Streptomyces sp.* strain ATCC 700974 and some strains of *Streptomyces griseus*.^{161,244,245}

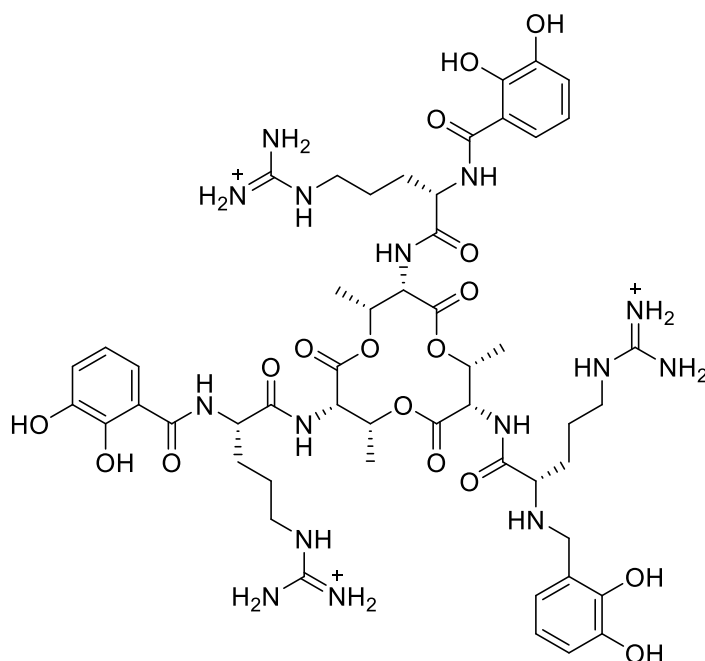


Figure 16. Structure of griseobactin

Since it has been described that aforementioned compounds are mostly coexpressed with desferrioxamines, it is no wonder that antiSMASH predicted another siderophore cluster as cluster 24.²⁴⁵ Its genes are identical to the desferrioxamine B BGC from *Streptomyces griseus* (BGC0000941).^{161,246} As mentioned above, desferrioxamine B (see **Figure 17**), like griseobactin, is required for iron uptake especially under starvation conditions.²⁴⁷

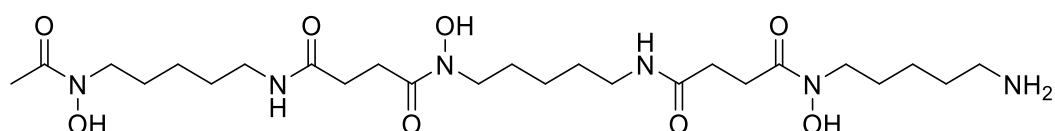


Figure 17. Structure of desferrioxamine B

The BGC of ectoin, another compound that is widespread among several species of bacteria and also within the family of *Streptomyces*, has been predicted to be on cluster 21.²⁴⁸ Ectoin (see **Figure 18**) serves as an osmolyte preventing especially halophilic bacteria from osmotic stress.²⁴⁹

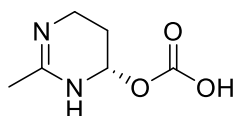


Figure 18. Structure of ectoin

Cluster 26 is the last cluster that shows a similarity of $\geq 95\%$ to an already characterised BGC. It has been predicted by antiSMASH to be a Type1-PKS-NRPS hybrid. The cluster showed sequence homology to the C-1027 BGC from *Streptomyces globisporus* C-1027 (BGC0000965). C-1027 belongs to the class of enediynes (see **Figure 19**) that is characterized by two acetylenic groups conjugated to a double bond within a nine- or ten-membered ring.^{250–252} This structural feature is the warhead of the enediynes, and its gene cassette organisation is highly conserved.²⁵³ Therefore, the identification of an enediyne gene cluster in the genome of *S. sp. Tü2401*, even though highly homologous to the cluster of an already known compound, is no proof that this strain produces indeed C-1027. It only emphasizes the potential of *S. sp. Tü2401* to produce an enediyne. These compounds are known for their cytotoxic as well as for antimicrobial activities.²⁵⁴ By creating a transient 1,4- benzenoid diradical due to cyclisation of the enediyne ring, a highly reactive nucleophile is formed, which abstracts up to two hydrogen atoms from the DNA backbone (see **Figure 20**).^{254,255} These DNA radicals in turn can

cause interstrand crosslinks by reacting with another DNA radical, or create reactive oxygen species (ROS) by reacting with O₂, which subsequently cause double- or single-stranded DNA cleavage.^{255,256} By exhibiting this MoA, enediynes could putatively induce the *yorB* reporter system of *Bacillus subtilis* 1S34 pHJS105-*yorB*-lacZ2. Enediynes are not known for inducing this system, which is most likely because they have never been tested in it, rather than because of inactivity. However, compounds causing double- or single-stranded DNA cleavage or inter-strand crosslinking similar to the enediyne MoA have been shown to induce the *yorB*- induction assay.^{159,161}

The ten-membered enediyne compounds were identified as discrete compounds.^{161,253} On the contrary, the nine-membered enediynes have been found to be attached to a protein, often called apoprotein that presumably works as a stabilizer for the enediyne group, preventing them from self-decomposition as well as a carrier to the double-stranded DNA.^{252,257–259} Therefore, they are also called chromoproteins.^{253,260} The compound C-1027 belongs to the group of nine-membered enediynes.²⁵⁰

It is very likely that *S. sp.* Tü2401 is indeed producing an enediyne compound. Since antiSMASH predicted similarity only to the cluster of C-1027, extraction methods that have been successfully applied for this enediyne should be used for the isolation of the *yorB*-inducing compound produced by *S. sp.* Tü2401.

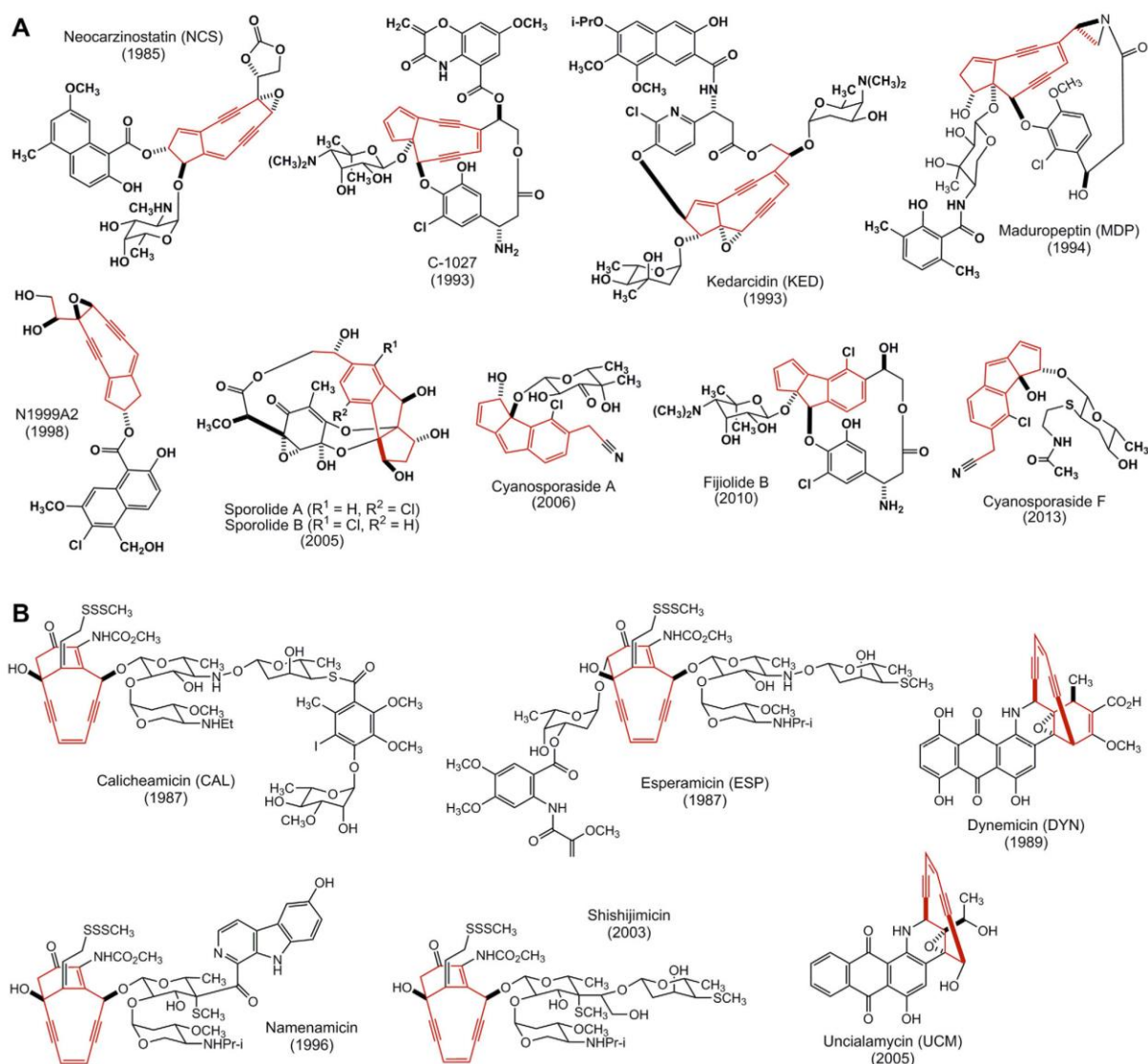


Figure 19. Structures of all enediyne compounds known to date and their respective year of identification (in parentheses). This compound family consists of (A) nine-membered ring compounds and (B) ten-membered ring compounds. The enediyne ring, which serves as their biological warhead, is highlighted in red. Even though sporolides, cyanosporolids and fijiolides do not contain this unique structural feature, they are presumably derived from nine-membered enediyne precursors due to their chlorine substitution pattern after cycloaromatization. Adapted from Shen *et al.* (2015)^{161,250}

3.4.4 Agar extraction

As mentioned above (see **3.4.2**), the *yorB*- inducing compound is only produced when *S. sp.* Tü2401 is grown on solid media (ISP2 agar). Therefore, in order to identify the bioactive compound(s), it was mandatory to develop an extraction method from agar.

As mentioned above, *S. sp.* Tü2401 features a gene cluster with sequence homology to a known enediyne BGC (see **3.4.3.1**), i.a. C-1027. Thus, a protocol that had been successfully applied to the isolation of C-1027 has been used.¹⁶⁰ However, this protocol was originally developed for the extraction of the compound from liquid culture, therefore in our case it was required to liquefy the agar prior to the isolation. According to the safety data sheet of the supplier (Sigma Aldrich), the melting point of the used agar was between 85 °C and 95 °C. Even the melting point of low melting point agarose was at 65.5 °C (Thermo Fisher Scientific). Extraction at these high temperatures could lead to an enhanced degradation of the compounds of interest and has therefore not been tested. A second attempt to liquefy the agar prior to the isolation aimed at pressing the medium out of the gel structure. Hence, standard ISP2 agar plates (approx. 20 ml) were sliced and transferred into a 50 ml tube and subsequently centrifuged at 20,000 g for 30 min, resulting in 10 ml supernatant. The following procedure was adapted from Yan *et al.* (2018).¹⁶⁰ After filtration through a folded filter, the pH was adjusted to pH 4.0 using 0.1 M HCl. After centrifugation, (NH₄)₂SO₄ was added to the supernatant up to the saturation point and incubated for 4 h at 4 °C. This step aimed at the denaturation and subsequent precipitation of the apoprotein as a complex with the chromophore. Afterwards, the precipitate was separated, dissolved in 10 ml 0.1 M K₂HPO₄ at a pH of 8.0 and finally extracted with 10 ml ethyl acetate. During this step, chromophore and apoprotein were finally separated. While the denaturated apoprotein remained as a pellet, the chromophore was dissolved in the organic phase. After drying under reduced pressure, the pellet was dissolved in 2.0 ml MeOH.

3.4.4.1 Dereplication of the bioactive compound produced on solid medium

In order to identify and dereplicate the *yorB*-inducing compound, the dissolved pellet obtained from the agar extraction (see 3.4.4) was submitted to HPLC-MS analysis. Since antiSMASH predicted 95 % cluster identity with the BGC of C-1027, the total ion chromatogram has been analysed for the presence of m/z 844.3 ($[M+H]^+$ of C-1027).²⁵² However, no matching mass could be identified in the chromatogram.

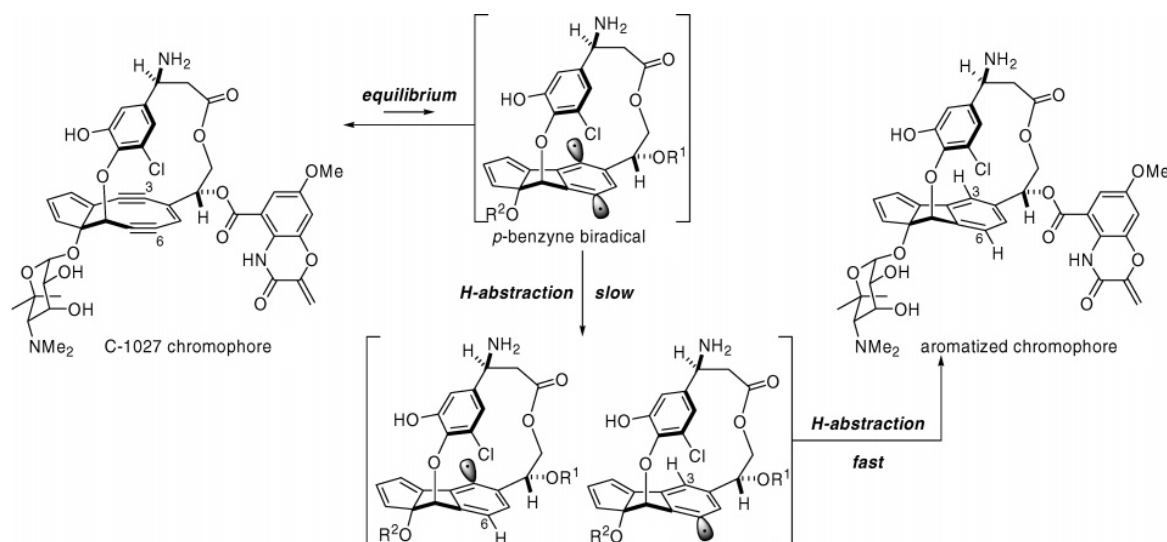


Figure 20. Scheme of the spontaneous aromatization of C-1027 at room temperature via a Masamune–Bergman rearrangement (Adapted from Inoue *et al.* (2006))^{252,261}

During the isolation process, the apoprotein was denaturated and later separated from the chromophore. In several studies it has been reported that the chromophore without the apoprotein is prone for self-decomposition and further degradation (see **Figure 20**), which is also likely to happen during isolation.^{262,263} Therefore, the chromatogram has been analysed in a second attempt in regard to the aromatized chromophore that should have a mass compared to the original chromophore of m/z +2. In fact, the corresponding mass of the aromatized C-1027 chromophore (m/z 846.3 $[M+H]^+$ and also m/z 868.3 $[M+Na]^+$) was detectable in the chromatogram. Additionally, the isotope pattern of the aromatized C-1027 chromophore in the spectrum was in accordance with literature data from Inoue *et al.* (2006) (see **Figure 21**).²⁵² The peak at m/z 847.3 represents most probably the aromatized C-1027 chromophores, where one ¹²C atoms has been substituted by one ¹³C atom. Since the natural incidence for ¹³C atoms is 1 %, the peak intensity for this molecule should be ca. 43 % of the parent ion, which is indeed

represented in the spectrum (see **Figure 21**). The peak at m/z 848.3 is probably the isotope peak were the ^{35}Cl atom is exchanged by a ^{37}Cl atom. The peak intensity should be due to the natural incidence ca. 1/3 of the parent ion peak. However, the peak intensity is increased to ca. 40 % which might be due to other substitution products, like for example a two atom substitution of $^{12}\text{C}/^{13}\text{C}$ atom (incidence 0.1 ‰) or a two atom substitutions of $^1\text{H}/^2\text{H}$ (incidence 0.1 ‰) or a one atom substitution of $^{12}\text{C}/^{13}\text{C}$ and of $^1\text{H}/^2\text{H}$. But also substitutions with other naturally occurring isotopes like e.g. ^{15}N (incidence 0.36 ‰), ^{17}O (incidence 0.37 ‰), ^{18}O (incidence 0.2 ‰) might contribute to the characteristic isotope pattern of C-1027.

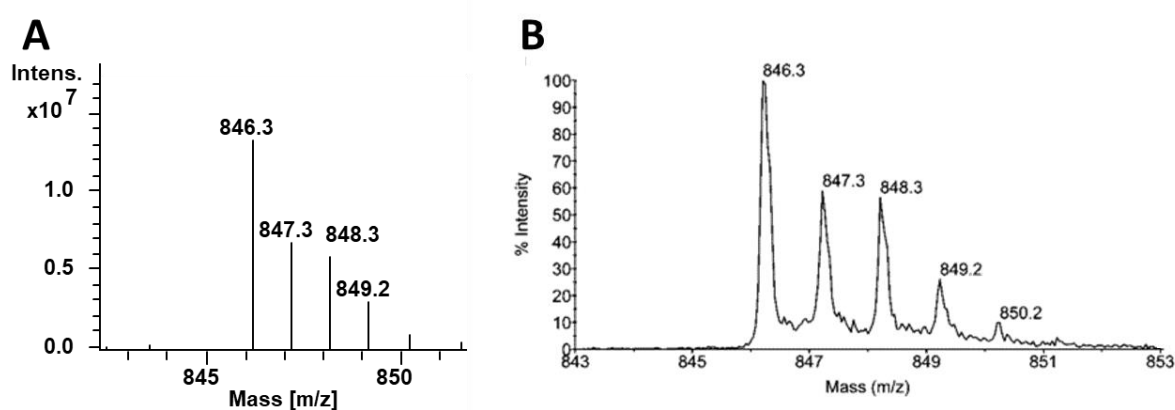


Figure 21. ESI-MS spectra of the aromatized C-1027 chromophore. (A) MS spectrum of the aromatized C-1027 chromophore after agar extraction. (B) MS spectrum of the aromatized C-1027 chromophore according to Inoue et al. (2006)²⁵²

Thus, these data confirm that *S. sp.* Tü2401 is indeed capable of producing an enediyne compound, most likely C-1027.

C-1027 was initially isolated from *Streptomyces globisporus* C-1027 in 1988, as a highly potent antitumor antibiotic.^{264,265} It showed exceptional cytotoxicity to cultured cancer cells ($\text{IC}_{50} = 1.5 \times 10^{-17} - 3.2 \times 10^{-16} \text{ M}$) as well as against a panel of transplantable tumour cells in mice.^{265,266}

The C-1027 holoprotein consists of a labile chromophore, also called lidamycin that is, like most nine-membered ring enediynes bound noncovalently to its apoprotein (10489 Da). The chromophore is linked to the apoprotein via hydrophobic interactions between the hydrophobic groups (benzoxazine and the macrocycle) of the chromophore and the hydrophobic side chains of the apoprotein^{252,256,267} In general, nine-membered ring enediyne compounds need an external activation by e.g. nucleophiles to initiate the electronic rearrangement that

leads to the aromatization via a Masamune-Bergman reaction. Except for maduropeptin and C-1027, once they are detached from their stabilizing apoproteins they spontaneously aromatize at room temperature (see **Figure 20**) ($T_{1/2}$ (C-1027) = 0.8 h in ethanol).^{252,268} That is why especially C-1027 has the highest reactivity within the enediyne family.²⁵² It is causing multiple DNA damages including single- and double-strand breaks, abasic sites, alteration of cell cycle progression, induction of chromosomal aberrations and telomere dysfunction at a low nanomolar concentration.^{266,269} The interplay between the benzoxazine moiety and the nine-membered enediyne ring is the reason for the extreme toxicity. It has been shown through high-resolution NMR studies of the complex of double-stranded DNA and aromatized chromophore that while the enediyne ring is placed in the minor DNA groove, the benzoxazine moiety is oriented parallel to the DNA bases.^{252,270,271} The necessity of the benzoxazine moiety for DNA binding has been shown by Yu *et al.*, since the absence of this moiety lead to a loss of binding affinity by ca. 400-fold.^{252,272} Moreover, it has been reported that interaction with the DNA is highly sequence specific. Accordingly, the following five-nucleotide sequences are prone for double-strand lesions CTTTI/AAAAG, ATAAT/ATTAT, CTTIA/TAAAG, CTCTT/AAGAG, and especially GTTAT/ATAAC (underlining the cutting sites).^{252,266,273}

The remarkable cytotoxic activities of many enediyne compounds have made them a promising target for drug candidates. However, the toxicity is not only extreme, but also delayed, which limits their application.^{268,274} Therefore, conjugation of enediynes with either polymers like e.g. poly(styrene-co-maleic acid) (SMA), or its derivatives, or monoclonal antibodies have shown great promise, as they improve uptake and toxicological profile at the same time.²⁶⁸ Hence, when in 1994 the conjugate of neocarzinostatin and SMA (SMANCS[®]) has been approved for the treatment of hepatoma in Japan, it was the first enediyne drug used in clinics. This drug has also been successfully used for antitumor treatment in lung, stomach, pancreas, gall bladder, lymphoma, and melanoma in combination with Lipidol[®] - a lipid contrast agent.²⁷⁵ Calicheamicin is another enediyne compound that is successfully employed in tumour therapy. In an antibody-drug conjugate (ADC) with a CD33 monoclonal antibody (mAB) (e.g. Mylotarg[®]) it is used to treat acute myeloid leukaemia and as an ADC with a CD22 mAB (e.g. Besponsa[®]) for non-Hodgkin lymphoma.^{250,275,276} Furthermore, there are currently several mAB-C-1027 conjugates against hepatoma in phase II clinical trials in China.^{256,277-280}

Given the fact that only 11 enediynes are structurally characterized to date, with four additional compounds that have only been isolated in the aromatized form yet, it is remarkable that 3 of these have already been used in clinics, representing a success rate of ca. 30%.²⁵⁰ Bioinformatic analysis of bacterial genomes have revealed that enediyne BGC are highly abundant among Actinobacteria (6.3 %). Therefore, it is even more astonishing that the number of compounds belonging to this group is still small.

The identification of C-1027 as a secondary metabolite of *S. sp.* Tü2401 on the one hand shows the great potential of the Tübingen strain collection to produce highly potent compounds. It is the first time an enediyne compound has been identified from the collection, but presumably not the only one. Taken into account, the abundance of 6.3 % of enediyne BGC among Actinobacteria genomes and the number of 1200 Actinobacteria strains comprising the Tübingen strain collection, it can be assumed that statistically 75 enediyne producing strains are yet to be identified.

On the other hand, these findings also reveal that the *yorB* reporter gene assay is a powerful tool to identify enediyne producing strains.

3.4.5 Purification of hydrophilic metabolites from *S. sp.* Tü2401 submerge cultures

As mentioned above, *S. sp.* Tü2401 is capable of producing at least two different compounds with different MoA, but similar activity spectra, depending on the cultivation conditions. While the compound produced on solid medium is most probably the enediyne C-1027, the compound produced in submerge culture remained unknown in the early process of dereplication due to multiple reasons.

On the one hand, it was impossible to extract the compound(s) from the CFS into organic solvents. Standard extraction protocols (see **2.4.6**) employing various pH of the CFS (pH 2; 5; 7; 9; and 11) and several organic solvents e.g. ethyl acetate, methyl acetate, ethyl formate, and butanol (data not shown) were unable to extract the active compound(s). The extraction success was analysed using standard *E. coli* K12 agar diffusion bioassays (see **2.3.1**). In all cases the aqueous phase remained active, while the organic extract was not bioactive (see **Figure 22**).

On the other hand, standard RP-HPLC-DAD dereplication methods could not be applied, since the hydrophilicity of the compound(s) did result in almost no retention on different reversed phase HPLC columns (see **Table 29**).

Moreover, the elution in the injection peak led to an overlay of signals, therefore, no significant absorption in the DAD could be assigned to the compound(s). However, further analysis indicated that the compounds putatively lack chromophores and thus do not show any signals in the DAD at all.

Due to these first observations, high hydrophilicity, and lack of chromophores, it was necessary to develop an entirely new strategy for the isolation and identification of the bioactive compounds produced by *S. sp.* Tü2401 submers cultures.

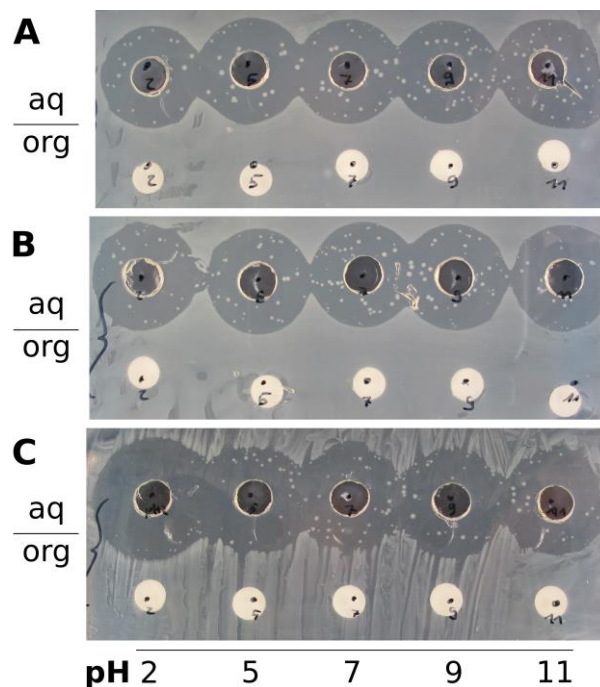


Figure 22. Results of *E. coli* K12 agar diffusion bioassays of OM CFS extracts of *S. sp* Tü2401.

CFS of OM cultures of *Streptomyces* sp. Tü2401 were extracted with either (A) ethyl acetate, (B) methyl acetate or (C) ethyl formate. pH of CFS were adjusted prior to extraction to 2, 5, 7, 9 or 11. 50 μ L of each phase were analysed in agar diffusion assay against *E. coli* K12. Aqueous phases were pipetted directly into the wells in the upper row (aq). Organic phases were applied to sterile filter discs and placed on the bottom row (org). (Adapted from Schneider 2018)¹⁶¹

Consequently, after cultivation of *S. sp.* Tü2401 in a 10 l fermenter (see 2.2.4), the entire culture was separated by multiple sheet filtration in CFS and mycelium, resulting in 8.5 l CFS (see 2.4.4). Subsequently, the CFS was extracted five times with each 2.0 l of EA. The organic phases were combined and concentrated under reduced pressure, resulting in 235 g crude extract (see 2.4.4.2).¹⁶¹ The aqueous phase was collected and lyophilized (see 2.5), resulting in 91 g reverse extract.¹⁶¹ Both crude and reverse extract were analysed for antibacterial activity against *E. coli* K12 in agar diffusion assays (see 2.3.1), revealing that only the reverse extract showed inhibition zones, while the crude extract was inactive. HPLC chromatograms of the reverse extract unveiled a substantial reduction of the number of peaks.¹⁶¹ Clearly, this first step of the isolation aimed at the removal of lipophilic compounds, dissolvable in EA. However, since *S. sp.* Tü2401 has been cultivated in a complex medium, besides the lipophilic compounds a plethora of hydrophilic compounds, e.g. sugars, salts, and amphiphilic metabolites still remained in the reverse extract.

Table 26. Results of the extraction of the reverse extract of *S. sp.* Tü2401.

Solvent	pH	Inhibition zone after the 1 st extraction [cm]	Inhibition zone after the 2 nd extraction [cm]	Undissolved pellet [%]
Water	2	1.9	0.0	25
	7	1.9	0.0	27
30 % MeOH	2	1.9	1.0	9
	7	1.8	1.0	18
50 % MeOH	2	1.9	0.8	45
	7	1.8	1.1	26
80 % MeOH	2	1.7	1.0	82
	7	1.9	1.0	73

Therefore, another isolation step was necessary, aiming at the removal of highly hydrophilic sugars and salts. For this purpose, several mixtures of MeOH and water (0 %; 30 %; 50 %; 80 % MeOH), each at pH of 2 and 7, have been analysed regarding their potential to dissolve the bioactive compound from the reverse extract (see 2.4.7). In short, 11 mg of the reverse extract have been dissolved in 1.0 ml of the respective mixture. After shaking for 30 min in the ultrasonic bath, the supernatants have been removed and subsequently analysed using *E. coli* K12 agar diffusion assays (see 2.3.1). The pellets were once more dissolved in 1 ml of the respective mixture and treated as described above. The resulting supernatants were also analysed using *E. coli* K12 agar diffusion assays (see 2.2.2). Meanwhile, the pellets were dried for 10 min at 60 °C and subsequently weighted (see Figure 23). As a result, already the first

dissolution of the mixture of 80 % MeOH showed inhibition zones the same size as the water control samples, indicating that this mixture was sufficient to dissolve a considerable amount of the bioactive compounds. However, the supernatant of the second dissolution of the mixture of 80 % MeOH was still bioactive even though the halo size was only half the size of the first dissolution. At the same time, the weight of the pellet after two extractions remained 80 % of the initial weight, indicating that a substantial amount of the other hydrophilic compounds remained in the pellet and were not soluble in 80 % MeOH (see **Table 26**). Hence, the whole reverse extract was extracted two times with 80 % MeOH and dried under reduced pressure, resulting in 18.2 g enriched reverse extract. Subsequently, this extract was analysed via HPLC-DAD, revealing a chromatogram that still contained several peaks. Therefore, additional purification steps were needed.

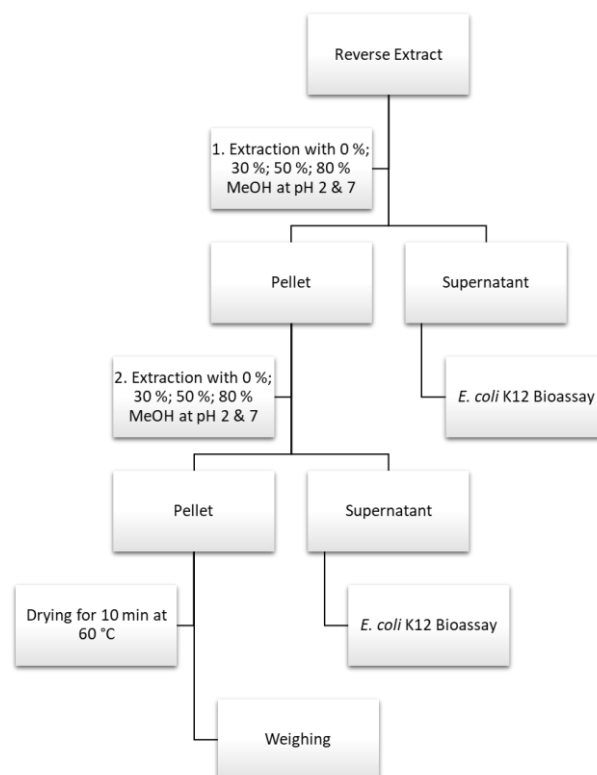


Figure 23. Workflow for the extraction of the reverse extract of *S. sp* Tü2401.

3.4.5.1 Gel filtration chromatography

The technique of SEC has already been introduced in chapter 3.3.4.1. However, there are basically two different types of SEC: One, gel permeation chromatography, being described *ibidem*. The other is gel filtration chromatography (GFC), here, a hydrophilic stationary phase and an aqueous mobile phase is used to separate water soluble molecules. The separation is in both cases based on the analytes size and affinity towards the stationary or mobile phase. GFC has at first been described in 1959 by Dr. Jerker Porath and Dr. Per Flodin as “A method for desalting and group separation”.²⁸¹ Thus, this method seemed perfect for the final removal of salts and sugars from the purified reverse extract. Additionally, the retention time could give a first hint towards the size of the bioactive compound(s).^{282,283}

In order to identify the most suitable separation conditions, four different stationary phases, have been investigated (see **Table 27**) according to 2.6.2., Sephadex™ LH20; Sephadex™ G15, Bio-Gel® P2, and Toyopearl® HW40, each covering large exclusion limits starting from a few Dalton up to 5 kDa (Sephadex™ LH20)

Table 27. Comparison of different stationary phases for GFC of the purified reverse extract.

Material	Exclusion Limits [Da]	Column dimensions [cm]	Flow rate [ml/h]	Loading mass [mg]	Fractionation interval [1/h]	K_d^*
Sephadex™ LH20	≤ 5000	2.5 x 90	34	104	3	0.60
Sephadex™ G15	≤ 1500	2.5 x 90	36	105	3	0.44
Bio-Gel® P2	100 - 1800	2.5 x 90	45	103	3	0.46
Toyopearl® HW40	100 - 10000	2.5 x 90	36	105	3	0.71

* K_d ... distribution coefficient

To compare the 4 stationary phases, the distribution coefficient K_d , a parameter, independent of column dimensions, has been determined (3).²⁸⁴ K_d values describe the extent to which a molecule diffuses into the pores of the stationary phase.²⁸¹ Therefore, prior to the actual analysis, 1 ml of a 5mg/ml blue dextran solution has been subjected to each column. Blue dextran has an approximate molecular mass of 2000 kDa, therefore it is not able to penetrate into the pores of the stationary phase, thereby allowing the determination of each columns void vol-

ume (V_0). The total column volumes V_t has been estimated according to the column dimensions. Finally, the purified reverse extract has been fractionated on each column. Each fraction has been analysed via *E. coli* K12 agar diffusion assays, giving the elution volumes V_e of the bioactive compound(s). A K_d of 0 represents high molecular weight compounds without any retention like blue dextran, whereas a low molecular weight compound, strongly interacting with the stationary phase will have a $K_d \geq 1$. Accordingly, K_d values between 0 and 1 represent intermediate molecular weight compounds.²⁸⁴

$$(3) \quad K_d = \frac{V_e - V_0}{V_t - V_0}$$

In the case of the separation of known compounds, it would be beneficial to choose the stationary phase where K_d differs the most. However, for this separation, neither the bioactive compounds are known, nor the other matrix components from the purified reverse extract. Therefore, Toyopearl® HW40 has been chosen as stationary phase, since it exhibited the broadest exclusion limits on the one hand. And on the other hand, its K_d value of 0.71 points towards the biggest extend of diffusion of the bioactive compound(s) into the pores compared to all other stationary phases. Thus, Toyopearl® HW40 seemed to provide a sufficient separation of high molecular weight compounds and low molecular weight compounds simultaneously.

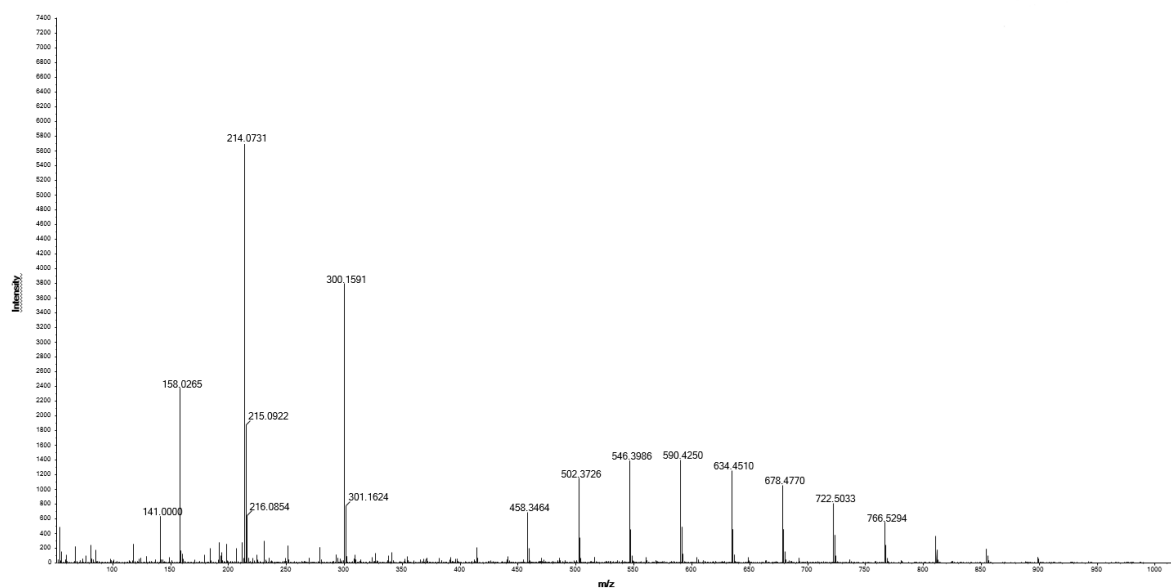


Figure 24. MS spectrum of the bioactive fraction at $t_R = 16$ min. A cluster from m/z 458 to m/z 898 can be observed, with $\Delta m/z$ of 44, indicating the presence of PEG in the sample.

Since this gravity flow chromatography was very time consuming, not the entire 18.2 g of the purified reverse extract have been separated, but rather 10.0 g. The active fractions have been combined and dried under reduced pressure, giving 1.1 g of bioactive fractions. However, the chromatograms of HPLC-DAD-ELSD analysis (see **2.6.4; Table 12**) still exhibited a few peaks in the DAD ($0 \text{ min} \leq t_R \leq 12 \text{ min}$), and also large peaks in the ELSD ($12 \text{ min} \leq t_R \leq 18 \text{ min}$) (see **Figure 26**). Interestingly, microfractionation (see **2.6.4; Table 6**) and subsequent *E. coli* K12 agar diffusion bioassays (see **2.3.1**) revealed a broad bioactive fraction ranging from $t_R = 16 \text{ min}$ to $t_R = 18 \text{ min}$. In order to determine the respective masses, these fractions have been submitted to HPLC-MS analysis (see **Table 8**). As a result, the spectrum showed cluster with an m/z of 44, indicating the presence of PEG (see **Figure 24 & Figure 25**). These vast amounts of PEG might neither be a part of the media components, nor a metabolite from *S. sp* Tü2401. It might more likely originate from the antifoam agent Ucolub N115[®] (Fragol, Mülheim, Germany), consisting of Polypropylen- PEG, from which 2.0 ml had been added during large scale fermentation of *S. sp.* Tü2401 (see **2.2.4**).²⁸⁵ Therefore, in order to identify the masses of the bioactive compounds, a method for the removal of the overlaying PEG needed to be developed.

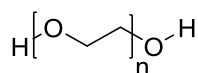


Figure 25. Structure of Polyethylene glycol (PEG), a polymere of ethylene oxide ($\text{C}_2\text{H}_4\text{O}$;
 $M = 44.052 \text{ g/mol}$)

A fast and efficient separation method is medium pressure liquid chromatography (MPLC). It allows the purification of large compound quantities and is therefore most suitable for the purification of crude extracts or preparative isolation of NP. In comparison to the widespread HPLC, where pressures of 400 - 500 bar are reached, MPLC is performed in general at pressures between 5 – 20 bar.²⁸⁶ Particle sizes of the stationary phases in MPLC columns range from $25 \mu\text{m} - 40 \mu\text{m}$, compared to $3 - 5 \mu\text{m}$ in HPLC columns. Therefore, in general MPLC can be operated at higher flow rates up to 100 ml/min .²⁸⁷

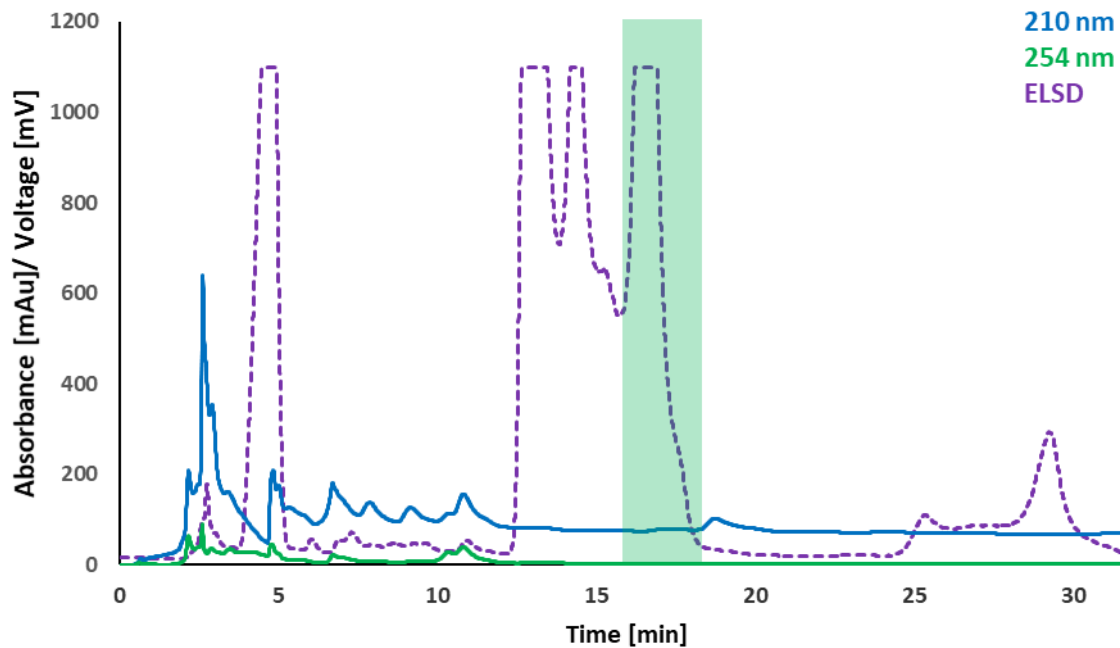


Figure 26. HPLC-DAD-ELSD chromatogram of the combined active fractions after GFC of the purified reverse extract. The active fractions of the GFC have been combined and fractionated (see 2.6.4; Table 6). The fractions have been subsequently analysed in the *E. coli* K12 agar diffusion assays (see 2.3.1). Timeframe corresponding to fractions with antibiotic activity is highlighted with the green overlay. MPLC

In order to determine the best separation conditions and the most suitable stationary phase material for MPLC purifications, it is most common to use thin-layer chromatography (TLC), since these results can be directly translated into MPLC.²⁸⁸ For this purpose two different, normal phase stationary phases (Silica gel 60 F₂₅₄, Silica gel 60 Diol F₂₅₄) and multiple mobile phases have been used to separate the bioactive fractions derived from GFC (see 2.6.2). Bioautography has been used to visualize the bioactive fractions on the TLC plate (see 2.3.4). It is a microbial screening method used to detect antimicrobial or antifungal activity in combination with TLC.

$$(4) \quad R_f = \frac{\text{migration distance in the mobile phase}}{\text{migration distance of the solvent}}$$

Table 28. Results of TLC experiments. Bioactive fractions from GFC have been separated on two different, normal phase stationary phases (Silica gel 60 F₂₅₄, Silica gel 60 Diol F₂₅₄), using various mobile phase compositions. The R_f values of the bioactive compound(s) have been determined via bioautography. The shape of the corresponding halo is described in parenthesis.

Stationary Phase	Mobile Phase	Bioactivity R _f
Silica gel 60 F ₂₅₄	EA/MeOH/H ₂ O (1:8:1; v/v/v)	0.2 (spot)
Silica gel 60 F ₂₅₄	EA/MeOH/H ₂ O [0.1 M citrate; pH 6] (1:8:1;v/ v/v)	0.25 (spot)
Silica gel 60 F ₂₅₄	EA/MeOH/H ₂ O [0.1 M citrate; pH 6] (1:7:2; v/v/v)	0.6 (spot)
Silica gel 60 F ₂₅₄	EA/MeOH/H ₂ O [HCl- KCl (0.1 M, pH 2] (1:8:1; v/v/v)	0.35 (spot)
Silica gel 60 F ₂₅₄	EA/MeOH/H ₂ O [HCl- KCl (0.1 M; pH 2] (1:7:2; v/v/v)	0.35 (spot)
Silica gel 60 F ₂₅₄	MeOH/H ₂ O (9:1; v/v)	0.15 (smear)
Silica gel 60 F ₂₅₄	MeOH/H ₂ O (9.5:0.5; v/v)	0.1 (smear)
Silica gel 60 F ₂₅₄	MeOH/H ₂ O (8:2; v/v)	0.6 (spot)
Silica gel 60 F ₂₅₄	MeOH/H ₂ O (7:3; v/v)	0.7 (spot)
Silica gel 60 F ₂₅₄	DCM/MeOH/H ₂ O (1:8:1; v/v/v)	0.2 (smear)
Silica gel 60 F ₂₅₄	DCM/MeOH (2:8; v/v)	0.1 (smear)
Silica gel 60 Diol F ₂₅₄	MeOH/H ₂ O (2:8; v/v)	no activity
Silica gel 60 Diol F ₂₅₄	MeOH/H ₂ O (2:8; v/v) + 1 % glacial acetic acid	no activity

In MPLC, column volumes (CV) (**formula 5**) instead of R_f values are used (**formula 4**). Literally, CV is the volume needed to elute the compound after injection.²⁸⁸

$$(5) \quad CV = \frac{1}{R_f}$$

The TLC experiments have shown that Silica gel 60 Diol F₂₅₄ stationary phases lead to a total loss of bioactivity. This is somehow surprising, since Diol phases are generally behaving as deactivated silica gel with less polar activity.²⁸⁹ In contrast, normal phase Silica gel 60 F₂₅₄ plates showed good separation capabilities, since variation of the media composition led to strong shifts of the R_f values. The two component mixture of MeOH and H₂O, with no pH modification needed, had shown the greatest potential for the separation. An increase of the H₂O ratio from 5 % to 30 %, lead to a drastic increase of R_f values from 0.1 to 0.7, corresponding to a

shift from 10 CV to 1.4 CV. Hence, a gradient MPLC using silica stationary phase and a MeOH/H₂O gradient from 100 % MeOH to 70 % MeOH was assumedly most promising (see **2.6.1**).

In addition to the development of a suitable MPLC method, the TLC experiments were also used to get insights into the molecular structure of the bioactive compound(s). There are a number of staining methods to visualize the compounds on the TLC plate, which additionally allow the determination of functional groups that are contained within the molecule.²⁹⁰ In this study, orcinol, as an agent typically used to detect sugars has been used (see **2.6.1.1.1**).²⁹¹ This test is also called Bial's test in honour of its inventor Manfred Bial.²⁹² Orcinol in combination with Fe³⁺ forms under acidic conditions a blue-green complex with pentose sugars, and a brown complex with hexose sugars.²⁹² However, no sugars could be detected in the proximity of the bioactive spots. Additionally, also the presence of functional groups whose pK_a is ≤ 5 has been tested using bromocresol green (see **2.6.1.1.2**). At pH values below 5.4 this sulfonephthalein gets protonated, and thus turning from its dianionic form (blue) into the monoanionic form (yellow). However, no yellow spots could be detected in the proximity of the bioactive spots, indicating that the bioactive compound does not contain functional groups whose pK_a is ≤ 5. Moreover, the presence of primary amines, e.g. amino acids and ammonia, has been analysed using ninhydrin (see **2.6.1.1.3**). Ninhydrin condenses with a primary amine to form a Schiff base. After decarboxylation, amino-ninhydrin is formed, which subsequently condensates with another molecule of ninhydrin to form a purple product, also called Ruhemann's purple.²⁹³ But also this test was negative.

After all, these staining tests did not give new insights into the structure of the bioactive compound(s). But even though all tests were negative, it would be wrong to conclude that the bioactive compound(s) do not feature one or more of the tested functional groups. These staining assays always bear the risk that the compound(s) are bioactive in the bioautography tests, although their concentration is below the limit of detection in the staining assays.

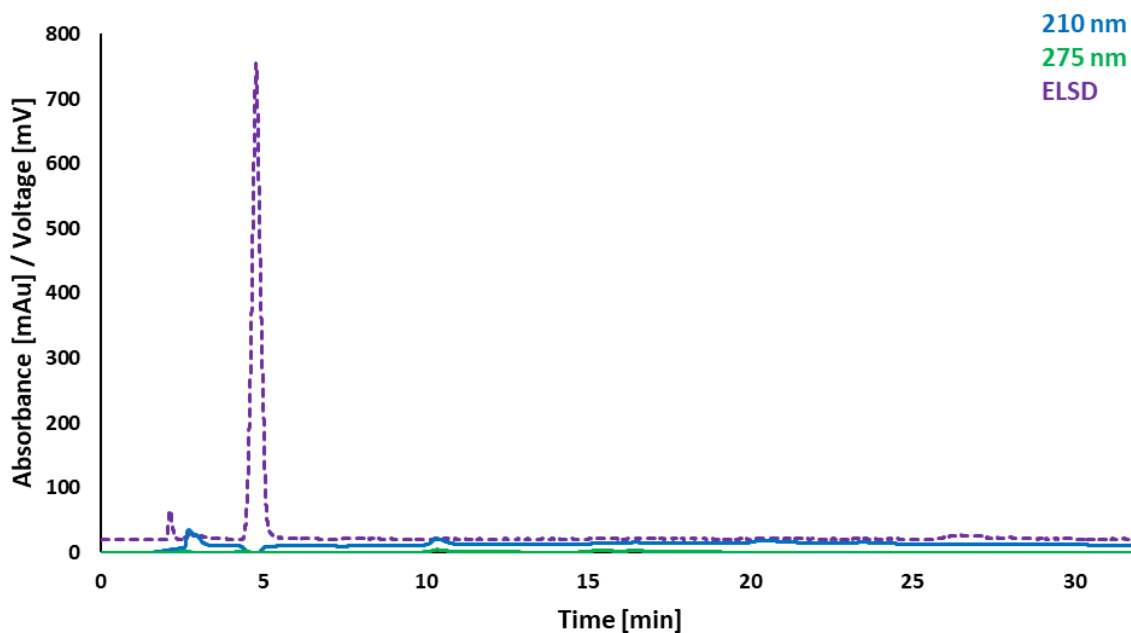


Figure 27. HPLC-DAD-ELSD chromatogram of the combined bioactive fractions after MPLC.

The bioactive fractions after MPLC have been analysed via HPLC using the Merck SeQuant® ZIC®-HILIC (see 2.6.4; Table 12) The chromatogram indicates the absence of PEG, since no signals occur in the ELSD.

For the MPLC separation, 40 mg of the bioactive fractions from the GFC have been applied via dry loading (see 2.6.3) onto a 12 g Sepacore Silica HP column (Büchi Labortechnik AG, Flawil, Switzerland) and subsequently separated, using a gradient from 100 % MeOH to 50 % MeOH in 15 min at a flow rate of 18 ml/min. Samples were taken every minute and analysed using *E. coli* K12 agar diffusion assays (see 2.3.1). As a result, the bioactive fractions elute between 10 and 19 CV with a maximum after of bioactivity after 16 CV. HPLC-DAD-ELSD analysis (see 2.6.4; Table 12) of the bioactive fractions revealed the absence of any signals in the ELSD. Thus, this method is suitable for the removal of PEG (see Figure 27). In total 200 mg of the bioactive fractions from the GFC have been separated using MPLC, resulting in 9 mg of PEG free bioactive fractions.

Further analysis of the not bioactive fractions unveiled the elution of PEG very early during the separation, after 2 to 4 CV.

3.4.5.2 HPLC

As mentioned above (see **3.4.5**), already the first HPLC-DAD analysis of the CFS of *S. sp. Tü2401* submerge cultures have disclosed one major challenge for the identification of the bioactive compound(s). Since the normal ACN/H₂O screening gradient, ranging from 5-100 % ACN on a Phenomenex Luna® C-18 column led to elution of the bioactive compound(s) contemporaneous with the injection peak (see **Table 29**)

This indicates that the interactions between the bioactive compound(s) from *S. sp. Tü2401* submerge cultures and the mobile phase were much stronger, than the interactions with the stationary phase. Therefore, it was inevitable to develop an entire new method for these highly hydrophilic compound(s). For this purpose, different stationary phases have been analysed in order to increase retention. Therefore, an HPLC coupled to a fraction collector was used for the separations. The t_R of the bioactive compound(s) was determined via *E. coli* K12 agar diffusion assays (see **2.3.1**). For the analysis, the freeze dried reverse extract (see **3.4.5**) was dissolved in water and subsequently ACN was added until the solution finally consisted of 80 % ACN. After centrifugation, the supernatant was used for the separation.

It is well known that reversed phase columns differ in their separation behaviour depending on the aliphatic chain length and the degree of endcapping. The longer the carbon chain and the more thoroughly endcapped, the less polar interactions between the solute and the stationary phase can be observed.^{294,295} But not only these obvious differences lead to altered retention times, also endcapped C-18 columns from different vendors can have different separation characteristics.²⁹⁵

Therefore, the Nucleosil 100 C-18 column has been tested as an alternative reversed phase to the Phenomenex Luna® C-18 column. However, using the same separation conditions did not improve the separation of the bioactive compound(s), as they still eluted at the same time as the injection peak (see **Table 29**)

Furthermore, the Nucleosil 100 C-8 column has also been tested as a less unpolar reversed phase column. Referring to the producer, its separation is still based on hydrophobic (van der Waals) interactions but offers column additional slight residual silanol interactions compared to the Nucleosil C-18, since they are not endcapped.²⁹⁶ These hydroxyl groups are now able to

have dipole-dipole interactions or to form hydrogen bonds with the analyte(s). For the separation, the same method as for the Phenomenex Luna[®] C-18 column has been applied. However, the bioactive compound(s) were not retained (see **Table 29**).

Table 29. Columns & conditions for the separation for albomycin δ_1 & δ_2

Column	Separation conditions				t_R of the bio-active compound(s)[min]
	mobile Phase	Gradient [%]	Flow [ml/min]	Time [min]	
Nucleosil 100 C-8; 5 μm ; 100 \AA ; 4.6 mm x 125 mm	A: H ₂ O;B: ACN + 0.1 % FA	B: 0 - 100	2.0	15	0
Nucleosil 100 C-18; 5 μm ; 100 \AA ; 4.6 mm x 125 mm	A: H ₂ O;B: ACN + 0.1 % FA	B: 0 - 100	2.0	15	0
Luna [®] C-18; 5 μm ; 100 \AA ; 4.6 mm x 250 mm	A: H ₂ O;B: ACN + 0.1 % FA	B: 5 - 100	2.5	20	0
Kinetex [®] Polar C-18; 2.6 μm ; 100 \AA ; 4.6 mm x 150 mm	A: H ₂ O;B: ACN + 0.1 % FA	B: 5 - 100	1.2	20	0 - 2
Luna [®] NH ₂ ; 5 μm ; 100 \AA ; 4.6 mm x 250 mm	A: H ₂ O;B: ACN + 0.1 % FA	B: 80 (isocratic)	2.0	20	2.5 - 5.5
SeQuant [®] ZIC [®] -HILIC; 3.5 μm ; 100 \AA ; 4.6 mm x 150 mm	A: 10 mM NH ₄ CH ₃ COO; B: ACN + 0.1 % FA	B: 80 (isocratic)	0.8	45	12.5 - 22.5
XBridge BEH Amide; 5 μm ; 130 \AA ; 4.6 mm x 250 mm	A: ACN/H ₂ O/100mM NH ₄ COO pH3 (5:4:1; v/v/v) B: ACN/100mM NH ₄ COO pH3 (9:1)	B: 80 - 60	1.0	35	21.0 - 23.0; 27.0 - 29.0

The Kinetex[®] Polar C-18 column from Phenomenex is a silica based stationary phase, modified with C-18 chains, TMS endcaps and small polar groups.²⁹⁷ It provides therefore as well polar and non-polar retention. Due to the reduced particle size the column was operated at a flow rate of 1.2 ml/min instead of 2.0 ml/min. Hence, to maintain comparable separation conditions to the other reversed phases, it was necessary to prolong the run by 25 % to 20 min, while the gradient from 5 % to 100 % ACN remained unchanged. The agar diffusion assay revealed an increase in retention since the bioactive compound(s) eluted between 0 and 2 min (see **Table**

29). Even though the Kinetex[®] Polar C-18 column slightly improved the retention of the bioactive compound(s), the spread of the bioactivity over 2 min indicate a very broad peak and thus poor selectivity.

Hydrophilic Interaction Liquid Chromatography (HILIC), using either the Luna[®] NH₂ column, the SeQuant[®] ZIC[®]-HILIC column, or the XBridge BEH Amide column substantially improved the separation in terms of retention time and selectivity. HILIC is an alternative normal phase liquid chromatography approach, designed for the separation of small polar compounds on polar stationary phases.²⁹⁸ Nevertheless, it also has intersections with other chromatographic application, since it combines normal phase chromatography with ion chromatography and even with reversed phase chromatography.²⁹⁸ The stationary phases are in general traditional polar stationary phases, as used in normal phase LC, like silica, amino or cyano.^{298–303} However, the mobile phases are more similar to those used in classical reversed phase LC.^{298,302–304} Furthermore, like in ion chromatography, even charged compounds can be analysed using HILIC. These characteristics makes HILIC a perfect method for the analysis of compounds that elute near the void in reserved-phase chromatography.²⁹⁸ Additionally, it has also been successfully combined with MS analysis.²⁹⁸ HILIC has been used to analyse a broad variety of hydrophilic compounds like carbohydrates and peptides, and is becoming more popular also in terms of pharmaceutical analysis.^{305–307} Even though the separation of polar compounds on polar stationary phases with unpolar/aqueous mobile phases has been used for 30 years, mostly in carbohydrate analysis, it was Dr. Andrew Alpert who introduced the acronym HILIC in 1990.^{304,308} Ever since, the interest in the method is rising, evident in the number of scientific HILIC papers since 2003, reaching 500 new publications in 2012.^{298,303,309} Even though significant progress has been made in elucidating the retention mechanism of HILIC, there are still questions to be answered.³⁰³ Various techniques (e.g. frontal analysis, titration, etc.) have confirmed the presence of a water-rich layer on the surface of the stationary phase.³⁰³ This indicates that partition of the analyte between this layer and the mobile phase is the predominant factor for retention.³⁰⁸ However, the actual retention mechanism of HILIC is much more complex, since also adsorption and electrostatic interactions might be involved in the separation.^{303,309,310} It is assumed that the individual separation mechanism depends on the analyte, the mobile phase composition, and also the functionalities of the stationary phase, also termed “LC Retention Troika”.^{303,311} Hence, also mobile phase pH, its ionic strength, and the organic phase itself have an effect on the separation.^{161,303,312}

Three different polar stationary phases, Phenomenex Luna[®] NH₂, SeQuant[®] ZIC[®]-HILIC, and XBridge BEH Amide, have been analysed for their potential to separate the bioactive compound(s) from reverse extract of *S. sp. Tü2401* (see **Table 29**).

The Phenomenex Luna[®] NH₂ column consists of a silica base modified with aminopropyl groups. In combination with acidic pH values, the positively charged amino functions facilitate great selectivity for acidic compounds due to coulomb interactions.¹⁶¹ In order to separate the bioactive compound(s), an isocratic method was used, where the mobile phase consists of 80 % ACN, 20 % H₂O and 0.1 % FA (see **Table 29**). As a result, the t_R of the bioactive compounds was between 2.5 - 5.5 min, thus enabling a better retention than on all the reversed phases. However, the signal was still very broad, indicating once more poor selectivity. Moreover, in contrast to the vendor's description, the application of this method to HPLC-MS analysis revealed insufficient stability of the stationary phase, leading to a high signal-to-noise ratio. Therefore, the Phenomenex Luna[®] NH₂ column was unsuitable for the isolation and dereplication of the bioactive compound(s).

The Merck SeQuant[®] ZIC[®]-HILIC column is composed of a zwitterionic sulfobetaine silica base. These zwitterionic phases are known to form a firm water layer on the surface and provide additional coulomb interactions to ionic analytes.³¹⁰ As recommended by Merck, the column was operated at a flow rate of 0.8 ml/min. Accordingly, the analysis time was increased to 45 min. Also with this column, an isocratic separation method was used, with a mobile phase consisting of 20 % of a 10 mM solution of NH₄CH₃COO and 80 % ACN (see **Table 29**). The t_R of the bioactive compound(s) ranged during the first analysis from 14 to 17 min. However, repetition of this separation resulted in considerable fluctuations of the t_R over a range from 12.5 min to 22.5 min. Since the equipment as well as all the solvents and even the sample were the same, this is an indication for insufficient column equilibration or the sensitivity of the bioactive compound(s) towards a yet unknown and uncontrolled factor. MS analysis of the bioactive fractions compared to non-bioactive fractions did not reveal any masses unique to the bioactive fractions. Interestingly, there are no signals detectable in the chromatogram during the time the bioactive fractions elute - neither UV-signals nor ELSD-signals. The light scattering detector is used to detect and even quantify compounds that do not feature a chromophore and are less volatile than the mobile phase.^{313,314} Mobile phase composition, gas flow as well as nebulizer and vaporizer temperature are parameters that can influence the

sensitivity of the ELSD.^{161,315} An increase in sensitivity for carbohydrates has been reported to result from an increase in vaporizer temperature.^{161,315–317} Accordingly, vaporizer temperatures ranging from the standard 40 °C to 60 °C (5 °C steps) have been tested. An increase in sensitivity especially for compounds eluting between 8 and 12 min was observable.¹⁶¹ However, still no signals were detectable in the timeframe where the bioactive compound(s) elute.¹⁶¹ Hence, either the compound(s) are more volatile than the mobile phase, or their concentration is below the detection limit of the ELSD. Even though analysis using the Merck SeQuant® ZIC®-HILIC column resulted in good retention times, the inconsistency of the t_R of different runs as well as the broad range of elution still indicate no good selectivity for the bioactive compound(s) at the conditions chosen.

The last column that has been tested was the Waters XBridge BEH Amide. This column has been chosen, since it is stable over a broad range of mobile phase pH [2 – 11]. It is composed of a silica base that is trifunctionally-bonded via an ethylene bridged hybrid linker unit to an amide function. According to the manufacturer, this column has been especially designed to separate extremely polar compounds. This column has been operated at a flow rate of 1 ml/min. As mentioned above, the pH of the mobile phase is a crucial parameter in HILIC separations. Therefore, 3 different pH values have been compared, pH 3, 6, and 8.5. A 10mM NH_4CHOO solution at the respective pH was chosen as solvent A, whereas ACN served as solvent B. In contrast to the other columns, this time a gradient method was developed, starting with isocratic conditions (95 % B for 5 min), followed by a gradient over 20 min to 60 % B, which was finally kept for 5 min. In order to produce robust results, the equilibration time between injections is crucial for HILIC. Therefore, 10 CV have been used to equilibrate the column.³¹⁸ The t_R of the bioactive compound(s) varied just slightly, while at pH 8.5 the bioactive fractions eluted in the range between 21 and 26 min, it shifted to 23 to 26 min at pH 3 and 6. Even though the t_R are almost the same, the peaks shape became more narrow at lower pH values. Therefore, in all following experiments the pH was adjusted to 3.

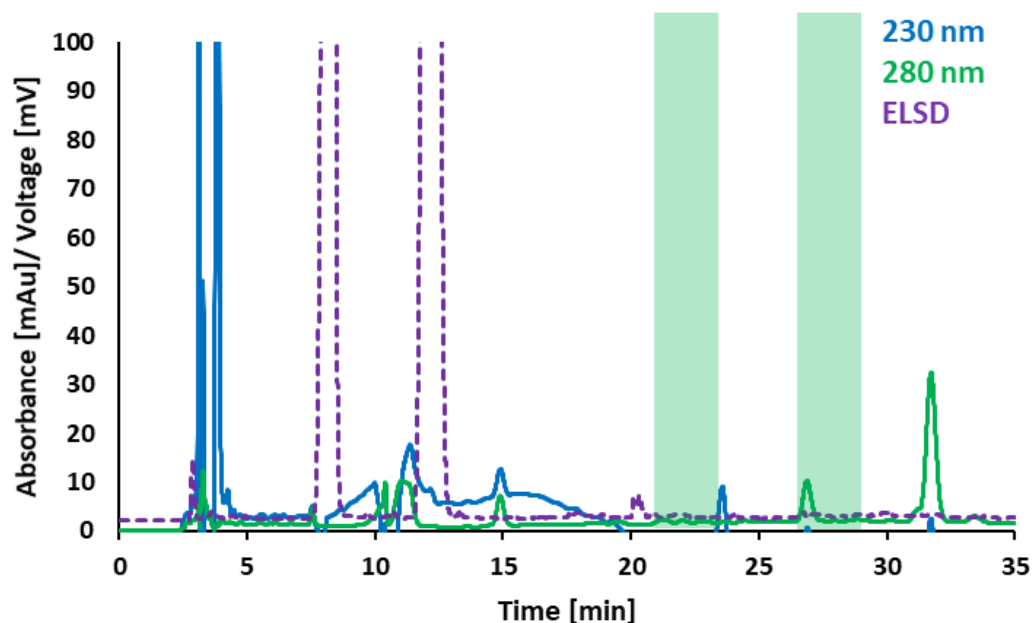


Figure 28. HPLC-DAD-ELSD chromatogram of the PEG free bioactive fractions after MPLC, using the Waters XBridge BEH Amide column

In addition to the pH, also the buffer concentration is crucial for HILIC separation.³⁰³ Accordingly, its influence on the separation was analysed. Thus, the mobile phase composition was changed, so that solvent A was composed of ACN/H₂O [pH3]/100mM NH₄CHOO (5:4:1 (v/v/v)) and solvent B of ACN/100mM NH₄CHOO [pH3] (9:1 (v/v)). The other separation parameters remained unchanged. The constant buffer concentration of 100mM NH₄CHOO indeed had an effect on the separation in this regard that the bioactive fractions elute in the narrow time frame between 27 and 29 min. Hence, in following analyses, the solvent composition was remained as described in order to maintain a constant buffer concentration. Moreover, in order to get a faster elution of the bioactive compound(s), the slope of the gradient has been reduced. Hence, the initial isocratic conditions were set to 80 %, respectively 70 % B. All other parameters remained unchanged. The separation, using initial isocratic conditions of 70 % B, decreased the t_R drastically, so that the bioactive compounds eluted between 6 and 9 min. However, during the same time many other uncharacterized peaks occurred. Therefore, this method seemed insufficient for separation of the bioactive compound(s). Meanwhile, the separation with the initial isocratic conditions of 80 % B did not decrease the t_R , since the bioactive fractions eluted between 21 and 29 min (see **Figure 28**). However, the bioassays revealed two separate bioactive fractions, one ranging from 21 to 23 min and the other ranging from 27 to 29 min. Subsequent analysis of the bioactive fraction $t_R = 27$ min revealed a single peak

(see **Figure 29**). Therefore, the Waters XBridge BEH Amide column in combination with this method has been used for all further isolation experiments (see **Table 29**).

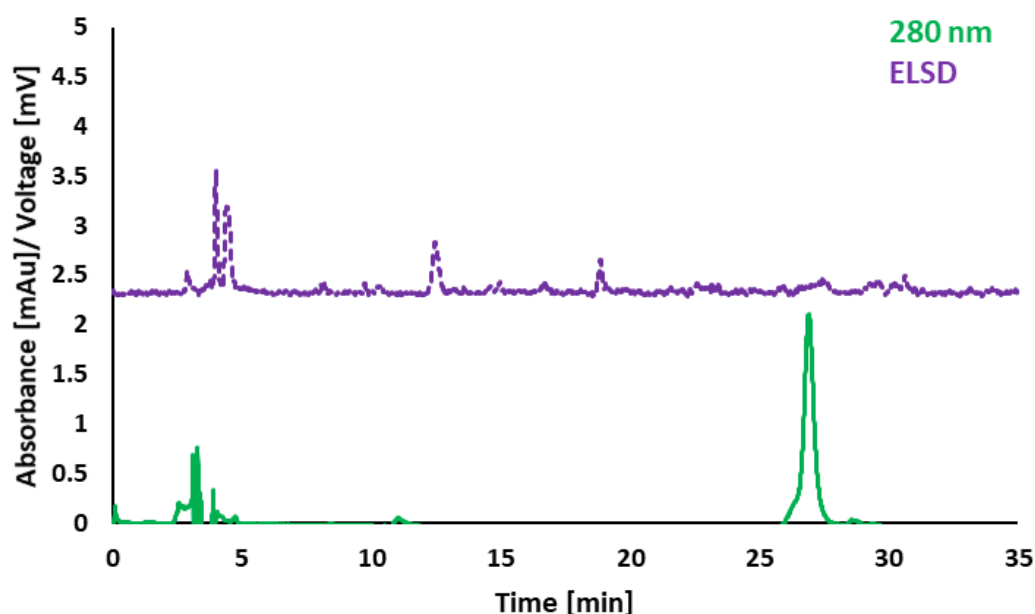


Figure 29. HPLC-DAD-ELSD chromatogram of the bioactive fraction $t_R = 27$ min using the Waters XBridge BEH Amide column

3.4.5.3 Dereplication of the hydrophilic metabolites from *S. sp.* Tü2401 liquid cultures

HPLC coupled with tandem mass spectrometry is a technique, where downstream to an HPLC multiple steps of mass spectrometry selection are performed. Leading to selection of defined masses during the first stage of mass spectrometry and subsequently to the fragmentation of these ions in between the first and the second mass spectrometry.³¹⁹ The second mass spectrometry step is needed to detect the fragment ions. The fragmentation pattern is compound specific and thus can be used to identify or dereplicate compounds.^{196,320–322} Several web tools use fragmentation patterns for dereplication, e.g. MetFrag, CFM-ID.^{323–327} These tools have in common that they need an accurate mass as well as the fragment pattern of the compound that needs to be dereplicated for precise predictions. In the next step, this pattern is compared to a database of fragmentation patterns. However, every tool has its own approach for the generation of the underlying database.

MetFrag creates in-silico fragmentation patterns, by simply breaking every bonds of candidate molecules from different databases e.g. ChemSpider.com, and subsequently scoring the likelihood for each break. Finally, these in-silico fragmentation patterns are matched against the mass list of the compound that needs to be dereplicated, resulting in a score, indicating the quality of the candidate spectrum assignment.³²³

CFM-ID is based on Competitive Fragmentation Modelling (CFM), a probabilistic generative model especially for ESI-MS² data that uses machine learning technique, able to learn from the data. Like MetFrag it finally ranks a list of candidate structures according to their matching score.³²⁵

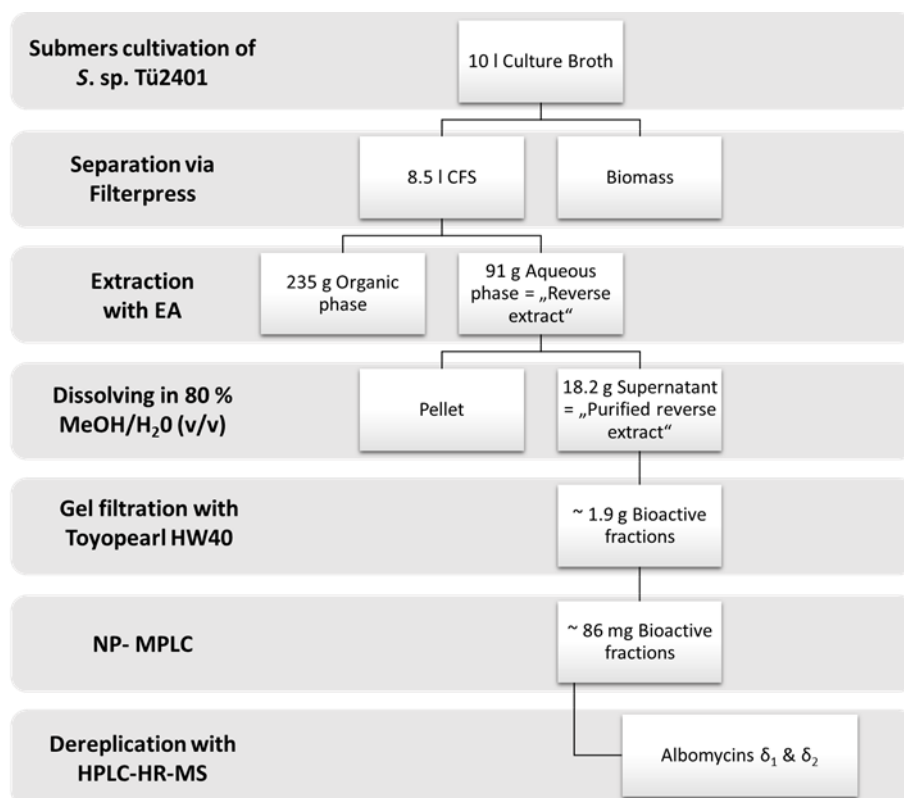


Figure 30. Isolation scheme for albomycin δ_1 and δ_2 .

In order to isolate the bioactive compounds produced by *S. sp. Tü2401* in submersive culture, many purification steps have been necessary to end up with bioactive single compound isolates (see **Figure 30**). The bioactive fractions $t_R = 21$ min and $t_R = 27$ min were finally analysed using HPLC-MS² (2.6.5), resulting in m/z $[M+H]^+$: 1004.2849 ($t_R = 21$ min) and 1046.3049 (27 min). The respective fragmentation pattern has been subsequently submitted to MetFrag. With the help of this tool, it was possible to identify the compounds albomycin δ_1 and δ_2 as

possible structures for the bioactive compounds. In order to confirm these findings, the HPLC-MS data were compared to those of albomycin δ_1 and δ_2 . After obtaining, these two compounds from an in-house compound library, they have been separately dissolved in 80 % ACN and submitted to the same analysis as the single compound isolates from *S. sp. Tü2401*. The data revealed equivalence in terms of retention times as well as of isotope patterns and masses (see **Figure 31**). Thus, it is legitimate to assign the bioactivity of *Streptomyces sp. Tü2401* to albomycin δ_1 and δ_2 .

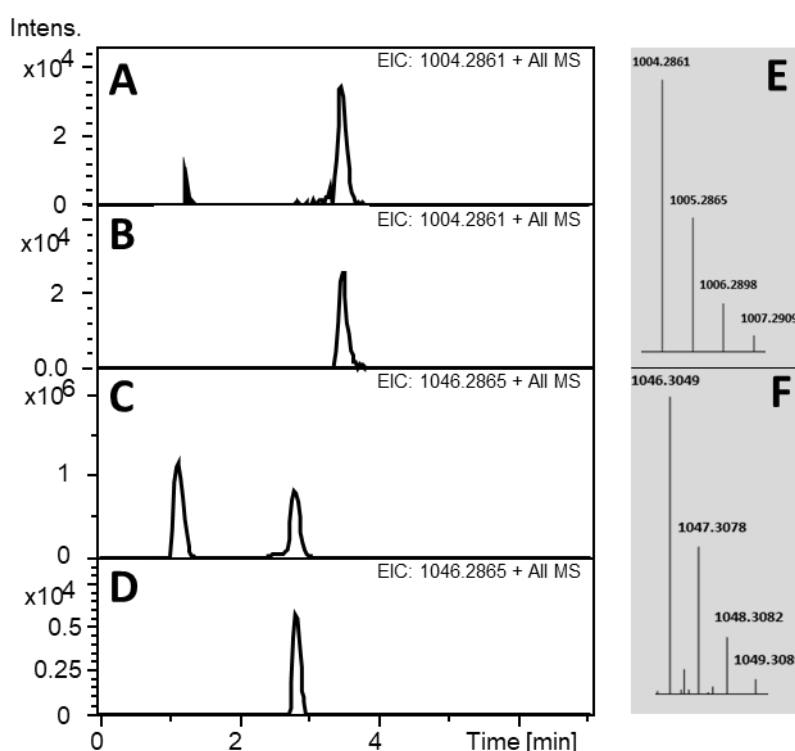


Figure 31. HPLC chromatograms and mass spectra of bioactive single compound isolates of *S. sp. Tü2401* and albomycin δ_1 and δ_2 control samples. A – D show the extracted ion chromatograms (EIC) of albomycin δ_1 (A), albomycin δ_2 (C), bioactive fraction $t_R = 21$ min from *S. sp. Tü2401* (B), and bioactive fraction $t_R = 27$ min from *S. sp. Tü2401*. The first peaks in A and C are due to control samples that were highly concentrated, leading to an additional peak contemporaneous with the injection peak. E & F depict the mass spectra of albomycin δ_1 (E) and δ_2 (F) that could be found in the control samples as well as the bioactive isolates of *S. sp. Tü2401*

Albomycins, originally called griseins, have been isolated from a *Streptomyces griseus* strain in 1947 in the Waksman Lab (see **1.3**).^{328–330} The structure of the albomycins were finally elucidated 35 years after the first reports in 1982 by Benz *et al.*^{331,332} Until now, three different albomycins are known: δ_1 , δ_2 , and ϵ (see **Figure 32**). They are composed of a

tri- δ -*N*-hydroxy-L-ornithine peptide siderophore and thioribosyl nucleoside moiety within six consecutive chiral centres.³³¹ This thionucleoside is considered to be the warhead of the albomycins, since it differs only in the C-4 substituent of the pyrimidine nucleobase.³³¹ The single thioribosyl nucleoside moiety of albomycin δ_2 , designated as SB-217452, has been isolated from a *Streptomyces* sp. ATCC 700974 strain.³³³ It had shown moderate inhibitory activity against bacterial seryl tRNA synthetases (SerRS) with IC₅₀ values of 8 mM.^{333,334} Besides this, SB-217452 exhibits weak antibacterial activity.³³³ Various studies have confirmed the importance of the siderophore moiety for the bioactivity of the albomycins.^{335,336} Gram-negative bacteria like *Escherichia coli* and *Salmonella facilitate* secrete the siderophore ferrichrome under iron limitation, which can subsequently be taken up again via a siderophore receptor.^{335,336} In fact, the siderophore moiety of albomycins mimics ferrichrome. Thus, they are taken up via the same route, hence this strategy is referred to as “Trojan Horse” strategy.^{335,336} Once internalised, the peptide is hydrolysed, releasing the active thioribosyl nucleoside moiety, and thus exerting the antibacterial activity.³³⁵ Accordingly, resistance mechanisms involve either a loss of peptidase activity or reduced uptake, and have been reported to develop rapidly.³³⁶ This phenomenon was confirmed in the *E. coli* K12 bioactivity tests using *S. sp.* Tü2401 (see **Figure 22**).

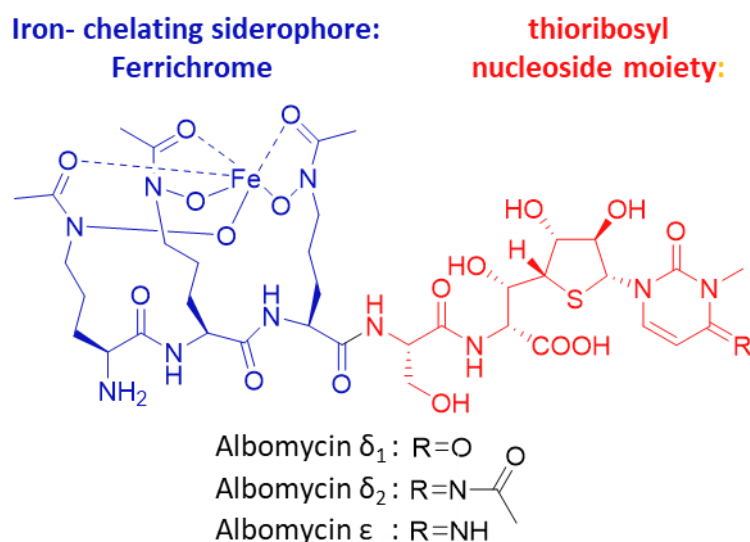


Figure 32. Structure of different albomycins contain a thioribosyl nucleoside moiety (red) linked to an iron- chelating hydroxamate siderophore (blue) through a serine residue (Adapted from Zeng *et al.* 2009)³³⁷

Due to their structures, the albomycins are assigned to the family of sideromycins that also comprises the naturally occurring compounds ferrimycin A1 from *Streptomyces griseoflavus* and the salmycins A – D from *Streptomyces violaceus*.^{335,338,339} They are all composed of hydroxamate-type siderophores and suffer all from the same resistance mechanism development that affects the siderophore uptake.³⁴⁰

Albomycins exhibit antibacterial activities against Gram-positive, including multi-drug resistant strains, but also against Gram-negative bacteria.^{331,341–343} Even though albomycin δ_2 was found to be more potent against most of the tested organisms, albomycin δ_1 turned out to be very active against *Neisseria gonorrhoeae* ATCC 49226 with a MIC of 3.9 ng/ml, while albomycin δ_2 was inactive.³³¹ This underlines the significance of the C-4 substituent for the biological activity towards different organisms. Particularly remarkable activities are the MIC values of 10 ng/ml against *Streptococcus pneumoniae* respectively 5 ng/ml against *Escherichia coli*, illustrating that albomycins are almost tenfold more potent than penicillin.^{331,344} This has also been confirmed in screening against 27 clinical isolates of *S. pneumoniae* and *S. aureus*, where albomycin δ_2 has been compared with ciprofloxacin, vancomycin, and penicillin G.³³¹ Albomycin δ_2 was mostly even more potent than all these antibiotics, showing in some case more 1000 times lower MIC values.³³¹ The presence of iron has a substantial influence on the biological activity of albomycin δ_2 against *S. pneumoniae*, since its antibiotic activity was not only increased during iron limitation, but also clinical isolates that were resistant under normal conditions became susceptible under iron-depleted conditions.³³¹ Activity against *S. aureus* and *E. coli* was not influenced by iron concentration.³³¹

In addition to these promising antibacterial activity data, albomycins did not exhibit toxicity during in-vivo studies in mice and have also been well tolerated.^{331,343} Thus it is no surprise that albomycins have already been successfully used in clinics in the Soviet Union.³⁴³

In recent years not only a total synthesis for albomycins δ_1 , δ_2 and ϵ has been developed, but also the BGC has been identified, making albomycin a valuable target for synthetic biology.^{331,334}

BLAST analysis of the genome of *S. sp. Tü2401* confirmed the presence of the albomycin BGC. However, since this genome cluster has not been identified by antiSMASH, the albomycins could not be identified earlier during the dereplication process.

3.5 *Streptomyces* sp. AcE210

In previous works, *Streptomyces* sp. AcE210 has been isolated from the root nodules of an alder tree. The ethyl acetate extract showed antibacterial activity against a co-isolated *Bacillus* sp. Subsequent HPLC analysis of this EA extract revealed 6 compounds that could not be dereplicated, using an in-house database (see **2.6.4; Table 8**). Within the course of this thesis, these compounds as well as another, co-eluting derivative could be identified as xanthocidin and congeners. Even though xanthocidin has first been described in 1966, the other 6 compounds have never been isolated from a *Streptomyces* sp. before.³⁴⁵ Xanthocidin belongs to the small group of cyclopentanone antibiotics, that in addition comprises of pentenomycins, vertimycin, sarkomycin and methylenomycins.^{346–349}

Moreover, the structural similarities of xanthocidin and some of its congeners to the methylenomycins A, B, and C, led to a biosynthesis hypothesis. Feeding studies with isotopically labelled [¹³C₅]-L-valine confirmed, that *Streptomyces* sp. AcE210 employs an isobutyryl-CoA starter unit, resulting in a branched side chain in xanthocidin. Moreover, analysis of the genome sequence of *Streptomyces* sp. AcE210 revealed a cluster of homologues to the *mmy* genes involved in methylenomycin biosynthesis.

The results have been summarized in the publications A and B.

A. Xanthocidin Derivatives from the Endophytic Streptomyces sp. AcE210 Provide Insight into Xanthocidin Biosynthesis

Ortlieb, Nico; Bretzel, Karin; Kulik, Andreas; Haas, Julian; Lüdeke, Steffen; Keilhofer, Nadine; Schrey, Silvia Diane; Gross, Harald; Niedermeyer, Timo Horst Johannes

ChemBioChem 19, 2472–2480 (2018); doi: 10.1002/cbic.201800467

Xanthocidin Derivatives from the Endophytic *Streptomyces* sp. AcE210 Provide Insight into Xanthocidin Biosynthesis

Nico Ortlieb,^[a, b, c] Karin Bretzel,^[a] Andreas Kulik,^[a] Julian Haas,^[d] Steffen Lüdeke,^[d]
Nadine Keilhofer,^[e] Silvia Diane Schrey,^[e, f] Harald Gross,^[b, g] and
Timo Horst Johannes Niedermeyer^{*[a, b, c]}

Xanthocidin and six new derivatives were isolated from the endophytic *Streptomyces* sp. AcE210. Their planar structures were elucidated by 1D and 2D NMR spectroscopy as well as by HRMS. The absolute configuration of one compound was determined by using vibrational circular dichroism spectroscopy (VCD). The structural similarities of xanthocidin and some of the isolated xanthocidin congeners to the methylenomycins A, B, and C suggested that the biosynthesis of these compounds might follow a similar route. Feeding studies with isotopically

labelled [¹³C₅]-L-valine showed that instead of utilizing acetyl-CoA as starter unit, which has been proposed for the methylenomycin biosynthesis, *Streptomyces* sp. AcE210 employs an isobutyryl-CoA starter unit, resulting in a branched side chain in xanthocidin. Further evidence for a comparable biosynthesis was given by the analysis of the genome sequence of *Streptomyces* sp. AcE210 that revealed a cluster of homologues to the *mmv* genes involved in methylenomycin biosynthesis.

Introduction

Xanthocidin (**1**), first isolated from *Streptomyces xanthocidicus* in 1966,^[1,2] is a compound with moderate antibiotic activity against *Escherichia coli*, *Bacillus agri*, and *Xanthomonas oryzae*.^[1] Additionally, its cytotoxic potential as topoisomerase II α inhibitor has been discussed.^[3] Since the original producer

strain had lost its ability to produce **1**,^[4] total synthesis^[5,6] was the only way to obtain this compound, and only few studies on the biological activity of xanthocidin have been performed.

Xanthocidin belongs to the small group of cyclopentanone antibiotics that have been found to be produced by various *Streptomyces* spp., and also by the fungus *Phialophora asteris*.^[7] Other representatives of the cyclopentanone antibiotics are pentenomycin,^[8] cryptosporiopsin,^[7] and sarkomycin.^[9] The latter has been used in antitumour therapy in Japan.^[10] The best studied members of this compound family, however, are methylenomycin A and B.^[11] The identification^[12] and sequencing of the *mmv* gene cluster of genes that encode the biosynthesis of the methylenomycins (Figure 5),^[13] as well as a re-investigation of the primary metabolic origin of the methylenomycins by radiolabelling studies, have led to a hypothesis of their biosynthesis.^[14] The methylenomycin biosynthesis is the only cyclopentanone antibiotic biosynthesis that has been studied to date.

In this study, we rediscovered xanthocidin (**1**) from the culture filtrate of *Streptomyces* sp. AcE210. In addition to **1**, six naturally occurring xanthocidin derivatives could be identified. Their structures were solved by HRMS, NMR spectroscopy, and VCD spectroscopy. Since the biosynthesis pathway of xanthocidin is yet undescribed, we set out to explore its biosynthesis. The isolated compounds show high analogy to compounds from the methylenomycin compound family. Due to the close structural resemblance between the xanthocidins and the methylenomycins, we assumed that their biosynthesis proceeds via a similar pathway. We hypothesized that *Streptomyces* sp. AcE210 employs isobutyryl-CoA instead of acetyl-CoA as starter unit, resulting in a branched side chain in xanthocidin. Based on this hypothesis, we report a precursor incorpora-

[a] N. Ortlieb, K. Bretzel, A. Kulik, Prof. Dr. T. H. J. Niedermeyer
Department of Microbiology and Biotechnology
Interfaculty Institute of Microbiology and Infection Medicine
Eberhard Karls University Tübingen
Auf der Morgenstelle 28, 72076 Tübingen (Germany)

[b] N. Ortlieb, Prof. Dr. H. Gross, Prof. Dr. T. H. J. Niedermeyer
German Centre for Infection Research (DZIF)
Partner Site Tübingen, Tübingen (Germany)


[c] N. Ortlieb, Prof. Dr. T. H. J. Niedermeyer
Department of Pharmaceutical Biology/Pharmacognosy
Institute of Pharmacy, Martin-Luther-University Halle-Wittenberg
Hoher Weg 8, 06120 Halle (Saale) (Germany)
E-mail: timo.niedermeyer@pharmazie.uni-halle.de

[d] Dr. J. Haas, Dr. S. Lüdeke
Institute of Pharmaceutical Sciences, Albert-Ludwigs-University Freiburg
Albertstrasse 25, 79104 Freiburg (Germany)

[e] Dr. N. Keilhofer, Dr. S. D. Schrey
Department of Physiological Ecology of Plants
Interfaculty Institute of Microbiology and Infection Medicine
Eberhard Karls University Tübingen
Auf der Morgenstelle 5, 72076, Tübingen (Germany)

[f] Dr. S. D. Schrey
IBG-2: Plant Sciences, Forschungszentrum Jülich
52425 Jülich (Germany)

[g] Prof. Dr. H. Gross
Department of Pharmaceutical Biology, Pharmaceutical Institute
Eberhard Karls University Tübingen
Auf der Morgenstelle 8, 72076 Tübingen (Germany)

 Supporting information and the ORCID identification numbers for the authors of this article can be found under <https://doi.org/10.1002/cbic.201800467>.

the presence of an additional proton ($\delta_{\text{H}}=4.38$ ppm) and hydroxy group ($\delta_{\text{H}}=3.90$ ppm). This finding, together with the molecular formula, determined to be $\text{C}_{11}\text{H}_{18}\text{O}_5$ by HRMS, and the UV spectrum, being similar to that of **1**, suggested that compound **2** is a derivative of xanthocidin, reduced at C-3. This was supported by the high-field shift of the signal of C-3 ($\delta_{\text{C}}=78.8$ ppm) compared to the signal of C-3 of xanthocidin ($\delta_{\text{C}}=206.4$ ppm).^[6] HMBC data (Table 1, Figure 1) also support-

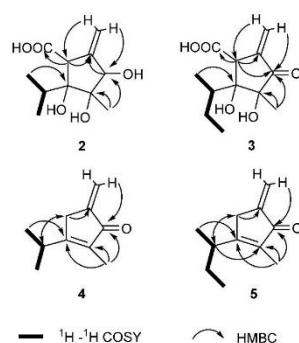


Figure 1. COSY and key HMBC correlations for compounds 2–5.

ed this structure. Thus, compound **2** was identified as dihydroxanthocidin. Interestingly, the methylene protons at C-7 couple with the proton at C-1 and C-3, resulting in ^1H spectra with coupling patterns that are more complex than initially expected. Compound **3** was isolated as a white, amorphous solid. The high similarity of the ^1H NMR spectrum to the spectrum of **1**, showing only two additional signals from diastereotopic methylene protons (H-11: $\delta_{\text{H}}=1.63, 1.14$ ppm; $\delta_{\text{C}}=23.4$ ppm) in the aliphatic range (Table 1), and the UV spectrum, which is similar to that of **1**, suggested that compound **3** is also a derivative of xanthocidin. Furthermore, the molecular formula of **3**, $\text{C}_{12}\text{H}_{18}\text{O}_5$ according to HRMS, differs from that of **1** by an additional CH_2 . Hence, we suspected a variation in the isopropyl

side chain of **1**. C-9 was assigned to be a tertiary carbon by ^1H NMR data. COSY data (Figure 1) showed it to have a neighbouring CH_2 (C-11) as well as a CH_3 group (C-10), which indicated another bond to a quaternary carbon. This was confirmed by HMBC correlations of H-9 to C-4 (Table 2, Figure 1). Thus, the structure of compound **3** was revealed to be homoxanthocidin. However, the absolute configuration of C-11 could not be deduced based on NMR experiments.

Compounds **4** and **5** showed similar UV spectra with maxima at 246 nm and 270 nm. After purification of the compounds by preparative HPLC, they were found to be highly volatile. It has not been possible to obtain them in dry form by evaporation of the HPLC mobile phase. Thus, upon isolation by preparative HPLC, solid phase extraction (SPE) was used to capture the compounds from the HPLC eluate. After adsorption of the compounds to the solid phase, compounds **4** and **5** were eluted from the respective SPE cartridges using $[\text{D}_3]\text{acetonitrile}$. Their ^1H NMR spectra looked similar, with **5** showing an additional CH_2 group ($\delta_{\text{H}}=1.51$ ppm). This was confirmed by the molecular formulae of the compounds determined by HRMS ($\text{C}_{10}\text{H}_{14}\text{O}$ for **4**, $\text{C}_{11}\text{H}_{16}\text{O}$ for **5**). Thus, **5** must possess an additional CH_2 group in the aliphatic side chain, comparable to **3**. The molecular formulae afforded four degrees of unsaturation. The ^1H NMR spectrum together with the HSQC spectrum indicated that all protons in the molecules are attached to carbons, proving the absence of OH or COOH groups. However, similar to xanthocidin (**1**), **4** and **5** showed diastereotopic methylene protons (H-6) as well as one methyl group (H-7) and an aliphatic side chain (**4**: H-8 and 9; **5**: H-8 to 11; Table 2). COSY experiments revealed that the side chain in the case of compound **4** is an isopropyl group (as also found in **1** and **2**), whereas it is a 1-methylpropyl group in compound **5** (as also found in **3**). The HMBC spectrum showed correlations between the methyl group protons (H-7) and the three quaternary carbons C-1, C-2, and C-3. C-1 showed the characteristic chemical shift of a keto group ($\delta_{\text{C}}=197.2$ ppm (**4**); 197.2 ppm (**5**)). The deshielded signals of C-2 and C-3 indicated the presence of a double bond between those carbons, while the low field shift of C-3 suggested that this double bond is conjugated to the keto group at C-1, and that C-3 is

Table 2. ^1H NMR and ^{13}C NMR data of compounds 4 and 5 in $[\text{D}_3]\text{acetonitrile}$ (600 MHz for ^1H , 150 MHz for ^{13}C).					
Position	Xanthocidin B (4)		HMBC ^[a]	Homoxanthocidin B (5)	
	δ_{C} , type	δ_{H} (ν [Hz])		δ_{C} , type	δ_{H} (ν [Hz])
1	197.2, C			197.2, C	
2	136.6, C			138.2, C	
3	174.8, C			173.7, C	
4	30.8, CH_2	3.13, m	2, 3, 5	31.4, CH_2	3.09, m
5	143.4, C			143.4, C	
6	114.9, CH_2	5.37, m	1, 4	115.2, CH_2	5.36, m
		5.91, m	1, 4, 5		5.91, m
7	8.0, CH_3	1.73, t (2.2)	1, 2, 3	8.9, CH_3	1.73, t (2.2)
8	29.5, CH	3.09, sept (7.0)	2, 3, 4, 9	37.0, CH	2.84, m
9	20.4, CH_3	1.12, d (7.0)	3, 8, 9	28.7, CH_2	1.51, m
10				12.5, CH_3	0.84, t (7.4)
11				18.6, CH_3	1.10, d (6.8)

[a] HMBC correlations are from proton(s) stated to the indicated carbon.

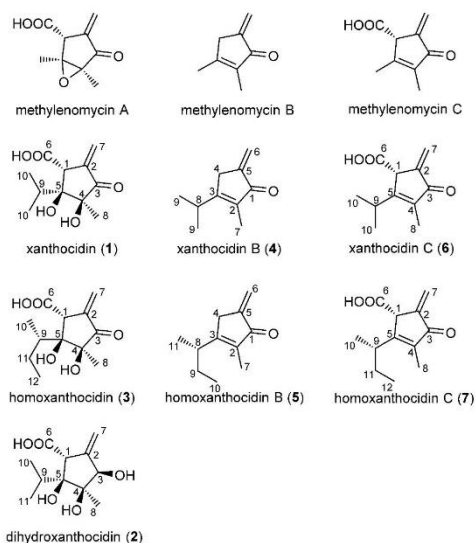
tion study with isotopically labelled [$^{13}\text{C}_5$]-L-valine, a potential biosynthetic precursor of the isobutyryl residue, confirming this hypothesis, and indicating that the starting building blocks for xanthocidin biosynthesis are derived from amino acids. Additionally, we performed a preliminary *in silico* analysis of the genome sequence, which allowed us to identify and annotate the corresponding candidate biosynthetic genes.

Results and Discussion

As part of our efforts to discover new bioactive compounds from microorganisms, we focused on isolating actinomycetes from selected ecological niches, since previous work has shown that such niches frequently harbour strains that produce compounds of interest.^[15] Alder (*Alnus glutinosa*) root nodules develop in response to N_2 -fixing actinomycetes of the genus *Frankia*, resulting in a symbiosis that hosts further associated microbes^[16] which can affect establishment and functioning of the nodule.^[17] *Streptomyces* sp. AcE210 was isolated from a mature root nodule of an alder tree, growing in Tübingen, Germany. The EtOAc extract from the acidified culture filtrate of *Streptomyces* sp. AcE210 showed several peaks in the HPLC chromatogram that could not be dereplicated using our in-house database (Figure S1). Consequently, the extract was fractionated using RP-flash chromatography, and the respective compounds were subsequently purified using preparative RP-HPLC, resulting in compounds 1–5. In addition, HR-MS helped to identify compounds 6 and 7 in the crude extract.

Structure elucidation of the xanthocidins

Compound 1 was isolated as a white amorphous powder. HRMS data for 1 were consistent with the molecular formula $\text{C}_{11}\text{H}_{16}\text{O}_5$. Based on this molecular formula and the compound's ^1H NMR data, compound 1 was identified as xanthocidin. In order to determine the relative stereochemistry, NOESY experi-



ments were performed, showing correlations between the two OH as well as between the COOH and H-10 and H-8. Additionally, the optical rotation was found to be $[\alpha]_{\text{D}}^{25} = +23.6^\circ$. As this agrees with the original data published in 1994, we identified compound 1 as (+)-xanthocidin.^[4]

Compound 2 was obtained as a white-yellow, amorphous solid. The ^1H NMR data (Table 1) showed three OH protons ($\delta_{\text{H}} = 4.99$, $\delta_{\text{H}} = 4.45$, $\delta_{\text{H}} = 3.90$ ppm) and one very broad COOH signal ($\delta_{\text{H}} = 12.18$ ppm). Comparison of these data with the ^1H NMR data of 1 revealed a high similarity of the spectra with the exception that the NMR spectrum of compound 2 showed

Table 1. ^1H NMR and ^{13}C NMR data of compounds 2 and 3 in $[\text{D}_6]\text{DMSO}$ (600 MHz for ^1H , 150 MHz for ^{13}C).

Position	δ_{C} , type	Dihydroxanthocidin (2)		δ_{C} , type	Homoxanthocidin (3)	
		δ_{H} (J [Hz])	HMBC ^[a]		δ_{H} (J [Hz])	HMBC ^[a]
1	56.5, CH	3.29, m	2, 4, 5, 6, 7	54.0, CH	3.71, t (2.0)	2, 3, 4, 6, 7
2	148.6, C			140.8, C		
3	78.8, CH	4.38, m	2, 4, 5, 7, 8	206.7, C		
3-OH		4.45, brs				
4	80.80, C			80.8, C		
4-OH		4.99, brs			5.30, s	1, 4, 5, 6
5	80.61, C			80.9, C		
5-OH		3.90, s	1, 4, 5, 6		4.29, s	3, 4, 5, 8
6	173.1, C	12.18, brs		172.3, C	12.68, brs	
7	106.7, CH_2	4.92, m	1, 2, 3	121.5, CH_2	5.61, m	1, 2, 3, 6
		5.10, m	1, 2, 3		6.13, m	1, 2, 3, 6
8	14.9, CH_3	1.09, s	3, 4, 5	19.3, CH_3	1.3, s	3, 4, 5
9	29.1, CH	2.28, sept (6.7)	4, 5, 11	35.8, CH	1.88, m	4, 10, 11, 12
10	16.7, CH_2	0.93, d (6.7)	4, 5, 9, 11	12.4, CH_2	0.97, d (6.6)	5, 9, 11, 12
11	17.6, CH_3	0.80, d (6.7)	4, 5, 9, 10	23.4, CH_3	1.15, m	9, 10
					1.63, m	5, 9, 10
12				11.6, CH_3	0.86, t (7.4)	9, 10, 11

[a] HMBC correlations are from proton(s) stated to the indicated carbon.

located in the β position with respect to the keto group. The HMBC spectrum revealed correlations between the diastereotopic methylene protons (H-6) and C-1, C-4 and C-5. C-5 must be connected to the methylene group, due to its low field carbon shift of $\delta_{\text{C}}=143.4$ ppm (**4**, **5**). Since H-8 shows correlations with C-4 as well as with C-2 and C-3 (Table 2; Figure 1), compounds **4** and **5** feature the same cyclopentane scaffold as xanthocidin (**1**). From these results, the structures of **4** and **5** were elucidated as xanthocidin B (**4**), and homoxanthocidin B (**5**). In order to determine the absolute configuration of C-8 in **5**, VCD experiments were performed and compared to a spectrum calculated for the *S*-enantiomer at the B3LYP/6-311G(d,p) level in Gaussian 09.^[18] Despite the low signal-to-noise ratio of the VCD spectrum, a good agreement between the calculated and observed spectra, particularly of the strong $-+-+$ pattern between 1340 and 1245 cm^{-1} (C–C single bond stretch vibrations of the ring and C–H wagging modes of the side chain) allows the unambiguous assignment of the *S*-configuration (Figure 2).

Compounds **6** and **7** showed UV spectra similar to those of **4** and **5** with maxima at 246 nm and 270 nm. Due to the chemical instability of **6** and **7**, it has not been possible to isolate these two compounds in pure form. Compound **6** degraded to compound **4**, while compound **7** degraded to **5**. However,

HRMS experiments revealed a molecular formula of $\text{C}_{11}\text{H}_{14}\text{O}_3$ for **6**, and $\text{C}_{12}\text{H}_{16}\text{O}_3$ for **7**, suggesting **6** and **7** to be carboxylated derivatives of **4** and **5**. Since the extraction of the *Streptomyces* sp. AcE210 supernatant was performed at pH 2, loss of CO_2 is presumably the result of an acid-promoted decarboxylation. This is in agreement with the observation that methylenomycin B, which shows high structural similarity to **4** and **5** (the only difference is found in the aliphatic side chain), is a degradation product of methylenomycin C, being produced under acidic conditions.^[14,19] Thus it is conceivable that, in analogy to the degradation of methylenomycin C to methylenomycin B, compounds **4** and **5** represent the decarboxylated degradation products of compounds **6** and **7** (xanthocidin C and homoxanthocidin C). Methylenomycin C has been shown by radiolabelling experiments to be a biosynthetic precursor of methylenomycin A.^[20] We assume that this is also the case for the xanthocidins (thus compounds **4** and **1** as well as **5** and **3**). Since **5** is the degradation product of **7**, while **7** is most likely a biosynthetic precursor of **3**, we assume that all three compounds with a chiral side chain (**3**, **5**, and **7**) have the same *S*-configuration at the side chain chiral carbon.

Biosynthesis of xanthocidin

Since the original xanthocidin producer strain *S. xanthocidicus* has lost its ability to produce the compound, no studies investigating xanthocidin biosynthesis have been performed.^[4] Due to the structural similarity of methylenomycins A, B, and C with **1**, **4**, and **6**, we suspected that both compound families are biosynthesized in a similar way. In the original methylenomycin producer strain *Streptomyces coelicolor* A3(2), the biosynthesis genes for methylenomycin (*mmy*) are located on the linear plasmid SCP1, which can remain autonomous or integrate into the chromosome.^[12] Even though this has been known since 1977, it took until 2004 to describe the full sequence of the *mmy* genes encoding the methylenomycin biosynthesis.^[21] Based on these findings, Corre and Challis proposed a putative biosynthetic pathway (Figure 3A), and confirmed it by isotope labelling experiments.^[14,22] In brief, the ketoacyl synthase III (KASIII) MmyC catalyses in a first step the condensation of acetyl-CoA with malonyl-MmyA (MmyA being an acyl carrier protein), forming acetoacetyl-MmyA. In the next step, this acetoacetyl-MmyA is condensed with a pentulose to form a butenolide intermediate, catalysed by MmyD. MmyD shows 47% amino acid similarity with the syringolide biosynthetic protein AvrD from *Pseudomonas syringae*,^[14] which has been proposed to catalyse the condensation of a β -ketoheptanoyl-CoA with xylose-5-phosphate to form a butenolide intermediate.^[23] Unfortunately, there is no direct evidence for the catalytic function of MmyD, for example from feeding experiments. Nevertheless, its feasibility has been shown by biomimetic synthesis studies.^[14,24] Methylenomycin A is finally formed from the butenolide intermediate by a complex rearrangement, undergoing an aldol condensation, a lactone hydrolysis and several reduction and oxidation steps.^[14] Radiolabelling studies showed that methylenomycin C is a biosynthetic precursor of methylenomycin A.^[20]

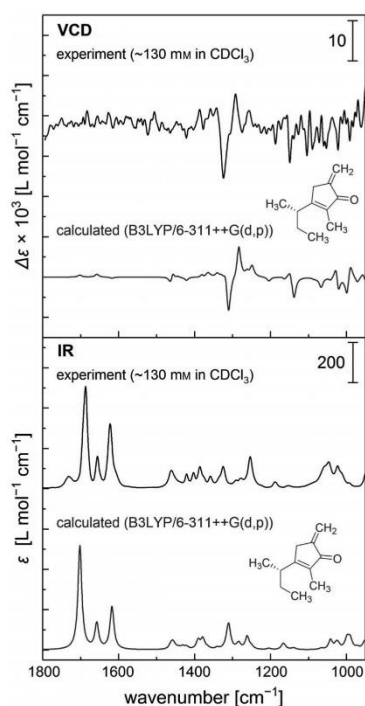


Figure 2. Experimental and calculated VCD and IR spectra of (*S*)-**5**.

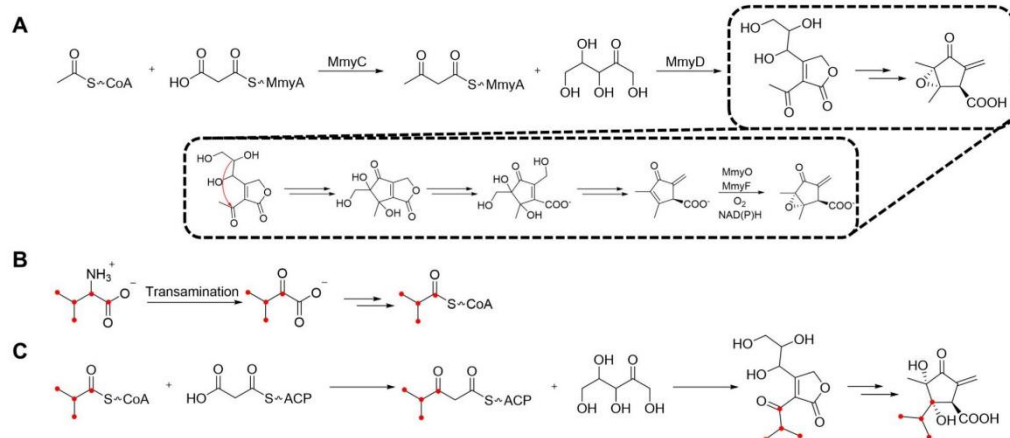


Figure 3. A) Biosynthesis of methylenomycin according to Corre and Challis,^{14,22} red arrow indicating aldol condensation. B) Metabolism of $^{13}\text{C}_5$ labelled valine to isobutyryl-CoA^{25,26} (red dots indicating labelled atoms). C) Putative biosynthesis of xanthocidin (red dots indicating labelled atoms).

Corre and Challis have proposed that MmyC is highly selective for acetyl-CoA over isobutyryl-, isovaleryl- or 2-methylbutyryl-CoA, which is surprising, since the KASIII in *Streptomyces* are usually more promiscuous.^{14,27}

From the structures of **1** and **3**, we hypothesized that the protein corresponding to MmyC in our strain, *Streptomyces* sp. AcE210, is rather selective for isobutyryl-, or 2-methylbutyryl-CoA, thus resulting in the production of **1–7** instead of methylenomycin (Figure 3C). It is known that these starter units are commonly used for the production of branched-chain fatty acids in *Streptomyces*,²⁸ and that these precursors are derived from valine or isoleucine, respectively (Figure 3B).^{25,26,29} Indeed, the *S*-configuration of the chiral carbon in the side chain of **3**, **5**, and **7** supported our hypothesis that the putative 2-methylbutyryl-CoA starter unit might be derived from L-isoleucine.

To confirm this hypothesis, we performed pulsed, stable-isotope-labelled feeding experiments using [$^{13}\text{C}_5$]-L-valine (1 mg mL^{-1}) at 24, 48, and 72 h after inoculation of the main culture. After 96 h of incubation, the cultures were extracted and analysed by HPLC-MS.

Since production of xanthocidin in *Streptomyces* sp. AcE210 was very sensitive regarding the culture conditions, the experiments were performed in a complex medium, so that [$^{13}\text{C}_5$]-L-valine was not the only carbon source. Thus, also non-labelled xanthocidin should have been produced. This was indeed the case. However, in the cultures fed with [$^{13}\text{C}_5$]-L-valine, besides the peaks for the non-labelled xanthocidin and its derivatives, we observed additional peaks with a shift to higher masses (+4). These additional peaks were detectable for **1**, **2**, **4**, and **6**, which all feature the isopropyl side chain putatively originating from an isobutyryl-CoA starter unit (Figure 4). These additional mass shifted peaks were not observed for **3**, **5**, and **7**. This is consistent with our hypothesis that these compounds do not utilize isobutyryl-CoA as a starter unit, but rather accept a dif-

ferent starter unit, most likely 2-methylbutyryl-CoA, originating from L-isoleucine. We did, however, not conduct feeding trials with labelled L-isoleucine to further substantiate this.

To prove that this +4 mass-shift was caused by the postulated isobutyryl-CoA starter unit, **4** has been isolated from control cultures and from cultures supplemented with [$^{13}\text{C}_5$]-L-valine. **4** and [$^{13}\text{C}_4$]-**4** were analysed by ^{13}C NMR spectroscopy. Labelling of C-3, C-8, and C-9 was confirmed both by peak intensity increase as well as signal splitting for C-3 (dd, $J=42.5$ and 1.5 Hz; calculated $J=44.1$ and 6.1 Hz), C-8 (dt, $J=42.7$ and 33.7 Hz; calculated $J=44.1$ and 34.3 Hz), and C-9 (dd, $J=33.7$ and 1.5 Hz; calculated $J=34.3$ and 6.1 Hz; Figure S24). Thus, the isopropyl side chain of the xanthocidins is indeed originating from isobutyryl-CoA, which in turn is derived from the amino acid valine.

AntiSMASH³⁰ analysis of the genomic sequence of *Streptomyces* sp. AcE210 revealed only a minor similarity to the methylenomycin biosynthetic gene cluster (BGC). Therefore, the genome analysis was complemented with manual BLAST analyses.³¹ The latter revealed the presence of a comparable equivalent of the intertwined *mmy*-*mmf* gene cluster coding for methylenomycins and methylenomycin furans, respectively, the *xc*i cluster of *Streptomyces* sp. AcE210. However, in contrast to the reported *mmy*-*mmf* BGCs from *S. coelicolor* A3(2) and *S. violaceoruber* SANK95570, the *xc*i gene cluster is shorter by one gene and is heavily rearranged (Figure 5). The genes *xc*iA, *xc*iC, and *xc*iD, homologues to the essential genes *mmy*A, *mmy*C and *mmy*D (Figure 3A) which are required for the early steps of methylenomycin biosynthesis,¹⁴ could be readily detected in the *xc*i cluster. We speculate that XciD possesses a different substrate specificity and prefers branched substrates over linear precursors. However, the genome of *Streptomyces* sp. AcE210 lacks direct homologues for the biosynthetic genes *mmy*YFPKGO (coding for redox, ATP-binding and hypothetical proteins) and the regulator gene *mmy*B. This is on one hand

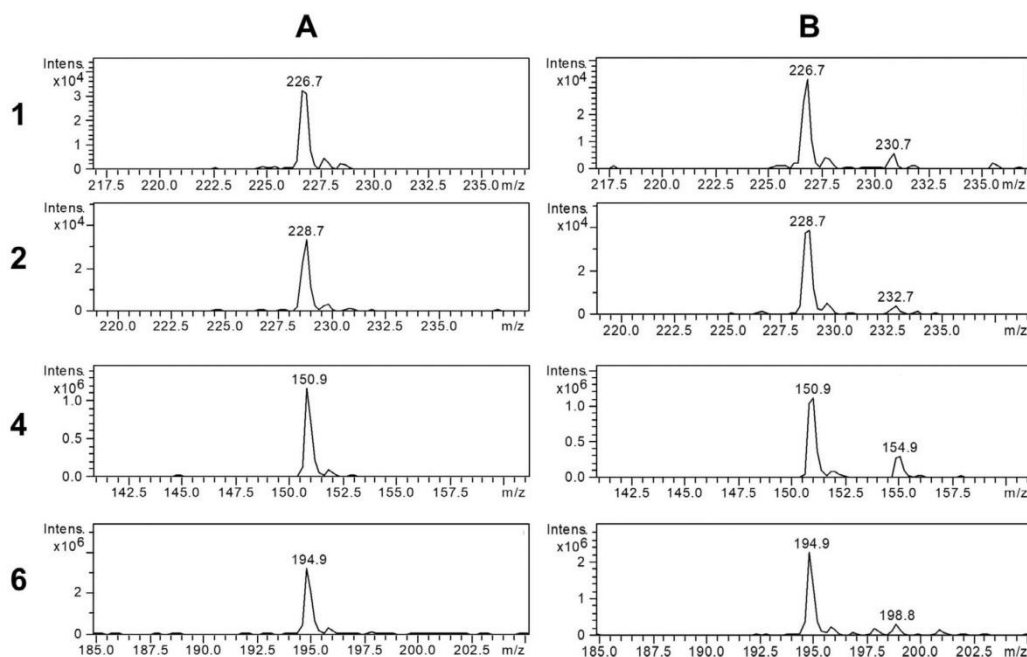


Figure 4. HPLC-MS analysis of the feeding experiments. Mass spectra at the peak apex of compounds **1** (m/z 227 $[M-H]^-$), **2** (m/z 229 $[M-H]^-$), **4** (m/z 151 $[M+H]^+$), **6** (m/z 195 $[M+H]^+$): A) the unlabelled control samples, and B) samples after $[^{13}C_4]$ -L-valine feeding. For all compounds an additional peak is visible in the extracts of the fed cultures, exhibiting a mass shift of +4, indicating the incorporation of four carbon atoms of one labelled $[^{13}C_4]$ -L-valine into the molecule.

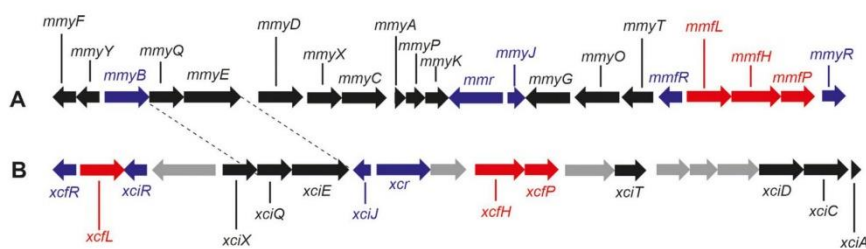


Figure 5. A) Organization of the *mmy*-*mmf* gene cluster on the SCP1 plasmid of *S. coelicolor* A3(2). B) Organization of the *mmy*-*mmf* gene cluster equivalent of *Streptomyces* sp. AcE210. Blue: regulation and resistance genes; black: methylenomycin biosynthesis genes (*mmy*); red: methylenomycin furan biosynthesis (*mmf*) genes; grey: hypothetical genes.

surprising since *mmyB*, *mmyF* and *mmyY* have been shown to be essential for methylenomycin production.^[32] On the other hand, six gene candidates are present in the *xci* cluster of strain *Streptomyces* sp. AcE210, the products of which do not show a significant level of AA identity with the products of *mmyYFPKGO*, but are predicted to have similar functions (Table S26) and might confer for the structural difference between methylenomycins and xanthocidins. Concerning *mmfLHP*, homologues of all three essential genes could be found.^[32] In contrast to their clustering in the reported methyl-

enomycin BGC, they are organized as a split cluster in *Streptomyces* sp. AcE 210 (Figure 5). However, they still might be functional, as a compound with the molecular mass of methylenomycin furan MMF2^[33] could be detected in an extract of *Streptomyces* sp. AcE210 by LC-MS/MS in cultures harvested and extracted within the timeframe of 20–60 h. Due to their postulated autoinducer function, furan production precedes slightly the production of the xanthocidins. The putative functions of the genes in the *xci* gene cluster are summarised in the Supporting Information (Table S26).

Conclusion

In conclusion, we have identified *Streptomyces* sp. AcE210 as a producer of xanthocidin and six new xanthocidin derivatives. This gave us the opportunity to revisit the biosynthesis of this compound class. The noticeable structural similarity of these compounds to methylenomycins A, B, and C led to the assumption that the biosynthesis of these compounds might be similar. Instead of utilizing acetyl-CoA as starter unit, *Streptomyces* sp. AcE210 employs isobutyryl-CoA for the biosynthesis of xanthocidin, resulting in an isopropyl side chain attached to the characteristic cyclopentane core structure. Feeding experiments with isotopically labelled [$^{13}\text{C}_5$]-L-valine confirmed this hypothesis. Additionally, analysis of the genome sequence of *Streptomyces* sp. AcE210 revealed clustered homologues to the *mmv* genes involved in methylenomycin biosynthesis. However, it would be necessary to perform knock-out and complementation experiments in order to confirm that this cluster is indeed responsible for xanthocidin biosynthesis.

Experimental Section

General experimental procedures: The optical rotation was measured using a Jasco P-2000 polarimeter at a wavelength of 589 nm (sodium D line) using a 10 mm cell with a total volume of 200 μL . The NMR experiments for structure elucidation were performed on a Bruker Avance-II spectrometer operating at 600 MHz (^1H) or 150 MHz (^{13}C). The NMR experiments for the incorporation study were done on a Bruker Avance III HD 400 spectrometer at 100 MHz (^{13}C). As solvents, [D_2]DMSO and [D_2]acetonitrile were used. The chemical shifts were referenced to the residual protonated solvent signals of [D_2]DMSO ($\delta_{\text{H}}=2.49$ ppm, $\delta_{\text{C}}=39.5$ ppm) and [D_2]acetonitrile ($\delta_{\text{H}}=1.94$ ppm, $\delta_{\text{C}}=118.7$ ppm), respectively. All NMR raw data are deposited in an OA repository (DOI: 10.6084/m9.figshare.6923447). NMR data were evaluated using ACD/Structure Elucidator 2017.2; for C–C coupling constants predictions, ACD/C+H NMR Predictors and DB 2017.2 was used (Advanced Chemistry Development, Inc.). HRESIMS analyses were performed using a Bruker Maxis-4G High Resolution ESI-TOF mass spectrometer and a Waters Synapt G2S High Resolution ESI-TOF mass spectrometer. HPLC analysis was carried out with a Nucleosil 100-C18 column (5 μm ; 125 \times 3 mm, precolumn [10 \times 3 mm]; Dr. Maisch GmbH, Ammerbuch, Germany) and a LC system 1260 (Agilent Technologies, Waldbronn, Germany) using a binary gradient of acetonitrile and deionized H_2O , each supplemented with 0.1% formic acid, with a flow rate of 1.5 mL min^{-1} from 5% to 100% acetonitrile over 15 min at a column temperature of 25 $^\circ\text{C}$. Data evaluation was conducted with ChemStation for LC 3D systems version B.04.03[16] software (Agilent Technologies, Waldbronn, Germany). HPLC-ESI-MS analysis was carried out with a Nucleosil 100-C18 column (3 μm ; 100 \times 2 mm, precolumn [10 \times 2 mm]; Dr. Maisch GmbH, Ammerbuch, Germany) and an LC/MSD Ultra Trap system XCT 6330 (Agilent Technologies, Waldbronn, Germany) using a method previously described by Jahn et al.^[34] Data evaluation was conducted with DataAnalysis for 6300 series Ion Trap LC/MS 6.1 version 3.4 software (Bruker Daltonik, Bremen, Germany).

Strain isolation and taxonomy: *Streptomyces* sp. AcE210 was isolated from root nodules of black alder trees (*Alnus glutinosa* (L.) Gaertn.). Root samples exhibiting mature nodules of 2–5 cm diameter were collected from alder trees close to Tübingen University,

Germany (48.537521, 9.031931) in April 2012. Root nodules were thoroughly cleaned by removing adhering soil particles using a toothbrush and running tap water before rinsing with sterile VE water. Under sterile conditions, nodules were cracked open and fragments of approximately 0.5 \times 0.5 cm size were added to 50 mL of HNC medium^[35] (6% yeast extract, 0.05% SDS, 0.05% CaCl_2 , pH 7.0) and incubated at 42 $^\circ\text{C}$ with shaking for 30 min. The suspension was filtered through a fine glass mesh, and a dilution series was prepared. The filtered suspensions were plated onto ISP-2 agar^[36] containing 5 g L^{-1} cycloheximide, 2 g L^{-1} nalidixic acid, and 5 g L^{-1} nystatin. After 8 d at 27 $^\circ\text{C}$, *Streptomyces* sp. AcE210 and eight further actinomycete isolates could be distinguished according to their morphological appearance.^[37] These were transferred to and subsequently maintained on ISP-2 agar.

Taxonomic classification of *Streptomyces* sp. AcE210 was carried out by whole genome sequencing. The genomic DNA extraction was performed using the Qiagen Genomic-tip 100/G kit (Qiagen, Hilden, Germany) following the manufacturer's protocol. The DNA sequence was subsequently submitted to the autoMLST program^[38] in order to automatically generate a species phylogeny with reference organisms, identifying the phylogenetic neighbours. As a result, *Streptomyces alboflavus* NRRL B-2373T and *Streptomyces avermitilis* DSM 46492 appeared as the closest relatives with an estimated average nucleotide identity (ANI) of 84.1% (Mash distance: 0.1586), which indicates that *Streptomyces* sp. AcE210 apparently belongs to a yet undescribed species (Figure S25). The genome sequencing of the strain has been described in the respective genome announcement.^[39] *Streptomyces* sp. AcE210 has been deposited in the Tübingen strain collection of actinobacteria.

Fermentation and extraction: A pre-culture was produced by growing *Streptomyces* sp. AcE210 in five 500 mL Erlenmeyer flasks, equipped with baffle and spiral, each containing 100 mL of NL410 medium (dextrose 1%, glycerol 1%, oat meal 0.5%, soy flour 1%, yeast extract 0.5%, BactoTM casamino acids 0.5%, CaCO_3 0.1% in deionized water, pH 7.0), for 3 days at 27 $^\circ\text{C}$ at 180 rpm. The pre-cultures were used to inoculate a sterile 10 L fermenter (Biostat E, B. Braun Melsungen AG, Melsungen, Germany) filled with 9.5 L NL 19 medium (mannitol 2%, soy flour 2% in deionized water, pH 7.5). The strain was cultivated at 27 $^\circ\text{C}$, 220 rpm and an aeration rate of 0.5 vvm. After 4 days of culturing, 2% Hyflo Super-cel was added and the entire culture was separated by multiple sheet filtration in culture filtrate and mycelium, resulting in 8 L of clarified culture filtrate. Subsequently, the pH of this filtrate was adjusted to pH 2 with 1 M HCl and extracted five times with each 2.0 L of EtOAc. The organic phases were combined and concentrated under reduced pressure, resulting in 6.5 g extract.

Incorporation of [$^{13}\text{C}_5$]-L-valine into 1, 2, 4 and 6: [$^{13}\text{C}_5$]-L-Valine was purchased from Sigma-Aldrich. The amino acid was dissolved in water to a concentration of 1 mg mL^{-1} and sterilized by filtration. For the HPLC-MS experiments, 2 mL of this solution were added after 24, 48 and 72 h to a culture of *Streptomyces* sp. AcE210 (20 mL), growing in NL 19 (composition see above) at 27 $^\circ\text{C}$ and 180 rpm. The cultures were harvested after 5 days of incubation and extracted with EtOAc after adjustment to pH 2, using 1 M HCl. The extract was dissolved in 100% MeOH, and subsequently analysed by HPLC-ESI-MS. For the NMR experiments, 10 mL of this solution were added after 24, 48 and 72 h to each of the five cultures of *Streptomyces* sp. AcE210 (100 mL), growing in NL 500 medium (soluble starch 1%, dextrose 1%, glycerol 1%, fish meal 1.5%, sea salts 1% in deionized water, pH 8.0) at 27 $^\circ\text{C}$ and 180 rpm. Deionized water (10 mL) instead of the [$^{13}\text{C}_5$]-L-valine solution was added to the control cultures. The cultures were

harvested after 5 days incubation and extracted with EtOAc after adjustment to pH 2 with 1 M HCl. The extracts were subjected to flash chromatography (Sepacore C-18 cartridges) using a MeOH/H₂O gradient from 5–100% in 60 min. Fractions were collected every 2 min. The fractions were analysed by HPLC. Fractions containing compound **4** were combined and dried under reduced pressure. Subsequently, **4** was isolated by preparative HPLC [Nucleosil100 C₁₈ (10 μm, 100 Å, 21 mm×250 mm)]. A binary gradient of acetonitrile and deionized H₂O with a flow rate of 24 mL min⁻¹ from 50% to 65% acetonitrile in 20 min was used at a column temperature of 23 °C to yield **4** (*t_R*=8.3 min). Fractions containing **4** were combined and diluted with deionized water to an organic solvent content of 12%. The compound was extracted from the diluted fraction using SPE (Phenomenex Strata C18-E cartridge; 200 mg/6 mL). Subsequently, **4** was eluted using [D₃]acetonitrile, and the incorporation pattern was analysed by ¹³C NMR spectroscopy.

Isolation of secondary metabolites: The extract was first separated by flash column chromatography (Sepacore C-18 cartridges) using a MeOH/H₂O gradient from 5–100% in 60 min to give two fractions, A and B. HPLC analysis revealed that fraction A contained **1–3**, while fraction B contained **4** and **5**. Compounds **1**, **2**, and **3** were isolated by semi-preparative HPLC [Phenomenex Luna C₁₈ (5 μm, 100 Å, 10 mm×250 mm)]. A binary gradient of acetonitrile and deionized H₂O with a flow rate of 4.5 mL min⁻¹ from 15% to 20% acetonitrile in 20 min was used at a column temperature of 30 °C to yield **1** (390 mg, *t_R*=4.5 min), **2** (5.5 mg, *t_R*=3.5 min) and **3** (74.8 mg, *t_R*=5.5 min). Compounds **4** and **5** were isolated by semi-preparative HPLC [Phenomenex Luna C₁₈ (5 μm, 100 Å, 10 mm×250 mm)]. A binary gradient of acetonitrile and deionized H₂O with a flow rate of 4.5 mL min⁻¹ from 45% to 75% acetonitrile in 20 min was used at a column temperature of 30 °C to yield **4** (*t_R*=7.1 min) and **5** (*t_R*=9.8 min). Compounds **4** and **5** were captured from the respective HPLC fractions using SPE as described above.

Xanthocidin (1): White amorphous powder; $[\alpha]_D^{24} = +23.6$ (*c*=1.65, MeOH); ¹H NMR data are identical to literature data;⁴¹ ESIMS *m/z* 227 [M–H]⁻; HRMS *m/z* 227.0921 [M–H]⁻ (calcd for C₁₁H₁₅O₅, 227.0920).

Dihydroxanthocidin (2): White-yellow amorphous powder; UV λ_{max} 232 nm; ¹H NMR ([D₂]DMSO, 600 MHz) and ¹³C NMR ([D₆]DMSO, 150 MHz) see Table 1; ESIMS *m/z* 229 [M–H]⁻; HRMS *m/z* 229.1097 [M–H]⁻ (calcd for C₁₁H₁₇O₅, 229.1076).

Homoxanthocidin (3): White amorphous powder; UV λ_{max} 232 nm; ¹H NMR ([D₂]DMSO, 600 MHz) and ¹³C NMR ([D₆]DMSO, 150 MHz) see Table 1; ESIMS *m/z* 241 [M–H]⁻; HRMS *m/z* 241.1082 [M–H]⁻ (calcd for C₁₂H₁₇O₅, 241.1076).

Xanthocidin B (4): UV λ_{max} 246 nm, 270 nm; ¹H NMR ([D₃]acetonitrile, 600 MHz) and ¹³C NMR ([D₃]acetonitrile, 150 MHz) see Table 2; ESIMS *m/z* 151 [M+H]⁺; HRMS *m/z* 151.1111 [M+H]⁺ (calcd for C₁₀H₁₅O₄, 151.1123).

Homoxanthocidin B (5): UV λ_{max} 246 nm, 270 nm; ¹H NMR ([D₃]acetonitrile, 600 MHz) and ¹³C NMR ([D₃]acetonitrile, 150 MHz) see Table 2; ESIMS *m/z* 165 [M+H]⁺; HRMS *m/z* 165.1291 [M+H]⁺ (calcd for C₁₁H₁₇O₄, 165.1279).

Xanthocidin C (6): UV λ_{max} 246 nm, 270 nm; ESIMS *m/z* 195 [M+H]⁺; HRMS *m/z* 195.1032 [M+H]⁺ (calcd for C₁₁H₁₅O₃, 195.1021).

Homoxanthocidin C (7): UV λ_{max} 246 nm, 270 nm; ESIMS *m/z* 209 [M+H]⁺; HRMS *m/z* 209.1177 [M+H]⁺ (calcd for C₁₂H₁₇O₃, 209.1178).

Determination of absolute configuration by VCD: To obtain a CDCl₃ solution of highly volatile **5**, the compound was eluted from a SPE column with 1 mL of CDCl₃. The first of seven eluted fractions contained the sample at an appropriate concentration for an IR/VCD experiment (maximum optical density of ≈0.7). The solution was placed in a 110 μm BaF₂ rotating cell and IR and VCD spectra (4 cm⁻¹ resolution) were recorded on a Tensor 27 FT-IR spectrometer with PMA 50 VCD side bench (Bruker Optics, Ettlingen, Germany). The wavenumber of optimum handedness of circularly polarized light (retardation: 1/4 λ) was set to 1400 cm⁻¹. The spectrum shown in Figure 2 corresponds to the average of 8 h of measuring at different angles from 0° to 360° (increments of 15°) after background subtraction. A concentration of ≈130 nm was estimated from the IR absorbance of the carbonyl stretch vibration at ≈1700 cm⁻¹ using the corresponding molar absorptivity value from density functional theory calculations (see below).

Quantum chemical calculations: Six conformers of **5** were modelled using the MMFF-based conformer search algorithm in SPARTAN. The six geometries were optimized and their relative energies and IR and VCD intensities were calculated at the B3LYP/6–311++G(d,p) level in GAUSSIAN 09. The calculated frequencies were scaled by 0.97. Theoretical spectra were constructed with Lorentzian line shapes (6 cm⁻¹ bandwidth) around calculated intensities. The simulated IR and VCD spectra shown in Figure 2 were obtained from averaging the conformer spectra according to their Boltzmann weights (66.7:25.9:3.1:2.5:1.5:0.2%, determined in respect to their relative energies).

Acknowledgements

We thank Prof. Dr. Michael Lalk, University of Greifswald, Germany, for recording the NMR data, and the ZMG MS Core Facility (CFP-MS), University Halle–Wittenberg, Germany, for the acquisition of HRMS data. This work was in part financially supported by the German Center for Infection Research (Partner Site Tübingen, TTU 09.706 and TTU 09.) and the DFG (SFB 766). Calculations were performed on the bwForCluster JUSTUS supported by the state of Baden-Württemberg through bwHPC and the German Research Foundation (DFG) through Grant No. INST 40/467-1 FUGG.

Conflict of Interest

The authors declare no conflict of interest.

Keywords: biosynthesis • methylenomycin • natural products • Streptomyces • xanthocidin

- [1] K. Asahi, J. Nagatsu, S. Suzuki, *J. Antibiot.* **1966**, *19*, 195.
- [2] K.-I. Asahi, S. Suzuki, *Agric. Biol. Chem.* **1970**, *34*, 325.
- [3] S. Takeda, K. Yaji, K. Matsumoto, T. Amamoto, M. Shindo, H. Aramaki, *Biol. Pharm. Bull.* **2014**, *37*, 331.
- [4] K. Mori, A. Horinaka, M. Kido, *Liebigs Ann. Chem.* **1994**, 817.
- [5] a) D. Boschelli, A. B. Smith, *Tetrahedron Lett.* **1981**, *22*, 3733; b) A. B. Smith, D. Boschelli, *J. Org. Chem.* **1983**, *48*, 1217; c) M. A. Tius, D. J. Drake, *Tetrahedron Lett.* **1996**, *52*, 14651.

- [6] K. Yaji, M. Shindo, *Tetrahedron Lett.* **2010**, *66*, 9808.
- [7] R. J. J. C. Lousberg, Y. Tirilly, M. Moreau, *Experientia* **1976**, *32*, 331.
- [8] K. Umino, T. Furumai, N. Matsuzawa, Y. Awataguchi, Y. Ito, *J. Antibiot.* **1973**, *26*, 506.
- [9] H. Umezawa, T. Takeuchi, K. Nitta, T. Yamamoto, S. Yamaoka, *J. Antibiot.* **1953**, *6*, 101.
- [10] J. H. Burchenal, C. E. Crandall, A. Gellhorn, R. B. Golbey, D. A. Karnofsky, G. B. Magill, C. P. Rhoads, C. C. Stock, S. N. Yorukoglu, *Cancer Res.* **1956**, *16*, 960.
- [11] T. Haneishi, N. Kitahara, Y. Takiguchi, M. Arai, S. Sugawara, *J. Antibiot.* **1974**, *27*, 386.
- [12] R. Kirby, D. A. Hopwood, *J. Gen. Microb.* **1977**, *98*, 239.
- [13] Genebank Accession number: AJ276673.
- [14] C. Corre, G. L. Challis, *ChemBioChem* **2005**, *6*, 2166.
- [15] a) J. Riedlinger, S. D. Schrey, M. T. Tarkka, R. Hampf, M. Kapur, H.-P. Fiedler, *Appl. Environ. Microbiol.* **2006**, *72*, 3550; b) S. D. Schrey, E. Erkenbrack, E. Früh, S. Fiedler, K. Hommel, N. Horlacher, D. Schulz, M. Ecke, A. Kulik, H.-P. Fiedler, R. Hampf, M. T. Tarkka, *BMC Microbiol.* **2012**, *12*, 164.
- [16] E. E. Chaia, L. G. Wall, K. Huss-Danell, *Symbiosis* **2010**, *51*, 201.
- [17] M. Solans, *J. Basic Microbiol.* **2007**, *47*, 243.
- [18] *Gaussian 09*, Revision D.01, M. J. Frisch, G. W. Trucks, H. B. Schlegel, G. E. Scuseria, M. A. Robb, J. R. Cheeseman, G. Scalmani, V. Barone, B. Menonucci, G. A. Petersson, H. Nakatsuji, M. Caricato, X. Li, H. P. Hratchian, A. F. Izmaylov, J. Bloino, G. Zheng, J. L. Sonnenberg, M. Hada, M. Ehara, K. Toyota, R. Fukuda, J. Hasegawa, M. Ishida, T. Nakajima, Y. Honda, O. Kitao, H. Nakai, T. Vreven, J. A. Montgomery, Jr., J. E. Peralta, F. Ogliaro, M. Bearpark, J. J. Heyd, E. Brothers, K. N. Kudin, V. N. Staroverov, R. Kobayashi, J. Normand, K. Raghavachari, A. Rendell, J. C. Burant, S. S. Iyengar, J. Tomasi, M. Cossi, N. Rega, J. M. Millam, M. Klene, J. E. Knox, J. B. Cross, V. Bakken, C. Adamo, J. Jaramillo, R. Gomperts, R. E. Stratmann, O. Yazyev, A. J. Austin, R. Cammi, C. Pomelli, J. W. Ochterski, R. L. Martin, K. Morokuma, V. G. Zakrzewski, G. A. Voth, P. Salvador, J. J. Dannenberg, S. Dapprich, A. D. Daniels, Ö. Farkas, J. B. Foresman, J. V. Ortiz, J. Cioslowski, D. J. Fox, Gaussian, Inc., Wallingford CT, **2009**.
- [19] G. L. Challis, K. F. Chater, *Chem. Commun.* **2001**, 935.
- [20] U. Hornemann, D. A. Hopwood, *Tetrahedron Lett.* **1978**, *19*, 2977.
- [21] S. D. Bentley, S. Brown, L. D. Murphy, D. E. Harris, M. A. Quail, J. Parkhill, B. G. Barrell, J. R. McCormick, R. I. Santamaria, R. Losick et al., *Mol. Microbiol.* **2004**, *51*, 1615.
- [22] G. L. Challis, *J. Ind. Microbiol. Biotechnol.* **2014**, *41*, 219.
- [23] S. L. Midland, N. T. Keen, J. J. Sims, M. M. Midland, M. M. Stayton, V. Burton, M. J. Smith, E. P. Mazzola, K. J. Graham, J. Clardy, *J. Org. Chem.* **1993**, *58*, 2940.
- [24] a) H. Yoda, M. Kawauchi, K. Takabe, K. Hosoya, *Heterocycles* **1997**, *45*, 1895; b) J. P. Henschke, R. W. Rickards, *Tetrahedron Lett.* **1996**, *37*, 3557; c) C.-m. Zeng, S. L. Midland, N. T. Keen, J. J. Sims, *J. Org. Chem.* **1997**, *62*, 4780; d) R. Chênevert, M. Dasser, *J. Org. Chem.* **2000**, *65*, 4529.
- [25] S. Omura, K. Tsuzuki, Y. Tanaka, H. Sakakibara, M. Aizawa, G. Lukacs, *J. Antibiot.* **1983**, *36*, 614.
- [26] M. M. Sherman, S. Yue, C. R. Hutchinson, *J. Antibiot.* **1986**, *39*, 1135.
- [27] Y. Li, G. Florova, K. A. Reynolds, *J. Bacteriol.* **2005**, *187*, 3795.
- [28] a) T. A. Cropp, A. A. Smogowicz, E. W. Hafner, C. D. Denoya, H. A. I. McArthur, K. A. Reynolds, *Can. J. Microbiol.* **2000**, *46*, 506; b) K. H. Choi, R. J. Heath, C. O. Rock, *J. Bacteriol.* **2000**, *182*, 365.
- [29] O. Sprusansky, K. Stirrett, D. Skinner, C. Denoya, J. Westpheling, *J. Bacteriol.* **2005**, *187*, 664.
- [30] T. Weber, K. Blin, S. Duddela, D. Krug, H. U. Kim, R. Brucocoleri, S. Y. Lee, M. A. Fischbach, R. Müller, W. Wohlleben, R. Breitling, E. Takano, M. H. Medema, *Nucleic Acids Res.* **2015**, *43*, W237-43.
- [31] S. F. Altschul, W. Gish, W. Miller, E. W. Myers, D. J. Lipman, *J. Mol. Biol.* **1990**, *215*, 403.
- [32] S. O'Rourke, A. Wietzorrek, K. Fowler, C. Corre, G. L. Challis, K. F. Chater, *Mol. Microbiol.* **2009**, *71*, 763.
- [33] C. Corre, L. Song, S. O'Rourke, K. F. Chater, G. L. Challis, *Proc. Natl. Acad. Sci. USA* **2008**, *105*, 17510.
- [34] L. Jahn, T. Schafhauser, D. Wibberg, C. Rückert, A. Winkler, A. Kulik, T. Weber, L. Flor, K.-H. van Pée, J. Kalinowski, J. Ludwig-Müller, W. Wohlleben, *J. Biotechnol.* **2017**, *257*, 233.
- [35] H. M. Nonomura in *Biology of Actinomycetes 88* (Ed.: Y. Okami, T. Beppu, H. Ogawara), Japan Scientific Societies Press, Tokyo, **1988**, pp. 288–293.
- [36] E. B. Shirling, D. Gottlieb, *Int. J. Syst. Evol. Microbiol.* **1966**, *16*, 313.
- [37] C. F. Hirsch, D. L. Christensen, *Appl. Environ. Microbiol.* **1983**, *46*, 925.
- [38] a) M. Alanjary, K. Steinke, M. Adamek, D. Huson, N. Ziemert, "autoMLST: Automatic Multi-Locus Species Tree" <http://automlst.ziemertlab.com/index#>, accessed Oct. 08, **2018**; b) M. Richter, R. Rosselló-Móra, F. O. Glöckner, J. Peplies, *Bioinformatics* **2016**, *32*, 929.
- [39] N. Ortlieb, N. Keilhofer, S. D. Schrey, H. Gross, T. H. J. Niedermeyer, *Microbiol. Resour. Announc.* **2018**, *7*, e01190-18.

Manuscript received: August 11, 2018

Accepted manuscript online: October 9, 2018

Version of record online: November 6, 2018

B. Draft Genome Sequence of the Xanthocidin-Producing Strain Streptomyces sp.**AcE210, Isolated from a Root Nodule of *Alnus glutinosa* (L.)**

Ortlieb, Nico; Keilhofer, Nadine; Schrey, Silvia Diane; Gross, Harald; Niedermeyer, Timo Horst Johannes;

Microbiol Resour Announc 14, 277 (2018); doi: 10.1128/MRA.01190-18



GENOME SEQUENCES



Draft Genome Sequence of the Xanthocidin-Producing Strain *Streptomyces* sp. AcE210, Isolated from a Root Nodule of *Alnus glutinosa* (L.)

Nico Ortlieb,^{a,b,c} Nadine Keilhofer,^d Silvia D. Schrey,^{d,e} Harald Gross,^{b,f} Timo H. J. Niedermeyer^{a,b,c}

^aDepartment of Microbiology and Biotechnology, Interfaculty Institute of Microbiology and Infection Medicine, University of Tübingen, Tübingen, Germany

^bGerman Centre for Infection Research (DZIF), partner site Tübingen, Tübingen, Germany

^cDepartment of Pharmaceutical Biology/Pharmacognosy, Institute of Pharmacy, University of Halle-Wittenberg, Halle (Saale), Germany

^dDepartment of Physiological Ecology of Plants, Interfaculty Institute of Microbiology and Infection Medicine, Universität Tübingen, Tübingen, Germany

^eIBG-2: Plant Sciences, Jülich, Germany

^fDepartment of Pharmaceutical Biology, Pharmaceutical Institute, University of Tübingen, Tübingen, Germany

ABSTRACT *Streptomyces* sp. strain AcE210 exhibited antibacterial activity toward Gram-positive microorganisms and turned out to be a rare producer of the specialized metabolite xanthocidin. The 10.6-Mb draft genome sequence gives insight into the complete specialized metabolite production capacity and builds the basis to find and locate the biosynthetic gene cluster of xanthocidin.

As part of our ongoing efforts to investigate bioactive natural products from the *Actinobacteria* (1–9), we investigated the endophytic strain *Streptomyces* sp. AcE210. It exhibited antibacterial activity toward Gram-positive bacteria, and a chemical analysis revealed its ability to produce the natural product xanthocidin (10, 11). This compound belongs to the family of cyclopentenoid antitumor antibiotics that have been clinically applied in antitumor therapy (12). However, the fact that the original producing strain, *Streptomyces xanthocidicus*, lost the ability to biosynthesize xanthocidin (13) precluded biotechnological production and strain optimization as well as the conduct of biosynthetic and genetic studies. With strain AcE210 in hand, biosynthetic studies can now be revisited. To locate, analyze, and prove the biosynthetic gene cluster, the sequencing of this strain was initiated.

Strain AcE210 was isolated from root nodules of *Alnus glutinosa* (L.) Gaertn. growing in Tübingen, Germany. After surface cleaning using sterile water, nodules were cracked open. Fragments were added to 50 ml of higher nitrogen content (HNC) medium (6% yeast extract, 0.05% SDS, 0.05% CaCl₂ [pH 7.0]) and incubated at 42°C with shaking for 30 min. The suspension was filtered, and a dilution series was prepared. The filtered suspensions were plated onto International *Streptomyces* Project 2 (ISP-2) agar containing 5 g/liter cycloheximide, 2 g/liter nalidixic acid, and 5 g/liter nystatin. After 8 days at 27°C, strain AcE210 and eight other actinomycetes could be distinguished and separately isolated according to their morphological appearances.

DNA of strain AcE210 was harvested from cultures grown for 3 days at 27°C in 100 ml of NL410 medium (1% dextrose, 1% glycerol, 0.5% oatmeal, 1% soy flour, 0.5% yeast extract, 0.5% Bacto Casamino Acids, and 0.01% CaCO₃ in deionized water) under agitation (180 rpm) using a Qiagen Genomic-tip 100/G kit following the manufacturer's protocol. Subsequently, a 10-kb SMRTbell library was generated from sheared genomic DNA (gDNA) using protocols and reagents according to the manufacturers' instructions and was sub-

Received 27 August 2018 Accepted 24 September 2018 Published 11 October 2018

Citation Ortlieb N, Keilhofer N, Schrey SD, Gross H, Niedermeyer THJ. 2018. Draft genome sequence of the xanthocidin-producing strain *Streptomyces* sp. AcE210, isolated from a root nodule of *Alnus glutinosa* (L.). *Microbiol Resour Announc* 7:e01190-18. <https://doi.org/10.1128/MRA.01190-18>.

Editor Irene L. G. Newton, Indiana University Bloomington

Copyright © 2018 Ortlieb et al. This is an open-access article distributed under the terms of the Creative Commons Attribution 4.0 International license.

Address correspondence to Timo H. J. Niedermeyer, timo.niedermeyer@pharmazie.uni-halle.de.

Ortlieb et al.



jected to sequencing using a PacBio RS II sequencing platform. Sequencing reads were processed, filtered (PreAssembler filter v1), and mapped using SMRT Analysis v2.3.0, while *de novo* assembly was performed utilizing Falcon v0.2.1 (14) with the Falcon sense options multi output, 0.70 min idt, min cov 4, local match count threshold 2, max n read 200, and n core 6 and the overlap filtering settings max diff 240, max cov 360, min cov 5, and bestn 10. The length cutoff for seed reads was set at 6,000 bp for initial mapping as well as for preassembly. Quiver v1 was used for consensus polishing using the “only unambiguously mapped reads” option. Overall, 254,702 reads (N_{50} 6,342 bp; mean subread length, 5,265 bp) were assembled into a 10,567,477-nucleotide draft genome at 127-fold coverage. The resulting draft genome sequence consists of 4 contigs in total with a G+C content of 70.4%. The assembled contigs were annotated with the Prokaryotic Genome Annotation Pipeline (PGAP) (15), yielding a total of 8,873 predicted protein-coding sequences. The closest related type strains based on a multilocus sequence type (MLST) analysis are *Streptomyces alboflavus* NRRL B-2373 and *Streptomyces avermitilis* DSM 46492. Automated specialized metabolism analysis using AntiSMASH v4.0.2 (16) predicted 23 biosynthetic gene clusters. The biosynthetic genes involved in xanthocidin biosynthesis will be discussed in more detail elsewhere.

Data availability. This whole-genome shotgun (WGS) project has been deposited in DDBJ/ENA/GenBank under the accession number QJRC00000000. Raw sequencing data sets have been registered in the NCBI SRA database under the accession number SRP159767.

ACKNOWLEDGMENTS

Research in H.G.'s and T.H.J.N.'s laboratories was funded by the German Center for Infection Research (DZIF). We acknowledge financial support within the funding program “Open Access Publishing” by the German Research Foundation (DFG).

REFERENCES

- Iftime D, Kulik A, Härtner T, Rohrer S, Niedermeyer THJ, Stegmann E, Weber T, Wohlleben W. 2016. Identification and activation of novel biosynthetic gene clusters by genome mining in the kirromycin producer *Streptomyces collinus* Tü 365. *J Ind Microbiol Biotechnol* 43: 277–291. <https://doi.org/10.1007/s10295-015-1685-7>.
- Spohn M, Edenhart S, Alanjary M, Ziemert N, Wibberg D, Kalinowski J, Niedermeyer THJ, Stegmann E, Wohlleben W. 2018. Identification of a novel aminopolycarboxylic acid siderophore gene cluster encoding the biosynthesis of ethylenediaminesuccinic acid hydroxyarginine (EDHA). *Metallomics* 10:722–734. <https://doi.org/10.1039/C8MT00009C>.
- Zeyhle P, Bauer JS, Kalinowski J, Shin-ya K, Gross H, Heide L. 2014. Genome-based discovery of a novel membrane-bound 1,6-dihydroxyphenazine prenyltransferase from a marine actinomycete. *PLoS One* 9:e99122. <https://doi.org/10.1371/journal.pone.0099122>.
- Spohn M, Kirchner N, Kulik A, Jochim A, Wolf F, Muenzer P, Borst O, Gross H, Wohlleben W, Stegmann E. 2014. Overproduction of ristomycin A by activation of a silent gene cluster in *Amycolatopsis japonicum* MG417-CF17. *Antimicrob Agents Chemother* 58:6185–6196. <https://doi.org/10.1128/AAC.03512-14>.
- Zeyhle P, Bauer JS, Steimle M, Leipoldt F, Rösch M, Kalinowski J, Gross H, Heide L. 2014. A membrane-bound prenyltransferase catalyzes the O-prenylation of 1,6-dihydroxyphenazine in the marine bacterium *Streptomyces* sp. CNQ-509. *Chembiochem* 15:2385–2392. <https://doi.org/10.1002/cbic.201402394>.
- Buchmann A, Eitel M, Koch P, Schwarz PN, Stegmann E, Wohlleben W, Wolański M, Krawiec M, Zakrzewska-Czerwińska J, Méndez C, Botas A, Núñez LE, Moris F, Cortés J, Gross H. 2016. High-quality draft genome sequence of the actinobacterium *Nocardia terpenica* IFM 0406, producer of the immunosuppressant brasilicardins, using Illumina and PacBio technologies. *Genome Announc* 4:e01391-16. <https://doi.org/10.1128/genomeA.01391-16>.
- Wolf F, Bauer JS, Bendel TM, Kulik A, Kalinowski J, Gross H, Kaysser L. 2017. Biosynthesis of the β -lactone proteasome inhibitors belactosin and cystargolide. *Angew Chem Int Ed Engl* 56:6665–6668. <https://doi.org/10.1002/anie.201612076>.
- Jiao J, Paterson J, Busche T, Rückert C, Kalinowski J, Harwani D, Gross H. 2018. Draft genome sequence of *Streptomyces* sp. strain DH-12, a soilborne isolate from the Thar Desert with broad-spectrum antibacterial activity. *Genome Announc* 6:e00108-18. <https://doi.org/10.1128/genomeA.00108-18>.
- Schwarz PN, Buchmann A, Roller L, Kulik A, Gross H, Wohlleben W, Stegmann E. 2018. The immunosuppressant brasilicardin: determination of the biosynthetic gene cluster in the heterologous host *Amycolatopsis japonicum*. *Biotechnol J* 13:1700527. <https://doi.org/10.1002/biot.201700527>.
- Asahi K, Nagatsu J, Suzuki S. 1966. Xanthocidin, a new antibiotic. *J Antibiot (Tokyo)* 19:195–199.
- Sakurai T, Imura Y, Asahi K. 1980. Molecular structure of xanthocidin. *Agric Biol Chem* 44:2257–2258. <https://doi.org/10.1080/00021369.1980.10864313>.
- Burchenal JH, Crandall CE, Gellhorn A, Golbey RB, Karnofsky DA, Magill GB, Rhoads CP, Stock CC, Yorukoglu SN. 1956. Clinical experiences with sarkomycin in neoplastic diseases. *Cancer Res* 16:960–964.
- Yaji K, Shindo M. 2010. Total synthesis of (\pm)-xanthocidin using FeCl₃-mediated Nazarov reaction. *Tetrahedron* 66:9808–9813. <https://doi.org/10.1016/j.tet.2010.10.084>.
- Chin C-S, Peluso P, Sedlazeck FJ, Nattestad M, Concepcion GT, Clum A, Dunn C, O'Malley R, Figueroa-Balderas R, Morales-Cruz A, Cramer GR, Delledonne M, Luo C, Ecker JR, Cantu D, Rank DR, Schatz MC. 2016. Phased diploid genome assembly with single-molecule real-time sequencing. *Nat Methods* 13:1050–1054. <https://doi.org/10.1038/nmeth.4035>.
- Tatusova T, DiCuccio M, Badretdin A, Chetvernin V, Nawrocki EP, Zaslavsky L, Lomsadze A, Pruitt KD, Borodovsky M, Ostell J. 2016. NCBI Prokaryotic Genome Annotation Pipeline. *Nucleic Acids Res* 44: 6614–6624. <https://doi.org/10.1093/nar/gkw569>.
- Blin K, Wolf T, Chevrette MG, Lu X, Schwalen CJ, Kautsar SA, Suarez Duran HG, de los Santos ELC, Kim HU, Nave M, Dickschat JS, Mitchell DA, Shelest E, Breitling R, Takano E, Lee SY, Weber T, Medema MH. 2017. antiSMASH 4.0—improvements in chemistry prediction and gene boundary identification. *Nucleic Acids Res* 45:W36–W41. <https://doi.org/10.1093/nar/gkx319>.

4. Conclusion

The present work aimed at the identification of biologically active natural products from Actinobacteria. In order to facilitate a time and space efficient cultivation of the Tübingen strain collection of Actinobacteria, a suitable tool was developed, combinable with multiple agar diffusion assays, utilizing various monitor strains. As a proof of concept, the Tübingen strain collection was initially screened against one monitor strain, developed to identify compounds that interfere with a key player of QS signal transduction.

Furthermore, the aim of the theses was also the identification and characterisation of new natural products with rare structural features, independent from their bioactivity. Within this scope, *Streptomyces* sp AcE210 was analysed due to its potential to synthesise a rare cyclopentanone antibiotic – xanthocidin as well as several yet uncharacterized derivatives.

This chapter will summarize the key findings of the thesis and present resulting deductions.

4.1 Development of a screening system

In the present work a cultivation system for Actinobacteria was developed, allowing the cultivation of 96 different strains on agar in stainless steel MTP. All cultivation and screening systems reported to date are based on submerge cultivation systems. Even though Actinobacteria are able to grow and produce secondary metabolites in submerge cultures, their lifecycle indicates that they are naturally growing attached to any kind of surface. Keeping in mind the tremendous influence of the cultivation conditions on the production of secondary metabolites, the herein described combined cultivation and screening platform for Actinobacteria could be a promising tool for the fast and efficient identification of new bioactive NP. To the best of my knowledge, it is the first tool that allows simultaneous cultivation of multiple Actinobacteria strains on agar and subsequent analysis of these strains in agar diffusion assays.

4.2 Exploitation of the developed system to search for bioactive compounds

In order to proof the benefit of the developed cultivation and screening system, the Tübingen strain collection has been cultivated using ISP2 and ISP3 medium and subsequently screened against the *S. aureus* PC322 assay that has been developed by Nielsen *et al.*¹⁴⁷

82 strains showed quorum sensing inhibition activity, while 284 strains exhibited antibacterial activity, and 866 strains did not reveal any activity. These results indicate the great potential of this tool since it allows the identification of bioactive strains in a fast and comprehensive way. Moreover, the bioactivity assay that is coupled to the cultivation system is interchangeable. Hence, different bioactivities could be analysed using this tool. The only limit so far is that the bioactivity assay needs to be an agar diffusion assay. Hence, the scope of the screening has been extended and, in cooperation with other scientists, more monitor strains have already been used successfully.

Two of the most promising strains from the screening have been analysed in regard to their bioactive compounds, *S. sp.* Tü2700 exhibiting QS inhibition activity, and *S. sp.* Tü2401 showing antibacterial activity. Phylogeny analysis of these two strains using the bioinformatics tool autoMLST revealed their affiliation to the genus *Streptomyces*.

A sufficient purification protocol for the isolation of the bioactive compound of *S. sp.* Tü2700 was developed and led to the dereplication of oxazolomycin A. This oxazole polyene γ -lactam/ β -lactone antibiotic compound has been first isolated in 1985 by Uemura *et al.*²¹⁰ *S. aureus* PC322 bioactivity assays with and without staining agent revealed that oxazolomycin A doesn't inhibit QS, but instead exhibits partially antibacterial activity, resulting in misleading hazy halos. Even though it is known for its antiviral, cytotoxic and antibacterial behaviour as well as its potential to inhibit plant transformation, antibacterial activity against *S. aureus* has only been described for its methylated derivative KSM-2690 B so far. Moreover, except for glucose, no compounds have been reported yet that create hazy halos in the *S. aureus* PC322 assay, without interfering with its *agr* system yet. Therefore, oxazolomycin A and possibly KSM-2690 B could be considered as compounds leading to false positive outcomes. Hence, in order to eliminate those compounds early in the screening process, it would be advisable to analyse, in the future, every positive hit in a second assay. This second assay should be performed without supplementing X-Gal in the agar.

Characterisation of *S. sp.* Tü2401 revealed that this strain was able to produce two different compounds, depending on the cultivation conditions. On agar the highly cytotoxic compound C-1027 was produced. This compound was originally isolated in 1988 from *Streptomyces globisporus*. It belongs to the small family of enediyne compounds that comprises to date 11 members. Three of these, namely neocarcinostatin, calicheamicin and C-1027 are currently in clinical trials, or are already used in the clinic.²⁵⁰ The success rate for these compounds reaching the clinic of ca. 30 %, makes these compounds a very promising target for antitumor drug development. Since bioinformatic analysis of bacterial genomes have revealed that enediyne BGC are highly abundant among Actinobacteria (6.3 %), it is astonishing that the number of compounds belonging to this group is still small. On the other hand, this ratio indicates that, within the Tübingen strain collection, statistically 75 enediyne producing strains are yet to be identified. Since C-1027 was exclusively produced on agar, this compound serves as a prove of concept for the cultivation/screening tool and underlines the huge potential of the Tübingen strain collection for the identification of potential drug candidates. Moreover, many bioactive strains that have been identified during the screening are not characterized yet. Therefore, a profound dereplication process for those compounds is recommended in order to save time and resources.

The other antibacterial compounds produced by *S. sp.* Tü2401 could not be isolated, due to their hydrophilicity using classical isolation approaches. The development of a specific purification procedure led to the identification of albomycin δ_1 and δ_2 . Even though these sideromycins are known since 1947, their activity against Gram-negative bacteria like *E. coli* has put them back into the spotlight of researchers in recent years. Detailed bioactivity studies against a panel of clinical isolates as well as against multi resistant strains have shown their great potential, since albomycin δ_2 exhibited in some case more 1000 times lower MIC values against *S. pneumoniae* and *S. aureus* compared to ciprofloxacin, vancomycin, and penicillin G.³³¹ MIC values of 5 ng/ml against *Escherichia coli* illustrate that albomycins are almost tenfold more potent than penicillin.^{331,344} Besides, albomycins did not exhibit toxicity during in-vivo studies in mice and have also been well tolerated.^{331,343} In times where multi resistant strains are on the rise, and antibiotics active against Gram-negative bacteria are scarce, albomycins are promising drug candidates.

4.3 Investigations of the xanthocidin biosynthesis

The isolation and structural characterization of xanthocidin and six new derivatives from the endophytic *Streptomyces* sp. AcE210 led to the elucidation of the biosynthesis for this cyclopentanone antibiotic as well as to the identification of its putative BGC. The family of cyclopentanone antibiotics comprises 5 major compounds. However, the biosynthesis has previously only been studied for methylenomycin. Even though xanthocidin has already been isolated already in 1966, the biosynthesis has not been described yet. Since the original producer strain had lost its ability to produce xanthocidin, total synthesis has been the only way to obtain this compound.¹⁹³ Therefore, only few studies on the biological activity of xanthocidin have been performed.¹⁹³ The potential of the cyclopentanone antibiotics to serve as potential new drug candidates is exemplified by sarkomycin, another member of this family that has been used in antitumor therapy in Japan.¹⁹³ Hence, the identification of a new xanthocidin producer and the xanthocidin biosynthesis, as well as a putative BGC could enable a sustainable biotechnological production of xanthocidin. Additionally, feeding of unusual starter units/amino acids could result in the production of new derivatives with alternated bioactivity.

5. References

- (1) Atanasov, A. G.; Waltenberger, B.; Pferschy-Wenzig, E.-M.; Linder, T.; Wawrosch, C.; Uhrin, P.; Temml, V.; Wang, L.; Schwaiger, S.; Heiss, E. H. *et al. Biotechnol. Adv.* **2015**, *33*, 1582–1614
- (2) Newman, D. J.; Cragg, G. M.; Snader, K. M. *Nat. Prod. Rep.* **2000**, *17*, 215–234
- (3) Patwardhan, B. J. *Ethnopharmacol.* **2005**, *100*, 50–52
- (4) *Theophrastean studies: On natural science, physics and metaphysics, ethics, religion, and rhetoric*; Fortenbaugh, W. W., Ed.; Rutgers University studies in classical humanities 3; Transaction Books: New Brunswick, NJ, 1988
- (5) Sneader, W. *Drug Discovery*; John Wiley & Sons, Ltd: Chichester, UK, 2005
- (6) Cragg, G. M.; Newman, D. J. *Biochim. Biophys. Acta* **2013**, *1830*, 3670–3695
- (7) Klockgether-Radke, A. P. *Anesthesiol Intensivmed Notfallmed Schmerzther* **2002**, *37*, 244–249
- (8) Sertuerner. *Ann. Phys.* **1817**, *55*, 56–89
- (9) *Natural Products in the Chemical Industry*; Schaefer, B., Ed.; Springer Berlin Heidelberg: Berlin, Heidelberg, 2014
- (10) Weyer, J. *Geschichte der Chemie Band 2 - 19. und 20. Jahrhundert*; Springer Berlin Heidelberg: Berlin, Heidelberg, 2018
- (11) Kaiser, H. *Z Rheumatol* **2008**, *67*, 252–262
- (12) Mann, C. C.; Plummer, M. L. *The aspirin wars: Money, medicine, and 100 years of rampant competition*, 1. ed.; A Borzoi book; Knopf: New York, 1991
- (13) Katz, L.; Baltz, R. H. *J. Ind. Microbiol. Biotechnol.* **2016**, *43*, 155–176
- (14) Batra, S.; Seth, M.; Bhaduri, A. P. In *Progress in Drug Research; Chirality and future drug design*; Juchau, M. R., Walker, R. J., Fawcett, J. P., Sutherland, R., Preston, N. W., Batra, S., Seth, M., Bhaduri, A. P., Schoner, W., Fisher, J. W., Ohtaka, H., Fujita, T., Jucker, E., Eds.; Birkhäuser Basel: Basel, 1993; pp 191–248
- (15) Bérdy, J. J. *Antibiot.* **2012**, *65*, 385–395
- (16) Demain, A. L. *J. Ind. Microbiol. Biotechnol.* **2014**, *41*, 185–201
- (17) Chen, Y.; Bruyn Kops, C. de; Kirchmair, J. *J Chem Inf Model* **2017**, *57*, 2099–2111
- (18) Newman, D. J.; Cragg, G. M. *J. Nat. Prod.* **2016**, *79*, 629–661
- (19) Ecker, D. M.; Jones, S. D.; Levine, H. L. *mAbs* **2015**, *7*, 9–14
- (20) Urquhart, L. *Nature reviews. Drug discovery* **2018**, *17*, 232
- (21) *New Technologies in Clinical Laboratory Science*; Shinton, N. K., Ed.; Springer Netherlands: Dordrecht, 1985
- (22) Fleming, A. *Br. J. Exp. Pathol.* **1929**, *10*, 226–236
- (23) Fan, Q.; Ma, J.; Xu, Q.; Zhang, J.; Simion, D.; Carmen, G.; Guo, C. *Colloids Surf B Biointerfaces* **2015**, *128*, 181–190
- (24) Hogg, J. A. In *Drug Discovery; Drugs from Natural Products—Animal Sources*; Bloom, B., Ulliyot, G. E., Eds.; Advances in Chemistry; American Chemical Society: WASHINGTON, D. C., 1971; pp 14–32

- (25) CRC Press Taylor & Francis Group. *Dictionary of Natural Products*; CRC Press, 2018
- (26) Lewin, G. R.; Carlos, C.; Chevrette, M. G.; Horn, H. A.; McDonald, B. R.; Stankey, R. J.; Fox, B. G.; Currie, C. R. *Annu. Rev. Microbiol.* **2016**, *70*, 235–254
- (27) Ludwig W, Euzéby J, Schumann P, Buss HJ, Trujillo ME, Kämpfer P. In *Bergey's manual of systematic bacteriology*, 2. ed.; *Road map of the phylum Actinobacteria*; Goodfellow, M., Whitman, W. B., Bergey, D. H., Eds.; Springer: New York, NY, 2012; pp 1–28
- (28) Barka, E. A.; Vatsa, P.; Sanchez, L.; Gaveau-Vaillant, N.; Jacquard, C.; Meier-Kolthoff, J. P.; Klenk, H.-P.; Clément, C.; Ouhdouch, Y.; van Wezel, G. P. *Microbiol. Mol. Biol. Rev.* **2016**, *80*, 1–43
- (29) Aminov, R. I. *Front. Microbiol.* **2010**, *1*, 134
- (30) Bode, H. B.; Bethe, B.; Höfs, R.; Zeeck, A. *ChemBioChem* **2002**, *3*, 619–627
- (31) Hopwood, D. a. *Streptomyces in nature and medicine: The antibiotic makers*; Oxford University Press: Oxford, New York, 2007
- (32) Solecka, J.; Zajko, J.; Postek, M.; Rajnisz, A. *Cent. Eur. J. Biol.* **2012**, *7*
- (33) Kämpfer, P. In *The Prokaryotes: Volume 3: Archaea. Bacteria: Firmicutes, Actinomycetes; The Family Streptomycetaceae, Part I: Taxonomy*; Dworkin, M., Falkow, S., Rosenberg, E., Schleifer, K.-H., Stackebrandt, E., Eds.; Springer-Verlag: New York, NY, 2006; pp 538–604
- (34) Ilic, S. B.; Konstantinovic, S. S.; Todorovic, Z. B.; Lazic, M. L.; Veljkovic, V. B.; Jokovic, N.; Radovanovic, B. C. *Microbiology* **2007**, *76*, 421–428
- (35) Waksman, S. A.; Woodruff, H. B. *Proc. Soc. Exp. Biol. Med.* **1940**, *45*, 609–614
- (36) NobelPrize.org; *Award ceremony speech*. <https://www.nobelprize.org/prizes/medicine/1952/ceremony-speech/>
- (37) Schatz, A.; Bugle, E.; Waksman, S. A. *Proc. Soc. Exp. Biol. Med.* **1944**, *55*, 66–69
- (38) Watve, M. G.; Tickoo, R.; Jog, M. M.; Bhole, B. D. *Arch. Microbiol.* **2001**, *176*, 386–390
- (39) Waksman, S. A.; *The Actinomycetes and Their Antibiotics. Advances in Applied Microbiology Volume 5*; Advances in Applied Microbiology; Elsevier, 1963; pp 235–315
- (40) Béahdy, J.; *Recent Developments of Antibiotic Research and Classification of Antibiotics According to Chemical Structure. Advances in Applied Microbiology Volume 18*; Advances in Applied Microbiology; Elsevier, 1974; pp 309–406
- (41) Genilloud, O. *Nat. Prod. Rep.* **2017**, *34*, 1203–1232
- (42) Baltz, R. H. *Microbe* **2007**, *Volume 2*, 125–131
- (43) Běhal, V.; *Bioactive products from streptomyces*; Advances in Applied Microbiology; Elsevier, 2000; pp 113–156
- (44) Li, J. W.-H.; Vederas, J. C. *Science* **2009**, *325*, 161–165
- (45) Hug, J. J.; Bader, C. D.; Remškar, M.; Cirnski, K.; Müller, R. *Antibiotics* **2018**, *7*
- (46) Bentley, S. D.; Chater, K. F.; Cerdeño-Tárraga, A.-M.; Challis, G. L.; Thomson, N. R.; James, K. D.; Harris, D. E.; Quail, M. A.; Kieser, H.; Harper, D. *et al. Nature* **2002**, *417*, 141–147
- (47) Smanski, M. J.; Zhou, H.; Claesen, J.; Shen, B.; Fischbach, M. A.; Voigt, C. A. *Nat Rev Microbiol* **2016**, *14*, 135–149
- (48) Ochi, K.; Hosaka, T. *Applied microbiology and biotechnology* **2013**, *97*, 87–98

- (49) Hosaka, T.; Ohnishi-Kameyama, M.; Muramatsu, H.; Murakami, K.; Tsurumi, Y.; Kodani, S.; Yoshida, M.; Fujie, A.; Ochi, K. *Nat. Biotechnol.* **2009**, *27*, 462–464
- (50) Locatelli, F. M.; Goo, K.-S.; Ulanova, D. *Metallomics* **2016**, *8*, 469–480
- (51) Tanaka, Y.; Kasahara, K.; Hirose, Y.; Murakami, K.; Kugimiya, R.; Ochi, K. *J. Bacteriol.* **2013**, *195*, 2959–2970
- (52) Tiwari, K.; Gupta, R. K.; *Bioactive Metabolites from Rare Actinomycetes*; Studies in Natural Products Chemistry; Elsevier, 2014; pp 419–512
- (53) Thumar, J. T.; Dhulia, K.; Singh, S. P. *World J Microbiol Biotechnol* **2010**, *26*, 2081–2087
- (54) Bister, B.; Bischoff, D.; Ströbele, M.; Riedlinger, J.; Reicke, A.; Wolter, F.; Bull, A. T.; Zähler, H.; Fiedler, H.-P.; Süßmuth, R. D. *Angew Chem Int Ed Engl* **2004**, *43*, 2574–2576
- (55) Fiedler, H.-P.; Bruntner, C.; Riedlinger, J.; Bull, A. T.; Knutsen, G.; Goodfellow, M.; Jones, A.; Maldonado, L.; Pathom-aree, W.; Beil, W. *et al. J Antibiot (Tokyo)* **2008**, *61*, 158–163
- (56) Genilloud, O.; González, I.; Salazar, O.; Martín, J.; Tormo, J. R.; Vicente, F. *J. Ind. Microbiol. Biotechnol.* **2011**, *38*, 375–389
- (57) Subramani, R.; Aalbersberg, W. *Appl. Microbiol. Biotechnol.* **2013**, *97*, 9291–9321
- (58) Vartoukian, S. R.; Palmer, R. M.; Wade, W. G. *FEMS Microbiol Lett* **2010**, *309*, 1–7
- (59) Katz, M.; Hover, B. M.; Brady, S. F. *J. Ind. Microbiol. Biotechnol.* **2016**, *43*, 129–141
- (60) Hover, B. M.; Kim, S.-H.; Katz, M.; Charlop-Powers, Z.; Owen, J. G.; Ternei, M. A.; Maniko, J.; Estrela, A. B.; Molina, H.; Park, S. *et al. Nat. Microbiol.* **2018**
- (61) Waksman, S. A. *Mycologia* **1947**, *39*, 565
- (62) Dougherty, T. J.; Pucci, M. J. *Antibiotic Discovery and Development*; Springer US: Boston, MA, 2012
- (63) Tan, S. Y.; Grimes, S. *Singapore Med J* **2010**, *51*, 842–843
- (64) Williams, K. J. *JRSM Open* **2009**, *102*, 343–348
- (65) Silver, L. L. *Clin Microbiol Rev* **2011**, *24*, 71–109
- (66) Brown, E. D.; Wright, G. D. *Nature* **2016**, *529*, 336–343
- (67) Gould, K. J. *Antimicrob. Chemother.* **2016**, *71*, 572–575
- (68) Fischbach, M. A.; Walsh, C. T. *Science* **2009**, *325*, 1089–1093
- (69) Yoneyama, H.; Katsumata, R. *Biosci Biotechnol Biochem* **2006**, *70*, 1060–1075
- (70) Nathan, C. *Nature* **2004**, *431*, 899–902
- (71) Powers, J. H. *Clin. Microbiol. Infect.* **2004**, *10*, 23–31
- (72) Fleming, A. *Nobel lecture "Penicillin"*
- (73) Hawkey, P. M.; Jones, A. M. *J. Antimicrob. Chemother.* **2009**, *64 Suppl 1*, i3-10
- (74) Maragakis, L. L.; Perencevich, E. N.; Cosgrove, S. E. *Expert Rev Anti Infect Ther* **2008**, *6*, 751–763
- (75) Projan, S. J. *Curr. Opin. Microbiol.* **2003**, *6*, 427–430
- (76) Payne, D. J.; Gwynn, M. N.; Holmes, D. J.; Pompliano, D. L. *Nat Rev Drug Discov* **2007**, *6*, 29–40
- (77) Butler, M. S.; Blaskovich, M. A.; Cooper, M. A. *J. Antibiot.* **2013**, *66*, 571–591

- (78) Maurer, C. K.; *From in vitro to in vivo: Establishment of a Test System for the Biological Evaluation of Novel Quorum Sensing Inhibitors as Anti-infectives Against Pseudomonas aeruginosa*. PhD thesis, Universität des Saarlandes, Saarbrücken, 2015
- (79) Cegelski, L.; Marshall, G. R.; Eldridge, G. R.; Hultgren, S. J. *Nat Rev Microbiol* **2008**, *6*, 17–27
- (80) Deak, D.; Outtersson, K.; Powers, J. H.; Kesselheim, A. S. *Ann. Intern. Med.* **2016**, *165*, 363–372
- (81) Hesterkamp, T. *Curr. Top. Microbiol. Immunol.* **2016**, *398*, 447–474
- (82) Pendleton, J. N.; Gorman, S. P.; Gilmore, B. F. *Expert Rev. Anti-infect. Ther.* **2013**, *11*, 297–308
- (83) Tacconelli, E. *Global Priority List of Antibiotic-Resistant Bacteria to Guide Research, Discovery, and Development of New Antibiotics*; Geneva, 2017
- (84) Lomovskaya, O.; Watkins, W. J. *Mol. Microbiol. Biotechnol.* **2001**, *3*, 225–236
- (85) Drawz, S. M.; Bonomo, R. A. *Clin. Microbiol. Rev.* **2010**, *23*, 160–201
- (86) Muhlen, S.; Dersch, P. *Curr. Top. Microbiol. Immunol.* **2016**, *398*, 147–183
- (87) Kotra, L. P.; Haddad, J.; Mobashery, S. *Antimicrob. Agents Chemother.* **2000**, *44*, 3249–3256
- (88) Nussbaum, F. von; Sussmuth, R. D. *Angew. Chem. Int. Ed. Engl.* **2015**, *54*, 6684–6686
- (89) Pirofski, L.-a.; Casadevall, A. *BMC biology* **2012**, *10*, 6
- (90) Rasmussen, T. B.; Givskov, M. *Int. J. Med. Microbiol.* **2006**, *296*, 149–161
- (91) Clatworthy, A. E.; Pierson, E.; Hung, D. T. *Nat. Chem. Biol.* **2007**, *3*, 541–548
- (92) Baron, C. *Curr. Opin. Microbiol.* **2010**, *13*, 100–105
- (93) Lee, B.; Boucher, H. W. *Curr Opin Pulm Med* **2015**, *21*, 293–303
- (94) O'Connell, K. M. G.; Hodgkinson, J. T.; Sore, H. F.; Welch, M.; Salmond, G. P. C.; Spring, D. R. *Angew Chem Int Ed Engl* **2013**, *52*, 10706–10733
- (95) Rasko, D. A.; Moreira, C. G.; Li, D. R.; Reading, N. C.; Ritchie, J. M.; Waldor, M. K.; Williams, N.; Taussig, R.; Wei, S.; Roth, M. *et al. Science* **2008**, *321*, 1078–1080
- (96) Zambelloni, R.; Marquez, R.; Roe, A. J. *Chem Biol Drug Des* **2015**, *85*, 43–55
- (97) Beckham, K. S. H.; Roe, A. J. *Front Cell Infect Microbiol* **2014**, *4*, 139
- (98) Williams, P. *Expert Opin. Ther. Targets* **2002**, *6*, 257–274
- (99) Finch, R. G.; Pritchard, D. I.; Bycroft, B. W.; Williams, P.; Stewart, G. S. *J. Antimicrob. Chemother.* **1998**, *42*, 569–571
- (100) Smith, R. S.; Iglewski, B. H. *J. Clin. Investig.* **2003**, *112*, 1460–1465
- (101) Galloway, W. R. J. D.; Hodgkinson, J. T.; Bowden, S.; Welch, M.; Spring, D. R. *Trends Microbiol.* **2012**, *20*, 449–458
- (102) Bhardwaj, A. K.; Vinothkumar, K.; Rajpara, N. *Recent Pat Antiinfect Drug Discov* **2013**, *8*, 68–83
- (103) Scutera, S.; Zucca, M.; Savoia, D. *Expert Opin Drug Discov* **2014**, *9*, 353–366
- (104) Hirakawa, H.; Tomita, H. *Front. Microbiol.* **2013**, *4*, 114
- (105) Bassler, B. L. *Curr. Opin. Microbiol.* **1999**, *2*, 582–587
- (106) Waters, C. M.; Bassler, B. L. *Annu. Rev. Cell Dev. Biol.* **2005**, *21*, 319–346
- (107) Garg, N.; Manchanda, G.; Kumar, A. *Antonie van Leeuwenhoek* **2014**, *105*, 289–305

- (108) Williams, P.; Winzer, K.; Chan, W. C.; Camara, M. *Philos. Trans. R. Soc. Lond., B, Biol. Sci.* **2007**, *362*, 1119–1134
- (109) Miller, M. B.; Bassler, B. L. *Annu. Rev. Microbiol.* **2001**, *55*, 165–199
- (110) Defoirdt, T.; Brackman, G.; Coenye, T. *Trends Microbiol.* **2013**, *21*, 619–624
- (111) Defoirdt, T.; Boon, N.; Bossier, P. *PLOS Pathog.* **2010**, *6*, e1000989
- (112) Gerdt, J. P.; Blackwell, H. E. *ACS Chem. Biol.* **2014**, *9*, 2291–2299
- (113) Garcia-Contreras, R.; Maeda, T.; Wood, T. K. *ISME J.* **2016**, *10*, 4–10
- (114) Moore, J. D.; Gerdt, J. P.; Eibergen, N. R.; Blackwell, H. E. *ChemBioChem* **2014**, *15*, 435–442
- (115) Kalia, V. C. *Biotechnol. Adv.* **2013**, *31*, 224–245
- (116) Brackman, G.; Breyne, K.; Rycke, R. de; Vermote, A.; van Nieuwerburgh, F.; Meyer, E.; van Calenbergh, S.; Coenye, T. *Sci. Rep.* **2016**, *6*, 20321
- (117) Kim, Y. H.; Kim, Y. H.; Kim, J. S.; Park, S. *Biotechnol. Bioprocess Eng.* **2005**, *10*, 322–328
- (118) Lowy, F. D. *The New England journal of medicine* **1998**, *339*, 520–532
- (119) Wertheim, H. F. L.; Melles, D. C.; Vos, M. C.; van Leeuwen, W.; van Belkum, A.; Verbrugh, H. A.; Nouwen, J. L. *Lancet Infect Dis* **2005**, *5*, 751–762
- (120) Brackman, G.; Coenye, T. *Curr. Pharm. Des.* **2015**, *21*, 1–8
- (121) Rutherford, S. T.; Bassler, B. L. *Cold Spring Harb Perspect Med* **2012**, *2*
- (122) Kuehnert, M. J.; Hill, H. A.; Kupronis, B. A.; Tokars, J. I.; Solomon, S. L.; Jernigan, D. B. *Emerging Infect. Dis.* **2005**, *11*, 868–872
- (123) Chambers, H. F. *Emerging Infect. Dis.* **2001**, *7*, 178–182
- (124) Gurusamy, K. S.; Koti, R.; Toon, C. D.; Wilson, P.; Davidson, B. R. *Cochrane Database Syst Rev* **2013**, CD009726
- (125) Menichetti, F. *Clin Microbiol Infect* **2005**, *11 Suppl 3*, 22–28
- (126) Lyon, G. J.; Novick, R. P. *Peptides* **2004**, *25*, 1389–1403
- (127) Mansson, M.; Nielsen, A.; Kjaerulff, L.; Gotfredsen, C. H.; Wietz, M.; Ingmer, H.; Gram, L.; Larsen, T. O. *Mar. Drugs* **2011**, *9*, 2537–2552
- (128) Chan, P. F.; Foster, S. J. *Microbiology* **1998**, *144 (Pt 9)*, 2469–2479
- (129) Johnson, J. G.; Wang, B.; Debelouchina, G. T.; Novick, R. P.; Muir, T. W. *ChemBioChem* **2015**, *16*, 1093–1100
- (130) Kleerebezem, M.; Quadri, L. E.; Kuipers, O. P.; Vos, W. M. de. *Mol Microbiol* **1997**, *24*, 895–904
- (131) Dunman, P. M.; Murphy, E.; Haney, S.; Palacios, D.; Tucker-Kellogg, G.; Wu, S.; Brown, E. L.; Zagursky, R. J.; Shlaes, D.; Projan, S. J. *J. Bacteriol.* **2001**, *183*, 7341–7353
- (132) MDowell, P.; Affas, Z.; Reynolds, C.; Holden, M. T.; Wood, S. J.; Saint, S.; Cockayne, A.; Hill, P. J.; Dodd, C. E.; Bycroft, B. W. *et al. Mol Microbiol* **2001**, *41*, 503–512
- (133) Lyon, G. J.; Wright, J. S.; Muir, T. W.; Novick, R. P. *Biochemistry* **2002**, *41*, 10095–10104
- (134) Lina, G.; Jarraud, S.; Ji, G.; Greenland, T.; Pedraza, A.; Etienne, J.; Novick, R. P.; Vandenesch, F. *Mol Microbiol* **1998**, *28*, 655–662
- (135) Novick, R. P.; Geisinger, E. *Annu. Rev. Genet.* **2008**, *42*, 541–564

- (136) Reyes, D.; Andrey, D. O.; Monod, A.; Kelley, W. L.; Zhang, G.; Cheung, A. L. *J. Bacteriol.* **2011**, *193*, 6020–6031
- (137) Dunny, G. M.; Leonard, B. A. *Annu. Rev. Microbiol.* **1997**, *51*, 527–564
- (138) Balaban, N.; Goldkorn, T.; Nhan, R. T.; Dang, L. B.; Scott, S.; Ridgley, R. M.; Rasooly, A.; Wright, S. C.; Larrick, J. W.; Rasooly, R. *et al. Science* **1998**, *280*, 438–440
- (139) Shaw, L. N.; Jonsson, I.-M.; Singh, V. K.; Tarkowski, A.; Stewart, G. C. *Infect. Immun.* **2007**, *75*, 4519–4527
- (140) Kiran, M. D.; Adikesavan, N. V.; Cirioni, O.; Giacometti, A.; Silvestri, C.; Scalise, G.; Ghiselli, R.; Saba, V.; Orlando, F.; Shoham, M. *et al. Mol. Pharmacol.* **2008**, *73*, 1578–1586
- (141) Taga, M. E. *ACS Chem. Biol.* **2007**, *2*, 89–92
- (142) Schauder, S.; Shokat, K.; Surette, M. G.; Bassler, B. L. *Mol Microbiol* **2001**, *41*, 463–476
- (143) Rezzonico, F.; Duffy, B. *BMC Microbiol.* **2008**, *8*, 154
- (144) Doherty, N.; Holden, M. T. G.; Qazi, S. N.; Williams, P.; Winzer, K. J. *Bacteriol.* **2006**, *188*, 2885–2897
- (145) Zhao, L.; Xue, T.; Shang, F.; Sun, H.; Sun, B. *Infect. Immun.* **2010**, *78*, 3506–3515
- (146) Yu, D.; Zhao, L.; Xue, T.; Sun, B. *BMC Microbiol.* **2012**, *12*, 288
- (147) Nielsen, A.; Nielsen, K. F.; Frees, D.; Larsen, T. O.; Ingmer, H. *Antimicrob. Agents Chemother.* **2010**, *54*, 509–512
- (148) Baldry, M.; Nielsen, A.; Bojer, M. S.; Zhao, Y.; Friberg, C.; Ifrah, D.; Glasser Heede, N.; Larsen, T. O.; Frøkiær, H.; Frees, D. *et al. PloS one* **2016**, *11*, e0168305
- (149) Nielsen, A.; Månsson, M.; Bojer, M. S.; Gram, L.; Larsen, T. O.; Novick, R. P.; Frees, D.; Frøkiær, H.; Ingmer, H. *PloS one* **2014**, *9*, e84992
- (150) Hansen, A. M.; Peng, P.; Baldry, M.; Perez-Gassol, I.; Christensen, S. B.; Vinther, J. M. O.; Ingmer, H.; Franzyk, H. *Eur J Med Chem* **2018**, *152*, 370–376
- (151) Kotz, J. *Science* **2012**, *5*, 380
- (152) Lindsay, M. A. *Nat Rev Drug Discov* **2003**, *2*, 831–838
- (153) Imming, P.; Sinning, C.; Meyer, A. *Nat Rev Drug Discov* **2006**, *5*, 821–834
- (154) Lee, J. A.; Uhlik, M. T.; Moxham, C. M.; Tomandl, D.; Sall, D. J. *J Med Chem* **2012**, *55*, 4527–4538
- (155) Swinney, D. C.; Anthony, J. *Nat. Rev. Drug Discov.* **2011**, *10*, 507–519
- (156) Plowright, A. T.; Drowley, L. In *Platform Technologies in Drug Discovery and Validation; Chapter Eight - Phenotypic Screening*; Goodnow, R. A., Ed.; Annual Reports in Medicinal Chemistry; Academic Press, 2017; pp 263–299
- (157) LaPlante, K. L.; Rybak, M. J. *Expert Opin. Pharmacother.* **2004**, *5*, 2321–2331
- (158) Jones, R. N.; Fritsche, T. R.; Sader, H. S.; Ross, J. E. *Antimicrob. Agents Chemother* **2006**, *50*, 2583–2586
- (159) Urban, A.; Eckermann, S.; Fast, B.; Metzger, S.; Gehling, M.; Ziegelbauer, K.; Rubsamen-Waigmann, H.; Freiberg, C. *Appl. Environ. Microbiol.* **2007**, *73*, 6436–6443
- (160) Yan, X.; Hindra; Ge, H.; Yang, D.; Huang, T.; Crnovcic, I.; Chang, C.-Y.; Fang, S.-M.; Annaval, T.; Zhu, X. *et al. J. Nat. Prod.* **2018**

- (161) Schneider, P.; *Isolation of Antibacterial Natural Products from Streptomyces sp. Tü2401*. master's thesis, Eberhard-Karls Universität Tübingen, Tübingen, 2018
- (162) Micheletti, M.; Lye, G. J. *Curr. Opin. Biotechnol.* **2006**, *17*, 611–618
- (163) Kitaoka, M.; Robyt, J. F. *Enzyme Microb. Technol.* **1998**, *22*, 527–531
- (164) Fischer, E.; Sauer, U. *Eur. J. Biochem.* **2003**, *270*, 880–891
- (165) Betts, J. I.; Baganz, F. *Microb. Cell Fact.* **2006**, *5*, 21
- (166) Sohoni, S. V.; Bapat, P. M.; Lantz, A. E. *Microb. Cell Fact.* **2012**, *11*, 9
- (167) Duetz, W. A. *Trends Microbiol.* **2007**, *15*, 469–475
- (168) Duetz, W. A.; Rüedi, L.; Hermann, R.; O'Conner, K.; Büchs, J.; Witholt, B. *Appl. Environ. Microbiol.* **2000**, *66*, 2641–2646
- (169) Minas, W.; Bailey, J. E.; Duetz, W. *Antonie van Leeuwenhoek* **2000**, *78*, 297–305
- (170) Siebenberg, S.; Bapat, P. M.; Lantz, A. E.; Gust, B.; Heide, L. *J. Biosci. Bioeng.* **2010**, *109*, 230–234
- (171) Duetz, W. A.; Witholt, B. *Biochem. Eng. J.* **2004**, *17*, 181–185
- (172) Zang, E.; Brandes, S.; Tovar, M.; Martin, K.; Mech, F.; Horbert, P.; Henkel, T.; Figge, M. T.; Roth, M. *Lab Chip* **2013**, *13*, 3707–3713
- (173) Liu, X.; Painter, R. E.; Enesa, K.; Holmes, D.; Whyte, G.; Garlisi, C. G.; Monsma, F. J.; Rehak, M.; Craig, F. F.; Smith, C. A. *Lab Chip* **2016**, *16*, 1636–1643
- (174) Mahler, L.; Wink, K.; Beulig, R. J.; Scherlach, K.; Tovar, M.; Zang, E.; Martin, K.; Hertweck, C.; Belder, D.; Roth, M. *Sci Rep* **2018**, *8*, 13087
- (175) Kürsten, D.; Kothe, E.; Wetzels, K.; Bergmann, K.; Köhler, J. M. *Environ. Sci.: Process. Impacts* **2014**, *16*, 2362–2370
- (176) Boitard, L.; Cottinet, D.; Bremond, N.; Baudry, J.; Bibette, J. *Eng. Life Sci.* **2015**, *15*, 318–326
- (177) van Dissel, D.; Claessen, D.; van Wezel, G. P. *Adv. Appl. Microbiol.* **2014**, *89*, 1–45
- (178) Glazebrook, M. A.; Doull, J. L.; Stuttard, C.; Vining, L. C. *J. Gen. Microbiol.* **1990**, *136*, 581–588
- (179) Martin, S. M.; Bushell, M. E. *Microbiology* **1996**, *142*, 1783–1788
- (180) Rutala, W. A.; Weber, D. J. *Guideline for disinfection and sterilization in healthcare facilities*, 2008
- (181) Balouiri, M.; Sadiki, M.; Ibnsouda, S. K. *J. Pharm. Anal.* **2016**, *6*, 71–79
- (182) Brown, D. F.; Kothari, D. *J. Clin. Pathol.* **1975**, *28*, 779–783
- (183) Shin, S. H.; Lim, Y.; Lee, S. E.; Yang, N. W.; Rhee, J. H. *J. Microbiol. Methods* **2001**, *44*, 89–95
- (184) Rogers, A. M.; Montville, T. J. *Food Biotechnol* **1991**, *5*, 161–168
- (185) Bonev, B.; Hooper, J.; Parisot, J. *J Antimicrob Chemother* **2008**, *61*, 1295–1301
- (186) Dewanjee, S.; Gangopadhyay, M.; Bhattacharya, N.; Khanra, R.; Dua, T. K. *J. Pharm. Anal.* **2015**, *5*, 75–84
- (187) Li, H.; Balan, P.; Vertes, A. *Angew Chem Int Ed Engl* **2016**, *55*, 15035–15039
- (188) Shirling, E. B.; Gottlieb, D. *Int. J. Syst. Evol. Microbiol.* **1966**, *16*, 313–340

- (189) Waksman, S. A. *The Actinomycetes. Vol. II. Classification, identification and descriptions of genera and species.* **1961**
- (190) Altschul, S. F.; Gish, W.; Miller, W.; Myers, E. W.; Lipman, D. J. *J. Mol. Biol.* **1990**, *215*, 403–410
- (191) Alanjary, M.; Steinke, K.; Adamek, M.; Huson, D.; Ziemert, N.; *autoMLST: Automatic Multi-Locus Species Tree.* <http://automlst.ziemertlab.com/index>
- (192) Richter, M.; Rosselló-Móra, R.; Oliver Glöckner, F.; Peplies, J. *Bioinformatics* **2016**, *32*, 929–931
- (193) Ortlieb, N.; Bretzel, K.; Kulik, A.; Haas, J.; Lüdeke, S.; Keilhofer, N.; Schrey, S. D.; Gross, H.; Niedermeyer, T. H. *J. ChemBioChem* **2018**, 2472–2480
- (194) Liebhart, E.; *Isolierung von Quorum Sensing inhibierenden Naturstoffen aus Actinomyceten.* bachelor's thesis, Eberhard Karls Universität, Tübingen, 2017
- (195) Monod, J. *Annu. Rev. Microbiol.* **1949**, *3*, 371–394
- (196) Allard, P.-M.; Péresse, T.; Bisson, J.; Gindro, K.; Marcourt, L.; van Pham, C.; Roussi, F.; Litaudon, M.; Wolfender, J.-L. *Analytical chemistry* **2016**, *88*, 3317–3323
- (197) Wolfender, J.-L.; Nuzillard, J.-M.; van der Hooft, J. J. J.; Renault, J.-H.; Bertrand, S. *Anal. Chem.* **2018**
- (198) Yang, J. Y.; Sanchez, L. M.; Rath, C. M.; Liu, X.; Boudreau, P. D.; Bruns, N.; Glukhov, E.; Wodtke, A.; Felicio, R. de; Fenner, A. *et al. J. Nat. Prod.* **2013**, *76*, 1686–1699
- (199) Asano, T.; Matsuoka, K.; Hida, T.; Kobayashi, M.; Kitamura, Y.; Hayakawa, T.; Iinuma, S.; Kakinuma, A.; Kato, K. *J. Antibiot.* **1994**, *47*, 557–565
- (200) Ueno, M.; Amemiya, M.; Someno, T.; Masuda, T.; Iinuma, H.; Naganawa, H.; Hamada, M.; Ishizuka, M.; Takeuchi, T. *J. Antibiot.* **1993**, *46*, 1658–1665
- (201) Liu, S. Y.; Zhang, W. Y.; Li, H. Y.; Dai, X. J.; Zhang, Y.; Xu, J. C.; Chen, L. L.; Wang, S. Q.; Qian, C. H. *Sheng li xue bao* **1994**, *46*, 83–89
- (202) Henke, H. *Präparative Gelchromatographie an Sephadex LH-20*; Henke: Obernburg, 1994
- (203) Verdrengh, M.; Collins, L.; Bergin, P.; Tarkowski, A. *Microbes Infect.* **2004**, *6*, 86–92
- (204) Hong, H.; Landauer, M. R.; Foriska, M. A.; Ledney, G. D. *J. Basic Microbiol.* **2006**, *46*, 329–335
- (205) Walter, E. D. *J. Am. Chem. Soc.* **1941**, *63*, 3273–3276
- (206) Alves, R. C.; Almeida, I. M. C.; Casal, S.; Oliveira, M. B. P. *J. Agric. Food Chem.* **2010**, *58*, 3002–3007
- (207) Hazato, T.; Naganawa, H.; Kumagai, M.; Aoyagi, T.; Umezawa, H. *J. Antibiot.* **1979**, *32*, 217–222
- (208) Moloney, M.; Trippier, P.; Yaqoob, M.; Wang, Z. *Curr. Drug Discov. Technol.* **2004**, *1*, 181–199
- (209) Kawai, S.; Kawabata, G.; Kobayashi, A.; Kawazu, K. *Agric. Biol. Chem.* **1989**, *53*, 1127–1133
- (210) Mori, T.; Takahashi, K.; Kashiwabara, M.; Uemura, D.; Katayama, C.; Iwadare, S.; Shizuri, Y.; Mitomo, R.; Nakano, F.; Matsuzaki, A. *Tetrahedron Lett.* **1985**, *26*, 1073–1076
- (211) Aizawa, S.; Shibuya, M.; Shirato, S. *J. Antibiot.* **1971**, *24*, 393–396
- (212) Ryu, G.; Hwang, S.; Kim, S. *J. Antibiot.* **1997**, *50*, 1064–1066
- (213) Ryu, G.; Kim, S. *J. Antibiot.* **1999**, *52*, 193–197
- (214) Kawazu, K.; Kanzaki, H.; Kawabata, G.; Kawai, S.; Kobayashi, A. *Biosci. Biotechnol. Biochem.* **2014**, *56*, 1382–1385

- (215) Kanzaki, H.; Kagemori, T.; Asano, S.; Kawazu, K. *Biosci Biotechnol Biochem* **1998**, *62*, 2328–2333
- (216) Gräfe, U.; Kluge, H.; Thiericke, R. *Liebigs Ann. Chem.* **1992**, *1992*, 429–432
- (217) Grigorjev, P. A.; Schlegel, R.; Gräfe, U. *Die Pharmazie* **1992**, *47*, 707–709
- (218) Otani, T.; Yoshida, K. I.; Kubota, H.; Kawai, S.; Ito, S.; Hori, H.; Ishiyama, T.; Oki, T. *J. Antibiot.* **2000**, *53*, 1397–1400
- (219) Kjaerulff, L.; Nielsen, A.; Mansson, M.; Gram, L.; Larsen, T. O.; Ingmer, H.; Gotfredsen, C. H. *Mar Drugs* **2013**, *11*, 5051–5062
- (220) Sully, E. K.; Malachowa, N.; Elmore, B. O.; Alexander, S. M.; Femling, J. K.; Gray, B. M.; DeLeo, F. R.; Otto, M.; Cheung, A. L.; Edwards, B. S. *et al. PLOS Pathog.* **2014**, *10*, e1004174
- (221) Seidl, K.; Stucki, M.; Ruegg, M.; Goerke, C.; Wolz, C.; Harris, L.; Berger-Bächi, B.; Bischoff, M. *Antimicrob. Agents Chemother.* **2006**, *50*, 1183–1194
- (222) Regassa, L. B.; Novick, R. P.; Betley, M. J. *Infect. Immun.* **1992**, *60*, 3381–3388
- (223) Weber, T.; Blin, K.; Duddela, S.; Krug, D.; Kim, H. U.; Bruccoleri, R.; Lee, S. Y.; Fischbach, M. A.; Müller, R.; Wohlleben, W. *et al. Nucleic Acids Res.* **2015**, *43*, W237-43
- (224) Zhao, C.; Coughlin, J. M.; Ju, J.; Zhu, D.; Wendt-Pienkowski, E.; Zhou, X.; Wang, Z.; Shen, B.; Deng, Z. *J. Biol. Chem.* **2010**, *285*, 20097–20108
- (225) Otera, J. *Chem. Rev.* **1993**, *93*, 1449–1470
- (226) Joule, J. A.; Mills, K.; Smith, G. F. *Heterocyclic chemistry*, 3. ed.; Chapman & Hall: London, 1995
- (227) Himmler, S.; Hörmann, S.; Obert, K.; Wasserscheid, P. *Chem. Ing. Tech.* **2007**, *79*, 421–428
- (228) Krause, K. M.; Serio, A. W.; Kane, T. R.; Connolly, L. E. *Cold Spring Harb Perspect Med* **2016**, *6*
- (229) Durfee, T.; Nelson, R.; Baldwin, S.; Plunkett, G.; Burland, V.; Mau, B.; Petrosino, J. F.; Qin, X.; Muzny, D. M.; Ayele, M. *et al. J. Bacteriol.* **2008**, *190*, 2597–2606
- (230) Hutter, B.; Schaab, C.; Albrecht, S.; Borgmann, M.; Brunner, N. A.; Freiberg, C.; Ziegelbauer, K.; Rock, C. O.; Ivanov, I.; Loferer, H. *Antimicrob. Agents Chemother.* **2004**, *48*, 2838–2844
- (231) Hutter, B.; Fischer, C.; Jacobi, A.; Schaab, C.; Loferer, H. *Antimicrobial agents and chemotherapy* **2004**, *48*, 2588–2594
- (232) Mariner, K. R.; Ooi, N.; Roebuck, D.; O'Neill, A. J.; Chopra, I. *Antimicrob. Agents Chemother.* **2011**, *55*, 1784–1786
- (233) Blin, K.; Wolf, T.; Chevrette, M. G.; Lu, X.; Schwalen, C. J.; Kautsar, S. A.; Suarez Duran, H. G.; Los Santos, E. L. C. de; Kim, H. U.; Nave, M. *et al. Nucleic acids research* **2017**, *45*, W36-W41
- (234) Blodgett, J. A. V.; Oh, D.-C.; Cao, S.; Currie, C. R.; Kolter, R.; Clardy, J. *Proc. Natl. Acad. Sci. U.S.A.* **2010**, *107*, 11692–11697
- (235) Yu, F.; Zaleta-Rivera, K.; Zhu, X.; Huffman, J.; Millet, J. C.; Harris, S. D.; Yuen, G.; Li, X.-C.; Du, L. *Antimicrob. Agents Chemother.* **2007**, *51*, 64–72
- (236) Schobert, R.; Schlenk, A. *Bioorg. Med. Chem.* **2008**, *16*, 4203–4221
- (237) Graupner, P. R.; Thornburgh, S.; Mathieson, J. T.; Chapin, E. L.; Kemmitt, G. M.; Brown, J. M.; Snipes, C. E. *J. Antibiot.* **1997**, *50*, 1014–1019
- (238) Mo, X.; Li, Q.; Ju, J. *RSC Adv* **2014**, *4*, 50566–50593
- (239) Xie, Y.; Wright, S.; Shen, Y.; Du, L. *Nat Prod Rep* **2012**, *29*, 1277–1287

- (240) Ueda, K.; Oinuma, K.-I.; Ikeda, G.; Hosono, K.; Ohnishi, Y.; Horinouchi, S.; Beppu, T. *J. Bacteriol.* **2002**, *184*, 1488–1492
- (241) Maresca, J. A.; Romberger, S. P.; Bryant, D. A. *J. Bacteriol.* **2008**, *190*, 6384–6391
- (242) Takano, H.; Obitsu, S.; Beppu, T.; Ueda, K. *J. Bacteriol.* **2005**, *187*, 1825–1832
- (243) Imbert, M.; Béchet, M.; Blondeau, R. *Curr. Microbiol.* **1995**, *31*, 129–133
- (244) Patzer, S. I.; Braun, V. *J. Bacteriol.* **2010**, *192*, 426–435
- (245) Wang, W.; Qiu, Z.; Tan, H.; Cao, L. *Biometals* **2014**, *27*, 623–631
- (246) Ohnishi, Y.; Ishikawa, J.; Hara, H.; Suzuki, H.; Ikenoya, M.; Ikeda, H.; Yamashita, A.; Hattori, M.; Horinouchi, S. *J. Bacteriol.* **2008**, *190*, 4050–4060
- (247) Keberle, H. *Ann. N. Y. Acad. Sci.* **1964**, *119*, 758–768
- (248) Sadeghi, A.; Soltani, B. M.; Nekouei, M. K.; Jouzani, G. S.; Mirzaei, H. H.; Sadeghizadeh, M. *Microbiol Res* **2014**, *169*, 699–708
- (249) Bernard, T.; Jebbar, M.; Rassouli, Y.; Himdi-Kabbab, S.; Hamelin, J.; Blanco, C. *J. Gen. Microbiol.* **1993**, *139*, 129–136
- (250) Shen, B.; Hindra; Yan, X.; Huang, T.; Ge, H.; Yang, D.; Teng, Q.; Rudolf, J. D.; Lohman, J. R. *Bioorganic Med. Chem. Lett.* **2015**, *25*, 9–15
- (251) Nicolaou, K. C.; Smith, A. L.; Yue, E. W. *Proc. Natl. Acad. Sci. U.S.A.* **1993**, *90*, 5881–5888
- (252) Inoue, M.; Usuki, T.; Lee, N.; Hiramata, M.; Tanaka, T.; Hosoi, F.; Ohie, S.; Otani, T. *J. Am. Chem. Soc.* **2006**, *128*, 7896–7903
- (253) Liang, Z.-X. *Nat Prod Rep* **2010**, *27*, 499–528
- (254) Joshi, M. C.; Rawat, D. S. *Chem. Biodivers.* **2012**, *9*, 459–498
- (255) Chen, Y.; Yin, M.; Horsman, G. P.; Shen, B. *J. Nat. Prod.* **2011**, *74*, 420–424
- (256) Shao, R.-g.; Zhen, Y.-s. *Anticancer. Agents Med. Chem.* **2008**, *8*, 123–131
- (257) S-Tsuchiya, K.; Arita, M.; Hori, M.; Otani, T. *J. Antibiot.* **1994**, *47*, 787–791
- (258) Cobuzzi, R. J., JR.; Kotsopoulos, S. K.; Otani, T.; Beerman, T. A. *Biochemistry* **2002**, *34*, 583–592
- (259) Urbaniak, M. D.; Bingham, J. P.; Hartley, J. A.; Woolfson, D. N.; Caddick, S. *J Med Chem* **2004**, *47*, 4710–4715
- (260) Gao, Q.; Thorson, J. S. *FEMS Microbiol Lett* **2008**, *282*, 105–114
- (261) Darby, N.; Kim, C. U.; Salaün, J. A.; Shelton, K. W.; Takada, S.; Masamune, S. *J. Chem. Soc. D* **1971**, *0*, 1516–1517
- (262) Smith, A. L.; Nicolaou, K. C. *J Med Chem* **1996**, *39*, 2103–2117
- (263) Sugiura, Y.; Matsumoto, T. *Biochemistry* **1993**, *32*, 5548–5553
- (264) Otani, T.; Minami, Y.; Marunaka, T.; Zhang, R.; Xie, M. Y. *J. Antibiot.* **1988**, *41*, 1580–1585
- (265) Zhen, Y. S.; Ming, X. Y.; Yu, B.; Otani, T.; Saito, H.; Yamada, Y. *J. Antibiot.* **1989**, *42*, 1294–1298
- (266) Xu, Y. J.; Zhen, Y. S.; Goldberg, I. H. *Biochemistry* **1994**, *33*, 5947–5954
- (267) Matsumoto, T.; Okuno, Y.; Sugiura, Y. *Biochem. Biophys. Res. Commun.* **1993**, *195*, 659–666

- (268) Galm, U.; Hager, M. H.; van Lanen, S. G.; Ju, J.; Thorson, J. S.; Shen, B. *Chem. Rev.* **2005**, *105*, 739–758
- (269) McHugh, M. M.; Gawron, L. S.; Matsui, S.-I.; Beerman, T. A. *Cancer Res.* **2005**, *65*, 5344–5351
- (270) Okuno, Y.; Iwashita, T.; Otani, T.; Sugiura, Y. *J. Am. Chem. Soc.* **1996**, *118*, 4729–4730
- (271) Okuno, Y.; Iwashita, T.; Sugiura, Y. *J. Am. Chem. Soc.* **2000**, *122*, 6848–6854
- (272) Yu, L.; Mah, S.; Otani, T.; Dedon, P. *J. Am. Chem. Soc.* **1995**, *117*, 8877–8878
- (273) Xu, Y.-j.; Xi, Z.; Zhen, Y.-s.; Goldberg, I. H. *Biochemistry* **1995**, *34*, 12451–12460
- (274) Thorson, J. S.; Sievers, E. L.; Ahlert, J.; Shepard, E.; Whitwam, R. E.; Onwueme, K. C.; Ruppen, M. *Curr. Pharm. Des.* **2000**, *6*, 1841–1879
- (275) Maeda, H. In *Enediyne antibiotics as antitumor agents; Enediyne Antibiotics as Antitumor Agents*; Borders, D. B., Ed.; Dekker: New York, 1995; p 363
- (276) Sievers, E. L.; Senter, P. D. *Annu. Rev. Med.* **2013**, *64*, 15–29
- (277) Brukner, I. In *Current Opinion in Oncologic: Endocrine and Metabolic Investigational Drugs*, 2nd ed.; C-1027 Taiho Pharmaceutical Co Ltd; Brukner, I., Ed., 2000; pp 344–352
- (278) Li, J. Z.; Jiang, M.; Xue, Y. C.; Zhen, Y. S. *Zhongguo Yi Xue Ke Xue Yuan Xue Bao* **1993**, *28*, 260–265
- (279) Li, J.; Zhen, Y.; Yang, Z. *Zhongguo Yi Xue Ke Xue Yuan Xue Bao* **1994**, *16*, 328–333
- (280) Shao, R. G.; Zhen, Y. S. *Yao xue xue bao* **1992**, *27*, 486–491
- (281) Porath, J.; Flodin, P. *Nature* **1959**, *183*, 1657–1659
- (282) Hichrom Limited. *Size Exclusion Chromatography: The Physical Properties of the Base Beads for all Toyopearl Products*
- (283) Andrews, P. *Biochem. J.* **1964**, *91*, 222–233
- (284) GE Healthcare; *Gel Filtration: Principles and Methods* (accessed February 21, 2016)
- (285) Kroner, K. H.; Hummel, W.; Völkel, J.; Kula, M. R. In *Membranes and Membrane Processes; Effects of Antifoams on Cross-flow Filtration of Microbial Suspensions*; Drioli, E., Nakagaki, M., Eds.; Springer US: Boston, MA, s.l., 1986; pp 223–232
- (286) Hostettmann, K.; Terreaux, C.; *Medium Pressure Liquid Chromatography. Encyclopedia of Separation Science*; Elsevier, 2000; pp 3296–3303
- (287) Hostettmann, K.; Marston, A.; Hostettmann, M. *Preparative Chromatography Techniques: Applications in Natural Product Isolation*, Second, Completely Revised and Enlarged Edition; Springer Berlin Heidelberg: Berlin, Heidelberg, s.l., 1998
- (288) Stevens, W. C.; Hill, D. C. *Mol. Divers.* **2009**, *13*, 247–252
- (289) Gocan, S. *J. Chromatogr. Sci.* **2002**, *40*, 538–549
- (290) Pirrung, M. C. *The synthetic organic chemist's companion*; Wiley-Interscience: Hoboken, N.J, 2007
- (291) Timur, Z. K.; Akyildiz Demir, S.; Marsching, C.; Sandhoff, R.; Seyrantepe, V. *Mol Genet Metab Rep* **2015**, *4*, 72–82
- (292) Bial, M. *Dtsch med Wochenschr* **1903**, *29*, 477–478
- (293) Friedman, M.; David Williams, L. *Bioorg. Chem.* **1974**, *3*, 267–280

- (294) Enami, T.; Nagae, N.; Doshi, S. *LC GC Eur* **2003**, *16*, 418–425
- (295) Cledera-Castro, M.; Santos-Montes, A.; Izquierdo-Hornillos, R.; Gonzalo-Lumbreras, R. *J. Sep. Sci.* **2007**, *30*, 699–707
- (296) Chromatographie; *Nucleosil C8*
- (297) Phenomenex. *Kinetex Core-Shell Technology: These Phases Rock Your LC Laboratory*, 2017
- (298) Buszewski, B.; Noga, S. *Anal. Bioanal. Chem.* **2012**, *402*, 231–247
- (299) Oyler, A. R.; Armstrong, B. L.; Cha, J. Y.; Zhou, M. X.; Yang, Q.; Robinson, R. I.; Dunphy, R.; Burinsky, D. J. *J. Chromatogr. A* **1996**, *724*, 378–383
- (300) Garbis, S. D.; Melse-Boonstra, A.; West, C. E.; van Breemen, R. B. *Anal. Chem.* **2001**, *73*, 5358–5364
- (301) Olsen, B. A. *J. Chromatogr. A* **2001**, *913*, 113–122
- (302) Li, R.; Huang, J. *J. Chromatogr. A* **2004**, *1041*, 163–169
- (303) Guo, Y. *Analyst* **2015**, *140*, 6452–6466
- (304) Hemström, P.; Irgum, K. *J. Sep. Sci.* **2006**, *29*, 1784–1821
- (305) Dejaegher, B.; Vander Heyden, Y. *J. Sep. Sci.* **2010**, *33*, 698–715
- (306) Alpert, A. J.; Shukla, M.; Shukla, A. K.; Zieske, L. R.; Yuen, S. W.; Ferguson, M. A.; Mehlert, A.; Pauly, M.; Orlando, R. *Journal of chromatography. A* **1994**, *676*, 191–22
- (307) Yoshida, T. *J. Biochem. Biophys. Methods* **2004**, *60*, 265–280
- (308) Alpert, A. J. *J. Chromatogr. A* **1990**, *499*, 177–196
- (309) Hemström, P.; Irgum, K. *J. Sep. Sci.* **2006**, *29*, 1784–1821
- (310) Guo, Y.; Gaiki, S. *J. Chromatogr. A* **2011**, *1218*, 5920–5938
- (311) Schuster, G.; Lindner, W. *J. Chromatogr. A* **2013**, *1273*, 73–94
- (312) Gama, M. R.; da Costa Silva, R. G.; Collins, C. H.; Bottoli, C. B. *Trends Anal. Chem.* **2012**, *37*, 48–60
- (313) Douville, V.; Lodi, A.; Miller, J.; Nicolas, A.; Clarot, I.; Prilleux, B.; Megoulas, N.; Koupparis, M. *Pharmeur. Bio. Sci. Notes* **2006**, *2006*, 9–15
- (314) Adnani, N.; Michel, C. R.; Bugni, T. S. *J. Nat. Prod.* **2012**, *75*, 802–806
- (315) Condezo-Hoyos, L.; Pérez-López, E.; Rupérez, P. *Food Chem.* **2015**, *180*, 265–271
- (316) Young, C. S.; Dolan, J. W. *LCGC North Am.* **2003**, *21*, 120, 122, 126, 128
- (317) Young, C. S.; Dolan, J. W. *LCGC North Am.* **2004**, *22*, 244, 246–250
- (318) *HILIC: Method Development Guide*; Advanced Chromatography Technologies, Ed., 2017
- (319) *IUPAC Compendium of Chemical Terminology*; Nič, M.; Jirát, J.; Košata, B.; Jenkins, A.; McNaught, A., Eds.; IUPAC: Research Triangle Park, NC, 2009
- (320) Fraige, K.; Dametto, A. C.; Zeraik, M. L.; Freitas, L. de; Saraiva, A. C.; Medeiros, A. I.; Castro-Gamboa, I.; Cavalheiro, A. J.; Silva, D. H. S.; Lopes, N. P. *et al. Phytochem Anal* **2018**, *29*, 196–204
- (321) Vijlder, T. de; Valkenburg, D.; Lemièrre, F.; Romijn, E. P.; Laukens, K.; Cuyckens, F. *Mass Spectrom. Rev.* **2018**, *37*, 607–629

- (322) Wolfender, J.-L.; Waridel, P.; Ndjoko, K.; Hobby, K. R.; Major, H. J.; Hostettmann, K. *Analisis* **2000**, *28*, 895–906
- (323) Ruttkies, C.; Schymanski, E. L.; Wolf, S.; Hollender, J.; Neumann, S. *J. Cheminformatics* **2016**, *8*, 3
- (324) Wolf, S.; Schmidt, S.; Müller-Hannemann, M.; Neumann, S. *BMC Bioinform.* **2010**, *11*, 148
- (325) Allen, F.; Pon, A.; Wilson, M.; Greiner, R.; Wishart, D. *Nucleic Acids Res.* **2014**, *42*, W94-9
- (326) Allen, F.; Pon, A.; Greiner, R.; Wishart, D. *Anal. Chem.* **2016**, *88*, 7689–7697
- (327) Böcker, S.; Letzel, M. C.; Lipták, Z.; Pervukhin, A. *Bioinformatics* **2009**, *25*, 218–224
- (328) Reynolds, D. M.; Schatz, A.; Waksman, S. A. *Exp. Biol. Med.* **1947**, *64*, 50–54
- (329) Reynolds, D. M.; Waksman, S. A. *J. Bacteriol.* **1948**, *55*, 739–752
- (330) Stapley, E. O.; Ormond, R. E. *Science* **1957**, *125*, 587–589
- (331) Lin, Z.; Xu, X.; Zhao, S.; Yang, X.; Guo, J.; Zhang, Q.; Jing, C.; Chen, S.; He, Y. *Nat Commun* **2018**, *9*, 3445
- (332) Benz, G.; Schröder, T.; Kurz, J.; Wünsche, C.; Karl, W.; Steffens, G.; Pfitzner, J.; Schmidt, D. *Angew. Chem. Int. Ed. Engl.* **1982**, *21*, 527–528
- (333) Stefanska, A. L.; Fulston, M.; Houge-Frydrych, C. S.; Jones, J. J.; Warr, S. R. *J. Antibiot.* **2000**, *53*, 1346–1353
- (334) Zeng, Y.; Kulkarni, A.; Yang, Z.; Patil, P. B.; Zhou, W.; Chi, X.; van Lanen, S.; Chen, S. *ACS Chem. Biol.* **2012**, *7*, 1565–1575
- (335) Page, M. G. P. *Ann. N. Y. Acad. Sci.* **2013**, *1277*, 115–126
- (336) Hartmann, A.; Fiedler, H. P.; Braun, V. *Eur. J. Biochem.* **1979**, *99*, 517–524
- (337) Zeng, Y.; Roy, H.; Patil, P. B.; Ibba, M.; Chen, S. *Antimicrob. Agents Chemother.* **2009**, *53*, 4619–4627
- (338) Vértesy, L.; Aretz, W.; Fehlhaber, H.-W.; Kogler, H. *HCA* **1995**, *78*, 46–60
- (339) Bickel, H.; Mertens, P.; Prelog, V.; Seibl, J.; Walser, A. *Antimicrob. Agents Chemother.* **1965**, *5*, 951–957
- (340) Miyakawa, S.; Noto, T.; Okazaki, H. *Microbiol. Immunol.* **1982**, *26*, 885–895
- (341) Braun, V.; Pramanik, A.; Gwinner, T.; Köberle, M.; Bohn, E. *Biometals* **2009**, *22*, 3–13
- (342) Pramanik, A.; Stroeher, U. H.; Krejci, J.; Standish, A. J.; Bohn, E.; Paton, J. C.; Autenrieth, I. B.; Braun, V. *Int. J. Med. Microbiol.* **2007**, *297*, 459–469
- (343) Gause, G. F. *BMJ* **1955**, *2*, 1177–1179
- (344) Pramanik, A.; Braun, V. *J. Bacteriol.* **2006**, *188*, 3878–3886
- (345) Asahi, K.; Nagatsu, J.; Suzuki, S. *J. Antibiot.* **1966**, *19*, 195–199
- (346) Lousberg, R. J. J. C.; Tirilly, Y.; Moreau, M. *Experientia* **1976**, *32*, 331–332
- (347) Umino, K.; Furumai, T.; Matsuzawa, N.; Awataguchi, Y.; Ito, Y. *J. Antibiot.* **1973**, *26*, 506–512
- (348) Umezawa, H.; Takeuchi, T.; Nitta, K.; Yamamoto, T.; Yamaoka, S. *J. Antibiot.* **1953**, *6*, 101
- (349) Haneishi, T.; Terahara, A.; Hamano, K.; Arai, M. *J. Antibiot.* **1974**, *27*, 400–407

6. Appendix

6.1 List of abbreviations

aa	Amino acid
ACN	Acetonitrile
AIP	Autoinducing peptides
antiSMASH	Antibiotics and secondary metabolite analysis shell
BGC	Biosynthetic gene cluster
BLAST	Basic Local Alignment Search Tool
CFS	Cell free supernatant
CFU	Colony-forming units
CV	Column volumes
DAD	Diode array detector
DCM	Dichlormethane
DNA	Deoxyribonucleic acid
EA	Ethyl acetate
eDNA	Environmental DNA
ELSD	Evaporative light scattering detector
FA	Formic acid
FDA	U. S. Food and Drug Administration
GFC	Gel filtration chromatography
HCl	Hydrochloric acid
HPLC	High performance liquid chromatography coupled to a mass spectrometer
HPLC-MS	High performance liquid chromatography coupled to a mass spectrometer
HR-MS	High resolution mass spectrometry
HSAF	Heat-stable antifungal factor
HTP	High-throughput
ISP	International Streptomyces Project
LC	Liquid chromatography
MeOH	Methanol
MIC	Minimal inhibitory concentration
MoA	Mode of action
MPLC	Medium pressure liquid chromatography
MS ²	Tandem mass spectrometry
MTP	Microtiter plate
NaOH	Sodium hydroxide
NMR	Nuclear magnetic resonance spectroscopy
NP	Natural product
PEG	Polyethylene glycol
pHPLC	Preparative HPLC
PTM	Polycyclic tetramate macrolactams
QS	Quorum sensing
QSI	Quorum sensing inhibition
rpm	Revolutions per minute
rRNA	Ribosomal RNA
SEC	Size-exclusion chromatography
SMA	Styrene-co-maleic acid

TLC	Thin-layer chromatography
t_R	Relative retention time

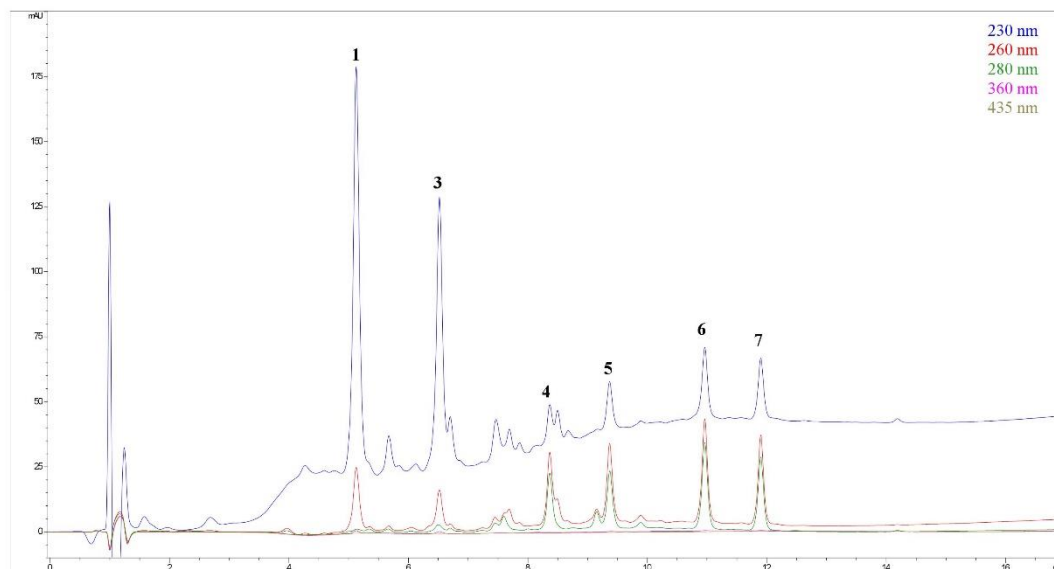
6.2 Supporting Information *Streptomyces* sp. AcE210

Supporting Information

Contents of the Supporting Information

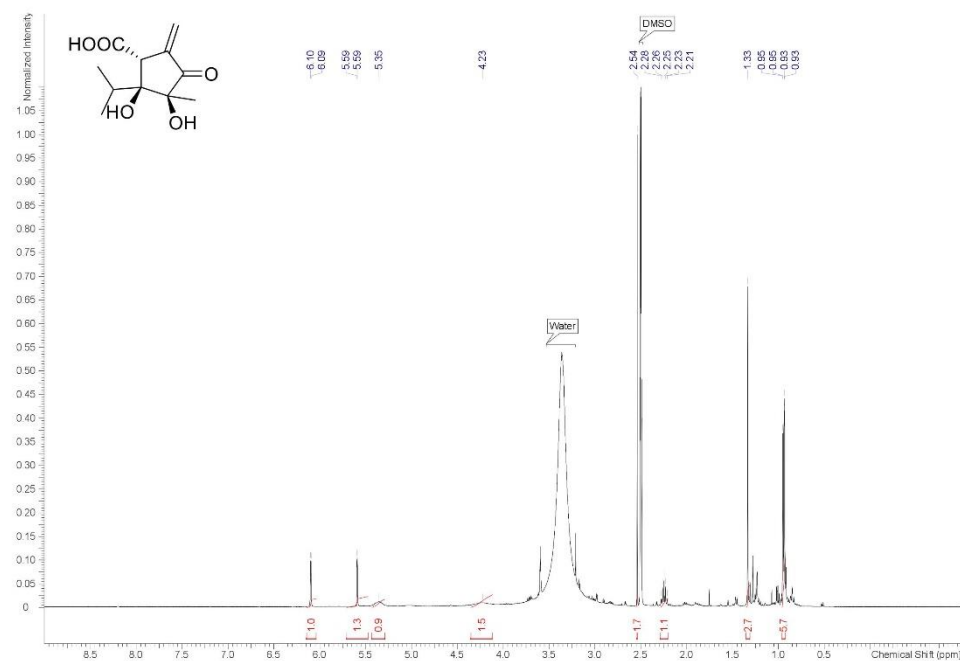
Figure S1. HPLC-UV chromatogram of the <i>S.</i> sp. AcE210 EtOAc extract.....	2
Figure S3. NOESY spectrum (600 MHz, DMSO- <i>d</i> ₆) used for dereplication of xanthocidin (1).....	4
Figure S4. ¹ H-NMR spectrum (600 MHz, DMSO- <i>d</i> ₆) of dihydroxanthocidin (2).....	5
Figure S5. ¹³ C-NMR spectrum (150 MHz, DMSO- <i>d</i> ₆) of dihydroxanthocidin (2).....	6
Figure S6. NOESY spectrum (600 MHz, DMSO- <i>d</i> ₆) of dihydroxanthocidin (2).....	7
Figure S7. HSQC-DEPT spectrum (600 MHz, 150 MHz, DMSO- <i>d</i> ₆) of dihydroxanthocidin (2) ...	8
Figure S8. ¹ H- ¹ H COSY spectrum (600 MHz, DMSO- <i>d</i> ₆) of dihydroxanthocidin (2).....	9
Figure S9. HMBC spectrum (600 MHz, 150 MHz, DMSO- <i>d</i> ₆) of dihydroxanthocidin (2).....	10
Figure S10. ¹ H-NMR spectrum (600 MHz, acetonitrile- <i>d</i> ₃) of homoxanthocidin (3).....	11
Figure S11. HSQC-DEPT spectrum (600 MHz, 150 MHz, acetonitrile- <i>d</i> ₃) of homoxanthocidin (3)	12
Figure S12. ¹ H- ¹ H COSY spectrum (600 MHz, acetonitrile- <i>d</i> ₃) of homoxanthocidin (3).....	13
Figure S13. HMBC spectrum (600 MHz, 150 MHz, DMSO- <i>d</i> ₆) of homoxanthocidin (3).....	14
Figure S14. ¹ H-NMR spectrum (600 MHz, acetonitrile- <i>d</i> ₃) of xanthocidin B (4).....	15
Figure S15. ¹³ C-NMR spectrum (150 MHz, acetonitrile- <i>d</i> ₃) of xanthocidin B (4).....	16
Figure S16. HSQC-DEPT spectrum (600 MHz, 150 MHz, acetonitrile- <i>d</i> ₃) of xanthocidin B (4) .	17
Figure S17. ¹ H- ¹ H COSY spectrum (600 MHz, acetonitrile- <i>d</i> ₃) of xanthocidin B (4).....	18
Figure S18. HMBC spectrum (600 MHz, 150 MHz, acetonitrile- <i>d</i> ₃) of xanthocidin B (4).....	19
Figure S19. ¹ H-NMR spectrum (600 MHz, acetonitrile- <i>d</i> ₃) of homoxanthocidin B (5).....	20
Figure S20. ¹³ C-NMR spectrum (150 MHz, acetonitrile- <i>d</i> ₃) of homoxanthocidin B (5).....	21
Figure S21. HSQC-DEPT spectrum (600 MHz, 150 MHz, acetonitrile- <i>d</i> ₃) of homoxanthocidin B (5).....	22
Figure S22. ¹ H- ¹ H COSY spectrum (600 MHz, acetonitrile- <i>d</i> ₃) of homoxanthocidin B (5).....	23
Figure S23. HMBC spectrum (600 MHz, 150 MHz, acetonitrile- <i>d</i> ₃) of homoxanthocidin B (5) ...	24
Figure S24. ¹³ C-NMR spectra (100 MHz, acetonitrile- <i>d</i> ₃) of xanthocidin B (4) and [¹³ C ₄]- xanthocidin B.....	25
Figure S25. Phylogenetic tree of <i>S.</i> sp. AcE210.....	26
Table S26. Results of the BLAST analysis.....	27

Figure S1. HPLC-UV chromatogram of the *S. sp.* AcE210 EtOAc extract, showing peaks for xanthocidin (1), homoxanthocidin (3), xanthocidin B (4), homoxanthocidin B (5), xanthocidin C (6), homoxanthocidin C (7). Dihydroxanthocidin (2) is not visible as isolated peak in the UV chromatogram. The other compounds observed in the chromatogram do not feature UV spectra similar to xanthocidin and the described derivatives, nor do they have molecular masses in the respective mass range.



2

Figure S2. $^1\text{H-NMR}$ spectrum (400 MHz, $\text{DMSO-}d_6$) used for the dereplication of xanthocidin (1)



3

Figure S3. NOESY spectrum (600 MHz, DMSO- d_6) used for dereplication of xanthocidin (**1**)

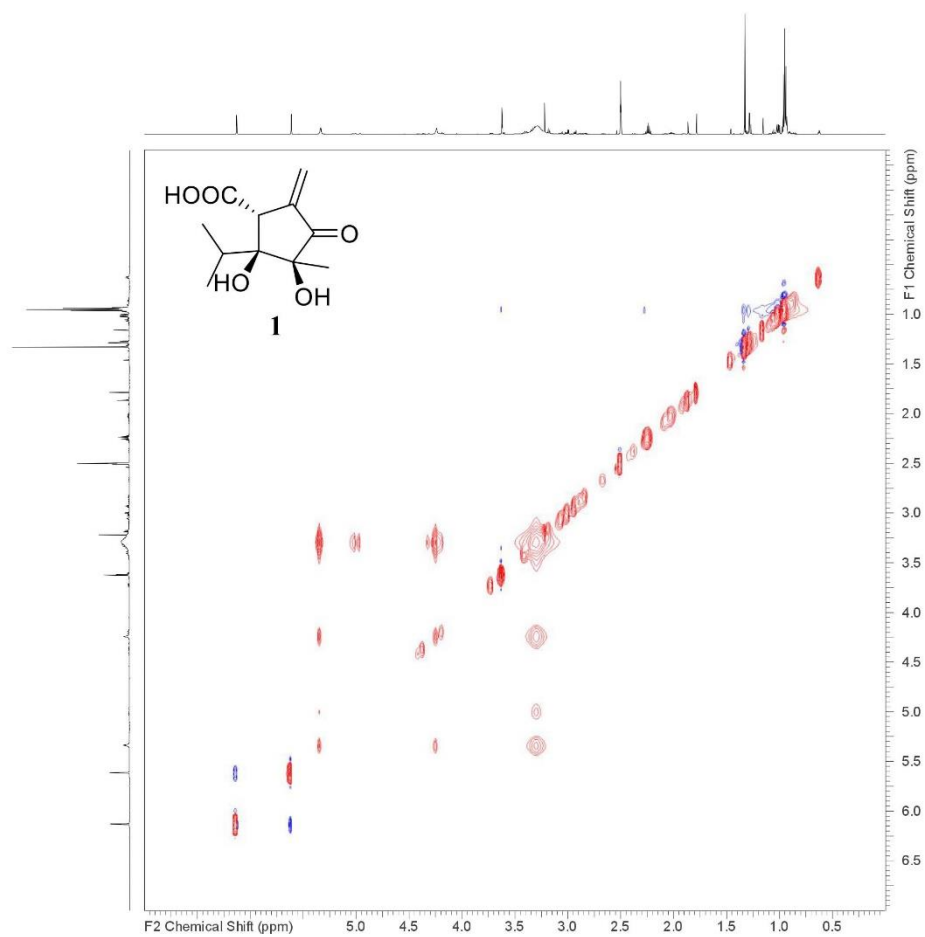
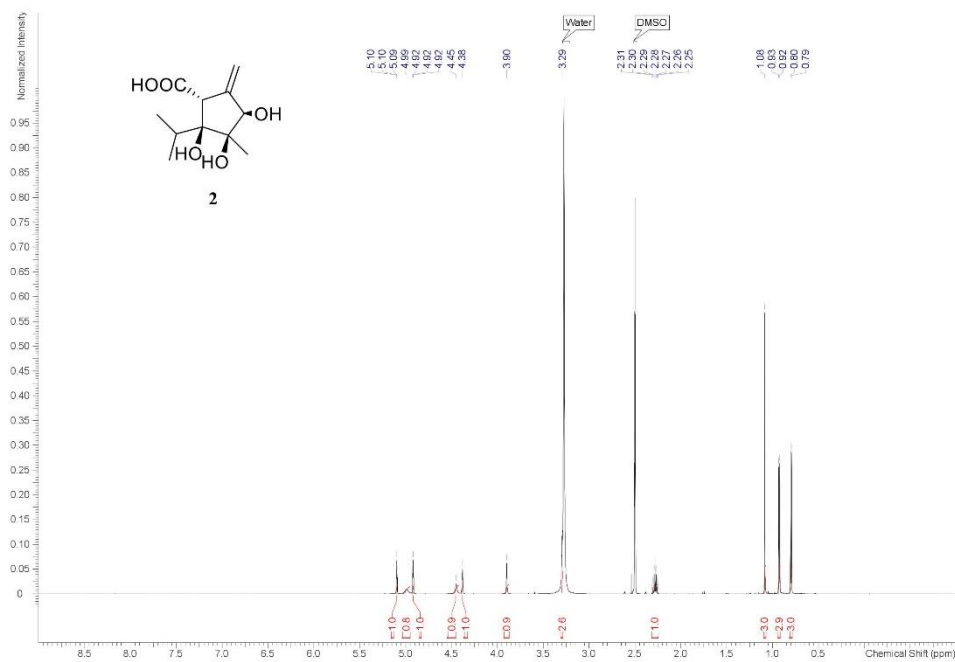
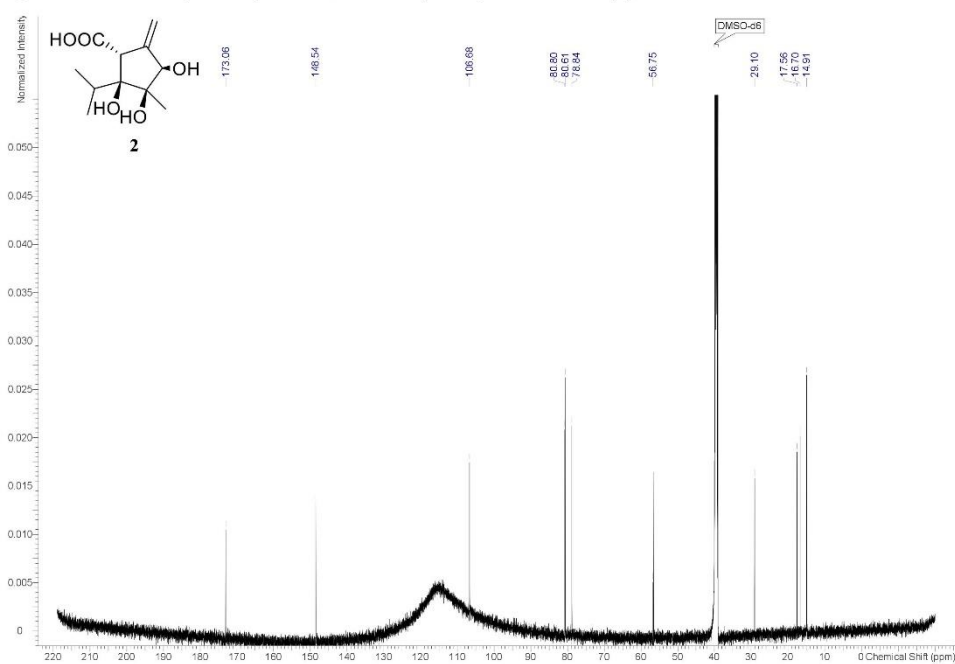


Figure S4. $^1\text{H-NMR}$ spectrum (600 MHz, $\text{DMSO-}d_6$) of dihydroanthocidin (**2**)

5

Figure S5. $^{13}\text{C-NMR}$ spectrum (150 MHz, $\text{DMSO-}d_6$) of dihydroanthocidin (**2**)

6

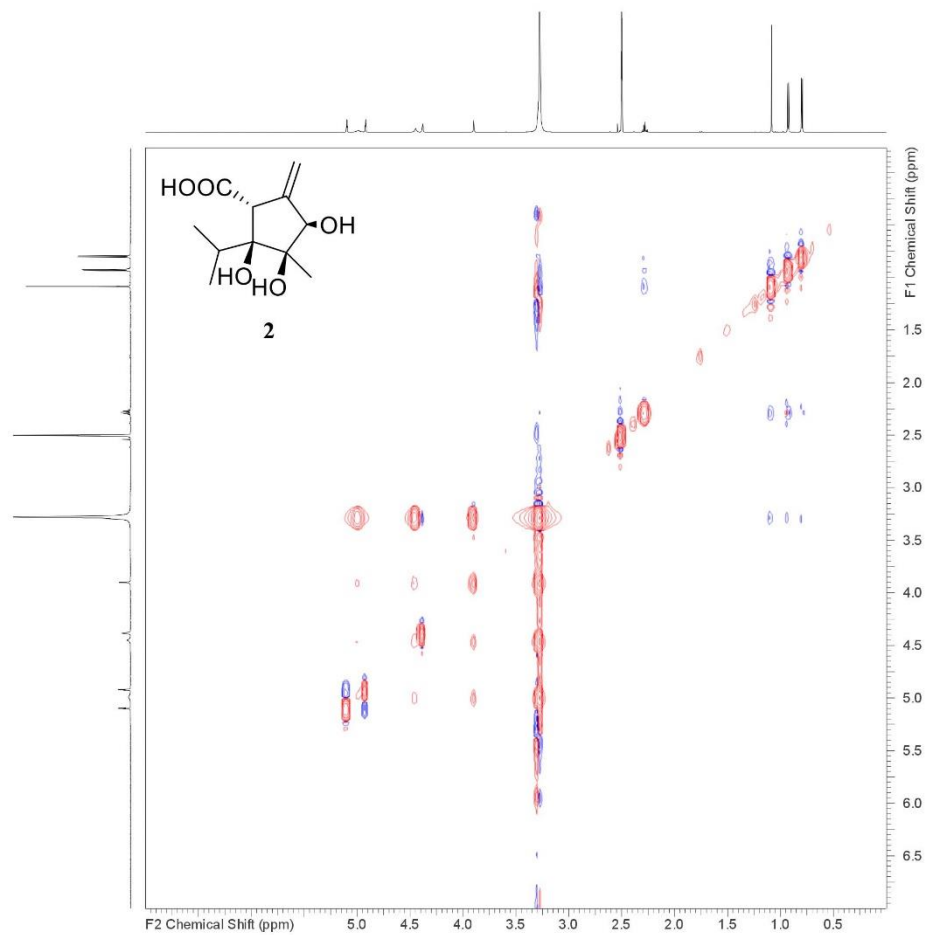
Figure S6. NOESY spectrum (600 MHz, DMSO-*d*₆) of dihydroxanthocidin (**2**)

Figure S7. HSQC-DEPT spectrum (600 MHz, 150 MHz, DMSO- d_6) of dihydroxanthocidin (**2**)

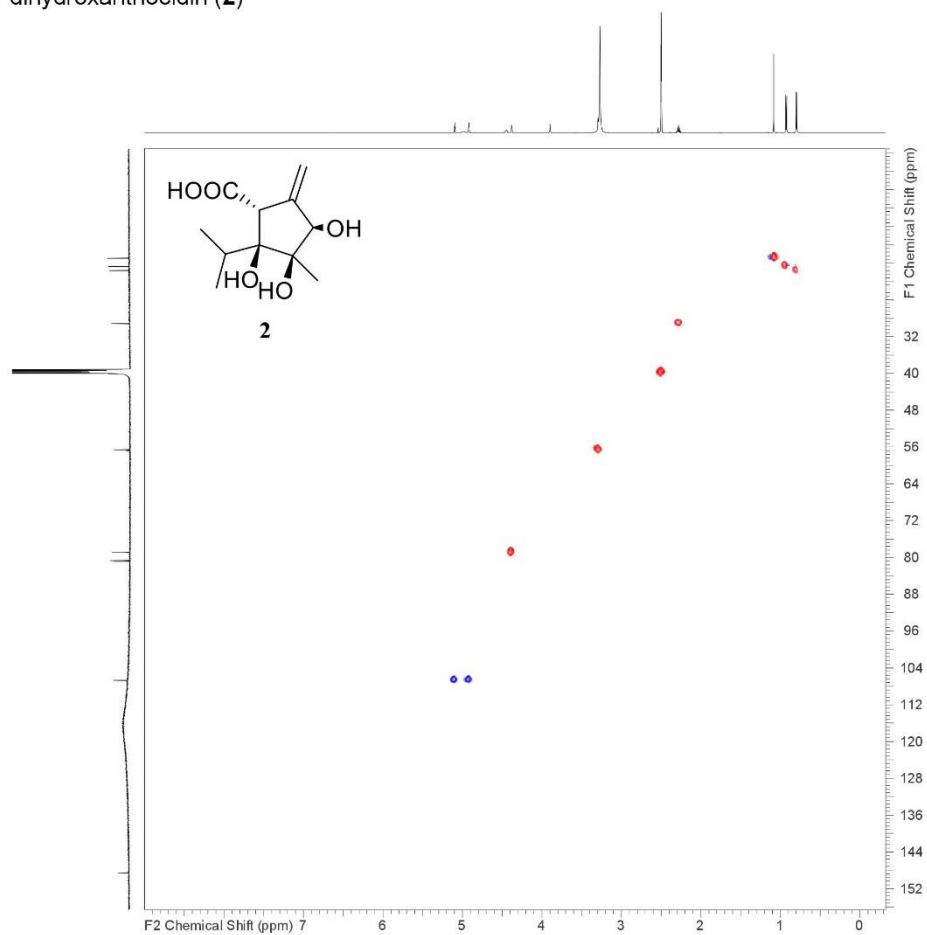


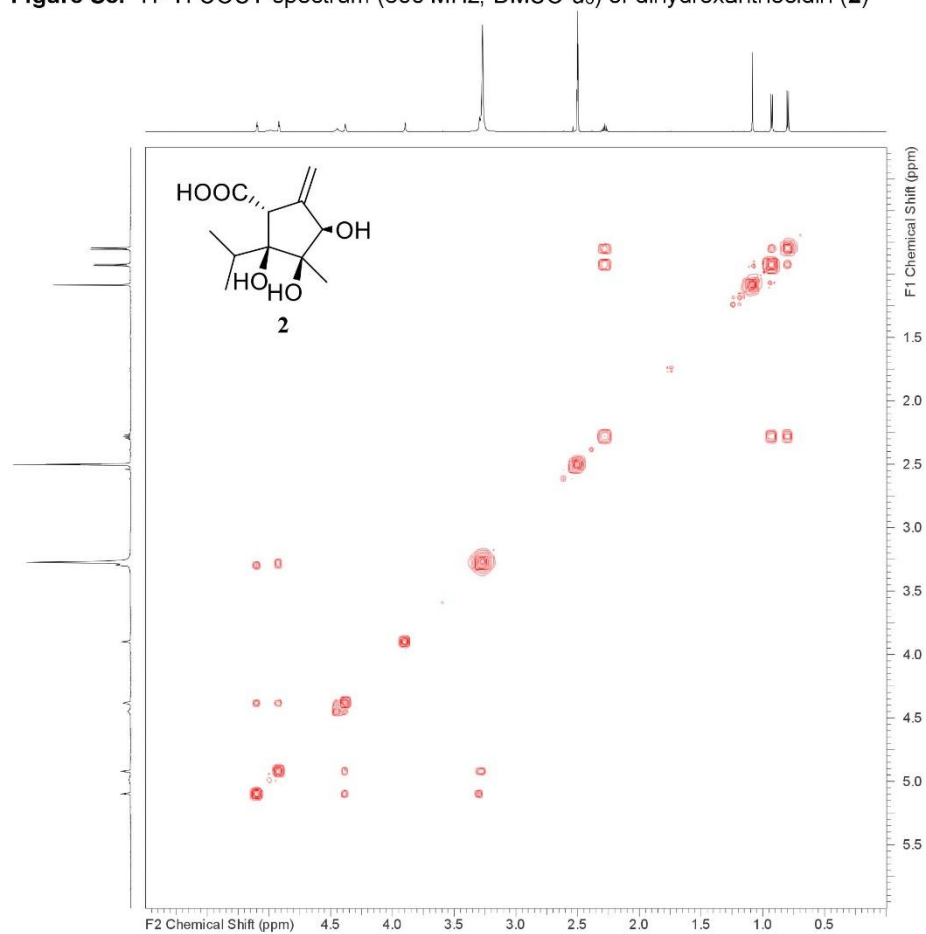
Figure S8. ^1H - ^1H COSY spectrum (600 MHz, $\text{DMSO-}d_6$) of dihydroxanthocidin (**2**)

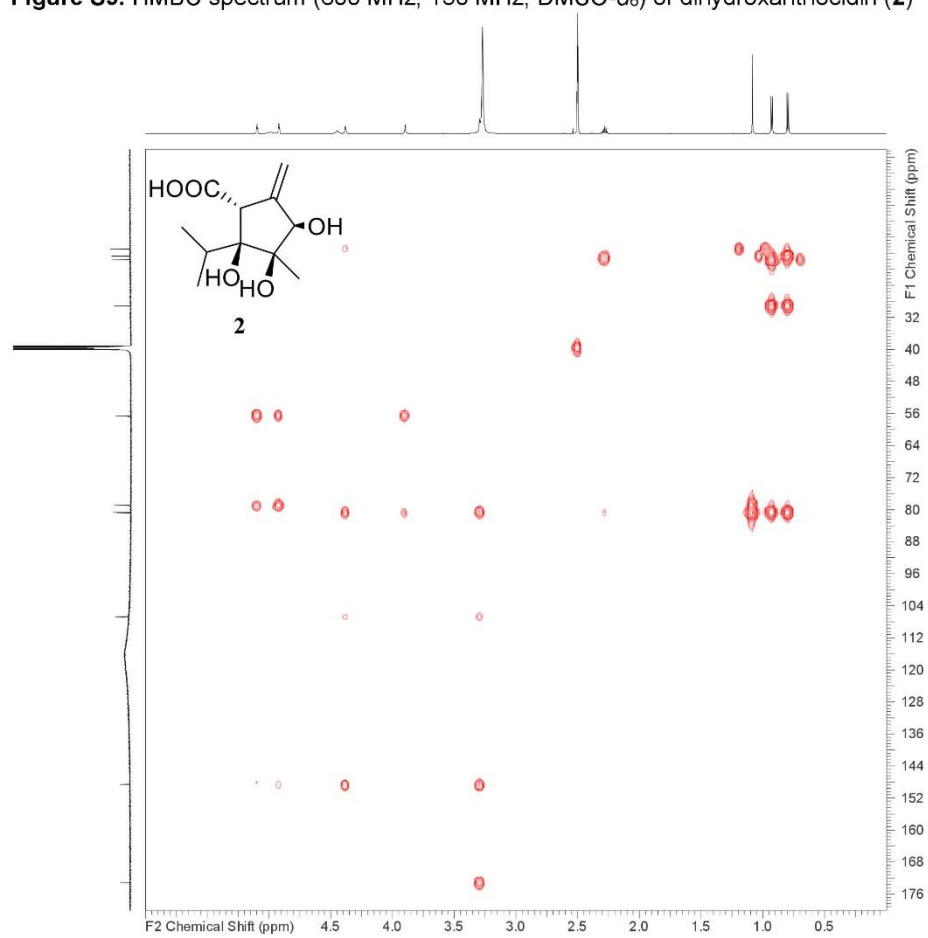
Figure S9. HMBC spectrum (600 MHz, 150 MHz, DMSO- d_6) of dihydroxanthocidin (**2**)

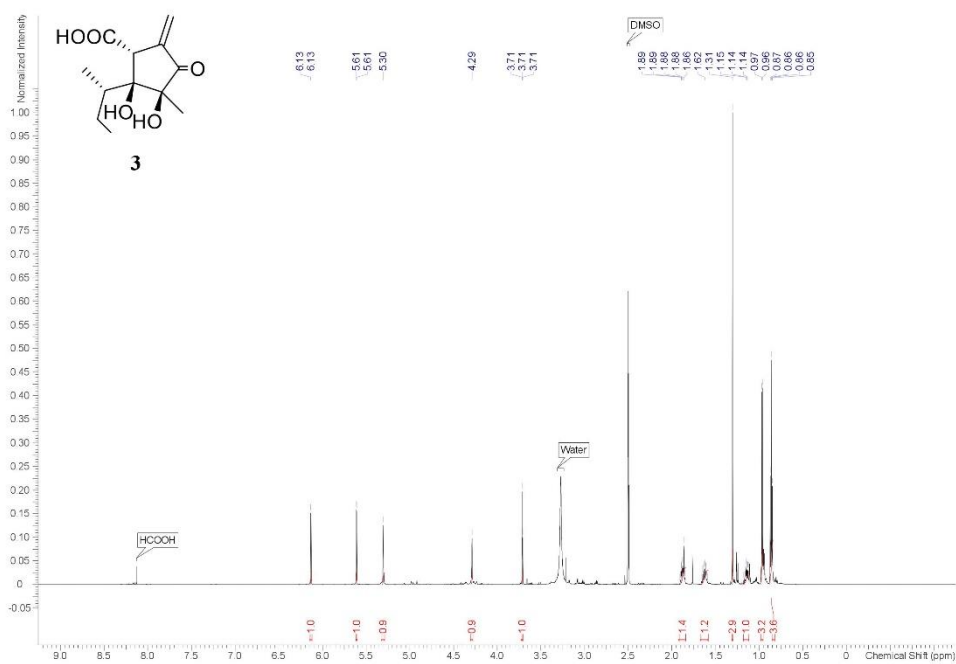
Figure S10. $^1\text{H-NMR}$ spectrum (600 MHz, acetonitrile- d_3) of homoxanthocidin (**3**)

Figure S11. HSQC-DEPT spectrum (600 MHz, 150 MHz, acetonitrile- d_3) of homoxanthocidin (**3**)

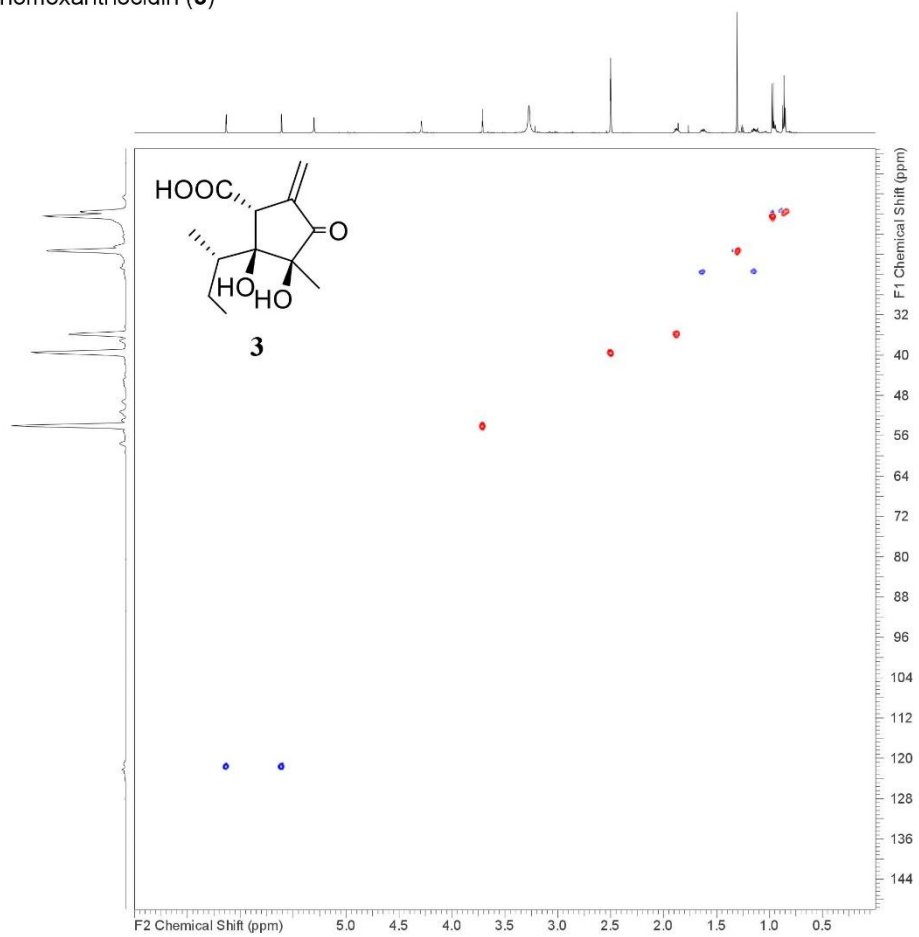


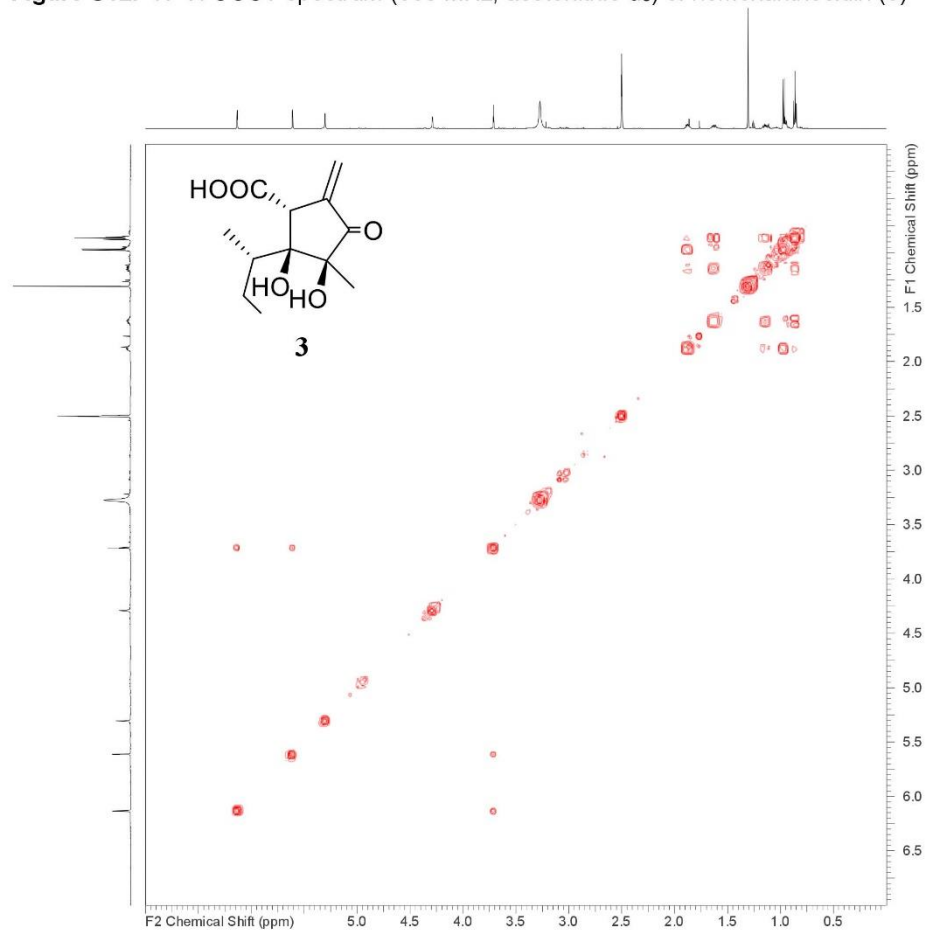
Figure S12. ^1H - ^1H COSY spectrum (600 MHz, acetonitrile- d_3) of homoxanthocidin (**3**)

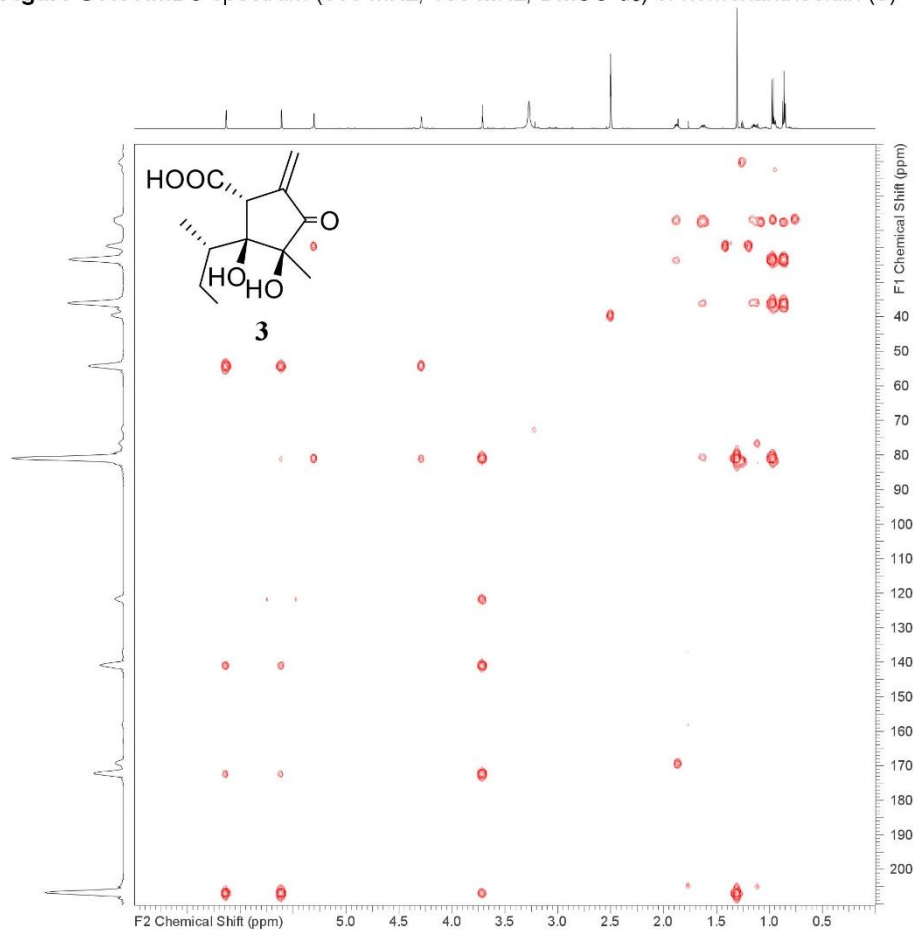
Figure S13. HMBC spectrum (600 MHz, 150 MHz, DMSO-*d*₆) of homoxanthocidin (**3**)

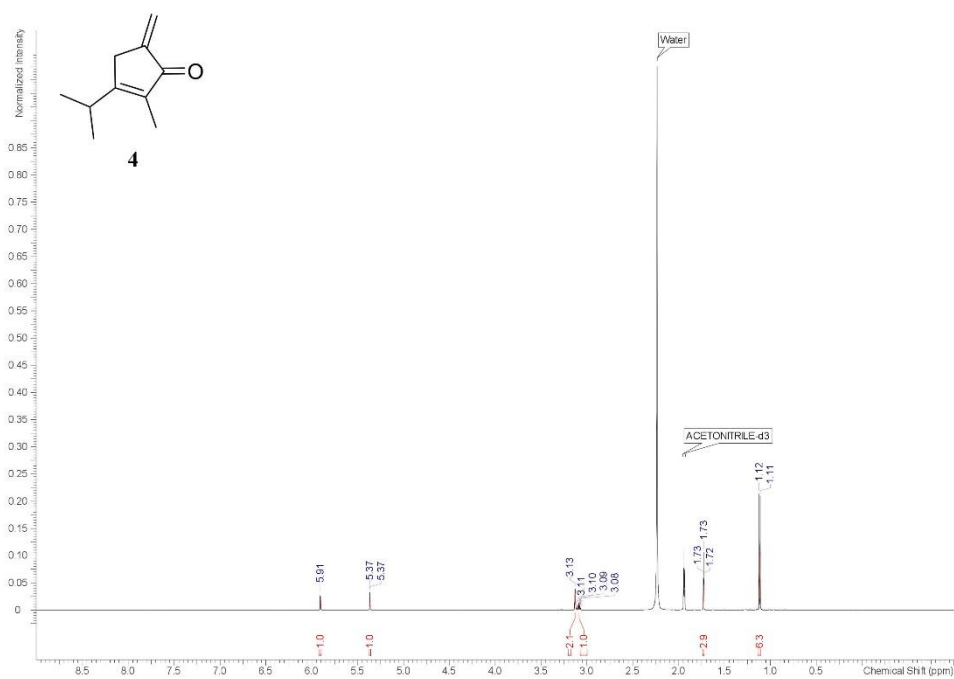
Figure S14. $^1\text{H-NMR}$ spectrum (600 MHz, acetonitrile- d_3) of xanthocidin B (**4**)

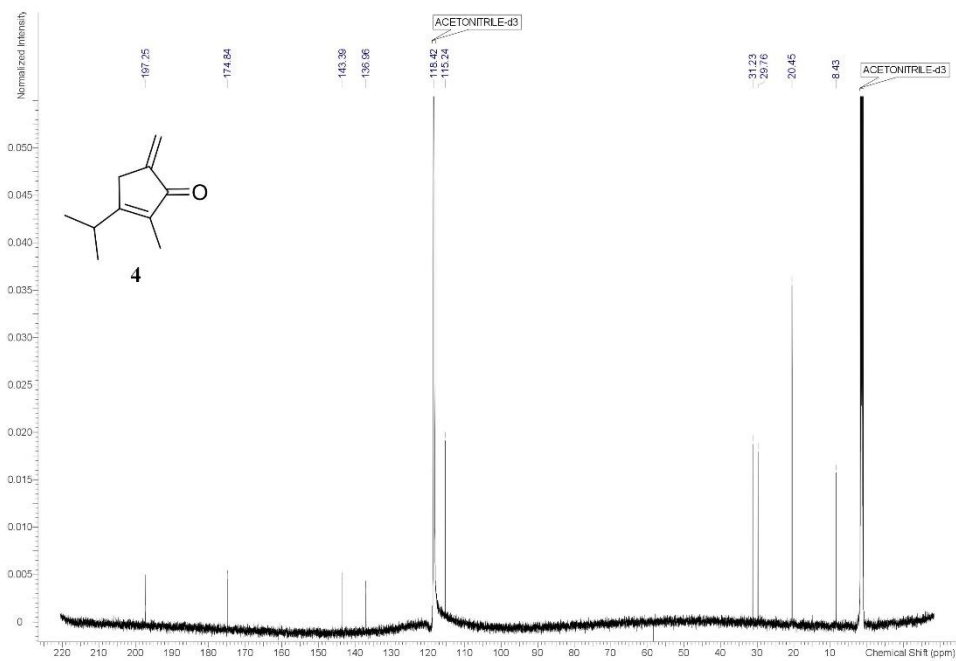
Figure S15. ^{13}C -NMR spectrum (150 MHz, acetonitrile- d_3) of xanthocidin B (**4**)

Figure S16. HSQC-DEPT spectrum (600 MHz, 150 MHz, acetonitrile- d_3) of xanthocidin B (4)

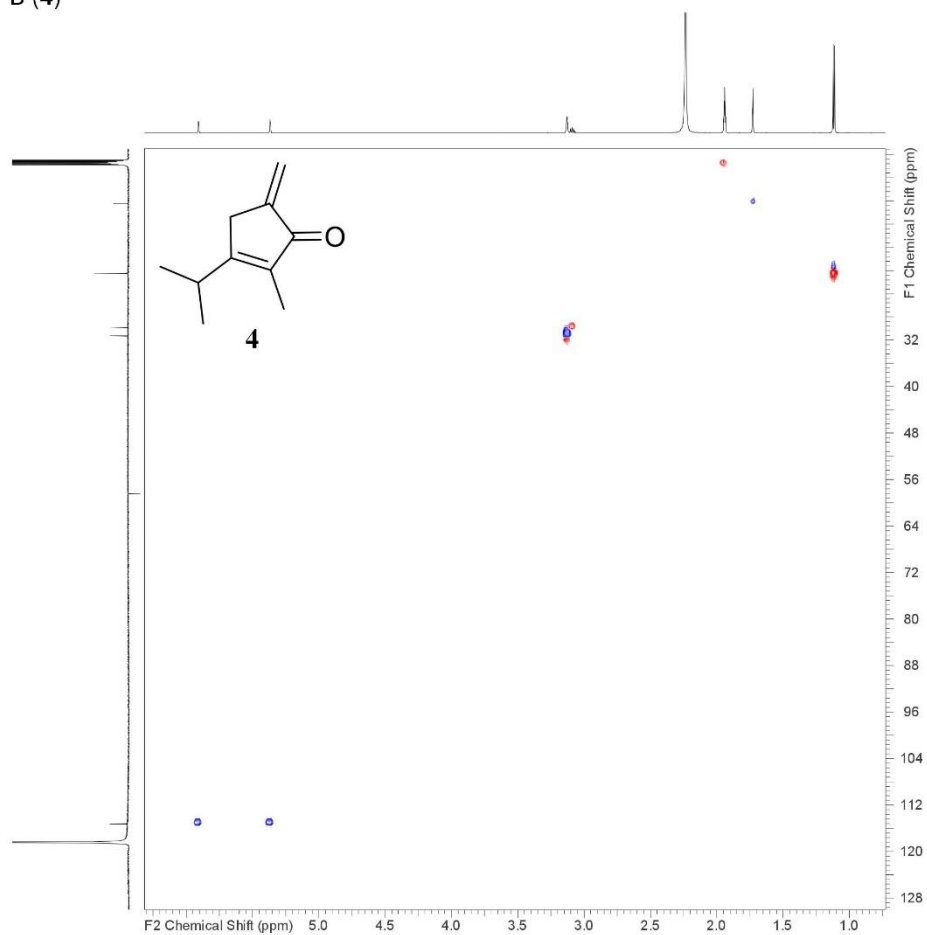


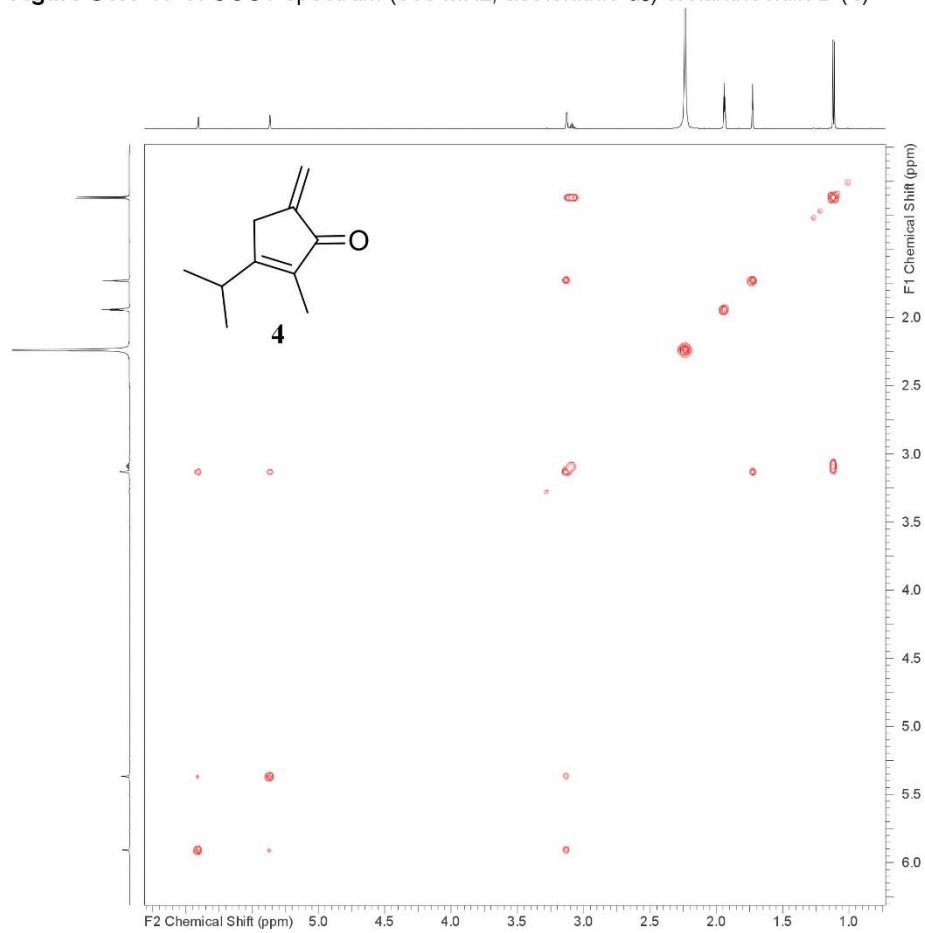
Figure S17. ^1H - ^1H COSY spectrum (600 MHz, acetonitrile- d_3) of xanthocidin B (**4**)

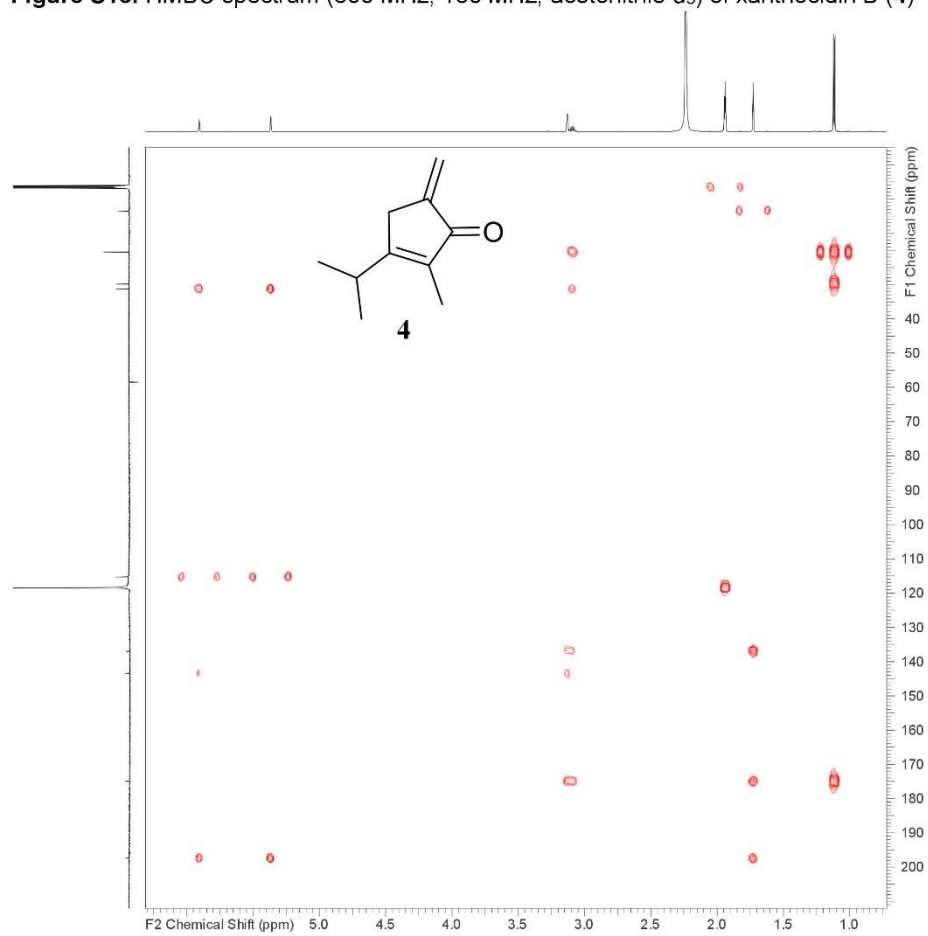
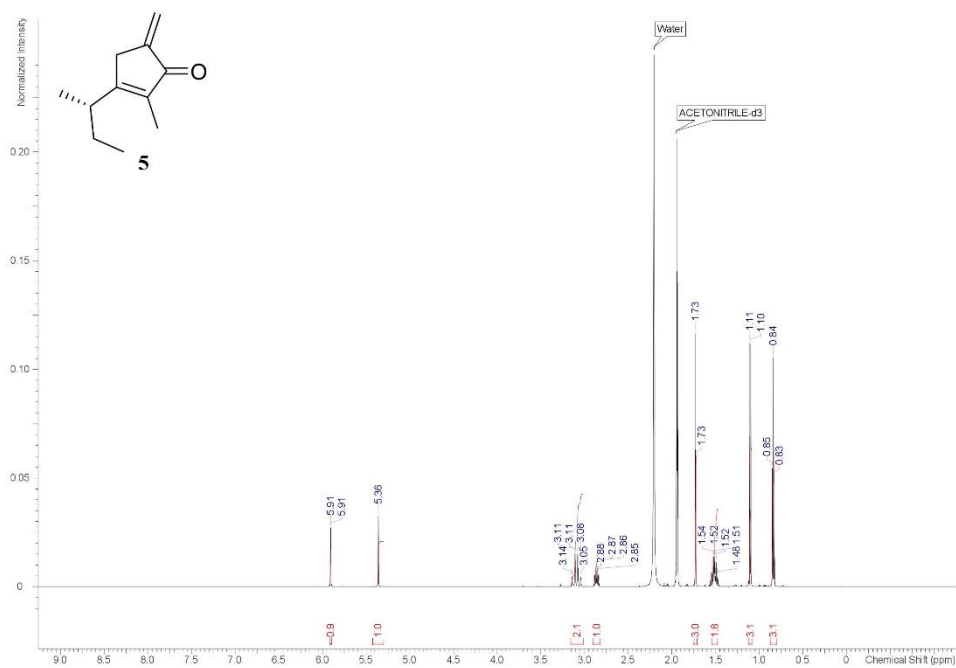
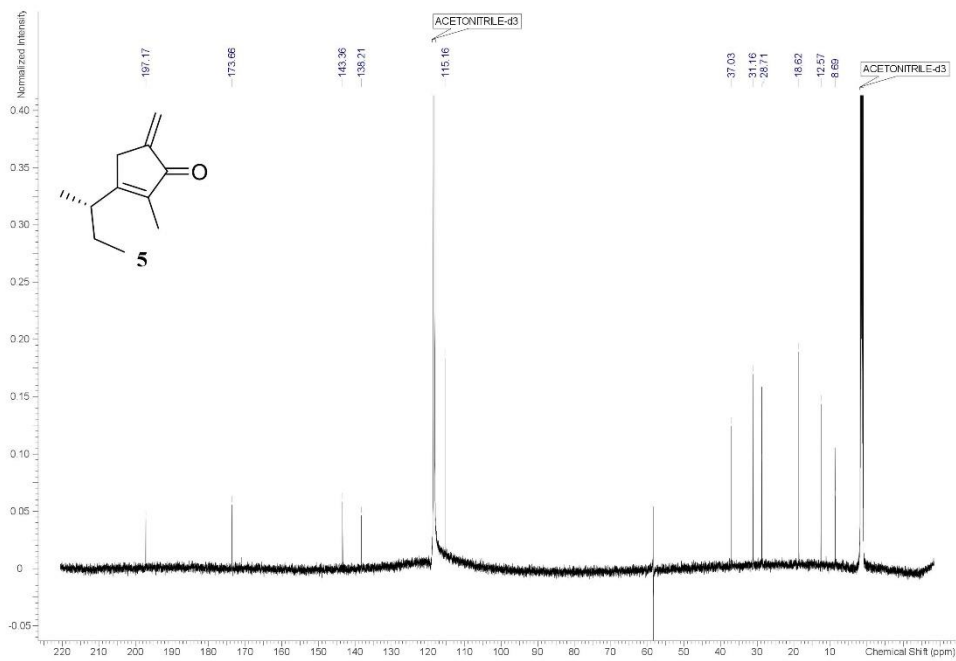
Figure S18. HMBC spectrum (600 MHz, 150 MHz, acetonitrile- d_3) of xanthocidin B (**4**)

Figure S19. $^1\text{H-NMR}$ spectrum (600 MHz, acetonitrile- d_3) of homoxanthocidin B (**5**)

20

Figure S20. $^{13}\text{C-NMR}$ spectrum (150 MHz, acetonitrile- d_3) of homoxanthocidin B (**5**)

21

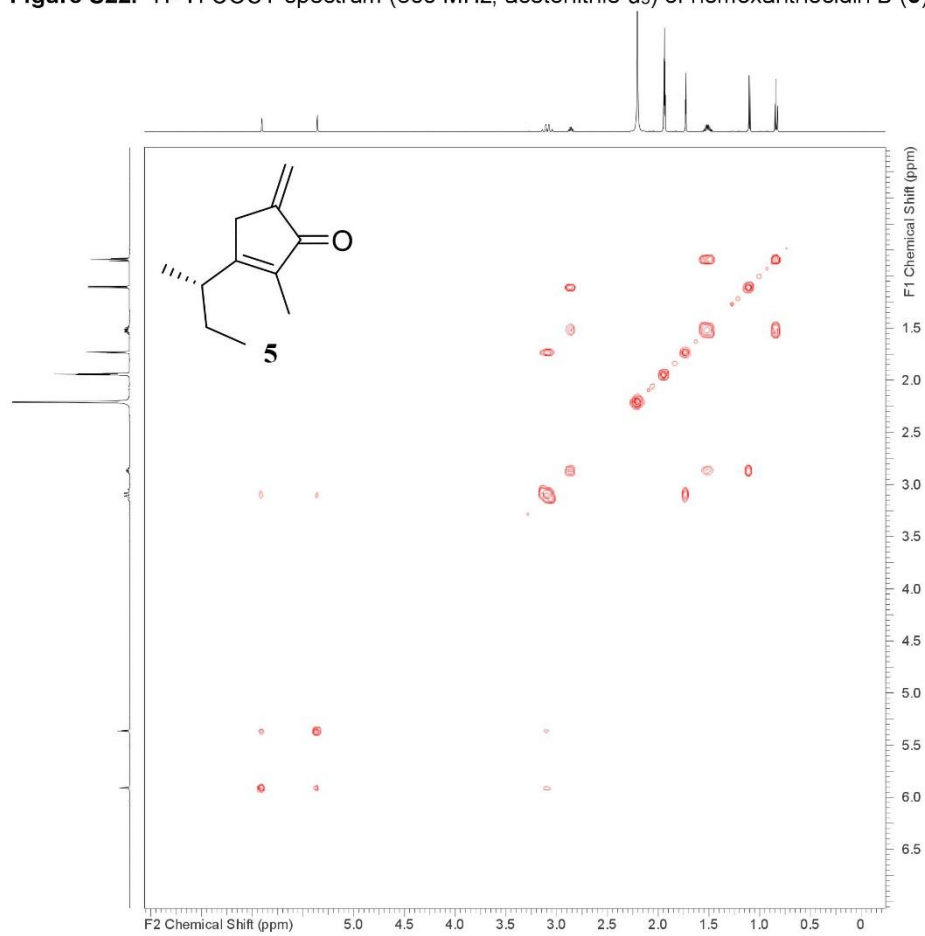
Figure S22. ^1H - ^1H COSY spectrum (600 MHz, acetonitrile- d_3) of homoxanthocidin B (**5**)

Figure S24. ^{13}C -NMR spectra (100 MHz, acetonitrile- d_3) of xanthocidin B (**4**) and $^{13}\text{C}_4$ -xanthocidin B; xanthocidin B control (bottom), $^{13}\text{C}_4$ -xanthocidin B (top); ^{13}C -labelled carbon multiplets highlighted

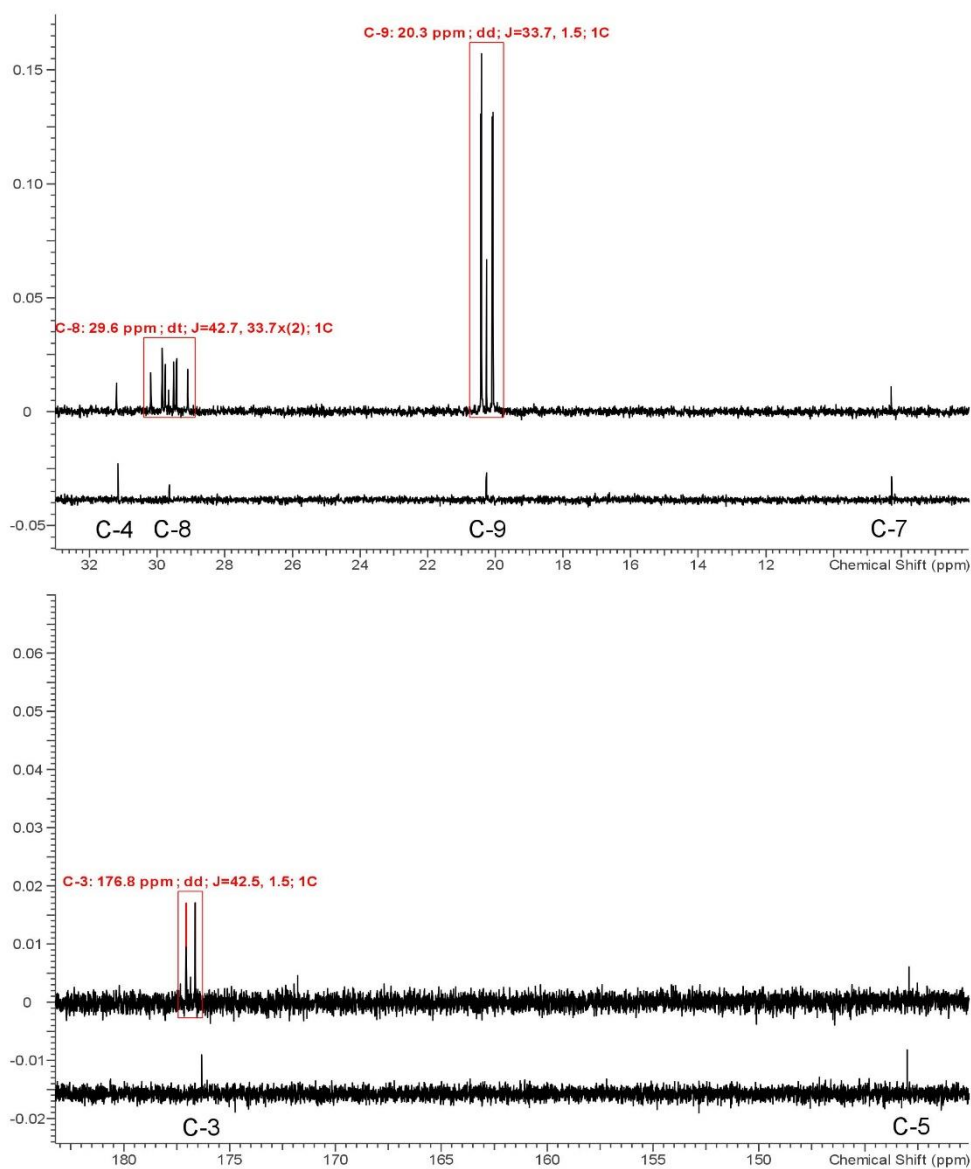


Figure S25. Phylogenetic tree of *S. sp. AcE210* (blue dot) inferred from gDNA sequence using the software autoMLST. The phylogeny is rooted with *Actinospica acidiphila* NRRL B24431 (red dot)

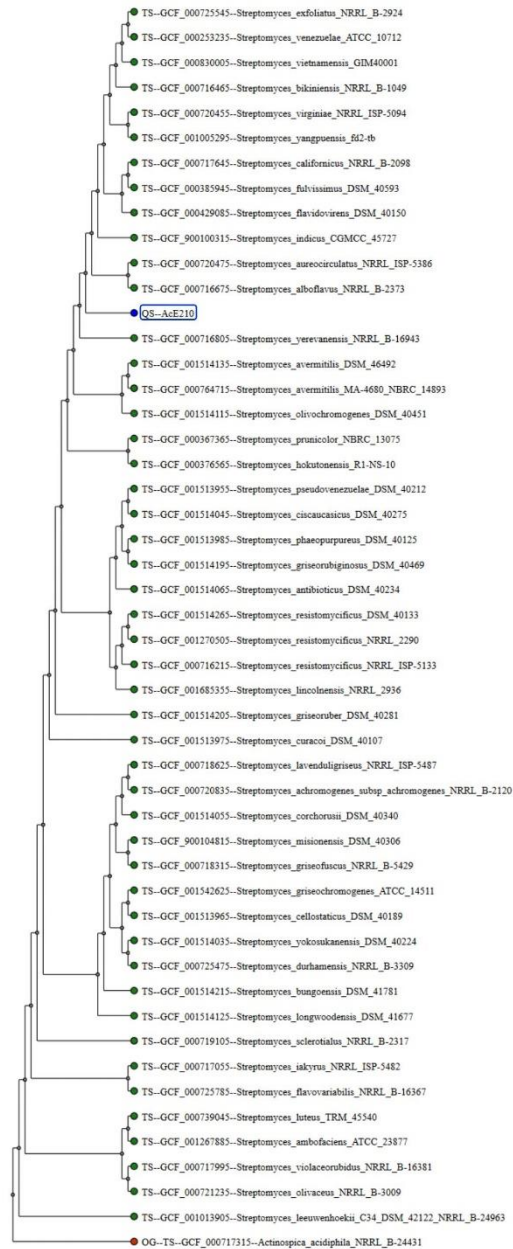


Table S26. Results of the BLAST analysis – comparison of the *mmy-mmf* gene cluster of *S. coelicolor* A3(2) and the putative xanthocidin (*xci*) gene cluster of *S. sp.* AcE210.

Gene	AA Identity [%]	AA Similarity [%]	AA Gaps [%]	Annotation / Proposed function
<i>xci_1_02270</i>	46	61	1	MmfR (transcriptional regulator, TetR family)
<i>xci_1_02269</i>	35	47	7	MmfL
<i>xci_1_02268</i>	33	50	4	MmyR (transcriptional regulator, TetR family)
<i>xci_1_02267</i>	n.s.	n.s.	n.s.	oxidase
<i>xci_1_02266</i>	66	81	0	MmyX (ATP/GTP-binding protein)
<i>xci_1_02265</i>	69	84	0	MmyQ (hypothetical function)
<i>xci_1_02264</i>	67	77	2	MmyE (putative enoyl reductase)
<i>xci_1_02263</i>	73	84	0	MmyJ (hypothetical protein)
<i>xci_1_02262</i>	74	83	2	Mmr (mmy A resistance protein)
<i>xci_1_02261</i>	n.s.	n.s.	n.s.	oxidoreductase
<i>xci_1_02260</i>	44	60	2	MmfH (oxidoreductase)
<i>xci_1_02259</i>	48	60	7	MmfP (phosphatase)
<i>xci_1_02258</i>	n.s.	n.s.	n.s.	hypothetical protein
<i>xci_1_02257</i>	46	56	8	MmyT (thioesterase)
<i>xci_1_02256</i>	n.s.	n.s.	n.s.	branched chain alpha keto dehydrogenase
<i>xci_1_02255</i>	n.s.	n.s.	n.s.	dehydrogenase
<i>xci_1_02254</i>	n.s.	n.s.	n.s.	acetyltransferase of dehydrogenase complex
<i>xci_1_02253</i>	45	58	2	MmyD
<i>xci_1_02252</i>	59	73	0	MmyC (putative ACP)
<i>xci_1_02251</i>	39	58	4	MmyA (ACP)

6.3 Acknowledgments

Ich möchte mich bedanken, bei

Prof. Dr. Timo Niedermeyer für das interessante Projekt, die Unterstützung, Betreuung und das Erstellen des Gutachtens sowie für seinen grenzenlosen Optimismus – „Alles wird gut.“. Außerdem möchte ich mich herzlich für die vielen Möglichkeiten bedanken, für Meetings und Tagungen, Deutschland und Europa bereist zu haben.

Prof. Dr. Harald Groß für die konstruktiven Diskussionen, die technische und fachliche Betreuung bei der Aufnahme von NMR Spektren sowie für seine Unterstützung – besonders in der letzten Phase dieser Arbeit, und darüber hinaus natürlich für das Erstellen des Gutachtens.

Prof. Dr. Wolfgang Wohlleben und seinen gesamten Arbeitsgruppen für die „Adoption“ und die Möglichkeit meine Forschungsarbeit an seinem Lehrstuhl für Mikrobiologie/Biotechnologie zu beenden. Ein besonderer Dank gilt hierbei der Arbeitsgruppe von Prof. Dr. Yvonne Mast für die Unterstützung bei der Einhaltung der gesetzlich geforderten (Eis-)Pausen.

Thomas Härtner für die schnelle und unkomplizierte Hilfe bei der Bewältigung der alltäglichen Probleme im Labor.

Andreas Kulik für die unzähligen HPLC-MS-Messungen und die Unterstützung bei der Kultivierung der Streptomyceten sowie bei der Aufreinigung der Naturstoffe.

Ronja, Julia, Steffen, Elke, allen ehemaligen Mitgliedern der AG Niedermeyer und insbesondere bei Tomasz für die schöne und lustige Zeit im Labor und auch darüber hinaus, für viele einzigartige Erinnerungen.

meinen Studenten Elisa Liebhart und Philipp Schneider für die gemeinsamen Bemühungen die aktiven Substanzen der Stämmen *S. sp. Tü2700* und *S. sp. Tü2401* zu isolieren.

den „Dienstags-Strategen“ für die heiteren Taktik-Seminare.

meinen Mitbewohnern und Wegbegleitern für die Feierabendgestaltung.

meinen Eltern und meinem Bruder für deren bedingungslosen Rückhalt aus der Ferne.

Vielen Dank Pia, für Deine grenzenlose, liebevolle Unterstützung und Deine Nachsicht!

6.4 Rights of use for third party property

Figure 19; S. 85

RightsLink Printable License

<https://s100.copyright.com/App/PrintableLicenseFrame.jsp?publis...>

ELSEVIER LICENSE TERMS AND CONDITIONS

Jan 25, 2019

This Agreement between University of Tübingen – Nico Ortlieb ("You") and Elsevier ("Elsevier") consists of your license details and the terms and conditions provided by Elsevier and Copyright Clearance Center.

License Number	4515830750181
License date	Jan 25, 2019
Licensed Content Publisher	Elsevier
Licensed Content Publication	Bioorganic & Medicinal Chemistry Letters
Licensed Content Title	Enediynes: Exploration of microbial genomics to discover new anticancer drug leads
Licensed Content Author	Ben Shen, Hindra,Xiaohui Yan,Tingting Huang,Huiming Ge,Dong Yang,Qihui Teng,Jeffrey D. Rudolf,Jeremy R. Lohman
Licensed Content Date	Jan 1, 2015
Licensed Content Volume	25
Licensed Content Issue	1
Licensed Content Pages	7
Start Page	9
End Page	15
Type of Use	reuse in a thesis/dissertation
Portion	figures/tables/illustrations
Number of figures/tables /illustrations	1
Format	both print and electronic
Are you the author of this Elsevier article?	No
Will you be translating?	No
Original figure numbers	Figure 1.
Title of your thesis/dissertation	Characterization of Natural Products from Ac-tinobacteria of the Tübingen strain collection – Screening, Isolation & Structure Elucidation
Expected completion date	Jan 2019
Estimated size (number of pages)	150
Requestor Location	University of Tübingen Auf der Morgenstelle 28 72076 Tübingen Tübingen, Baden-Württemberg 72076 Germany Attn: University of Tübingen
Publisher Tax ID	GB 494 6272 12
Total	0.00 EUR

Terms and Conditions

INTRODUCTION

1. The publisher for this copyrighted material is Elsevier. By clicking "accept" in connection with completing this licensing transaction, you agree that the following terms and conditions apply to this transaction (along with the Billing and Payment terms and conditions established by Copyright Clearance Center, Inc. ("CCC"), at the time that you opened your Rightslink account and that are available at any time at <http://myaccount.copyright.com>).

GENERAL TERMS

2. Elsevier hereby grants you permission to reproduce the aforementioned material subject to the terms and conditions indicated.

3. Acknowledgement: If any part of the material to be used (for example, figures) has appeared in our publication with credit or acknowledgement to another source, permission must also be sought from that source. If such permission is not obtained then that material may not be included in your publication/copies. Suitable acknowledgement to the source must be made, either as a footnote or in a reference list at the end of your publication, as follows:

"Reprinted from Publication title, Vol /edition number, Author(s), Title of article / title of chapter, Pages No., Copyright (Year), with permission from Elsevier [OR APPLICABLE SOCIETY COPYRIGHT OWNER]." Also Lancet special credit - "Reprinted from The Lancet, Vol. number, Author(s), Title of article, Pages No., Copyright (Year), with permission from Elsevier."

4. Reproduction of this material is confined to the purpose and/or media for which permission is hereby given.

5. Altering/Modifying Material: Not Permitted. However figures and illustrations may be altered/adapted minimally to serve your work. Any other abbreviations, additions, deletions and/or any other alterations shall be made only with prior written authorization of Elsevier Ltd. (Please contact Elsevier at permissions@elsevier.com). No modifications can be made to any Lancet figures/tables and they must be reproduced in full.

6. If the permission fee for the requested use of our material is waived in this instance, please be advised that your future requests for Elsevier materials may attract a fee.

7. Reservation of Rights: Publisher reserves all rights not specifically granted in the combination of (i) the license details provided by you and accepted in the course of this licensing transaction, (ii) these terms and conditions and (iii) CCC's Billing and Payment terms and conditions.

8. License Contingent Upon Payment: While you may exercise the rights licensed immediately upon issuance of the license at the end of the licensing process for the transaction, provided that you have disclosed complete and accurate details of your proposed use, no license is finally effective unless and until full payment is received from you (either by publisher or by CCC) as provided in CCC's Billing and Payment terms and conditions. If full payment is not received on a timely basis, then any license preliminarily granted shall be deemed automatically revoked and shall be void as if never granted. Further, in the event that you breach any of these terms and conditions or any of CCC's Billing and Payment terms and conditions, the license is automatically revoked and shall be void as if never granted. Use of materials as described in a revoked license, as well as any use of the materials beyond the scope of an unrevoked license, may constitute copyright infringement and publisher reserves the right to take any and all action to protect its copyright in the materials.

9. Warranties: Publisher makes no representations or warranties with respect to the licensed material.

10. Indemnity: You hereby indemnify and agree to hold harmless publisher and CCC, and their respective officers, directors, employees and agents, from and against any and all claims arising out of your use of the licensed material other than as specifically authorized pursuant to this license.

11. No Transfer of License: This license is personal to you and may not be sublicensed, assigned, or transferred by you to any other person without publisher's written permission.

12. No Amendment Except in Writing: This license may not be amended except in a writing signed by both parties (or, in the case of publisher, by CCC on publisher's behalf).

13. Objection to Contrary Terms: Publisher hereby objects to any terms contained in any purchase order, acknowledgment, check endorsement or other writing prepared by you, which terms are inconsistent with these terms and conditions or CCC's Billing and Payment terms and conditions. These terms and conditions, together with CCC's Billing and Payment terms and conditions (which are incorporated herein), comprise the entire agreement between you and publisher (and CCC) concerning this licensing transaction. In the event of any conflict between your obligations established by these terms and conditions and those established by CCC's Billing and Payment terms and conditions, these terms and conditions shall control.

14. Revocation: Elsevier or Copyright Clearance Center may deny the permissions described in this License at their sole discretion, for any reason or no reason, with a full refund payable to you. Notice of such denial will be made using the contact information provided by you. Failure to receive such notice

will not alter or invalidate the denial. In no event will Elsevier or Copyright Clearance Center be responsible or liable for any costs, expenses or damage incurred by you as a result of a denial of your permission request, other than a refund of the amount(s) paid by you to Elsevier and/or Copyright Clearance Center for denied permissions.

LIMITED LICENSE

The following terms and conditions apply only to specific license types:

15. Translation: This permission is granted for non-exclusive world **English** rights only unless your license was granted for translation rights. If you licensed translation rights you may only translate this content into the languages you requested. A professional translator must perform all translations and reproduce the content word for word preserving the integrity of the article.

16. Posting licensed content on any Website: The following terms and conditions apply as follows:

Licensing material from an Elsevier journal: All content posted to the web site must maintain the copyright information line on the bottom of each image; A hyper-text must be included to the Homepage of the journal from which you are licensing at <http://www.sciencedirect.com/science/journal/xxxxx> or the Elsevier homepage for books at <http://www.elsevier.com>; Central Storage: This license does not include permission for a scanned version of the material to be stored in a central repository such as that provided by Heron/XanEdu.

Licensing material from an Elsevier book: A hyper-text link must be included to the Elsevier homepage at <http://www.elsevier.com>. All content posted to the web site must maintain the copyright information line on the bottom of each image.

Posting licensed content on Electronic reserve: In addition to the above the following clauses are applicable: The web site must be password-protected and made available only to bona fide students registered on a relevant course. This permission is granted for 1 year only. You may obtain a new license for future website posting.

17. For journal authors: the following clauses are applicable in addition to the above:

Preprints:

A preprint is an author's own write-up of research results and analysis, it has not been peer-reviewed, nor has it had any other value added to it by a publisher (such as formatting, copyright, technical enhancement etc.).

Authors can share their preprints anywhere at any time. Preprints should not be added to or enhanced in any way in order to appear more like, or to substitute for, the final versions of articles however authors can update their preprints on arXiv or RePEc with their Accepted Author Manuscript (see below).

If accepted for publication, we encourage authors to link from the preprint to their formal publication via its DOI. Millions of researchers have access to the formal publications on ScienceDirect, and so links will help users to find, access, cite and use the best available version. Please note that Cell Press, The Lancet and some society-owned have different preprint policies. Information on these policies is available on the journal homepage.

Accepted Author Manuscripts: An accepted author manuscript is the manuscript of an article that has been accepted for publication and which typically includes author-incorporated changes suggested during submission, peer review and editor-author communications.

Authors can share their accepted author manuscript:

- immediately
 - via their non-commercial person homepage or blog
 - by updating a preprint in arXiv or RePEc with the accepted manuscript
 - via their research institute or institutional repository for internal institutional uses or as part of an invitation-only research collaboration work-group
 - directly by providing copies to their students or to research collaborators for their personal use
 - for private scholarly sharing as part of an invitation-only work group on commercial sites with which Elsevier has an agreement
- After the embargo period
 - via non-commercial hosting platforms such as their institutional repository
 - via commercial sites with which Elsevier has an agreement

In all cases accepted manuscripts should:

- link to the formal publication via its DOI
- bear a CC-BY-NC-ND license - this is easy to do
- if aggregated with other manuscripts, for example in a repository or other site, be shared in

alignment with our hosting policy not be added to or enhanced in any way to appear more like, or to substitute for, the published journal article.

Published journal article (JPA): A published journal article (PJA) is the definitive final record of published research that appears or will appear in the journal and embodies all value-adding publishing activities including peer review co-ordination, copy-editing, formatting, (if relevant) pagination and online enrichment.

Policies for sharing publishing journal articles differ for subscription and gold open access articles:

Subscription Articles: If you are an author, please share a link to your article rather than the full-text. Millions of researchers have access to the formal publications on ScienceDirect, and so links will help your users to find, access, cite, and use the best available version.

Theses and dissertations which contain embedded PJAs as part of the formal submission can be posted publicly by the awarding institution with DOI links back to the formal publications on ScienceDirect.

If you are affiliated with a library that subscribes to ScienceDirect you have additional private sharing rights for others' research accessed under that agreement. This includes use for classroom teaching and internal training at the institution (including use in course packs and courseware programs), and inclusion of the article for grant funding purposes.

Gold Open Access Articles: May be shared according to the author-selected end-user license and should contain a [CrossMark logo](#), the end user license, and a DOI link to the formal publication on ScienceDirect.

Please refer to Elsevier's [posting policy](#) for further information.

18. **For book authors** the following clauses are applicable in addition to the above: Authors are permitted to place a brief summary of their work online only. You are not allowed to download and post the published electronic version of your chapter, nor may you scan the printed edition to create an electronic version. **Posting to a repository:** Authors are permitted to post a summary of their chapter only in their institution's repository.

19. **Thesis/Dissertation:** If your license is for use in a thesis/dissertation your thesis may be submitted to your institution in either print or electronic form. Should your thesis be published commercially, please reapply for permission. These requirements include permission for the Library and Archives of Canada to supply single copies, on demand, of the complete thesis and include permission for Proquest/UMI to supply single copies, on demand, of the complete thesis. Should your thesis be published commercially, please reapply for permission. Theses and dissertations which contain embedded PJAs as part of the formal submission can be posted publicly by the awarding institution with DOI links back to the formal publications on ScienceDirect.

Elsevier Open Access Terms and Conditions

You can publish open access with Elsevier in hundreds of open access journals or in nearly 2000 established subscription journals that support open access publishing. Permitted third party re-use of these open access articles is defined by the author's choice of Creative Commons user license. See our [open access license policy](#) for more information.

Terms & Conditions applicable to all Open Access articles published with Elsevier:

Any reuse of the article must not represent the author as endorsing the adaptation of the article nor should the article be modified in such a way as to damage the author's honour or reputation. If any changes have been made, such changes must be clearly indicated.

The author(s) must be appropriately credited and we ask that you include the end user license and a DOI link to the formal publication on ScienceDirect.

If any part of the material to be used (for example, figures) has appeared in our publication with credit or acknowledgement to another source it is the responsibility of the user to ensure their reuse complies with the terms and conditions determined by the rights holder.

Additional Terms & Conditions applicable to each Creative Commons user license:

CC BY: The CC-BY license allows users to copy, to create extracts, abstracts and new works from the Article, to alter and revise the Article and to make commercial use of the Article (including reuse and/or resale of the Article by commercial entities), provided the user gives appropriate credit (with a link to the formal publication through the relevant DOI), provides a link to the license, indicates if changes were made and the licensor is not represented as endorsing the use made of the work. The full details of the license are available at <http://creativecommons.org/licenses/by/4.0>.

CC BY NC SA: The CC BY-NC-SA license allows users to copy, to create extracts, abstracts and new works from the Article, to alter and revise the Article, provided this is not done for commercial purposes, and that the user gives appropriate credit (with a link to the formal publication through the relevant DOI), provides a link to the license, indicates if changes were made and the licensor is not represented as endorsing the use made of the work. Further, any new works must be made available on the same

RightsLink Printable License

<https://s100.copyright.com/App/PrintableLicenseFrame.jsp?publis...>

conditions. The full details of the license are available at <http://creativecommons.org/licenses/by-nc-sa/4.0>.

CC BY NC ND: The CC BY-NC-ND license allows users to copy and distribute the Article, provided this is not done for commercial purposes and further does not permit distribution of the Article if it is changed or edited in any way, and provided the user gives appropriate credit (with a link to the formal publication through the relevant DOI), provides a link to the license, and that the licensor is not represented as endorsing the use made of the work. The full details of the license are available at <http://creativecommons.org/licenses/by-nc-nd/4.0>. Any commercial reuse of Open Access articles published with a CC BY NC SA or CC BY NC ND license requires permission from Elsevier and will be subject to a fee.

Commercial reuse includes:

- Associating advertising with the full text of the Article
- Charging fees for document delivery or access
- Article aggregation
- Systematic distribution via e-mail lists or share buttons

Posting or linking by commercial companies for use by customers of those companies.

20. Other Conditions:

v1.9

Questions? customer care@copyright.com or +1-855-239-3415 (toll free in the US) or +1-978-646-2777.

Figure 20; S. 87



The screenshot shows the Copyright Clearance Center RightsLink interface. At the top left is the Copyright Clearance Center logo. To its right is the RightsLink logo. Further right are navigation buttons for Home, Create Account, and Help, along with a chat bubble icon. Below the logos is the ACS Publications logo with the tagline 'Most Trusted. Most Cited. Most Read.' The main content area displays article details: Title: Antitumor Eneiyne Chromoprotein C-1027: Mechanistic Investigation of the Chromophore-Mediated Self-Decomposition Pathway; Author: Masayuki Inoue, Toyonobu Usuki, Nayoung Lee, et al; Publication: Journal of the American Chemical Society; Publisher: American Chemical Society; Date: Jun 1, 2006. A copyright notice at the bottom reads 'Copyright © 2006, American Chemical Society'. On the right side, there is a LOGIN button and a text box that says: 'If you're a copyright.com user, you can login to RightsLink using your copyright.com credentials. Already a RightsLink user or want to learn more?' with a link to 'learn more?'.

PERMISSION/LICENSE IS GRANTED FOR YOUR ORDER AT NO CHARGE

This type of permission/license, instead of the standard Terms & Conditions, is sent to you because no fee is being charged for your order. Please note the following:

- Permission is granted for your request in both print and electronic formats, and translations.
- If figures and/or tables were requested, they may be adapted or used in part.
- Please print this page for your records and send a copy of it to your publisher/graduate school.
- Appropriate credit for the requested material should be given as follows: "Reprinted (adapted) with permission from (COMPLETE REFERENCE CITATION). Copyright (YEAR) American Chemical Society." Insert appropriate information in place of the capitalized words.
- One-time permission is granted only for the use specified in your request. No additional uses are granted (such as derivative works or other editions). For any other uses, please submit a new request.

If credit is given to another source for the material you requested, permission must be obtained from that source.

[BACK](#)[CLOSE WINDOW](#)